THE UNIVERSITY *of* EDINBURGH

The Effect of Manipulating PI3K Pathway Components on Primordial Follicle Activation and DNA Damage Response in Bovine Ovarian Follicles *In vitro*

Mila Maidarti

Thesis submitted for the Degree of Doctor of Philosophy

University of Edinburgh

2020

Declaration

March 2020

I declare that all the work presented within this thesis was composed by myself and that it has not been submitted in any other degree or professional qualification. Except where stated otherwise in the text, the work presented is entirely my own.

Mila Maidarti

2020

Abstract

Developing immature follicles either from fresh or cryopreserved ovarian tissue to attain competent and fertilisable oocytes could provide an option for some patients undergoing fertility preservation to avoid the risk of ovarian micro-metastases following ovarian tissue transplantation. The first stage of an *in vitro* growth system (IVG) is activation of primordial follicles. Regulation of this process is critical as uncontrolled and precocious growth initiation of primordial follicles during *in vitro* activation (IVA) has been a major concern. A delicate balance between inhibitory and stimulatory signals is required to achieve activation but this can also be regulated by manipulating key signalling pathways associated with follicle activation.

Phosphatase and tensin homolog of chromosome 10 (PTEN), expressed by the oocyte, is a negative regulator of the Phosphoinositide 3-kinase (PI3K) pathway and has been utilised to initiate primordial follicle growth both *in vivo* and *in vitro* in a range of species. Pregnancies have been achieved after grafting small ovarian cortical fragments exposed to PI3K/protein kinase B (Akt) activators to reinitiate the growth of residual follicles in the ovarian tissue of premature ovarian insufficiency (POI) patients. However, activating growth in this way may be damaging to the ovarian follicles. PTEN also has a role in maintaining genomic integrity. Its effects on DNA double strand breaks (DSBs) repair capacity has been debatable. Notably, unrepaired DNA damage is related to ovarian ageing. Meiotic errors are also more likely, leading to chromosomal abnormalities and impacting on oocyte quality. Therefore, we hypothesised that inhibiting PTEN to increase the activation of primordial follicles could result in increased DNA damage and compromised DNA repair capacity in oocytes and granulosa cells. This technique may also affect further growth of isolated

preantral follicles selected for culture. The overall aim of this thesis was to determine the collective effects of PI3K/PTEN/Akt/mammalian target of rapamycin (mTOR) modulation pathway, either by inhibiting or activating the signals, on primordial follicle activation and DNA damage response (DDR) of bovine ovarian follicles *in vitro*.

These experiments demonstrated that short-term incubation of ovarian cortex with low (1μM) and high dose (10μM) dipotassium bisperoxo (5-hydroxypyridine-2-carboxyl) oxovanadate (V) (bpv(HOpic)), a PTEN inhibitor, increased primordial follicle activation but resulted in a reduction in the proportion of morphologically healthy follicles in the high dose group. In parallel, DNA damage increased with limited DNA repair function. This was observed both in low and high dose. The mTOR signalling pathway is a master regulator of cell growth and metabolism and its inhibition attenuates follicle growth activation. In the second part, the potential benefit of inhibiting PI3K/Akt/mTOR signalling on the regulation of *in vitro* follicular activation was investigated. The addition of a low dose rapamycin to bpv(HOpic) or rapamycin on its own reduced DNA damage and improved DNA repair capacity of the oocytes. In the last part, experiments were extended to isolated preantral follicles. None of the treatments had an effect on promoting isolated follicle growth and survival. Although DNA repair protein ataxia telangiectasia mutated (ATM) was significantly upregulated in the presence of rapamycin, it appeared that cumulative effects of increased gamma H2A histone family member X (γH2AX) and upregulation of ATM and Rad51 were not sufficient to support follicle growth.

Altogether, these data provide unimproved understanding into the regulation of the follicular activation and its relation with DDR, highlighting the significance of getting closer to physiological conditions to maintain follicle integrity. This may be a promising strategy for the derivation of mature oocytes *in vitro*. However, further investigations at the stage of isolated preantral follicle culture onwards are essential.

Lay Summary

Recent advances in cancer treatment including the improvement of chemotherapeutic regimens have led to increased survival of younger patients. This has resulted in greater consideration of future fertility and therefore an increased demand for fertility preservation prior to potentially damaging treatments. Cryo-preservation of ovarian material is now offered to young female cancer patients for subsequent ovarian tissue transplantation. Unfortunately, in certain cases, this method is not applicable due to the risk of transferring malignant cells during transplantation. Developing immature eggs (oocytes) either from fresh or cryopreserved ovarian tissue outside the body (i.e. entirely *in vitro*) to obtain mature eggs that could be fertilised would avoid this risk. The first stage in achieving a complete IVG system is activation of primordial follicles that contain the most immature eggs.

Primordial follicles are in a resting state within the ovary until they receive appropriate signals to initiate their growth initiation. Fragments of ovary containing primordial follicles can be cultured and this leads to activation of follicles and growth to developing follicles. However, the activation of these follicles is under control by the fine balance between inhibitory and stimulatory signals. PTEN is a factor known to have a major role in primordial follicle activation. Inhibition of PTEN will activate another signalling pathway called Akt that can increase the activation of immature eggs. These factors have been used to activate primordial follicle in range of species and has been applied clinically to reinitiate the growth of follicles in patients with very few follicles in their ovaries, and pregnancies have been achieved. A specific drug designed to stimulate Akt was used to incubate the tissue fragments prior to transplantation. However, this procedure might be damaging to the follicles as Akt is

also involved in cancer cell growth. Its activation may also affect DNA damage and its repair. In this study, the effects of these factors on DNA damage and DNA repair capacity of ovarian follicles have been studied using cow ovaries as a model for human.

This study has demonstrated that PTEN inhibition leads to increased primordial follicle activation, but also increases DNA damage and suppresses DNA repair capacity of cow ovarian follicle *in vitro*. As increasing the activation is associated with compromised DDR, it was hypothesised that decreasing the growth rate may improve DDR and prevent uncontrolled activation. This was tested by using a specific substance, mTOR inhibition that can slow the rate of activation. It was found that mTOR inhibition reduced DNA damage and improved DNA repair capacity of the follicles *in vitro*. To further analyse treatment effects on subsequent follicle growth, growing follicles were isolated from the fragments exposed to the treatments. However, no effect of treatments on follicle health, the number of antral follicles, expression of follicular health markers such as growth differentiation factor 9 (GDF9), connexin43 (Cx43) and laminin in isolated growing follicles cultured individually for another 6 to 8 days. Further analysis showed a reduction in expression of ATM and Rad51 in the PTEN inhibition group. These findings will help to improve and develop systems to grow eggs outside the body.

Publications and Presentations Relating to This Thesis

Publications

Inhibition of PTEN activates bovine non-growing follicles *in vitro* but increases DNA damage and reduces DNA repair response. Human Reproduction. 2018: pp. 1–11, 2018 doi:10.1093/humrep/dey354.

Crosstalk between PTEN/PI3K/Akt Signalling and DNA Damage in the Oocyte: Implications for Primordial Follicle Activation, Oocyte Quality and Ageing. *Cells* 2020, *9*(1), 200; http://doi.org/10.3390/cells 9010200.

Oral Presentations

Maidarti M, McLaughlin M, Clarkson YL, Telfer EE, Anderson RA (2017). Effect of PTEN inhibition on DNA damage and DNA repair capacity of bovine ovarian follicles in vitro. **Oral presentation at the 5th Biennial meeting of International Society for Fertility Preservation (ISFP); 2017 November 16-18; Vienna, Austria***.

Maidarti M, McLaughlin M, Clarkson YL, Telfer EE, Anderson RA (2018). Primordial follicle activation *in vitro* following PTEN inhibition is associated with increased DNA damage of bovine ovarian follicles. **Oral presentation at the 34th Annual Meeting of the European Society of Human reproduction and Embryology (ESHRE); 2018 July 1-4; Barcelona, Spain**.

Maidarti M, Clarkson YL, McLaughlin M, Telfer EE, Anderson RA (2018). The impact of PTEN inhibition and low dose rapamycin on primordial follicles activation and DNA damage response of bovine ovarian follicles *in vitro*. **Oral presentation at**

the 27th World Congress on Controversies in Obstetrics, Gynaecology and Infertility (COGI); 2018 November 23-25; London, UK.

Maidarti M, Clarkson YL, McLaughlin M, Telfer EE, Anderson RA (2019). Rapamycin reduces the adverse impact of PTEN inhibition on DNA damage response without preventing the increased follicle growth activation. **Oral presentation at Fertility meeting; 2019 January 3-5; Birmingham, UK.**

Maidarti M, McLaughlin M, Clarkson YL, Telfer EE, Anderson RA (2019). Primordial follicle activation *in vitro* following PTEN inhibition is associated with increased DNA damage of bovine ovarian follicles. **Oral presentation at the 35th Annual Meeting of the European Society of Human reproduction and Embryology (ESHRE); 2019 June 23-26; Vienna, Austria.**

Poster Presentations

Maidarti M, McLaughlin M, Clarkson Y, Telfer EE, Anderson RA (2018). Primordial Follicle Activation Following PTEN Inhibition Increased DNA Damage of Bovine Ovarian Follicles *In vitro*. **Poster presentation at 2nd UK fertility preservation meeting; 2018 September 16-17; Oxford, UK.**

* Awarded the outstanding abstract award winner

Acknowledgements

First and foremost, I would like to express my utmost gratitude to my supervisors, Professor Richard A Anderson and Professor Evelyn E Telfer for giving me this such an incredible opportunity. I can't thank you enough for believing in me, having faith in me, for teaching me to have faith in myself and for all the greatness you have helped me achieve during my PhD. Thank you for your words of encouragements and for always inspiring me during difficult times. I really appreciate everything you have taught me, for all the constructive advice and incredible ideas to enhance my knowledge and my critical thinking. I am also thankful that you have been very patient with all my questions and all the mistakes I made as I strive to learn everything that I can. Thank you for always being so keen to help me. I am so blessed to have you both as my supervisors.

I am equally grateful to thank Dr Marie McLaughlin for her time that she gave to assisting and teaching me all the technical skills in tissue culture. Thank you for being very patient with me, for the friendship and all the support throughout my PhD. I am also thankful for all the cakes and encouraging words. My sincere thanks also go to Dr Yvonne L Clarkson. I am so blessed to have her in our lab. Thank you very much for all your kindness, warm welcome, friendship, and your words to comfort me during the tough days. I can't thank you enough for your incredible support and great assistance in the lab. Your biomolecular knowledge is flawless. I am so lucky to have the opportunity to learn from one of the best.

This work would not have been possible without the help and support of many people who have given their invaluable support and assistance; John Binnie for being very

kind to help me with all trips to the abbatoir; Vivian Allison, Louise Dunn and Mike Molinek for their great technical assistance in histology and the DBUG lab over the last three years; Dr Anisha Kubasik ThayilI and Dr Martha Mikolajczak for their great technical assistance with confocal microscopy. I am also very thankful for their friendship, many chats and being such kind and fun people in the lab. I'd also like to thank all my fabulous friends Caroline Allen, Melissa Tharmalingam, Dr Roseanne Rosario and Lisa Campbell. Thanks for always listening to me, supporting me and encouraging me. The last year of my PhD has been great fun and full of laughs, thanks to Brenda Murage, Dr Emily Bailie, Dr Johanne Grosbois, Shannon Young, Min Ju Wu, Tara Doherty, Dr Kenichiro Sakaguchi and Dr Yvonne Clarkson.

My deepest gratitude to my colleagues, whom I cannot mention all individually (because there are too many), in the Obstetrics and Gynaecology Department, University of Indonesia. I am sincerely grateful to Faculty of Medicine, University of Indonesia for the permission I received to undergo this PhD. In addition, I would like to thank the Indonesia Endowment Fund for Education for the financial support without which I could not have undertaken these studies.

Last, but certainly not least I am deeply indebted to my family for their continuous support and unparalleled love. I am grateful to my late father for being such a great role model; my mother for her words of encouragement that have given me the strength to keep going. I am such a very fortunate child to have you as my parents. Thank you also to my sisters and my brother for all your support throughout the years. I love you all very much. My sincerely gratitude also goes to my husband Triono Sunaryo for always being there for me during the tough days, my lovely and amazing daughters

Azka Ajriya and Alma Mazaya for always cheering me up when things did not go according to plan and my experiments did not work. I love you all very much.

Table of Content

List of Figures

List of Tables

Abbreviations

Abbreviations	Description
ADSCs	Adipose-derived stem cells
Akt	Protein kinase B
APC	Anaphase-promoting complex
APLF	Aprataxin-and-PNK-like factor
ATM	Ataxia telangiectasia mutated
AMH	Anti-mullerian hormone
ATRIP	ATR-interacting protein
ATR	Ataxia telangiectasia and Rad3-related
bFGF	Basic fibroblast growth factor
Bcl-2	B-cell lymphoma/leukemia-2
Bad	Bcl-2-associated death promoter
Bax	Bcl- associated X protein
BMP	Bone morphogenetic protein
BMP4	Bone morphogenetic protein 4
BMP7	Bone morphogenetic protein 7
BMP15	Bone morphogenetic protein15
bpv(HOpic)	Dipotassium bisperoxo (5-hydroxypyridine-2-carboxyl) oxovanadate (V)
BL	Basal lamina
BRCA1	Breast cancer susceptibility gene1
BRCA2	Breast cancer susceptibility gene2
BSA	Bovine serum albumin
Cdc	Cell division cycle
Cdk2	Cyclin-dependent kinase-2
Chk1	Checkpoint kinase 1
Chk2	Checkpoint kinase 2
CP	Cyclophosphamide
CTGF	Connective tissue growth factor
Cx	Connexin

Cx37	Connexin 37
Cx43	Connexin 43
CXCR4	C-X-C chemokine receptor type 4
cAMP	Cyclic adenosine monophosphate
DAB	3, 3′-diaminobenzidine
DDR	DNA damage response
dH_2O	Distilled water
DPX	Dibutylphthalate Polystyrene Xylene
DNA-PKcs	DNA-dependent protein kinase catalytic subunit
dpc	Days post-coitum
DMSO	Dimethyl sulfoxide
DMC1	Disturbed meiotic cDNA1
DSBs	Double-strand breaks
DZN	Diazinon
ERK	Extracellular signal-regulated kinases
FIGLA	Factor in the germline-alpha
FGFs	Fibroblast growth factors
FSH	Follicle-stimulating hormone
FSHR	Follicle-stimulating hormone receptor
FOXL2	Forkhead box L2
FOXO3	Forkhead box O3
GC	Granulosa cells
GDF9	Growth differentiation factor 9
GPCR	G protein-coupled receptor
GV	Germinal vesicle
GVBD	Germinal vesicle breakdown
GWAS	Genome-wide association study
GSK3β	Glycogen synthase kinase 3
H & E	Haematoxylin and eosin
HGF	Hepatocyte growth factor
HR	Homologous recombination
IGF	Insulin-like growth factor

IVA	*In vitro* activation
IVF	*In vitro* fertilization
IVG	*In vitro* follicle growth
IVM	*In vitro* maturation
KGF	Keratinocyte growth factor
KL	KIT ligand
LHX8	LIM homeobox protein 8
LSD	Fisher least significant differences
LATS1/2	Large tumour suppressor homolog 1/2
LIF	Leukaemia inhibitory factor
LH	Luteinising hormone
LHR	Luteinising hormone receptor
MAPK	Mitogen-activated protein kinase
MC	Mesenchymal cells
MDC1	Mediator DNA damage checkpoint protein
M1	Metaphase I
M2	Metaphase II
mTORC1	Mammalian target of rapamycin complex I
mTORC2	Mammalian target of rapamycin complex 2
MMC	mitomycin C
MRN	MRE11, Rad50, NBS1
MRE11	Meiotic recombination 11
NBF	Normal buffered formalin
NBS1	Nijmegen breakage syndrome 1
NHEJ	Non-homologous end joining
NOBOX	Newborn ovary homeobox-encoding gene
PBS	Phosphate-buffered saline
PBST	Phosphate-buffered saline-triton
PCOS	Polycystic ovarian syndrome
PEG	Polyethylene glycol
PH	Pleckstrin homology
PIKK	Phosphatidylinositol 3-kinase-like kinase

PTEN	Phosphatase and tensin homolog deleted on chromosome 10
PDK1	Phosphatidylinositol-dependent kinase 1
PDGF	Platelet-derived growth factor
PGCs	Primordial germ cells
pGC	Primordial follicle granulosa cells
PI	Phosphatase Inhibitor
PI3K	Phosphoinositide 3-kinase
PIP2	Phosphatidylinositol-4,5-bisphosphate
PIP3	Phosphatidylinositol-3,4,5-bisphosphate
PKA	Protein kinase A
PKC	Protein kinase C
POF	Premature ovarian failure
POI	Premature ovarian insufficiency
PRISMA	Preferred reporting items for systematic reviews and meta-analyses
PUMA	p53 upregulated modulator of apoptosis
SDF1	Stromal cell-derived factor
Sohlh1	Spermatogenesis and oogenesis specific basic helix-loop-helix 1
STSW	Scott's tap water substitute
RIPA	Radioimmunoprecipitation assay
rpS6	Ribosomal protein S6 kinase
ROS	Reactive oxygen species
RPA	Replication protein A
SAC	Spindle assembly checkpoint
SCF	Stem cell factor
SGK	Serum-and glucocorticoid-induced kinase
SSBs	Single-strand breaks
SPSS	Statistical Package for the Social Sciences (SPSS)
S6K1	Ribosomal protein S6 kinase 1
TBS	Tris-buffered saline
TC	Theca cells
TBST	Tris-buffered saline-tween

TAp63	Trans-activating p63
TAZ	Transcriptional coactivator with PDZ-binding motif
TGFβ	Transforming Growth Factors-β
TID	Transcriptional inhibitory domain
TSC1/2	Tuberous sclerosis complex 1/2
TUNEL	Terminal deoxynucleotidyl transferase-mediated dUTP nick-end labelling
TZPs	Transzonal projections
XRCC4	X- ray cross complementing protein 4
XLF	XRCC4-like factor
YAP	Yes-associated protein
ZP	Zona pellucida
3D	Three dimensional
γH2AX	gamma H2A histone family member X

Chapter 1

General Introduction

1. Literature Review

A part of this chapter has been published as a review in Cells 2020, 9(1), 200; https://doi.org/10.3390/cells9010200.

1.1. Introduction

Cryopreservation of ovarian cortex prior to gonadotoxic treatments is used to preserve reproductive function and fertility of woman with cancer. Development of ovarian cryopreservation and subsequent transplantation has now resulted in the birth of almost 200 babies. However, in many cases, there is a risk of reintroducing malignant micro-metastases by transplanting the ovarian tissue, and this may lead to cancer recurrence (Dolmans *et al.*, 2013, Dolmans and Masciangelo, 2018).

The probability of reintroducing malignant cells is influenced by the stage and type of cancer with the risk of ovarian micro metastasis in leukaemia cancer patients being estimated as greater than 50% (Dolmans *et al.*, 2010) whilst the risk of ovarian metastasis in low-stage breast cancer and lymphoma is estimated as 0% (Meirow *et al.*, 1998, Rosendahl *et al.*, 2011). The risk tends to be variable across studies in cervical cancer patients, ranging from 0 to 14.3% (reviewed by (Bastings *et al.*, 2013)).These data highlight the potential risk of ovarian transplantation for certain patients and emphasise the need to develop in vitro systems (IVG and IVM) that could significantly improve reproductive outcomes for young female cancer survivors. In fact, it has recently been reported that the first live birth has been achieved using vitrification of oocytes from a female cancer survivor matured in vitro (IVM) (Grynberg *et al.*, 2020).

To avoid the risk of ovarian micro-metastases but still utilise the ovarian tissue, methods to grow immature follicles from fresh or cryopreserved ovarian tissue to

obtain mature oocytes are being developed as a solution to avoid the risk of ovarian micro-metastases after ovarian tissue transplantation (Barnes *et al.*, 1996, Gosden, 2000, Telfer *et al.*, 2008, Telfer and McLaughlin, 2012, Telfer and Zelinski, 2013, Thomas *et al.*, 2003a, Thomas *et al.*, 2003b). The primary focus in developing the IVG systems is increasing the number of developmentally competent oocytes (Telfer and McLaughlin, 2012). The first stage in this process is to activate and grow the most immature stage of follicle development (primordial follicles) contained within the tissue. To date, growth and maturation of primordial follicles entirely *in vitro* to produce developmentally competent oocytes capable of being fertilised and resulting in the birth of healthy offspring has only been achieved in mice (Eppig and O'Brien, 1996, O'Brien *et al.*, 2003).

Success in mouse models has led to the development of methods to support the growth of ovarian follicles *in vitro* starting from the early stages of follicle development in large mammals and human (Brito *et al.*, 2014, Hovatta *et al.*, 1997, Hovatta *et al.*, 1999, Picton and Gosden, 2000, Telfer and McLaughlin, 2012, Xiao *et al.*, 2015). Developing an optimal environment *in vitro* that supports follicular growth and survival is complex and challenging (Galloway *et al.*, 2000, McGee and Hsueh, 2000). It is now clear that *in vitro* follicle development from primordial stages requires a multistep culture system to initiate primordial follicle growth, preantral to antral follicle development and subsequently oocyte *in vitro* maturation (Telfer and McLaughlin, 2012, Telfer and Zelinski, 2013). Meiotically mature human oocytes derived from immature ovarian follicle grown in a multistep culture system has been achieved and represents a breakthrough in this field (McLaughlin *et al.*, 2018). In order

to optimise *in vitro* growth systems, it is crucial to have a greater understanding of the mechanisms regulating the activation of primordial follicles.

Activation of follicle growth is regulated by a combination of inhibitory, stimulatory and maintenance factors (Zhang and Liu, 2015). The PI3K/Akt signalling pathway within the oocyte has been shown to be a key regulator of primordial follicle activation. This system is a key signalling pathway in the regulation of primordial follicle growth and differentiation. Inhibition of PTEN, a major regulator of the PI3K pathway, has been widely used either *in vivo* (knockout mouse studies) or *in vitro* studies (use of a pharmacological inhibitor of PTEN) to induce primordial follicle activation in range of species (Adhikari *et al.*, 2012, Fan *et al.*, 2008, Jagarlamudi *et al.*, 2009, Reddy *et al.*, 2008). Pregnancy has been achieved after transplanted small ovarian cortical fragments exposed to pharmacological inhibitors of PTEN (Suzuki *et al.*, 2015). However, this method may be damaging to follicular growth and survival (Lerer-Serfaty *et al.*, 2013, McLaughlin *et al.*, 2014) implying that further investigation is required to fully understand the impact and implications of follicle activation using pharmacological approaches involving this pathway. Looking at its effects on the stage before the apoptosis occurs which is DDR is a major focus of this thesis using the bovine system as a model for human oocyte development. A thorough understanding of the impact of different culture conditions on DDR will be beneficial to optimise oocyte quality produced by a multistep culture system.

1.2. Primordial Follicle Formation and the Ovarian Reserve

Fetal life is a critical period of primordial follicle assembly as it has direct implications to determine female reproductive lifespan (Geber *et al.*, 2012). During embryogenesis, primordial germ cells (PGCs) undergo several phases of the migratory process, from

separation, migration and colonisation. In the human, these processes are completed at the end of 5 weeks of embryogenesis when the PGCs reach and settle in the genital ridge from the yolk sac through the dorsal mesentery of the hindgut to become oogonia (Faddy *et al.*, 1992, Mollgard *et al.*, 2010).

In other mammalian species, such as mice, PGCs have migrated to the genital ridge around ten days after conception. In the bovine, the genital ridge does not appear until 28-32 days of gestation and migration occurs around day 30 to 64 of pregnancy. In the genital ridge, the germ cells multiply and form oogonia. At 12 weeks of gestation, most of the germ cells are connected by intercellular bridges and appear as a nest/cyst of oogonia. Some oogonia start to enter meiosis and progress to diplotene stage of the first meiotic prophase and are referred to as primary oocytes (Bendsen *et al.*, 2006, Le Bouffant *et al.*, 2010). The high activity of germ cell proliferation at this stage is in line with the high somatic cell proliferation rate in the coelomic surface epithelium and blastemal cords that arise from regions within the ovaries. This intense proliferation can cause oocytes to be pushed to the cortical area of the ovary, included in the superficial epithelium or spread freely on the surface of the ovary, from which some may be lost (Motta *et al.*, 1986). It is estimated that the number of oogonia reaches a peak at five months of gestational age (Baker, 1963). Between 17 and 24 weeks of gestation, most oogonia have transformed into oocytes. During cyst breakdown, most of the oocytes experience apoptosis with just one third surviving. Pre-granulosa cells originated from the mesenchyme of the genital ridge establishes connections and surround these germ cells and ultimately form the primordial follicle pool (Pepling and Spradling, 2001, Pepling, 2012, Picton *et al.*, 1998, Wang *et al.*, 2017a). Oocytes are arrested at meiotic prophase I and only resume meiosis at the time

of ovulation (Picton *et al.*, 1998).

At birth, a pair of normal female human ovaries contains a finite stock of only 600,000 – 1,000,000 follicles (Baker, 1963). By the onset of puberty, the number of primordial follicles drops drastically with only approximately 500,000 follicles being present. Throughout life, approximately 400 - 600 oocytes will be released through ovulation (Wallace and Kelsey, 2010), whilst the remaining follicles undergo degeneration (atresia). The pool of primordial follicle serves as the source of growing follicles throughout the female's reproductive life span and will progressively dwindle with age leading to decreased ovarian reserve and ultimately reproductive senescence (Faddy and Gosden, 1995) (Fig 1.1). At the age of 50, a woman's primordial follicle pool will almost be exhausted, when there are only roughly 1000 follicles present in the ovary (de Bruin *et al.*, 2004, Faddy *et al.*, 1992).

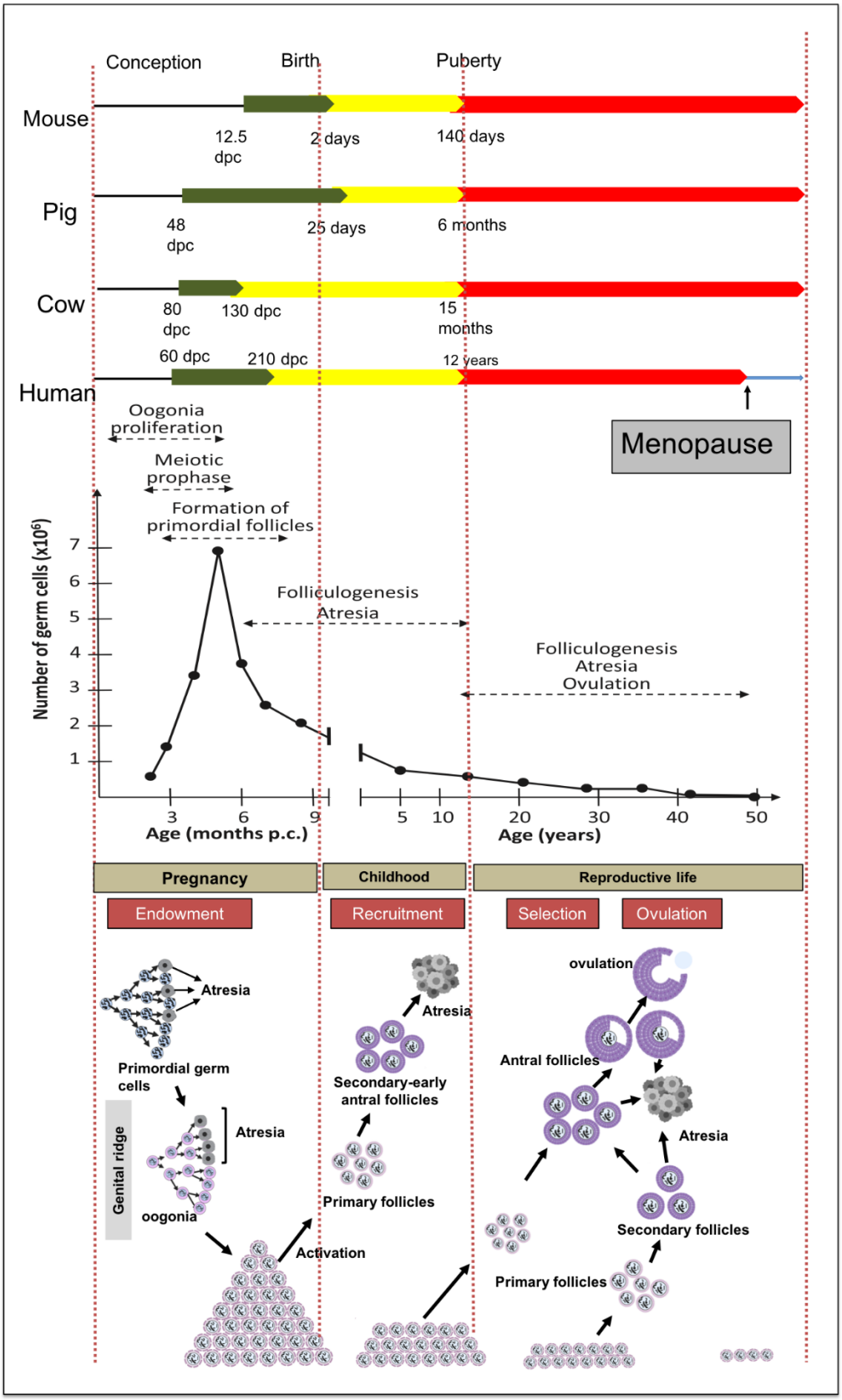

Figure 1.1. Germ cells attrition through oogonial cysts breakdown and atresia. After migration to

the genital ridge, germ cells will proliferate massively, and oogonia are formed. Most of the oogonia and germ cells undergo apoptosis during the process. The oogonia that survived the apoptosis are then encircled by pre-granulosa cells and transformed into primordial follicles. A small number of the follicles will be initiated to develop to growing follicles. The selected follicles then mature and ovulate in response to the pre-ovulatory gonadotrophin surge. Following repeated cycles of recruitment, atresia, or ovulation, the follicle reserve is depleted with increasing age leading to menopause. dpc= days post coitum (Adapted from (Kaipia and Hsueh, 1997, Monniaux *et al.*, 2014).

It is generally accepted that no new primordial follicles are formed postnatally (Hirshfield, 1991, Mandl and Zuckerman, 1951) but this idea has been challenged by the fact that reestablishment of the primordial follicle pool was observed following genotoxic drug treatment in mice (Johnson *et al.*, 2004). These results have been controversial (Eggan *et al.*, 2006, Gong *et al.*, 2010, Gosden, 2004, Johnson *et al.*, 2005, Pacchiarotti *et al.*, 2010, Telfer *et al.*, 2005, Woods *et al.*, 2013, Zhang *et al.*, 2008, Zou *et al.*, 2009). Some studies have identified the existence of putative oogonial stem cells in postnatal mammalian ovaries (Pan *et al.*, 2016), with cells that have characteristics of germline stem cells being isolated from adult human ovaries (Woods et al., 2012; Clarkson et al., 2018). However, there is still no evidence to conclusively show that these cells contribute to the ovarian reserve by forming new oocytes under normal physiological conditions.

Primordial follicles are quiescent, and the transition to the growing (primary) stage only occurs if they receive the appropriate signals. The number of primordial follicles activated at any given time is variable within different mammalian species (Elvin and Matzuk, 1998, Jagarlamudi *et al.*, 2010, Matzuk *et al.*, 2002). The exact mechanism of primordial follicle activation is not entirely understood (Jagarlamudi *et al.*, 2010). In the rodent, primordial follicle formation occurs shortly before and continues shortly

after birth, followed by primordial to primary follicle transition immediately thereafter. Around 15 days postpartum, the first group of antral follicles is established. Whereas in primates and most domesticated animals, this transition has started during fetal life and is a prolonged and asynchronous process whereby some follicles are gradually initiated to grow before other primordial follicles are formed (Fortune *et al.*, 2000, Fortune, 2003, Gougeon, 1996).

1.3. The General Concept of Mammalian Folliculogenesis

Folliculogenesis is the process in which primordial follicles develop into primary, secondary and antral stage follicles that can generate mature and fertilisable oocytes (Hernandez Gifford, 2015, Khan *et al.*, 2016). Folliculogenesis involves two principal phases, which are gonadotrophin independent and gonadotrophin dependent (Aerts and Bols, 2010, Edson *et al.*, 2009, Fortune, 1994, Hirshfield, 1991, Hummitzsch *et al.*, 2013b).

During folliculogenesis, the maturation of ovarian follicle involves several sequential stages, namely: initiation of primordial follicle growth, selection, ovulation and luteinisation. In initial recruitment, primordial follicles are recruited from the primordial follicle pool for further growth. Initial recruitment is a continuous process that initiates after primordial follicle assembly before the onset of puberty. Oocyte growth is the main characteristic of the growing follicles after this stage, though the oocyte remain arrested in the diplotene stage of prophase I. Follicles not recruited remain quiescent (Hsueh *et al.*, 2015, McGee and Hsueh, 2000). Once recruited, the activated primordial follicles develop into primary, secondary, and ultimately antral follicles. The multifaceted process of folliculogenesis does not just involve the

hypothalamic-pituitary-ovarian axis, but also several intra-ovarian and paracrine factors that affect the follicular development in a stage-specific manner (Richards and Pangas, 2010).

The first phase of follicle growth i.e. from primordial to preantral stages can take several weeks in humans and cows, during which the follicle increases in size from 30-50 μm (primordial follicles) to 100 - 200 μm (preantral follicles). The earliest phase of follicle development up to the preantral stage can occur independently of gonadotrophic hormones. These early stages are acutely dependent upon the bidirectional interaction between germ cells and surrounding somatic cells (McGee and Hsueh, 2000). It has been reported that follicle stimulating hormone (FSH) receptors (FSHR) are not present in primordial follicles until they enter the growth phase, as their expression may be induced during the primordial to primary stage transition (Oktay *et al.*, 1997). This may suggest that the role of FSH in primordial follicle growth initiation may not be essential. Nevertheless, it does not preclude the possibility of its direct effects on primary follicles onward or an indirect effect mediated by factors released by larger follicles or ovarian stromal cells (Silva *et al.*, 2004). Although FSH is not crucial for primordial follicle activation in bovine ovaries, it promotes the growth of primary and secondary follicles in humans (Abir *et al.*, 1997) and cows (Wandji *et al.*, 1996a).

Preantral to early antral follicle is often regarded as gonadotrophin sensitive stage. FSHR is present at this stage and the follicle is responsive to gonadotrophin hormones. At this stage granulosa and theca cells have become responsive to gonadotrophin hormones (Mori, 2016), but this is not a gonadotrophin-dependent stage (Craig et al.,

2007). Studies utilising FSH deficient mice (Abel *et al.*, 2000) and women lacking gonadotrophins (Goldenberg *et al.*, 1976) have demonstrated that follicle development can occur to the multilaminar stage in the absence of gonadotrophins (Kumar *et al.*, 1997). Whilst early follicle development can occur independently of FSH, the FSHR is present in granulosa cells of early preantral follicles and their growth may be enhanced by FSH (Oktay *et al.*, 1997). In a study utilising human ovarian tissue transplanted to hypogonadal mice, it was observed that follicles transplanted with two layers of granulosa cells did not form antral cavities in the absence of FSH. This data may infer that FSH is crucial for follicular growth beyond two granulosa cell layers, although growth activation is gonadotrophin independent (Oktay *et al.*, 1998). In addition, there is growing evidence to suggest that a low dose FSH is favourable to support preantral follicle growth and survival in bovine and human *in vitro* culture systems (McLaughlin and Telfer, 2010, McLaughlin *et al.*, 2018, Ribeiro *et al.*, 2015).

While follicle development from antral stage onward is completely dependent on the presence of gonadotrophins (Abir *et al.*, 2006). This stage depends on the circulating levels of FSH and luteinising hormone (Hummitzsch *et al.*) as the follicles become more sensitive to these hormones (Richards and Pangas, 2010). FSH regulates granulosa cell proliferation by binding to and activating the FSHR, which is located in granulosa cells. The interaction of FSH with its G protein-coupled receptor (GPCR) triggers the canonical intracellular signalling pathway activating adenylate cyclase-mediated cyclic adenosine monophosphate (cAMP) production and the protein kinase A (PKA) signalling pathway. These events have been reported as the main mechanism of FSH action in granulosa cells. However, it is increasingly evident that FSHR is also involved in the transduction of other signals through FSH binding, including PI3K,

Glycogen synthase kinase 3β (GSK3β), serum and serum-and glucocorticoid-induced kinase (SGK), and p38 mitogen-activated protein kinase (p38MAPK) (Gonzalez-Robayna *et al.*, 2000, Wayne *et al.*, 2007). Extracellular signal-regulated kinase (ERK) is an alternate pathway of FSH stimulation that allows robust mTOR activity upon TSC2 phosphorylation (Kayampilly and Menon, 2007, Manning *et al.*, 2002, Tee *et al.*, 2002), thereby enhancing granulosa cell proliferation (Kayampilly and Menon, 2007).

Increasing luteinising hormone (LH) level at this stage promotes follicular growth and steroidogenesis. An increase in estradiol production, triggered by FSH in granulosa cells, is essential for further follicle development at this stage (Findlay *et al.*, 2019). After the onset of puberty, a few preantral follicles will reach the preovulatory stage under cyclic gonadotrophin stimulation (Richards, 1980, Zeleznik, 2001). Preovulatory follicles are the major source of the cyclic estradiol secretion. In response to the preovulatory gonadotrophin surge, the dominant Graafian follicle ovulates to release the mature oocyte, whereas the remaining somatic cells transform into the corpus luteum (Hsueh *et al.*, 2015, McGee and Hsueh, 2000) (Figure 1.3).

1.3.1. Primordial Follicle Initiation and Growth: Sequence of Events Involved

In general, primordial follicle growth initiation can be distinguished by two phases, firstly the transformation of the pre-granulosa cells to a cuboidal shape, and then increasing numbers of granulosa cells which coincides with the rapid rise in oocyte size. Granulosa cell proliferation during these events involves a “rounding up” of cells before mitotic division occurs (van Wezel and Rodgers, 1996). Generally, follicle

activation occurs only in a small number of follicles each day and is independent of gonadotrophic hormones (Peters *et al.*, 1973). The timing of primordial follicle growth initiation varies between species. In human and sheep, it occurs when the oocytes are completely enclosed by approximately 15 cuboidal granulosa cells, and 40 cuboidal cells in bovine (reviewed by (Picton and Gosden, 2000)) (Figure 1.2).

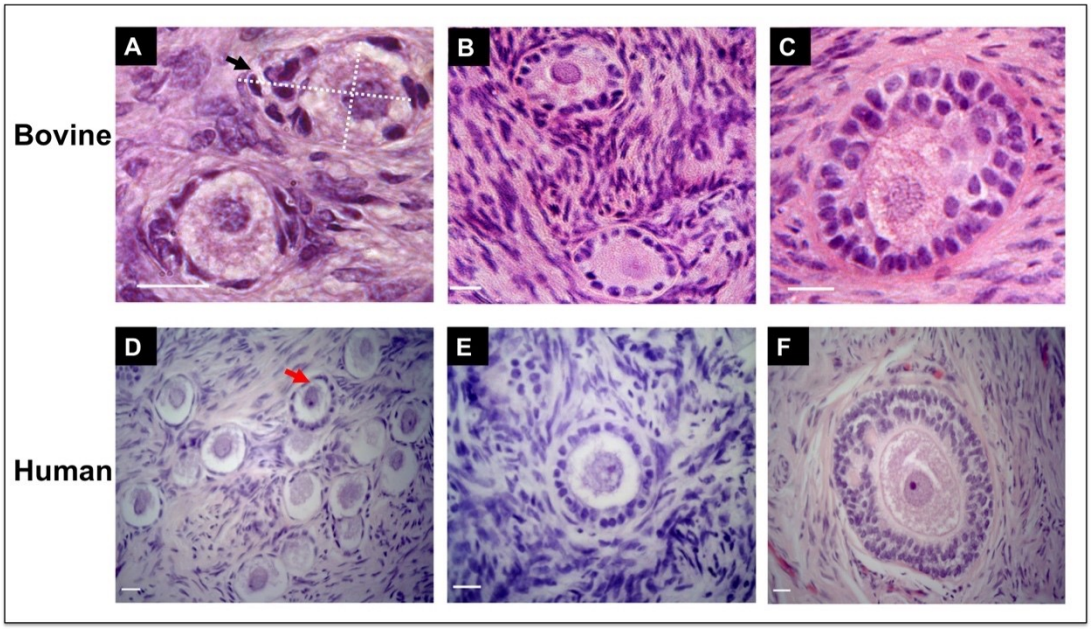

Figure 1.2. Histological sections of haematoxylin and eosin (H & E) staining showing bovine and human ovarian follicle development. (A) Non-growing bovine ovarian follicles are prolate in shape with granulosa cells cluster (black arrow) at opposite poles of the follicle's long axis, (B) Bovine primary follicles indicated by oocyte surrounded by cuboidal granulosa cells, (C) Multilayer secondary bovine ovarian follicles, (D) Primordial and transitory (red arrow) human ovarian follicles, (E) A human primary follicle and (F) A human secondary follicle (ovaries from transgender patients). Scale bar = 20 μm.

1.3.1.1. The Role of Follicular Microenvironment, Autocrine and Paracrine Signals in Primordial Follicle Activation

Primordial to primary follicle transition involves multiple pathways that serve as the activators or inhibitors (McLaughlin and McIver, 2009, Skinner, 2005). Primordial

follicle initiation depends on the response of each cell of the follicle to the activation or inhibition signals. The follicular microenvironment influencing pre-granulosa cell activation remains undetermined. However, a number of autocrine and paracrine signals derived from the follicular microenvironment other than oocytes and granulosa cells, including the stromal compartment, have been identified and implicated as being positive or negative regulators. Chemo-attractive cytokine stromal-derived factor-1 (SDF1) and its receptor C-X-C chemokine receptor type 4 (CXCR4) are known to be implicated in primordial germ cell formation and are also recognised recently as a negative regulator of the oocyte development at the early stage in neonatal mouse ovary (Holt *et al.*, 2006).

The role of locally acting growth factors is now widely understood to be essential in regulating primordial follicle activation. KIT ligand (KL) or stem cell factor (SCF), secreted by immature granulosa cells, is known to promote primordial follicle growth in mouse and rat ovaries (Parrott and Skinner, 1999, Reddy *et al.*, 2005) and pieces of monkey ovarian cortex (Gougeon and Busso, 2000). SCF has been confirmed to regulate theca cell growth and subsequent production of theca cell factors including transforming growth factor-α, keratinocyte growth factor (KGF), hepatocyte growth factor (HGF) and transforming growth factor β (TGFβ). Several growth factors including basic fibroblast growth factor (bFGF), platelet-derived growth factor (PDGF), KGF and connective tissue growth factor (CTGF) produced predominantly by oocytes and by all cells at a reduced rate have also been shown to activate primordial follicle initiation (Kezele *et al.*, 2005, Nilsson *et al.*, 2001, Nilsson *et al.*, 2006, Schindler *et al.*, 2010).

Studies conducted in rodents have supported the role of insulin-like growth factor (IGF) (Thomas *et al.*, 2007) and TGFβ superfamily members to promote primordial follicle growth. Bone morphogenetic factor 7 (BMP7) produced in stromal and theca cells, increases the number of growing follicle leading to primordial follicle pool depletion in rat (Lee *et al.*, 2001, Lee *et al.*, 2004). Similarly, bone morphogenetic factor 4 (BMP4) has been identified to increase the proportion of growing follicles in rat (Nilsson and Skinner, 2003). In addition, the microenvironment of primordial follicles including nutrition, reactive oxygen species (ROS), antioxidant and appropriate oxygen and energy support has been demonstrated to have a role in determining the fate of the follicle (Laplante and Sabatini, 2012, Praxedes *et al.*, 2018). It is an intriguing observation that total protein consumption may profoundly affect fertility performance, probably attributed to a functional relationship between amino acids and the mTOR activity. It has been reported that low protein diet attenuates primordial follicle activation in mice (Zhuo *et al.*, 2019). Insulin at low concentration has also been reported as an endocrine factor to support the coordination of primordial follicle activation by acting at the insulin receptor with the oocyte as the site of action (Kezele *et al.*, 2002) (Figure 1.3).

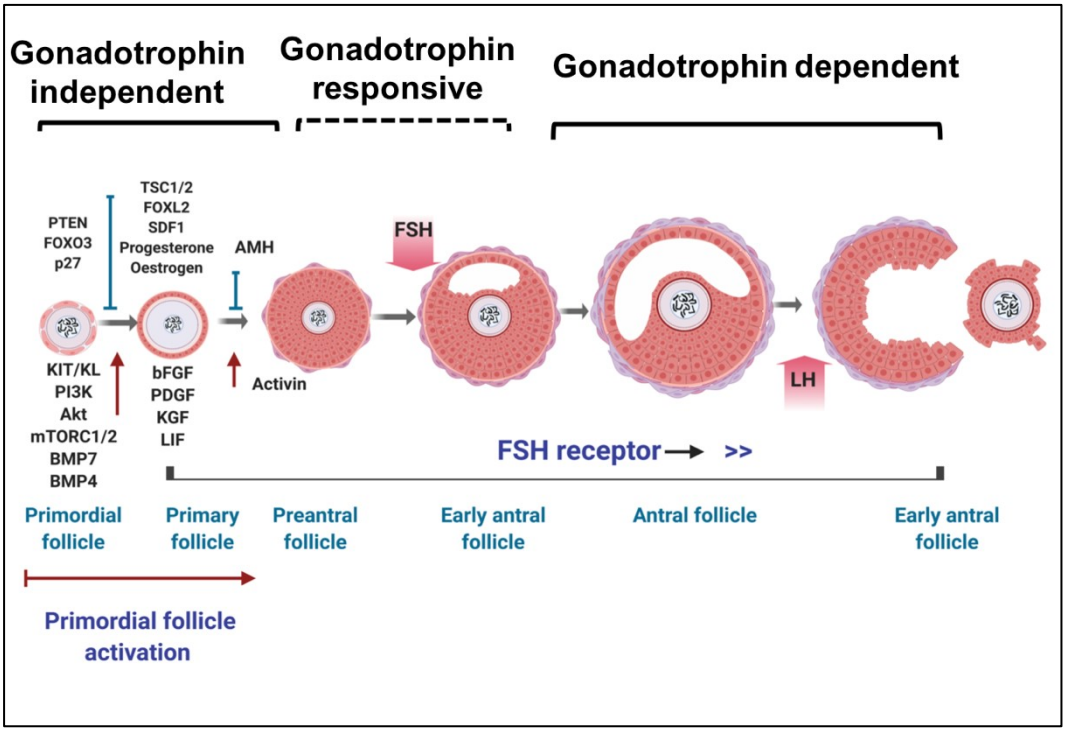

Figure 1.3. Folliculogenesis and factors involved in primordial follicle activation. The initiation phase is marked by the transformation of the flattened pre-granulosa cells surrounding the oocyte into cuboidal cells. Once recruited, the activated primordial follicles develop into primary, secondary, and ultimately antral follicles. In the earliest stage, the follicles grow in an FSH-independent fashion. Preantral stage is often regarded as a gonadotrophin independent stage, but FSHR is present at this stage and the follicle is responsive to gonadotrophin hormones, thus it can be more accurately regarded as being 'gonadotrophin responsive'. Primordial follicle initiation is determined by the balance between the inhibitory (blue line) and stimulatory factors (red line).

It has been proposed that primordial follicles are preserved in a resting state by nearby inhibitory factors released by surrounding growing follicles. Both Anti-mullerian hormone (AMH) (Durlinger *et al.*, 1999) and activin (Mizunuma *et al.*, 1999) are produced by growing follicles and function to limit the activation rate. Given that the more growing follicles that are present nearby primordial follicles, the greater the signals that will be exhibited, thus reducing the rate of activation. However, in contrast, a study relating ovarian follicle structure to its distance from potential local sources of

regulatory signals provided strong evidence for a local diffusing inhibitor (Da Silva-Buttkus *et al.*, 2009). Primordial follicle activation was unlikely to occur when the neighbouring primordial follicles were in close proximity. However, as the number of growing follicles nearby increases, it is more likely that the follicles will be activated. Thus it seems that growing follicles release a diffusing signal that employs a stimulatory effect on their neighbouring follicles (Da Silva-Buttkus *et al.*, 2009).

Importantly, recent studies have identified the role of the Hippo signalling pathway in primordial follicle initiation. The Hippo signalling pathway is a highly conserved cell signalling system. It functions to regulate cell proliferation, differentiation, apoptosis (Xiang *et al.*, 2015) and is essential in preserving optimal organ size (Kawamura *et al.*, 2013). Tissue shape and stromal density have been proposed to be attributed to the regulation of follicle growth initiation *in vitro* (Telfer and Zelinski, 2013). The follicular growth *in vitro* is hampered within the dense ovarian stroma and preparing ovarian cortical strips into cubes (1-2 mm^3) leads to significant primordial follicle activation compared to tissue slice (Scott *et al.*, 2004). Likewise, primordial follicle loss due to excessive activation is markedly increased in thin ovarian grafts compared to standard thickness graft (Gavish *et al.*, 2014). Mice and human ovaries fragmentation triggers actin polymerization and Hippo pathway disruption and subsequently enhances primordial follicle growth (Kawamura *et al.*, 2016, Li *et al.*, 2010b). Disrupting the Hippo pathway is intended to limit the activity of co-activators of the pathway, which are Yes-associated protein (YAP) and transcriptional co-activator with PDZ-binding motif (TAZ). YAP and TAZ are phosphorylated by the Large tumour suppressor homolog 1 (LATS1), a core kinase of the Hippo pathway. Increased in YAP in the nucleus may subsequently lead to cell proliferation (Hsueh *et*

al., 2015, Kawamura *et al.*, 2013).

1.3.1.2. Intra-oocyte Control and Regulation

The insulin signalling pathway acts through insulin receptors located in granulosa and thecal cells of different species (Lighten *et al.*, 1997, Samoto *et al.*, 1993). The PI3K signalling pathway appears to be the primary non-gonadotropic insulin signalling pathway that regulates the growth and differentiation of follicles (Dupont and Scaramuzzi, 2016). PI3K is composed of a heterodimer of the p85 regulatory subunit and p110 catalytic subunit. In response to growth factors including KL, all regulatory subunits of PI3K interact with the insulin receptor substrate, and thereby activate the catalytic subunit. This interaction leads to the phosphorylation of membrane phospholipid phosphatidylinositol 4, 5-biphosphonate (PIP2). The PIP2 converts to phosphatidylinositol 3, 4, 5-trisphosphate (PIP3), which then serves as a second messenger to enable phosphoinositide-dependent kinase 1(PDK1) activation. PTEN, expressed by the oocyte, reverses this process by converting PIP3 to PIP2.

PIP3 binds to Pleckstrin homology (PH) domain of PDK1 and Akt and recruits these two kinases to the subcortical area, which in turn activates PDK1 and Akt phosphorylation at Threonine (Thr308). Akt is further phosphorylated by mammalian target of rapamycin complex 2 (mTORC2) at serine 473 (Ser473) for its full activation, which then regulates a number of downstream targets. PDK1 also phosphorylates SGK, atypical isoforms of protein kinase C (PKC) and p70 ribosomal S6 kinase 1 (S6K1). S6K1 is the kinase of ribosomal protein S6 (rpS6).

PDK1 is indispensable in maintaining primordial follicle survival and preserving reproductive lifespan. In mice lacking PDK1 in oocytes, Akt/S6K1/rpS6 signalling is

suppressed leading to a rapid depletion of primordial follicles and ultimately ovarian senescence (Reddy *et al.*, 2009). Although PTEN loss is associated with increased Akt activation, coexisting loss with PDK1 prevents upregulation of rpS6 due to inactivation of Akt and S6K1. It seems likely that both PTEN and PDK1 loss leads to premature ovarian failure (POF) but through different mechanisms. PTEN loss is associated with excessive primordial follicle activation and subsequent follicular atresia, whereas PDK1 deficiency instigates accelerated clearance of primordial follicles straight from their quiescent state (Reddy *et al.*, 2009). However, PTEN deletion in oocytes of primary and further developed follicles does not reveal any significant effects on follicular growth (Reddy et al., 2008). This may indicate follicle stage specific functions of the PTEN/PI3K pathway within the oocyte (Jagarlamudi *et al.*, 2009). In addition, selective PTEN disruption in the granulosa cells of mice enhances granulosa cell proliferation and differentiation and thereby improves follicular growth (Fan *et al.*, 2008).

Another downstream substrate of Akt is mTOR, an atypical serine/threonine kinase. mTOR comprises of two distinct protein complexes, which are mTORC1 and mTORC2. Akt activates the mTOR1 pathway through the destabilization of the heterodimeric complex of tuberous sclerosis complex 1 (TSC1 or hamartin) and tuberous sclerosis complex 2 (TSC2 or tuberin). mTORC1 phosphorylates S6K1 at Thr389 and 4E-binding protein 1 (4EBP1) at Thr37, 46, 70 (Thr37, 46, 70) and Ser65 and eventually promotes cell growth and proliferation. The lack of TSC 1 and TSC2 in mouse oocytes has been proven to cause massive primordial follicle activation, leading to POF. Activated Akt, in turn, phosphorylates glycogen synthase kinase-3 (GSK3), Bcl-2-associated death promoter (Bad), transcription factor forkhead box O

(FOXO3) and p27 (Adhikari *et al.*, 2009, Adhikari and Liu, 2010). Once activated, FOXO3 is shuttled from the nucleus to the cytoplasm, which then suppresses their transcriptional function.

The FOXO3 deleted mouse model displays global primordial follicle activation at the neonatal stage leading to primordial follicle loss and ovarian failure (Castrillon *et al.*, 2003, John *et al.*, 2007). Conversely, overexpression of constitutively active FOXO3 in the nucleus of mouse oocytes preserves the oocytes in a dormant state, enhance ovarian reserve and reproductive capacity (Pelosi *et al.*, 2013). Within this framework, FOXO3 can be considered as a guardian of the primordial follicle pool, enhancing ovarian reserve and maintaining reproductive capacity (Castrillon *et al.*, 2003, John *et al.*, 2007, Pelosi *et al.*, 2013). As a substrate of Akt, the function of FOXO3 is controlled by PI3K, and the expression is downregulated in oocytes of larger follicles (Liu *et al.*, 2007). Upregulation of the downstream PI3K pathway also increases p27 activity that can inhibit cyclin-dependent kinase 2 (Cdk2) activity in oocytes of primordial follicles (Rajareddy *et al.*, 2007) (Figure 1.4).

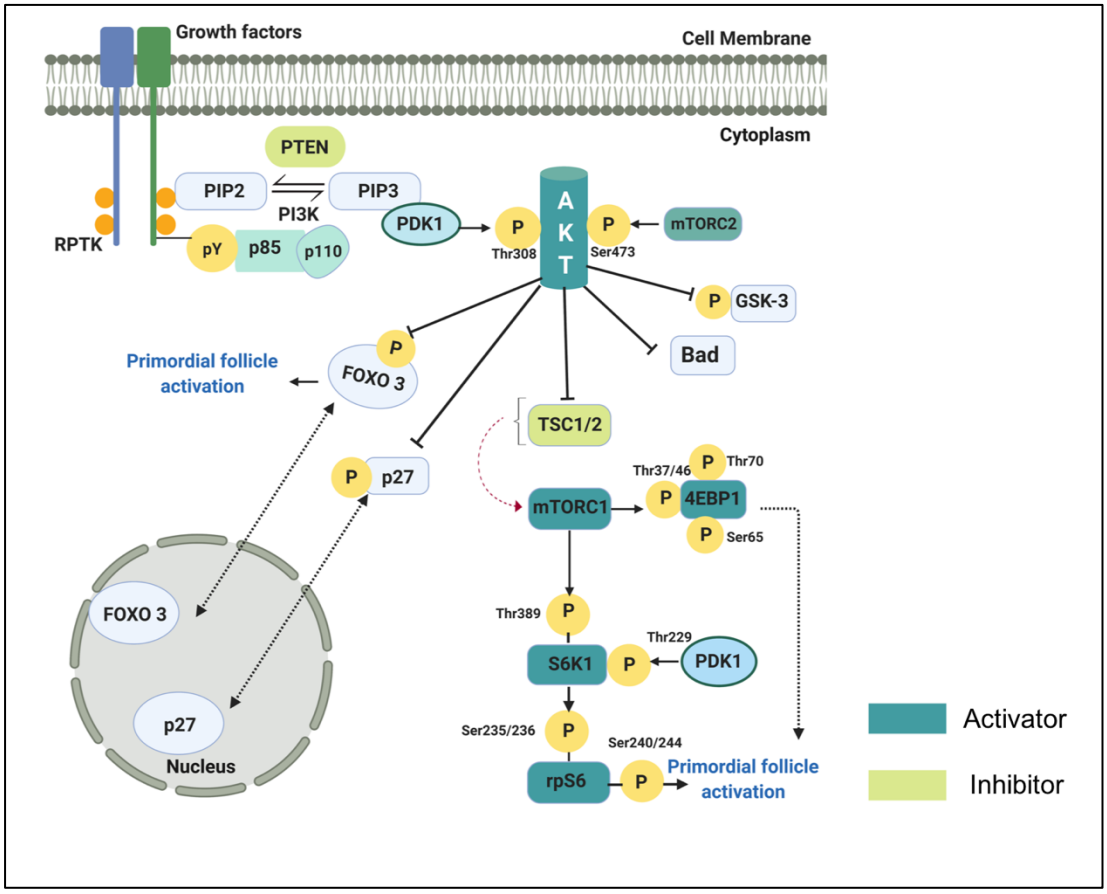

Figure 1.4. PI3K pathway involved in Primordial follicle activation. Activation of follicles from the quiescent state is regulated by the PI3K pathway through the balance of activating and inhibitory factors. Activation of follicles from the quiescent state is regulated by the PI3K pathway through the balance of activating and inhibitory factors. A p85 regulatory subunit and a p110 catalytic subunit of PI3K are localised in cytoplasm and is initiated by growth factor receptor tyrosine kinases at the plasma membrane. Upon growth factor stimulation, all regulatory subunits of PI3K interact with the insulin receptor substrate, and thereby activate the catalytic subunit. This interaction leads to the recruitment of PI3K from the cytoplasm to the inner membrane induces phosphorylation of PIP2 to PIP3, which then enables PDK1 activation. PTEN reverses this process and increases PIP2 expression. Akt is phosphorylated by PDK1 at Thr308 and mTORC2 at Ser473. These events then trigger a cascade of PI3K downstream reactions involving proteins such as p27, Bad, FOXO3, TSC2, and GSK β3. Phosphorylation of TSC2 then increases mTORC1 activity which, in turn, phosphorylates S6K1 and leads to activation of rpS6. mTORC1 controls protein translation through S6K1 and 4EBP1 phosphorylation (adapted from (Adhikari and Liu, 2009)).

Other factors that have been documented as oocyte-specific genes of the primordial follicle and are capable of either promoting or preventing primordial follicle activation are spermatogenesis and oogenesis specific basic helix-loop-helix 1 (Sohlh1), Sohlh2, factor in the germ-line alpha (FIGLA), newborn ovary homeobox gene (NOBOX) and LIM homeobox8 (LHX8) (reviewed by (Pangas and Rajkovic, 2006)). These genes are expressed in oogonia and oocytes within primordial and growing follicles. A study in a transgenic mouse model showed that NOBOX is a positive regulator of FOXO3 in the oocyte of primordial follicles suggested that NOBOX functions to maintain the primordial follicle pool (reviewed by (Zhang *et al.*, 2014)). LHX8 and NOBOX upregulate expression of several oocyte genes, including the TGFβ family members GDF9 and bone morphogenetic protein-15 (BMP15). GDF9 is crucial for oocyte growth beyond the primary follicle stage (Dong *et al.*, 1996), but GDF9 transcript in mice is also present in germ cell nests and primordial follicle. Mice deficient in NOBOX leads to increased oocyte nest and primordial follicle number and GDF9 expression is downregulated in the ovaries (Choi and Rajkovic, 2006, Rajkovic *et al.*, 2004). While in human, NOBOX is essential during follicle formation in the human fetal ovary and GDF9 is increased at the same developmental period indicating the role of NOBOX in regulating GDF9 expression (Bayne *et al.*, 2015). Unlike mice, GDF9 expression in sheep and cow oocytes emerge at the primordial follicle stage (Aaltonen *et al.*, 1999). Such species specific GDF9 expression and activity may in part reflect that NOBOX activity throughout folliculogenesis is stage specific and may be varied among species.

1.3.1.3. Granulosa Cells Secreted Factors

Accumulating lines of evidence suggest a role of granulosa cells in follicular growth and development. Primordial follicle pre-granulosa cells initiate primordial follicle growth and are indispensable in regulating the dormancy or awakening of quiescent oocytes within primordial follicles (Zhang *et al.*, 2014). A study utilising a mutant mouse model found that mTORC1 signalling in pre-granulosa cells has a major role in governing pre-granulosa cells differentiation into granulosa cells and eventually activates the growth of the oocyte through the mTORC1-mediated expression of KL. This process will then continue with a cascade of PI3K signalling pathway activation and subsequent oocyte awakening (Zhang *et al.*, 2014). A transgenic mouse study targeting molecules constituting mTORC1 revealed that the absence of mTORC1 activity in pre-granulosa cells prevents their differentiation into cuboidal cells and eventually inhibits the activation of primordial follicles. On the other hand, excess mTORC1 expression is associated with growth acceleration and differentiation and ultimately ovarian failure (reviewed by (Monniaux, 2016)).

In addition, both estradiol and progesterone have been shown to inhibit primordial follicle growth initiation (Kezele and Skinner, 2003). In mice, high levels of maternal estradiol and progesterone have been suggested as inhibitory factors to germline nest breakdown during pregnancy and that the decline in these hormones after birth leads to primordial follicle formation (Jefferson *et al.*, 2006). The addition of progesterone *in vitro*, and to a lesser extent, estradiol significantly increases the number of unassembled follicles in neonatal mice (Kezele and Skinner, 2003, Lei *et al.*, 2010).

Other factors contributing to the dormancy of the primordial follicle pool include Forkhead box L2 (FOXL2), which is expressed in pre-granulosa cells (Schmidt *et al.*,

2004). Pre-granulosa cells deficient gene encoding FOXL2 in mice fail to differentiate, resulting in oocyte death and massive follicular depletion (Schmidt *et al.*, 2004). In addition, granulosa cell-derived factors KL and leukaemia inhibitory factor (LIF) are expressed at higher levels in granulosa cells of primordial and primary follicles and are imperative in granulosa cell proliferation. LIF triggers KL activity in granulosa cells and eventually promotes primordial follicle activation (Nilsson *et al.*, 2002) (Figure 1.5).

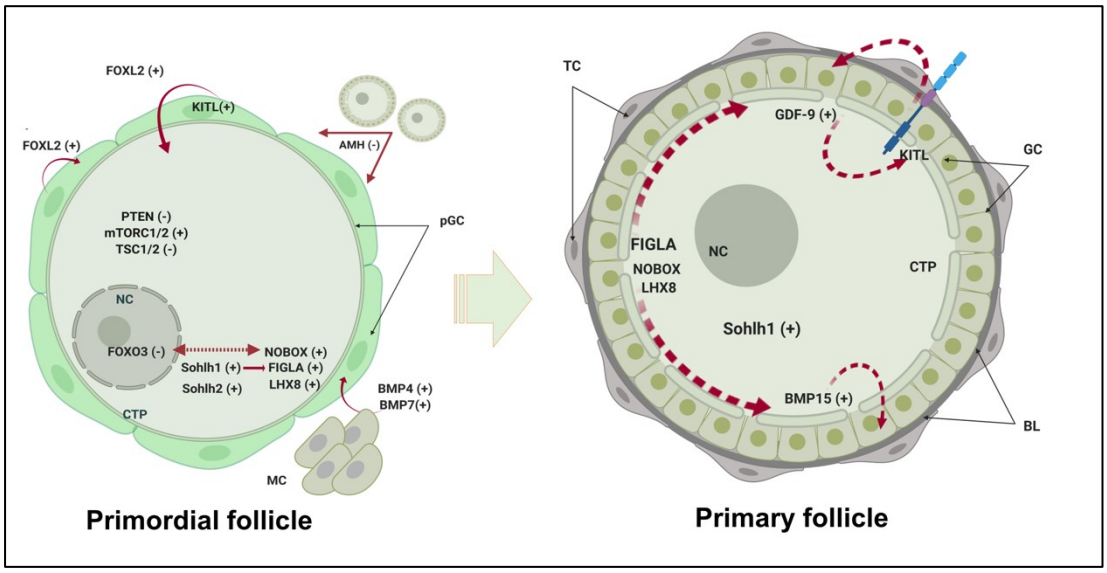

Figure 1.5. The localisation of follicular microenvironment key factors involved in primordial follicle activation. The figure shows the location of known factors contributing to primordial follicle activation, including factors produced by stromal cells. Primordial follicle activation is a result of the collective actions of these factors. AMH produced by surrounding early growing follicles inhibit primordial follicle development. Sohlh1 and Sohlh2 are positive regulator of NOBOX, LHX8 and FIGLA. FOXL is exclusively expressed in pre-granulosa cells. Its activation increases granulosa cells proliferation. PTEN and TSC1/2 in oocyte cytoplasm are the negative regulator of primordial follicle activation. While FOXO is located in the nucleus and NOBOX is a positive regulator of FOXO3. NOBOX activate GDF9 in stage and species-specific manner (more in growing follicle). GDF9 is oocyte secreting factor that may activate the activity of KL in granulosa cells and lead to granulosa cells proliferation. BMP4 and 7 produced by stromal cells act on granulosa cells and lead to primordial

follicle activation. BL (basal lamina), CTP (cytoplasm), NC (nucleus), pGC (primordial follicle granulosa cells), GC (granulosa cells), TC (theca cells), MC (mesenchymal cells), (+) activator, (-) inhibitor. Adapted from (Williams and Erickson, 2000).

1.3.2. Primary and Preantral Follicle Development

From primary stage onward, the granulosa cells become mitotically active and begin to express FSH receptor at the preantral stage (Oktay *et al.*, 1997). Thereafter, the proliferation rate dramatically increases, and oocytes enlarge with multilayer granulosa cells surrounding the oocyte (reviewed by (Monniaux, 2016)). Oocytes become transcriptionally active to produce adequate proteins and mRNA transcript (Albertini, 2015, Pangas and Rajkovic, 2015) which are a prerequisite for oocyte development. At this stage, oocyte and granulosa cell growth do not predominantly depend on gonadotrophins until follicle growth reaches the late preantral or early antral stage (Oktay *et al.*, 1997).

Preantral follicles are distinguished from primary by the formation of the zona pellucida (ZP) and differentiation of theca cells (Albertini *et al.*, 2001). Preantral follicle development is exemplified by several events, including the appearance of GDF9 and BMP15 and junctional connexin (Cx) proteins. GDF9 emerges during early stages and acts on granulosa cells throughout folliculogenesis. Sheep and cow oocytes begin to express GDF9 at the primordial follicle stage whereas it is very highly expressed in primary follicles in human (Aaltonen *et al.*, 1999), mouse, and rat (Findlay et al. 2019). The expression of BMP15 occurs slightly later than GDF9 in human oocytes. In mouse oocytes, BMP15 is co-expressed with GDF9 during folliculogenesis (Laitinen *et al.*, 1998). It is reported that short exposure to GDF9 and BMP15 collectively increases mouse preantral follicle growth *in vitro* compared to

either BMP15 or GDF9 alone. Chronic use of BMP15 has been shown to decrease the growth rate and eventually induce atresia. Intriguingly, environmental low BMP15 expression is favourable for oocyte development in mouse preantral follicles. SMAD 2/3 expression is a downstream target of GDF9 activity and is predominantly observed in early-stage follicular development. In contrast, BMP15 acts on granulosa cells of preantral follicles, and increases the expression of SMAD 1/5/8, which act downstream of BMP15 and are more noticeable from the preantral stages (Fenwick *et al.*, 2013).

Another TGFβ superfamily member known to be involved in preantral follicle development is activin (Findlay, 1993, Findlay *et al.*, 2002, Knight and Glister, 2001). Activin is produced by both oocyte and granulosa cells and is composed of a dimer of two beta subunits, A or B with activin A being the most prevalent isoform. During folliculogenesis, activin stimulates FSH production from the anterior pituitary (Katayama *et al.*, 1990). Its intraovarian properties comprise increased aromatase activity, development of antral cavity and increased granulosa cell proliferation (Findlay, 1993, Mizunuma *et al.*, 1999). Activin activity to promote preantral follicle growth *in vitr*o has been shown in ovine, caprine and human (McLaughlin *et al.*, 2010a, Silva *et al.*, 2006, Telfer *et al.*, 2008, Thomas *et al.*, 2003a). The regulation of KL, GDF9, and BMP15 is involved in a paracrine negative feedback mechanism. KL activation mediated by BMP15 and GDF9 leads to granulosa cell proliferation. Partly grown oocytes secrete BMP15 leading to KL activation in granulosa cells, while fully grown oocytes mainly produce GDF9 resulting in subsequent inhibition of KL expression in surrounding granulosa cells. In response to the accumulating effects of GDF9, BMP15 and KL secretion, granulosa cells actively proliferate and express FSH,

estrogen and androgen receptors that will be more pronounced with the growth of the follicles (Hutt *et al.*, 2006, Joyce *et al.*, 1999, Joyce *et al.*, 2000).

Secondary follicles increase in size and form multiple layers of granulosa cells to reach approximately 100-200 μm in diameter. At this point onwards, oocytes enlarge, and theca cells differentiate into external and internal theca. The formation of theca cells is accompanied by angiogenesis leading to the neoformation of numerous small blood vessels. On completion of preantral phase, the follicle contains five distinct and interacting structures. These are a fully-grown oocyte encircled by a zona pellucida, multilayer (approximately 9) granulosa cells, a basal lamina, theca cells and a capillary net in the theca tissue. LH receptor (LHR) is expressed in internal theca cells (Williams and Erickson, 2000).

1.3.3. Antral Follicle Growth and Ovulation

The final stage of folliculogenesis i.e. ovulation occurs at puberty. Once follicles develop antral cavities and become dependent upon FSH, they are subject to follicle selection and maturation of dominant follicles, with only one follicle being ovulated in mono-ovular species such as human and cows. Once an antral cavity is formed, the granulosa cells differentiate into two distinct cell types that respond differently to hormonal cues: the cumulus and mural cells (McGee and Hsueh, 2000). Cumulus cells and oocytes form a complex known as the cumulus oocyte complex (COC). From this stage onward, FSHR and LHR are expressed abundantly and folliculogenesis depends on pituitary-secreted gonadotrophin (FSH and LH) support.

The presence of FSH activity induces LHR mRNA expression. The interaction of LH with its receptors on the theca cells surface stimulates the cells to produce androgen,

which subsequently aromatises in the granulosa cells to produce estrogen (Fujita *et al.*, 1981, Sanchez and Smitz, 2012, Tajima *et al.*, 2007). Both theca and granulosa cells in antral stage follicles proliferate with concurrent accumulation of follicular fluid in the antrum. The largest follicle contains a higher number of FSH receptors and therefore is more receptive to lower FSH levels, thus is selected as the dominant follicle. This process is concomitant with increased oocyte size. Other factors involved in antral follicle growth are activin and inhibin, both of which are secreted by granulosa cells. These are necessary to regulate the androgen producing activity of theca cells. Both activin and inhibin function to regulate granulosa cells proliferation, differentiation and oocyte maturation (reviewed by (Sanchez and Smitz 2012)).

Oocyte-secreted factors, BMP15 and GDF9, are compulsory in regulating cumulus cell expansion. As evidenced in rat and human, these oocyte factors, either in combination or on their own enhance granulosa cell proliferation and differentiation (Hobeika *et al.*, 2019, Shimasaki *et al.*, 2004, Vitt *et al.*, 2000). Lastly, on completion of the whole process, follicles containing fully-grown oocytes are ready to undergo ovulation, induced by the LH surge. At this point, oocytes undergo final nuclear and cytoplasmic maturation that results in dissolution of the nuclear envelope germinal vesicle breakdown (GVBD). Oocyte maturation progresses to metaphase 2 (M2) with emission of the first polar body and then arrests until fertilisation (McGee and Hsueh, 2000). Suboptimal cytoplasmic and nuclear maturation may result in lower oocyte developmental capacity (Yerushalmi *et al.*, 2014). Only oocytes that have accomplished both cytoplasmic and nuclear maturation are able to be fertilised (Eppig *et al.*, 1994, Fan and Sun, 2019). A sequence of processes in oocytes occur in accordance with cumulus cell expansion. Following follicle wall rupture, the COC is

then released and subsequent tissue remodelling results in formation of the corpus luteum.

1.4. Oocyte and Somatic Cell Bidirectional Communication

Bidirectional intercellular connection between the oocyte and somatic cells is fundamental at every stage of folliculogenesis and is essential for the healthy maturation of the oocyte until the time of ovulation (Albertini *et al.*, 2001, Eppig, 1991). Gap junctions or intercellular channels regulate a distinctive form of communication between cells through a direct exchange of molecules. These intercellular channels are present in most cell types at some point during their development in mammals (Bruzzone *et al.*, 1996). In every stage of folliculogenesis, gap junctions couple the granulosa cells with each other and with oocytes, thus, establishing a functional syncytium allowing the diffusion of ions, second messengers, and metabolite molecules, between adjacent cells (Ackert *et al.*, 2001, Eppig, 1991, Kidder and Vanderhyden, 2010).

Several types of connexins have been recognised and act in different tissue. Ovarian granulosa cells primarily express Cx43 while the oocyte predominantly expresses connexin37 (Cx37) (reviewed by (Granot and Dekel, 1998)). Cx37 and 43 have been known to be critical at each stage of folliculogenesis to maintain follicular development. Cx37 is localised in the oocyte interfaces both in developing (primary and preantral) and in Graafian follicle but not in primordial follicle while Cx43 is localised in gap junctions between granulosa cells but not on the surface of the oocyte and does not contribute significantly to oocyte-granulosa cell junctions. The fundamental role of Cx37 is demonstrated by the deletion of the gene encoding Cx37

in mice, abolishing the gap junctions between the oocyte and granulosa cells. The oocytes stop growing and ultimately degenerate, probably due to diminishing oocyte and granulosa cell connections that then causes premature luteinisation of granulosa cells (Simon *et al.*, 1997). In contrast to Cx37, Cx43 is mainly expressed in the early stages of folliculogenesis in mouse ovaries (Juneja *et al.*, 1999).

In bovine ovaries, Cx37 is present in granulosa cells of primordial to the preantral stage and not restricted to the interface between the oocyte and granulosa cells. Oocytes exhibit diffuse cytoplasmic Cx37 labelling; hence, Cx37 contributes to the formation of channels between granulosa cells in bovine preantral follicles. Its expression is less detectable in antral stage follicle, whereas Cx43 is present in granulosa cells of follicular development at all stages. Cx43 begins to be expressed in the early stages of follicular development; its expression remains at a low level thereafter but then increases at the onset of antral follicle formation. Its expression increases gradually with an increase in follicular size to reach the highest level in antral follicles. Cx43 expression is not observed between the oocyte and granulosa cells or between atretic granulosa cells at any follicular stage (Nuttinck *et al.*, 2000). It has been reported that connexin activity is determined by FSH level. It increases significantly with FSH but then declines subsequently at the peak LH level that triggers meiosis and ovulation. At the onset of meiosis, the high level of LH induces the closure of gap junctions through the activation of mitogen-activated protein kinase (MAPK)-dependent gap junction that is a prerequisite for the oocyte to resume meiosis (Norris *et al.*, 2008). LH surge consequently closed all Cx43 junctions, while the Cx37 junctions remain open (Norris *et al.*, 2008).

1.5. DNA Damage and DNA Damage Repair Pathway

The DNA of a cell is continuously threatened by various types of damage that may cause a depreciation in cellular function, cell cycle progression and DNA repair (reviewed by (Branzei and Foiani, 2008)). Damage to DNA may cause errors in replication or transcription (Altieri *et al.*, 2008). Exogenous sources of DNA damage include environmental agents such as ultraviolet, radiation, chemotherapeutic drugs, and thermal disruption. Endogenous sources of damage that are not preventable include spontaneous reactions such as ROS generated by respiration and lipid peroxidation, and DNA base lesions like hydrolysis and alkylation (Lindahl and Barnes, 2000). DSBs do not occur as frequently as the other lesions, but persistent unrepaired DNA DSBs are the most severe type of damage and may substantially lead to genomic instability (Jackson and Bartek, 2009, Khanna and Jackson, 2001, Menezo *et al.*, 2010, Titus *et al.*, 2013).

Generally, DNA damage constitutes a major issue in non-dividing or slowly dividing cells due to DNA damage accumulating over time. Any damage that does not provoke cell cycle arrest will tend to induce replication errors leading to mutations. Nonetheless, all cells have the potential to repair the damage, which occurs predominantly at the G1/S and G2/M-phase transition (Oktay *et al.*, 2015). Cells with DNA damage react in different ways to trigger a proper signalling pathway of DDR. A mild injury may not cause significant consequences as it can be restored directly without cell cycle arrest. Meanwhile, severe DNA damage may result in cell cycle arrest to allow sufficient time to repair the damage. During this time, a sequence of DNA damage repair proteins is activated. Once the repair mechanism is completed, the checkpoint proteins are deactivated, and the cells resume cell cycle progression.

The target of DNA damage repair responses can either stimulate the apoptotic pathways that eventually lead to cell demise, or endure the DNA lesions by commencing the repair process (Menezo *et al.*, 2010). In this respect, the cell's fate depends on the ability of the cells to repair the damage, as sufficient repair capacity permits cells to resist apoptosis (Kujjo *et al.*, 2010).

There are two major pathways to repair DNA DSBs: the non-homologous end joining (NHEJ) and homologous recombination (HR). HR is considered as error-free and limited to S and G2 phase of the cell cycle when sister chromatids are available as a template for the DNA repair process. On the other hand, NHEJ is error-prone since it arbitrates the direct re-ligation of the two ends of damaged DNA and is not based on a DNA sequence. NHEJ does not implicate a complementary DNA template. Mutations are more likely, including deletion or insertion of base pairs. NHEJ can occur during all stages of the cell cycle, but it primarily occurs in the G0/G1 phase (Heijink *et al.*, 2013) and can be independent of the cell cycle (Bekker-Jensen and Mailand, 2010). NHEJ is the most common type of DNA damage repair in mitotic cells. HR is essential in DNA DSBs repair in all cell types (Hong *et al.*, 2013), but it predominantly exists in meiotic cells (Sung and Klein, 2006).

In NHEJ, the initial step is the detection and binding of the Ku heterodimer to the DNA DSBs. Ku is a heterodimer comprised of two subunits, Ku70 and Ku80 (Ku86). The capability of protein Ku to recognise and localise the DNA DSBs is likely due to its extraordinary binding affinity to DNA ends, its capacity to interact with DSBs in a sequence-independent manner, and its high concentration (~500,000 Ku molecules/cell). The Ku protein bound to the DSBs end, recruits DNA-dependent protein kinase catalytic subunit (DNA-PKcs), X-ray cross-complementing protein 4

(XRCC4), DNA Ligase IV, XRCC4-like factor (XLF), and Aprataxin-and-PNK-like factor (APLF) to DNA DSBs sites. Protein and DNA-PKcs interaction results in translocation of the Ku heterodimer on the dsDNA strand and eventually initiates the activity of DNA-PKcs kinase. Ku protein and DNA-PKcs recruit the processing enzymes to the DSBs, and XRCC4/ Ligase IV complex is finally recruited to mediate ligation of the DSB. This interaction then allows the end processing that might require nucleus enzyme, Artemis. End processing results in overhang strands and DNA polymerase μ and λ then interact with protein Ku. Once the DNA polymerisation process is completed, DNA ligase enzymes are engaged and seal the nicks to complete the entire process (Chang *et al.*, 2017) (Figure 1.6).

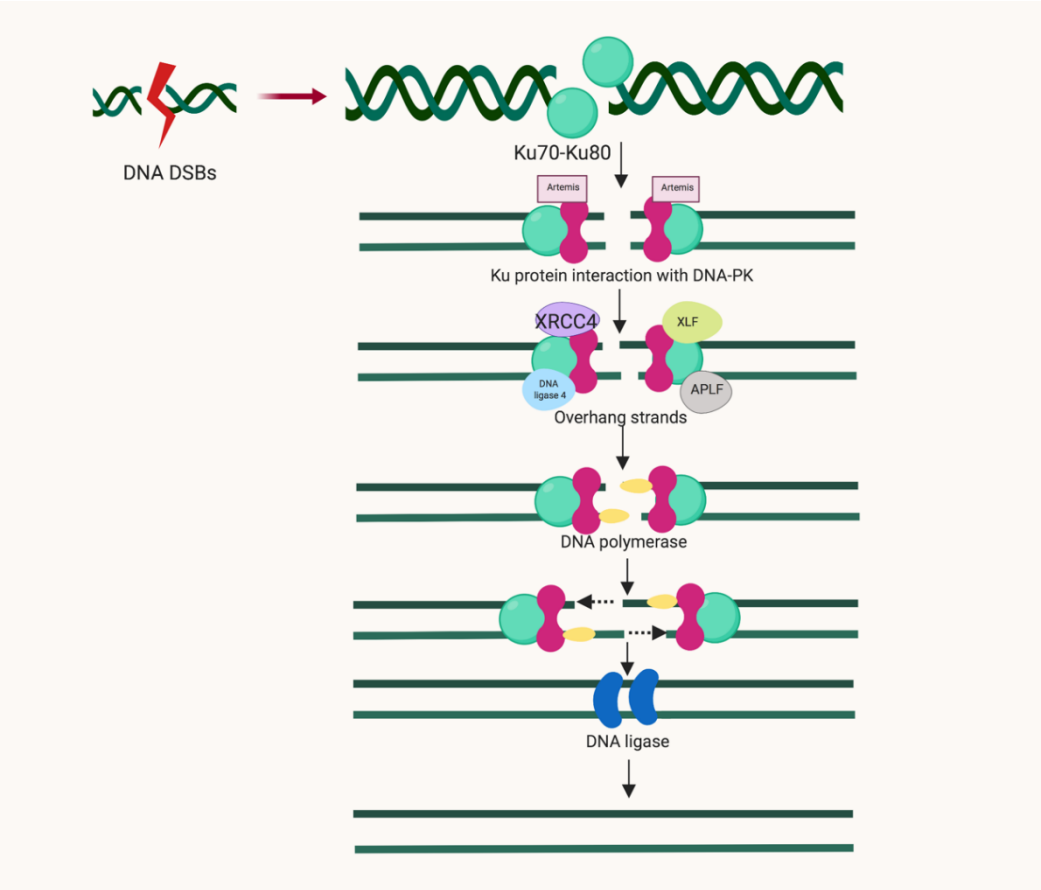

Figure 1.6. DNA DSBs NHEJ repair pathway. Unlike HR, NHEJ does not require a template strand of DNA repair. Following a detection and recognition of DNA breaks, protein Ku70/80 is activated and

bind to the free ends of the DNA. This interaction then recruits DNA-PKcs, XRCC4, DNA Ligase IV, XLF, and APLF to interact with Ku protein and form a complex. At this stage nucleus enzyme Artemis binds to the DNA-PKcs and protein Ku complex. This interaction then leads to the end processing resulting in overhang strands following when DNA polymerase is recruited, and the whole process is completed and finalised by DNA ligase.

Initiation of HR necessitates the detection of the DSBs by the meiotic recombination 11 (MRE11)-Rad50, Nijmegen breakage syndrome 1 (NBS1) (MRN) complex (Rein and Stracker, 2014). The MRN complex is an early DSBs sensor bound to the two free ends of DNA DSBs, and it maintains DNA ends in adjacency to enable the repair which, in turn, induces the activation of DNA repair mechanism downstream pathway. The binding of MRN complex to DNA DSB free ends then permits the NBS1 protein to interact with ATM dimers leading to autophosphorylation of ATM at a serine residue. ATM, in turn, phosphorylates H2AX at the c-terminal serine 139 (γH2AX). γH2AX binds specifically to DNA damage site and initiates the downstream pathway resulting in DNA repair or cell cycle arrest (reviewed by (Oktay *et al.*, 2015)). γH2AX is considerably phosphorylated from minutes to hours following DNA breaks and the intensity increases in line with the severity of the damage (Nazarov *et al.*, 2003, Rogakou *et al.*, 1998, Tomilin *et al.*, 2001). Mediator DNA damage checkpoint protein (MDC1) is another protein involved in this pathway and is activated and bound to γH2AX mediated by breast cancer susceptibility gene 1 (BRCA1). MDC1 forms foci that co-localise with γH2AX and provides positive feedback to further recruits MRN complexes leading to propagation of γH2AX at the sites of DNA breaks (Jungmichel and Stucki, 2010).

ATM and ataxia telangiectasia and Rad3-related (ATR) are members of the

phosphatidylinositol 3-kinase-like kinases (PIKKs) family. In single strand breaks (SSBs) repair mechanism, activation of ATM and ATR is generated by replication protein A (RPA) coated SSB. ATM is recruited by MRN complex (Falck *et al.*, 2005, Lee and Paull, 2005), whereas ATR is recruited by ATR-interacting protein (ATRIP) to RPA coated SSB (Cortez *et al.*, 2001, Falck *et al.*, 2005). Phosphorylation of ATM activates DNA repair proteins downstream pathway leading to either HR/NHEJ or phosphorylates checkpoint kinase 2 (Chk2) resulting in cell cycle arrest. On the other hand, checkpoint kinase 1 (Chk1) is a downstream target of ATR. Although it is commonly accepted that ATM and ATR activity are not interconnected, it has been shown that activation of ATM may depend on ATR in DDR, but it is restricted to S and G2 phase of the cell cycle (Jazayeri *et al.*, 2006).

In somatic cells, activation of Chk1 and Chk2 leads to p53 phosphorylation at Serine 20, which is also a downstream target of either ATM or ATR. p53 is essential to maintain checkpoint at G1/S of the cell cycle (Basu and Haldar, 1998, Heijink *et al.*, 2013). Initiation of Chk1 and Chk2 simultaneously inhibit cell division cycle (Cdc) 25 phosphatase that, in turn, activates cyclin-dependent kinase (Cdk) and restrain the cell cycle progression from G1 to S phase. p21 transcription is a downstream target of p53 that inhibits Cdk2 and cyclin-dependent kinase 4 (Cdk4) transcription and ultimately leads to cell cycle arrest (reviewed by (Collins and Jones, 2016)) and allows DNA repair. Nevertheless, this repair mechanism does not function appropriately in severe DNA damage that may cause the accumulation of DNA DSBs. Pro-apoptotic gene Bcl- associated X protein (Bax) and p53 upregulated modulator of apoptosis (PUMA) are then activated and ultimately leading to apoptosis (Kerr *et al.*, 2012b).

In germ cells, RPA is replaced by Rad51 and DNA meiotic recombinase 1 (DMC1)

(reviewed by (Oktay *et al.*, 2015)). DNA repair process in meiosis requires an intact DNA strand as a template and the strand from homologous chromosome is preferred compared to DNA from sister chromatid to obtain the organised homologous chromosome segregation. Strand exchange at meiotic recombination is completed by the activation of Rad51 and DMC1. Rad51 is essential in mitotic and meiotic recombination, whilst DMC1 is specifically involved in meiotic recombination as it acts particularly in interhomolog rather than sister chromatid exchange (Hong *et al.*, 2013) (Figure 1.7).

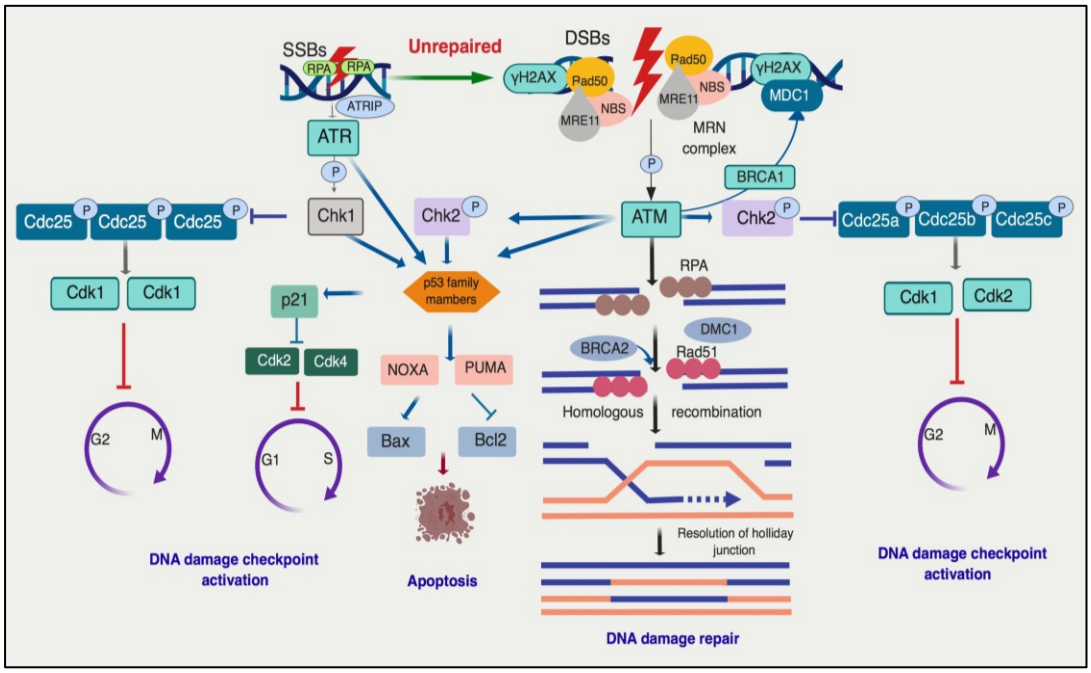

Figure 1.7. The intersection between DDR pathway and apoptosis. Detection and recognition of DNA breaks by MRN complex triggers a cascade of reactions involved in DNA damage repair downstream signalling pathways. The MRN complex activation, in turn, phosphorylates ATM in DNA DSBs response mechanism and ATR in SSB repair pathway. The ATR is recruited by ATRIP to RPA coated SSB. ATM, in turn, phosphorylates H2AX at serine 139 (γH2AX). Phosphorylation of ATM and ATR may either result in Chk2 and Chk1 phosphorylation or activation of p53 family member depending on the cell type. p53 induces cell-cycle arrest by activating the transcription of p21, which may hamper cell cycle progression through inhibition of Cdk2 and Cdk4 activity. MDC1 binds to

γH2AX via BRCA1 and forms foci that co-localise with γH2AX foci. In oocytes, the DNA strand resection is activated and leads to HR. The single-stranded DNA (ssDNA) is then coated by the ssDNA binding protein complex RPA. In germ cells, RPA is replaced by Rad51 and DMC1. Activation of Chk1 and Chk2 inhibits Cdc25 and ultimately induces Cdk1 and Cdk2 activations leading to cell cycle arrest. p53 activates PUMA and NOXA as the consequences of severe DNA damage with a limited repair. Apoptosis is more likely as a result of the balance between pro-apoptosis (Bcl2) and anti-apoptosis (Bax) activity.

1.5.1. DNA Damage and DNA Repair Response of Oocytes and Granulosa Cells

During reproductive life, oocytes and granulosa cells can be subjected to DNA damage as the consequence of external and internal insults of the cells to a considerable number of genotoxic agents (Titus *et al.*, 2013). The ability of cells to respond to such damage is critical considering that severe damage during meiosis can end up with significant consequences when the cells cannot respond to such damage accordingly (Bzymek *et al.*, 2010, Torgovnick and Schumacher, 2015). All types of follicles have different reactions to genotoxic agents, given the probability of changes in sensitivity concomitant with development and follicle growth (Hanoux *et al.*, 2007, Winship *et al.*, 2018).

Oocytes within primordial follicles, non-dividing and remained arrested at the diplotene stage of meiosis prophase 1 for an extraordinary length of time, are more prone to DNA induced damage compared to other follicle types. Meanwhile, granulosa cells, as actively dividing cells, are more sensitive to DNA DSBs. Granulosa cells maintain genomic integrity by activating DNA damage DSBs repair signalling pathway and transmit signals to checkpoint proteins to arrest the cell cycle. Compared

to germ cells, somatic cells are more proficient of actuating the DNA damage repair pathway dynamically. Apoptosis of the somatic cells ensues if a G1/S arrest is persistent, and the damage is irreparable (Roos and Kaina, 2006). The fate of oocytes with DNA DSBs depends on the severity of the damage. Oocytes with slight DNA DSBs can resume meiosis and progress to M2. As DNA DSBs are also a part of meiotic recombination process in oocytes during fetal life, it is important to ensure that this process runs properly as permanent DNA damage with limited repair may lead to DNA damage accumulation. A meiotic error is more likely leading to infertility. Given that oocytes are arrested at germinal vesicle (GV) stage for a long period of time, it is important to ensure that the DNA repair machinery in both oocytes and granulosa cells of immature follicles functions properly starting from sensing, recognising the damage, and regulating the DNA repair downstream pathway.

1.5.2. DNA Damage and Apoptosis Intersection in Non-growing and Early Growing Follicles, a Unique Regulation of p53 Family Members in the Oocyte Surveillance Mechanism

Although the mechanism underpinning oocytes vulnerability toward DNA damage has not been fully understood, high susceptibility to apoptosis signals is thought to be one of the causes (Hanoux *et al.*, 2007). The apoptosis process of oocytes within primordial follicle is mediated by a very distinct cell surveillance mechanism involving trans-activating p63α (TAp63α) pathway (Amelio *et al.*, 2012, Kerr *et al.*, 2012b, Livera *et al.*, 2008, Suh *et al.*, 2006), a family member of p53 (Levine *et al.*, 2011). TAp63α functions to respond to DNA damage primarily after prophase 1 of meiosis and is constitutively active only in female germ cells once DNA breaks occur (Livera *et al.*, 2008). The essential role of TAp63α in the apoptosis process makes it an important

regulator in follicle loss during chemotherapy which may result in a reduced primordial follicular pool. Oocytes in the quiescent state show a high TAp63α expression that reduces gradually during follicular development. Mouse oocytes exposed to radiation resulted in primordial follicle loss that coincided with diminished TAp63α in the oocytes. Interestingly, the larger follicles survived the same radiation dose, revealing the indispensable role of TAp63α in the DNA damage response of the oocytes ((Suh *et al.*, 2006).

TAp63α is maintained in dimeric form by transcriptional inhibitory domain (TID) and further stabilised by the interaction of N-terminal transactivation (TAD) with TID and the oligomerisation domain. Inactivation of TID alters the dimeric to tetrameric state (Deutsch *et al.*, 2011b, Deutsch *et al.*, 2011a, Straub *et al.*, 2010). In the dimeric state, the transactivation of TAp63α is suppressed by decreasing its DNA binding affinity and repressing the activity of the domain responsible for the transcriptional process (Deutsch *et al.*, 2011a). Exposure to genotoxic agents such as radiation has been displayed to increase TAp63α in its tetrameric state (Deutsch *et al.*, 2011b, Deutsch *et al.*, 2011a, Straub *et al.*, 2010) that, in turn, reduces TAp63α levels in oocytes and may finally cause apoptosis (Straub *et al.*, 2010) and elimination of damaged oocytes. The presence of TAp63α in oocytes of immature follicles stresses the need for effective surveillance mechanism to ensure only oocytes with complete DNA damage repair are recruited to ovulation (Gebel *et al.*, 2017, Livera *et al.*, 2008, Suh *et al.*, 2006) (Figure 1.8).

Phosphorylation of ATM is the first step in the initiation of G2 checkpoint activation in the DNA damage repair pathway (Carroll and Marangos, 2013). Inhibition of ATM

in mouse oocytes exposed to irradiation failed to activate TAp63α that consequently blocked the apoptosis pathway and prevented oocyte death (Kim and Suh, 2014). Phosphorylation of Chk2 by ATM, in turn, leads to TAp63α phosphorylation on serine 582 (Coutandin *et al.*, 2016). Meanwhile, p53, a tumour suppressor gene, is known to be essential in somatic cell apoptosis. In the physiologic state, the p53 level is low. Activation of the apoptotic pathway due to unrepaired DNA damage increases p53 expression, which consequently triggers cell cycle arrest or cell death (Deutsch *et al.*, 2011a) (Figure 1.8). Unlike in somatic cells, p53 is dispensable in oocytes against DNA damage (Coutandin *et al.*, 2016).

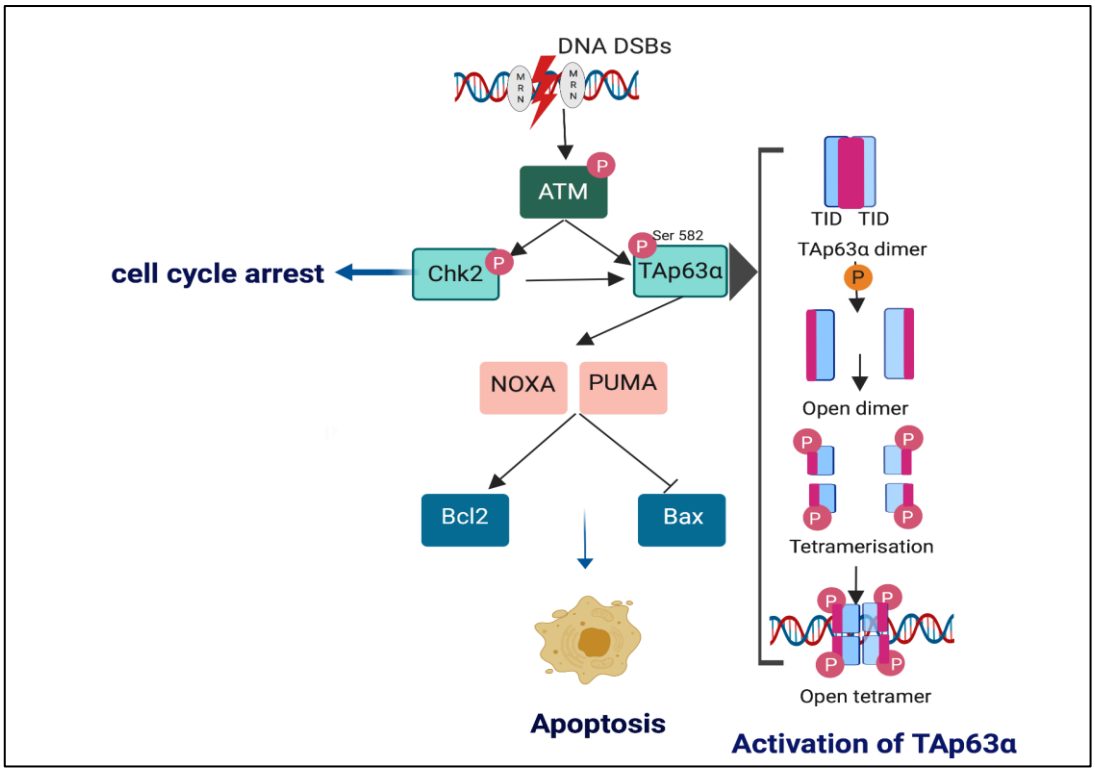

Figure 1.8. Oocytes within primordial follicles surveillance mechanism involving an interplay of dimeric to the tetrameric formation of TAp63α. The DNA DSBs recognition by MRN complex triggers ATM phosphorylation leading to Chk2 activation. TAp63α is a downstream target of phosphorylated ATM and Chk2. Phosphorylation of TAp63α ultimately transform inactive dimeric form of TAp63α to active form (tetramer), proapoptotic proteins PUMA and NOXA, transcriptional

targets of TAp63α will be activated resulting in apoptosis by repressing the initiation of Bcl2 and inducing the activity of Bax.

1.5.3. DDR in Fully Grown Oocytes of Growing Follicles

The capacity of oocytes in fully grown follicles to activate G2 checkpoint during DDR is not as efficient as somatic cells and immature oocytes within non-growing follicles (Carroll and Marangos, 2013). The transcriptional silence of oocytes within ovulatory follicles is likely to underlie their inability to respond to DNA induced damage (Martin *et al.*, 2018). GV oocytes with some DNA damage are able to progress to GVBD, enter Metaphase 1 (M1) and are capable of being fertilised (Carroll and Marangos, 2013). However, this may increase the risk of DNA damage in the embryo. The presence of severe DNA damage in GV oocytes will lead to an oocyte-specific checkpoint or spindle assembly checkpoint (SAC) activation which, in turn, prevents GV oocytes from exiting M-phase of the cell cycle leading to GV arrest at M-phase (Collins *et al.*, 2015, Marangos *et al.*, 2015). In this respect, SAC may function to prevent the production of abnormal oocytes and embryos by inhibiting anaphase-promoting complex (APC) before chromosome separation (Marangos *et al.*, 2007).

However, severe DNA breaks due to exposure to high etoposide concentrations causes GVBD rate to decline. In addition, oocytes with high γH2AX expression following prolonged culture in a high concentration of etoposide are able to enter M phase suggesting that inadequate DNA damage checkpoints are more likely in severe DNA damage and the checkpoint adaptation does exist in the oocyte DNA damage response (Marangos and Carroll, 2012).

DNA damage in oocytes involves ATM and Chk1 activation dependent on the severity of the damage. However, the fact that oocytes can enter M phase in the presence of γH2AX hints to the lack of a checkpoint mechanism in the oocytes of fully grown follicles due to lower ATM sensitivity to DNA damage response (Carroll and Marangos, 2013). Though the exact cause of increasing the checkpoint activation threshold is not clear, the lack of ATM phosphorylation appears to be the cause of less responsive DNA damage checkpoints in fully grown oocytes (Mayer *et al.*, 2016). Conversely, Rad51 functions efficiently in oocytes of fully-grown follicles. Mature oocytes exposed to doxorubicin *in vitro* exhibited a high Rad51 expression that is associated with a higher rate of oocyte survival (Kujjo *et al.*, 2010).

It is, however, worth noting that each species reacts differently to DNA damage. It has been reported that the DNA damage response in rodent oocytes was superior to the response in primates (Wang *et al.*, 2017b). In addition, co-localisation of Rad51 and γH2AX was predominantly observed in mouse compared to monkey oocytes (Wang *et al.*, 2017b) suggesting efficient DNA damage repair in mouse oocytes. However, bovine oocytes were less vulnerable to irradiation-induced DNA damage compared to mouse oocytes, demonstrated by more mouse oocytes undergoing necrosis, while no significant morphological changes were observed in bovine oocytes over the same time frame (Kujjo *et al.*, 2012). However, it is pertinent to note that although bovine oocytes exposed to doxorubicin were able to be fertilised, further development of embryos was compromised suggesting that intact DNA damage repair is needed to ensure complete development of the oocytes to the embryo and to produce healthy offspring (Kujjo *et al.*, 2012).

1.6. DNA damage Associated with Ovarian Ageing, a Crosstalk between PI3K/Akt/PTEN Signalling Pathway, Ageing, and DNA Damage Response

Ovarian ageing as a physiological process varies substantially among women depending on the number of primordial follicles and the degree of follicle loss (de Bruin *et al.*, 2004, Faddy *et al.*, 1992). It is also intensely associated with reduced oocyte quality (Li *et al.*, 2012). However, the relationship between ovarian ageing and deviations in the follicular microenvironment are still far from being fully understood (Broekmans *et al.*, 2009, Tatone *et al.*, 2008).

There is increasing evidence of a strong association between DNA damage and repair capacity of oocytes and increasing maternal age, with DNA repair becoming less efficient with ageing (Govindaraj *et al.*, 2015, Govindaraj *et al.*, 2017, Oktay *et al.*, 2015, Titus *et al.*, 2013). A study in non-human primates confirmed a lack of DNA repair efficiency with advancing age. In the non-human primate, γH2AX expression is considerably elevated in granulosa cells and oocytes of early growing follicles with the advancing age. This may be related to less efficient DNA repair function, as is shown by lower BRCA1 expression in both oocytes and granulosa cells (Zhang *et al.*, 2015). In line with these findings, mouse oocytes of all follicle types exhibit high expression of γH2AX with increasing age. At the same time point, the oocyte appears to have an ineffective DNA repair mechanism as is shown by a profound drop in BRCA1, MRE11, ATM but not breast cancer susceptibility gene 2 (BRCA2). In a genetic BRCA1 mutation mouse model, the oocytes are overwhelmed by DNA damage that might be due to compromised DSBs repair regulatory or the damage exceeds its physiological repair capacity. In addition, BRCA1 mutations but not

BRCA2 perturb ovarian stimulation leading to yielded smaller litter size (Titus *et al.*, 2013). Similarly, women with BRCA2 mutations do not show a reduced response to ovarian stimulation (Oktay *et al.*, 2010). However, it is worth considering that BRCA2 deficient mice are able to produce competent and fertilised oocytes but more abnormal embryos are observed (Sharan *et al.*, 2004) representing the decisive role of BRCA2 in female mouse meiosis.

The depreciation in reproductive performance is a major challenge in women with increasing age due to chromosomal abnormalities in oocytes. The decline in reproductive performance is also closely related to diminished ovarian reserve that seems to accelerate with age (Titus *et al.*, 2013). Likewise, a diminished ovarian reserve mirrored by low AMH levels in women with BRCA1 mutation but not BRCA2 (Phillips *et al.*, 2016), validates the findings from transgenic mouse model. Increased γH2AX expression in oocytes after the age of 36 is not associated with increased DNA repair proteins MRE11, BRCA1, Rad51, and ATM but BRCA2 expressions (Titus *et al.*, 2013). In addition, primordial follicles with BRCA1 mutations are more susceptible to DNA damage accumulation shown by high γH2AX expression in primordial follicles, which rises in BRCA mutation groups (Lin *et al.*, 2017).

As described above, mature oocytes have propensity to tolerate the damage. However, as an intact DNA repair process is obligatory to produce healthy offspring, the oocytes that survive despite the accumulation of DNA damage may be functionally impaired (Titus *et al.*, 2013). Although some evidence leads to normal BRCA2 expression with age, complete loss of BRCA2 function results in ovarian dysgenesis leading to primary amenorrhea. Further analysis indicates that Rad51 expression is low at the site of DNA

damage (Weinberg-Shukron *et al.*, 2018). Genome-wide association study (GWAS) investigation also displays the association between DNA damage repair and age at menopause (Day *et al.*, 2015), specifically emphasising links with BRCA1.

In contrast, granulosa cells of growing follicles are unlikely to be affected by age, proposing the lack of an age-linked escalation of DSBs in the non–germ cell component of the ovarian follicles (Titus *et al.*, 2013). It seems likely that granulosa cells capacity to respond to DNA damage is sufficient to prevent apoptosis (Titus *et al.*, 2013). Follicles with both γH2AX and ATM expression in granulosa cells following exposure to doxorubicin do not show apoptosis (Soleimani *et al.*, 2011). These findings are consistent with a previous study in rodents (Govindaraj *et al.*, 2015). However, a study using monkey ovaries showed that DNA damage in granulosa cells (and cumulus cells) increased significantly with advancing age in all follicle types including antral follicles (Zhang *et al.*, 2015). These highly variable results can be caused by the nature of dynamic behaviour of granulosa cells as is generally observed in highly proliferative cells with high metabolic activity, particularly in developing follicles that seemingly generate an oxygen radical–rich milieu (Titus *et al.*, 2013). These cells are more prone to DNA insults, but with the ability to exhibit dynamic DNA repair functions (Roos and Kaina, 2006).

ROS accumulation in mitochondria can be an underlying factor of ageing, by increasing oxidative damage leading to a gradual decrease in ovarian quality (Shi *et al.*, 2016). ROS overexpression in a cell may increase lipid peroxidation, oxidative stress and damage to macromolecules, including DNA leading to either SSBs or DSBs (Yang *et al.*, 2006). Mitochondria have been hypothesised to be the first organelle

affected by ROS. Ageing has been linked to mitochondria dysfunction as mitochondria DNA deletions increase with age (Keefe *et al.*, 1995, Kitagawa *et al.*, 1993). PTEN upregulation, through modulation of the PI3K/Akt pathway, decreases ROS production in cells (reviewed by (Kitagishi and Matsuda, 2013, Nogueira and Hay, 2013). Increased ROS production in mitochondria due to ageing can thus inhibit PTEN and increase Akt activation and further increase ROS production (Figure 1.9).

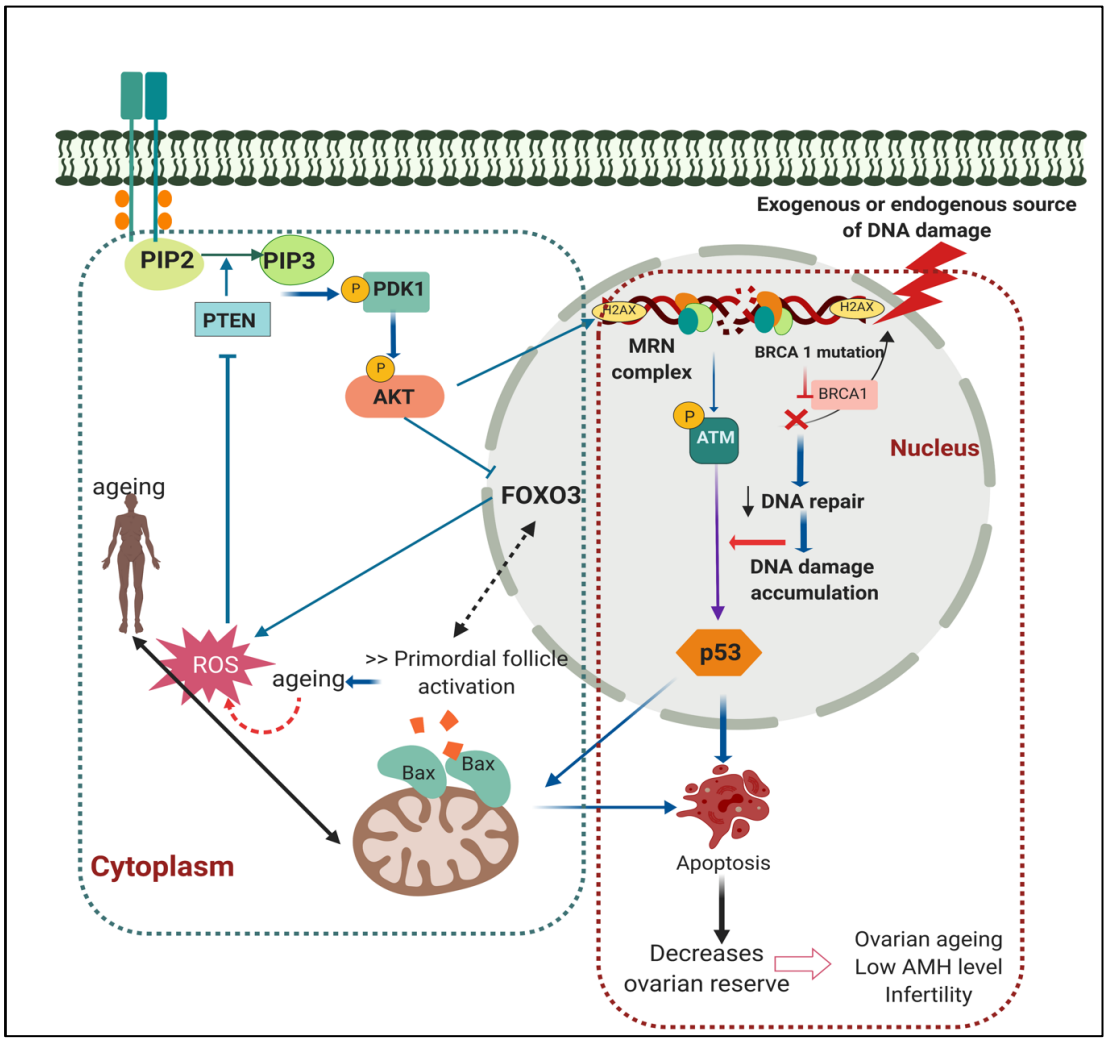

Figure 1.9. Molecular relationship between PTEN/Akt activation, DNA damage and decreased ovarian reserve in ovarian ageing due to exogenous or endogenous DNA insults. The green dashed line represents ovarian ageing due to excessive activation of primordial follicles that can be an indirect effect of DNA induced damage agents. The red dashed line represents the direct effects of DNA induced damage agents or BRCA mutations. This figure shows that BRCA1 mutations may lead to compromised

DNA repair pathways. In addition, mitochondria are also one of the major sources of DNA damage. Excessive ROS production may harm macromolecules in the cells, including DNA, leading to SSBs or DSBs. High ROS expression in the mitochondria may lead to PTEN inhibition and increased Akt activation that may eventually further increase ROS production (Maidarti *et al.*, 2020).

1.7. The Development of an IVG System

The growth of follicles *in vitro* is influenced by various factors such as the type of tissue, the method of culture, the composition of the medium, temperature, oxygen or CO_2 concentration and supplements to the medium (Sadeu JC, 2008, Schubert B, 2010). The complete development of oocytes from primordial germ cells *in vitro* has been demonstrated from mice and these have been able to promote normal follicle formation and subsequent yield of fertile offspring (Morohaku *et al.*, 2016). Additionally, after a long process and trials, the entire process of oogenesis from mouse pluripotent stem cells has been successfully reconstituted *in vitro* yielding normal progeny (Hikabe *et al.*, 2016). These cutting-edge studies have shed light on the development of IVG systems following the ground-breaking studies by the Eppig group (Eppig and Schroeder, 1989, Eppig and O'Brien, 1996, O'Brien *et al.*, 2003). Since then, IVG systems starting from the early stages of follicle development have been persistently pushed further and have led to systems being developed to support oocyte development of large mammals and humans.

Progress has been made to support the growth of ovarian follicles *in vitro* starting from the early stages of follicular development in a range of species (Brito *et al.*, 2014, Hovatta *et al.*, 1997, Hovatta *et al.*, 1999, Picton and Gosden, 2000, Telfer and McLaughlin, 2012, Xiao *et al.*, 2015). Work in our lab has shown that the multistep *in vitro* follicle systems utilising serum-free medium demonstrated significant follicle

growth and survival in human and domestic animal models (McCaffery *et al.*, 2000, McLaughlin *et al.*, 2018, Telfer *et al.*, 2008, Thomas *et al.*, 2007, Walters *et al.*, 2006) (Figure 1.10).

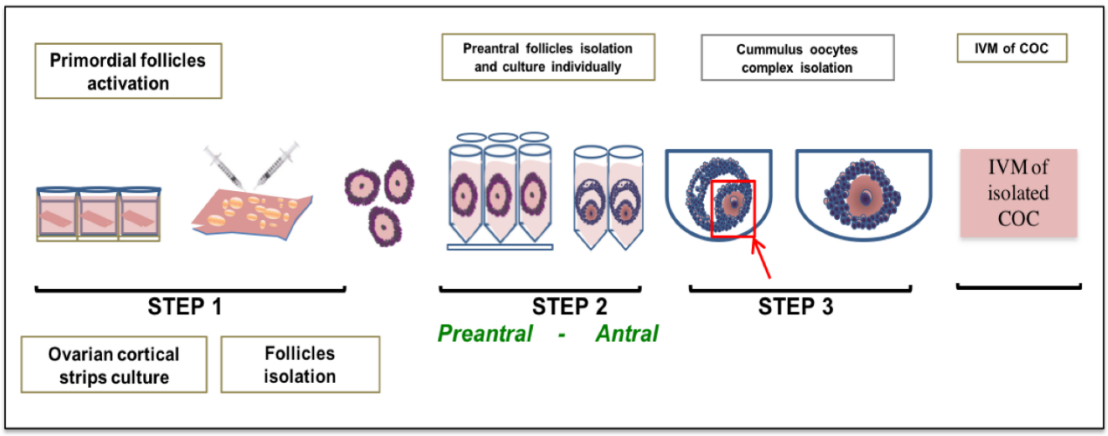

Figure 1.10. Proposed multistep IVG system to support complete oocyte development. Four steps IVG system consists of primordial follicle activation. Once a follicle is initiated and reaches multilaminar stages, isolated follicles are cultured individually in V-shaped microwell culture plates to support the development of follicles from preantral to antral stage. The fourth step of the IVG system is *in vitro* maturation (IVM) of the oocytes (Adapted from (Telfer *et al.*, 2008, Telfer and McLaughlin, 2012)).

After initiation of follicle growth, the growing follicles consisting of multilaminar granulosa cells will not survive within the cortical environment thus preantral follicle isolation following primordial follicle activation is a prerequisite for the further growth of the growing follicles (McLaughlin and Telfer, 2010, Telfer *et al.*, 2008). Two main techniques that are most frequently used to isolate preantral follicles are enzymatic and microdissection techniques. Microdissection allows the isolation of morphologically normal follicles with an intact basement membrane, thus allowing better interaction between oocytes and granulosa cells. However, this method is laborious and time-consuming with a low follicle yield (Telfer and McLaughlin, 2012).

Well preserved gap junctions are needed to maintain the interaction between cells and ensure the direct transport of important factors for follicular growth and oocyte maturation (Diaz *et al.*, 2007, Eppig and Schroeder, 1989, Murray and Spears, 2000) during the culture period. Damage to gap junctions will interfere with the oocyte and somatic cells communication resulting in follicle atresia, as this communication is obligatory to overcome the lack of particular factors required for oocyte metabolism, including amino acids that are required for glycolysis and biosynthesis of cholesterol (Eppig *et al.*, 2005, Su *et al.*, 2009).

The main issue currently is how to develop an appropriate IVG system that can preserve the three-dimensional (3D) structure of isolated ovarian follicles, maintain cell to cell communication, and enable their full growth and development. The importance of the spatial arrangement between cells has triggered several studies related to 3D hydrogel-based culture systems to support physiologic environment (Bissell *et al.*, 2003, Weaver *et al.*, 1996). A line of evidence suggests that a 3D system is capable of establishing oocyte and somatic cells communication, thus allowing direct transport of nutrients, hormones and oxygen (Bissell *et al.*, 2003, Weaver *et al.*, 1996).

It is worth considering that gene expression profiles of cells in 3D culture system are better at mimicking *in vivo* conditions (Hwa *et al.*, 2007). Furthermore, the 3D structure has an essential role in determining the organisation of communication between cells and controlling cell differentiation (Griffith and Swartz, 2006). The use of V-shaped microwell culture plates in our lab has been shown to maintain the three-dimensional structure of the follicles and promote interaction between oocyte and granulosa cells (Telfer *et al.*, 2008, Thomas *et al.*, 2007, Walters *et al.*, 2006). Bovine

preantral follicles isolated mechanically and cultured for 6 to 8 days in V-shaped microwells are able to maintain inter-granulosa cells communication indicated by the presence of Cx43 between granulosa cells. In addition, activin is associated with a peripheral distribution pattern of Cx43 protein that may be indicative of a similar spatial pattern of growth with extensive intercellular communication. It is most likely that activin fosters some degree of granulosa cell adhesion to the zona pellucida (McLaughlin *et al.*, 2010a).

In addition to 3D culture systems, *in vitro* follicle co-culture with adipose-derived stem cells (ADSCs) for 14 days is a promising opportunity in developing the IVG system. This system is able to maintain cell to cell communication throughout the culture period and produces competent oocytes, improves steroidogenesis and increases the expression of transzonal projections (TZPs) (Green *et al.*, 2019). Similarly, human preantral follicles enzymatically isolated and cultured in 3D matrices are able to preserve TZP networks surrounding oocytes and granulosa cells and produce GV stage oocytes (Xu *et al.*, 2009). However, a complete IVG system starting from primordial follicle activation has been only achieved in human using a multistep IVG system. Preantral follicles isolated mechanically from cultured unilaminar ovarian cortical strips are capable of achieving M2 stage oocytes. Nevertheless, oocyte morphology is compromised with a larger polar body than *in vivo* grown oocytes and with less cumulus expansion (McLaughlin *et al.*, 2018). These findings indicate the need to optimise the culture system at every stage of follicular development.

1.8. Potential Consequences of Pharmacological Activation of Primordial Follicles

Evidence from genetically modified mouse models supports the notion that

accumulated effects of PI3K/Akt/PTEN modulation can determine the rate of primordial follicle activation. PTEN is an essential key factor in promoting normal cell proliferation both in somatic and germ cells (Jagarlamudi *et al.*, 2009, Reddy *et al.*, 2008). As described above, investigation using knockout mice, where particular genes involved in this process have been eliminated or disrupted, shows a critical role of PTEN/PI3K/Akt to regulate primordial follicle initiation and growth (Adhikari *et al.*, 2009, Adhikari and Liu, 2009, Adhikari *et al.*, 2010, Reddy *et al.*, 2008, Reddy *et al.*, 2009).

A lower dose of PTEN inhibitor has successfully triggered the growth of primordial follicles in mice and resulted in mature and fertilisable IVG oocytes (Adhikari *et al.*, 2012). Healthy mouse progeny has been achieved following ovarian tissue transplantation under kidney capsules and *in vitro* fertilization (IVF) procedure (Li *et al.*, 2010a). These findings have been implemented translationally to human as a prospective approach in women with POI to optimise *in vitro* oocytes yield. Pregnancies have been attained after grafting ovarian cortical fragments exposed to PTEN inhibition into POI patients (Kawamura *et al.*, 2013, Suzuki *et al.*, 2015). This method has been acknowledged as a breakthrough to revolutionise reproductive capacity in women with POI. However, this pharmacological approach might impair follicle function (Grosbois and Demeestere, 2018, Lerer-Serfaty *et al.*, 2013, McLaughlin *et al.*, 2014). Despite a significant rise in primordial follicle activation perceived in ovarian cortical strips exposed to the PTEN inhibitor, bpv(HOpic), the growth of apparently healthy preantral follicles was compromised after 6 days of culture (McLaughlin *et al.*, 2014). In addition, the use of alginate scaffold and polyethylene glycol (PEG)-fibrinogen to culture human ovarian cortical strips in the

presence of 100 μM bpv(pic) did not improve follicular development (Lerer-Serfaty *et al.*, 2013).

Similarly, constitutive PI3K activation in Cre+ transgenic mouse oocyte leads to nonparallel oocyte and granulosa cell growth, indicated by enlarged oocyte size surrounded by immature pre-granulosa cells. Although expression of the cell death markers Terminal deoxynucleotidyl transferase-mediated dUTP nick-end labelling (TUNEL) and Bax was low, multioocytic follicles were noticeable with follicles exhibited a high inhibin A and B expression due to overgrowth of excess follicles with ovulation failure (Kim *et al.*, 2015). These findings infer that this treatment may provoke an unsynchronised growth phase between oocyte and granulosa cells, which may underlie the poor follicle growth.

PIKKs are envisaged as the central regulators of DNA damage repair capacity of cells. Akt activation implicates the Chk1 that has a principal role in DNA damage repair process as it will delay the cell cycle progression in S and G2 phase to repair an error of DNA damage prior to cell division (Hunt *et al.*, 2012). PTEN is hypothesised to have a role in conserving genomic integrity. Nonetheless, the outcome of some studies with regards to the role of PTEN in DNA DSBs repair are debatable (Altiok *et al.*, 1999, Fraser *et al.*, 2012, Plo *et al.*, 2008). High level of Akt compromises HR mechanism of DNA DSBs capacity, which is considered as the more precise repair mechanism for DSBs in oocytes (Jia *et al.*, 2013, Plo *et al.*, 2008).

Conversely, low Akt activity has been shown to impair the DNA damage repair mechanism by NHEJ (Kao *et al.*, 2007). Cells with PTEN deficiency lead to incomplete DNA DSBs repair capacity and high prevalence of spontaneous DNA

DSBs (Puc *et al.*, 2005). Furthermore, PTEN deletion is sufficient to markedly reduce the level of Rad51 that, in turn, leads to chromosomal instability (Brunet *et al.*, 1999, Thacker, 2005). These findings indicate that the absence of PTEN may instigate the accumulation of spontaneous DNA damage, and DNA damage repair capacity might be weakened in the loss of PTEN (Shen *et al.*, 2007). This mechanism is also imperative in cancer pathology as Akt impedes apoptosis and increases cell proliferation (Altiok *et al.*, 1999, Plo *et al.*, 2008). Whilst in normal cells, increased Akt level and DNA damage accumulation due to inefficient DNA repair are associated with Ras-induced senescence (Astle *et al.*, 2012) (Figure 1.11).

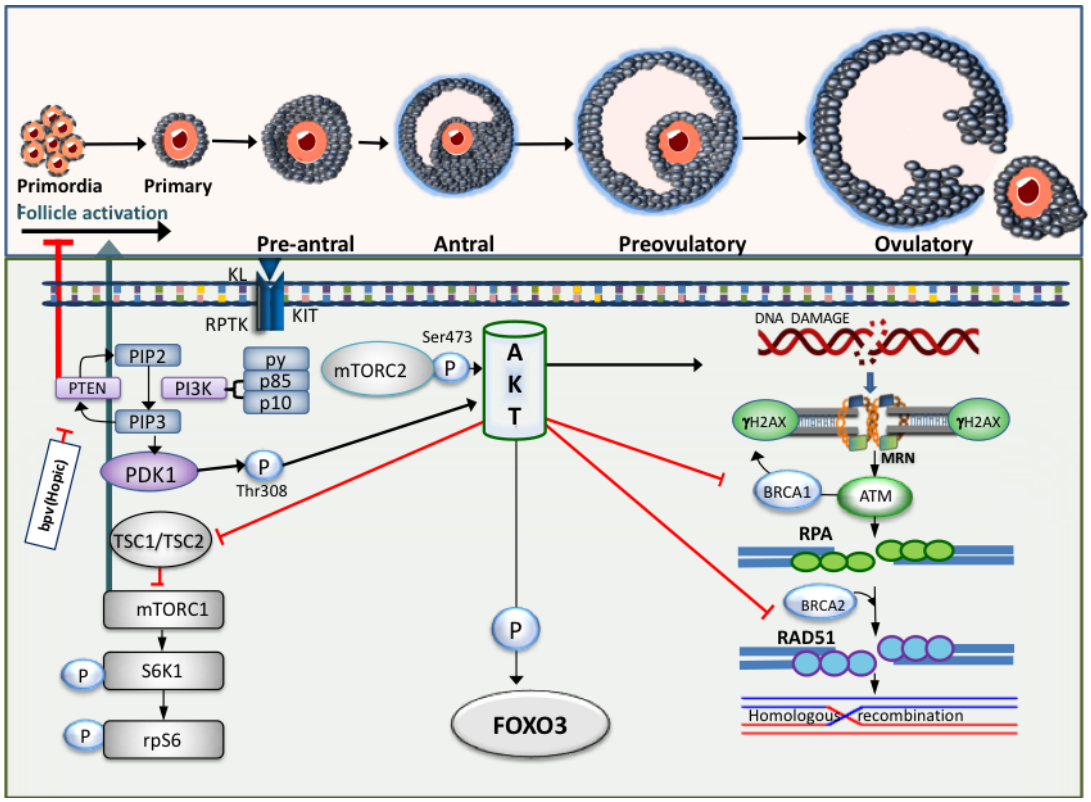

Figure 1.11. Crosstalk between AKT and DNA damage repair response. Intracellular high level of Akt increases DNA damage, represses nuclear and compromise HR in breast cancer cell line (Maidarti *et al.*, 2020).

Although the mechanism by which PI3K/Akt upregulation induces DNA damage in

oocytes has not been investigated further, this rapid grow leads to uncoordinated oocyte and granulosa cell growth (Kim *et al.*, 2015) and is associated with granulosa cell tumour (GCT) due to excessive granulosa cells proliferation in mice (Kim *et al.*, 2016). While in human model, accelerated primordial follicle growth has been linked to decreased estradiol production, suggesting impaired granulosa cells function. Furthermore, lowering the activation rate seems to result in more physiological follicle development, with normal estradiol production in culture media following ovarian cortical fragments culture (Grosbois and Demeestere, 2018). These findings imply that the rapid growth is associated with a disordered intrafollicular oocyte and somatic cell relationship (Smitz and Cortvrindt, 2002). However, the cellular basis was not clarified, but this outcome could be due to a theca cell defect, as the site of androgen production that is then converted to estrogen. Intriguingly, the presence of theca cells in mouse preantral follicle culture reveals insufficient oocyte growth (Morohaku *et al.*, 2016). In contrast, removal of theca cells from the follicle leads to an increase in estradiol and progesterone production (Morohaku *et al.*, 2016). In this context, the function of theca cells *in vitro* might not be essential as it can be replaced by appropriate medium culture.

The PI3K/Akt/mTORC signalling pathway has been related to follicle loss during chemotherapy. It was shown that cyclophosphamide (CP) reduced primordial follicles density in mouse ovaries through the activation of PI3K/Akt/mTOR. Taking advantage of this relationship, mTOR inhibition has been investigated as a means to safeguard the ovaries during chemotherapy in mice (Goldman *et al.*, 2017, Zhou *et al.*, 2017). This positive effect is due to mTOR downregulation that subsequently reduced phosphorylation of Akt, 4EBP1 and S6K1 leading to decreased spontaneous loss of

primordial follicle, thus maintaining ovarian reserve and fertility (Goldman *et al.*, 2017).

Similar to Akt activation, mTOR inhibition effects on DDR study has been limited to cancer cells with diverse outcomes. Constitutive mTOR activation enhances apoptosis triggered by chemotherapy through persistent DNA damage as is shown by the upregulation of γH2AX protein in mouse embryonic fibroblast cell lines. In parallel, the absence of both PTEN and TSC2 upregulates γH2AX expression. Intriguingly, mTOR inhibition prior to treatment is able to protect the cells from etoposide-induced apoptotic cell death, as evidenced by improved cell viability and decreased apoptosis rate with reduced γH2AX expression (Wang *et al.*, 2013). However, further investigations towards its effects on the DNA DSBs and the repair capacity of the oocytes and granulosa cells are needed. Additional insights into the interaction of these aspects may provide a better understanding of DDR during primordial follicle activation. Importantly, as defects in DDR are the starting events of apoptosis, this insight may provide opportunities to find an effective strategy to improve the IVG system.

Despite the unfavourable consequences of DNA damage to oocytes and granulosa cells, the investigation with regards to primordial follicle activation is mostly focused on the later stages of apoptotic events. If an approach leading to a decrease in endogenous DNA damage can be developed, the survival of follicular growth *in vitro* might be substantially increased. A summary of recent studies investigating the impact of PI3K/Akt/mTOR pathway is detailed in Table 1.1. The studies were retrieved systematically from PubMed (Medline) database as recently published (Maidarti *et al.*,

2020). Specific articles focused on primordial follicle activation was selected using specific terms such as ‘primordial follicle activation’, ‘PI3K/ Akt’. Articles selection is as presented in Figure 1.12.

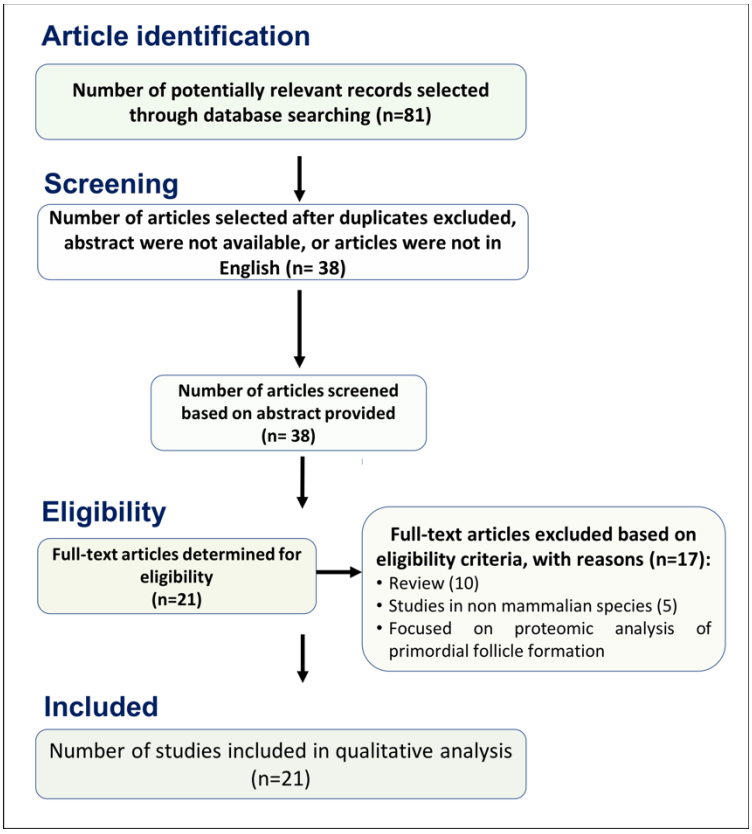

Figure 1.12. Methods for study selection. Flow chart following preferred reporting items for systematic reviews and meta-analyses (PRISMA) guidelines to determine the study included into qualitative analysis (Moher *et al.*, 2015).

Table 1.1. Recent studies investigating the impact of PI3K/Akt/mTOR pathway either as a part of genetic modification/pharmacological activation, chemotherapy treatment or ovotoxicity exposure on primordial follicle activation, follicular growth and survival (Maidarti *et al.*, 2020).

Study	Agents used/compounds/concentration	Mechanism of action	Species/ methods	Effects on follicular growth/survival	Specific effects on granulosa cells/oocyte
(Maidarti *et al.*, 2019)	1 and 10 μM bpv(HOpic) for 24 hours/ PTEN inhibitors.	Increase PI3K/Akt	Bovine/ ovarian cortical fragments cultured.	Decreases in higher dose.	Compromises DDR.
(Wang *et al.*, 2019a)	20, 40, 60, 80, 120, and 140 μM DZN	Inhibit PI3K/Akt	Porcine isolated granulosa cells.	Granulosa cells death	Increase DNA damage, mRNA level of ATM, Rad51, and BRCA1 increase p53.
(Grosbois and Demeestere, 2018)	30μM bpv(HOpic) + 150 μg/ml 740Y-P for 24 and 48 hours, or 100 nM everelimus.	Increase PI3K/Akt and inhibit mTOR activation respectively	Cryopreserved human ovarian cortical fragments cultured	Lowering the rate of activation improves follicular growth.	PTEN inhibition compromises granulosa cells estradiol production.
(Zhou *et al.*, 2017)	CP 75 mg, 100 mg, 150 mg per kg body weight and 5mg/kg body weight per day	PI3K/Akt activation	Mice, *in vivo*	CP induces non-growing and growing follicle loss. Rapamycin prevents	AMH expression decreases after CP exposure.

	1 week before and after CP administration.			CP induced primordial follicle activation.	
(Kim *et al.*, 2016)	Transgenic mice model	Increase PI3K activation in transgenic mice, Cre+	Transgenic mice, Cre+ and Cre-	Normal secondary follicles, GCT in primordial and primary follicles.	Bilateral GCT due to increase activin A.
(Ganesan and Keating, 2016b)	440 μM BPA.	Increases PI3K/Akt activation	Rat ovarian fragment culture exposed to BPA.	BPA induces DNA damage both in oocytes and granulosa cells. PI3K signalling pathway involved in BPA-induced DNA damage.	Primordial follicle is activated to replace the larger follicle depletion.
(Kim *et al.*, 2015)	Transgenic mice model	Increase PI3K activation in transgenic mice, Cre+	Transgenic mice, Cre+ and Cre-	Increases follicles survival,	Asynchronous oocytes and granulosa cells growth.
(Novella-Maestre *et al.*, 2015)	100 μM bpv(pic) for a total of 25 hours	Increase PI3K/Akt activation	Human ovarian cortical fragments cultured.	No damage to the follicular growth.	Improves estradiol production without any damage.

(Sun *et al.*, 2015)	200 µM phosphatidic acid (PA) and 50 µM propranolol (PRO) for 24 hours in mice.; bpv (100 µM) /740Y-P (250 µM /ml) for 24 hours, 740Y-P (250 µM /ml) only for another 24 hours; PA (100 mM)/740Y-P (200 µM)/PRO (50 µM) for 24 hours in human.	Increase PI3K/Akt /mTOR activation.	Mice and human ovaries transiently incubated in mTOR activators followed by grafting into female mice.	No damage to the follicular growth.	Not available (NA)
(Suzuki *et al.*, 2015)	30 µM of bpv(HOpic), and 150 µM /ml of 740YP for 24 hours followed by incubation with 740YP alone for another 24 hours (IVA).	Increase PI3K/Akt activation.	Human ovarian cortical fragments transplantation following IVA.	Autografting of ovarian fragments following IVA procedure to infertility related POI patients.	NA
(McLaughlin *et al.*, 2014)	1 µM bpv(HOpic) and 10 and 100 µM bpv(HOpic) (unpublished)	Increase PI3K/Akt activation	Human ovarian cortical fragments and isolated preantral follicle culture.	Higher dose compromises follicular growth. The lower dose is associated with deleterious effects on subsequent growth of preantral follicles.	NA
(Chang *et al.*, 2015)	Once daily at doses of 0.5, 1.0, 1.5, and 2.0 mg/ kg for 5 to 14 days.	Activation of PI3K/Akt	Intraperitoneal injection of	Increases the proportion of growing	Induces ovarian failure.

			cisplatin in mice	follicles.	
(Lerer-Serfaty *et al.*, 2013)	100 µM bpv(pic) and 500 µM /ml 740Y-P for 24 and 48 hours.	Increase PI3K/Akt activation.	Human ovarian cortical fragments cultured in PEG-fibrinogen hydrogels.	Compromises follicle survival.	NA
(Kawamura *et al.*, 2013)	30 µM bpv(HOpic) and 150 µg/mL 740YP for 24 hours	Increase PI3K/Akt activation.	Mice ovarian transplantation and human ovarian fragments transplantation following IVA.	Promotes primordial follicle activation both in mice and human.	NA
(Adhikari *et al.*, 2013)	Female mice deficient PTEN	Increase PI3K/Akt activation	PTEN knockout mice	Rapamycin reduces the primordial follicles activation in PTEN knockout mice.	Rapamycin prevents global primordial follicles activation induced by the absence of PTEN.
(Adhikari *et al.*, 2012)	1 µM bpv(HOpic) for 24 hours.	Increase PI3K/Akt activity.	Mice cortical fragments IVA followed by transplantation and bpv(HOpic) directly injected to female mice.	Does not compromise follicular health.	More mature and fertilised oocytes in PTEN inhibition group.

(Li *et al.*, 2010b)	100 μM bpv(pic) and/or 500 μg/ml 740Y-P for 48 hours or bpv(pic) plus 740Y-P together with the Akt inhibitor SH-550 μM or the PI3K inhibitor Wortmannin 25 μM.	Increase PI3K/Akt, Akt inhibitor decreases the activation.	Mice and human cortical fragments incubated in Akt activators followed by xenografting.	Increases in the number of secondary and antral stage follicles following xenografting and does not affect follicular health.	No malignancy observed after long term ovarian transplantation.
(Adhikari *et al.*, 2010)	Mice lacking TSC1, PTEN; TSC1 and PTEN; PDK1 and PDK1 and TSC1 in oocytes.	Enhances mTOR activation.	Mutant female mice	Degenerated activated primordial follicles (short term) diminished follicular health (long term).	Rapamycin prevents global primordial follicle activation; activation does not cause tumor development.
(Adhikari *et al.*, 2009)	Homozygous mutant female mice deficient TSC2 in oocytes.	Enhances mTOR activation.	Mutant female mice.	Massive primordial follicle activation.	Depletion of follicles reserve.
(Reddy *et al.*, 2009)	Female mice lacking PTEN, PDK1 and rpS6	Increases PI3K/Akt	Mutant female mice.	Follicles with degenerating oocytes in PDK1 deletion and enlarge oocytes in PTEN deletion.	The absence of PTEN causes POI that can be reversed by PDK1 deletion.
(Reddy *et al.*, 2008)	PTEN deletion mice.	Increases PI3K/Akt	PTEN mutant mice	Tend to be normal follicle morphology with enlarge oocytes and flattened granulosa cells.	PTEN deletion leads to excessive primordial follicle activation.

1.9. Hypothesis and Aims

Hypothesis

The studies in this Thesis address the Hypothesis that the use of a PTEN inhibitor to initiate and promote primordial follicle growth may compromise DNA repair capacity in oocytes and granulosa cells.

Secondly, reducing the rate of activation may improve the DDR of oocytes and granulosa cells *in vitro* and subsequent preantral follicle growth and development.

Aims

To test the hypothesis, the following specific aims were defined:

1. To investigate the effect of PTEN inhibitor on primordial follicle activation, DNA DSBs and DNA damage repair capacity of oocytes and granulosa cells *in vitro*
2. To investigate the effects of mTOR inhibition on primordial follicle activation, DNA DSBs and DNA damage repair capacity of oocytes and granulosa cells *in vitro.*
3. To investigate whether isolated preantral follicles originated from tissue exposed to PTEN and mTOR inhibitors can grow optimally to antral follicle stages, recover DNA repair capacity of the oocytes and granulosa cells and maintain oocyte and companion somatic cells communication throughout the culture period.

Chapter 2

General Materials and Methods

2.1. Ovarian Cortical Fragment Preparation and Dissection

2.1.1. Collection of Bovine Ovaries

Bovine ovaries were obtained from the local abattoir and transported in pre-warmed holding medium (section 2.1.2). At the laboratory, ovaries were rinsed in 70% alcohol and thin slices of ovarian cortex were removed by peeling from the ovary using a scalpel blade no. 24 in a laminar flow hood. Then the tissue was transferred into fresh dissection medium comprising preheated supplemented Leibovitz medium (Gibco BRL, Life Technologies Ltd. Paisley, Renfrewshire, UK) (section 2.1.3).

2.1.2. Holding Medium for Ovarian Transport

Holding medium for transport comprised of M199 (HEPES buffered) (Gibco BRL, Life Technologies Ltd., Paisley, Renfrewshire, UK) supplemented with sodium pyruvate (2 mM), penicillin G (75 μg/ml), streptomycin (50 μg/ml) and amphotericin B (2.5 μg/ ml) (all chemicals from Sigma-Aldrich Chemicals, Poole, Dorset, UK). pH was adjusted to 7.2 - 7.4.

2.1.3. Dissection Medium

Dissection medium was utilised as handling or holding medium for pieces of ovarian cortical strips and ovarian follicle isolation prior to treatment allocation and culture. Dissection medium was prepared from Leibovitz medium (GIBCO BRL, Life Technologies Ltd., Paisley, Renfrewshire, UK) supplemented with sodium pyruvate (2 mM), glutamine (2 mM), BSA (Fraction V. 3 mg/ml), penicillin G (75 μg/ml) and streptomycin (50 μg/ml). This dissection medium was preheated to 37ºC before use.

2.1.4. Ovarian Cortical Tissue Dissection

Ovarian cortical fragments were placed in a petri dish in dissection medium and

examined carefully under light microscopy to characterise ovarian cortex and underlying stroma. One to two pieces of ovarian cortical tissue sized approximately 1 x 0.5 x 0.1 cm were removed from each ovary. Damaged and/or haemorrhagic tissue was excised thus allowing the strips to flatten. Excess stromal tissue was trimmed away from the ovaries using forceps and scalpel blade. The tissue was gently stretched using the blunt edge of a scalpel blade with the cortex uppermost. Using an angled incision, the tissue was cut into small strips (sized 4 x 2 x 1 mm) equal to the number of treatment groups, then randomly distributed to each group to ensure that each group consisted of strips from different ovaries (Figure 2.1). Each fragment was examined under a dissecting microscope (Olympus, UK) for the presence of follicles. Any follicles measuring more than 40 μm were excised from the tissue fragments using the 25-gauge needles attached to 1 ml syringe barrels and a blade no 15 and fine forceps to ensure a presumptive population of unilaminar follicles. Some tissue fragments, depending on the aim of the experiments, were selected from each biopsy as 0-hour control and fixed in 10% neutral buffered formalin (NBF) for histological examination. The remaining bovine cortical strips were cultured in flat-bottomed 24-well culture plates (Corning Costar Europe, Badhoevedorp, The Netherlands).

2.2. Tissue Culture

2.2.1. Culture Medium

Basic culture medium comprised of McCoys 5A medium with bicarbonate and HEPES (20 mM) (GIBCO BRL, Life Technologies Ltd. Paisley, Renfrewshire, UK) supplemented with BSA (1 mg/ml), glutamine (3 mM), penicillin G (0.1 mg/ml), streptomycin (0.1 mg/ml), transferrin (2.5 μg/ml), selenium (4 ng/ml), insulin (10 ng/ml), FSH (1 ng/ml), and ascorbic acid (50 μg/ml) (all obtained from Sigma-Aldrich

Chemicals, Dorset, UK, unless otherwise stated). Following preparation and prior to use, the medium was filter sterilised (Corning Costar Europe, Badhoevedorp, The Netherlands) and equilibrated in a humidified incubator at 37ºC and an air atmosphere with 5% CO_2. Basic culture medium was used for all experiments including tissue and individual isolated follicles culture.

2.2.2. Ovarian Cortical Fragments Culture

Pieces of bovine cortical strips were cultured in flat-bottomed 24-well culture plates. One cortical slice was randomly placed in individual well containing 300 µl of culture medium or treated medium, depending on the aim of the experiment, at 37ºC in a humidified air atmosphere with 5% CO_2 for 24 hours. Medium was removed from the tissue fragments and replaced with fresh culture medium without treatment after 24 hours. Some of the fragments were subjected to western blotting and the remaining fragments were incubated for a further 5 days. During this time, half of the volume of medium per well was removed and replaced with fresh medium every two days. Each experiment was performed under constant conditions (Figure 2.1).

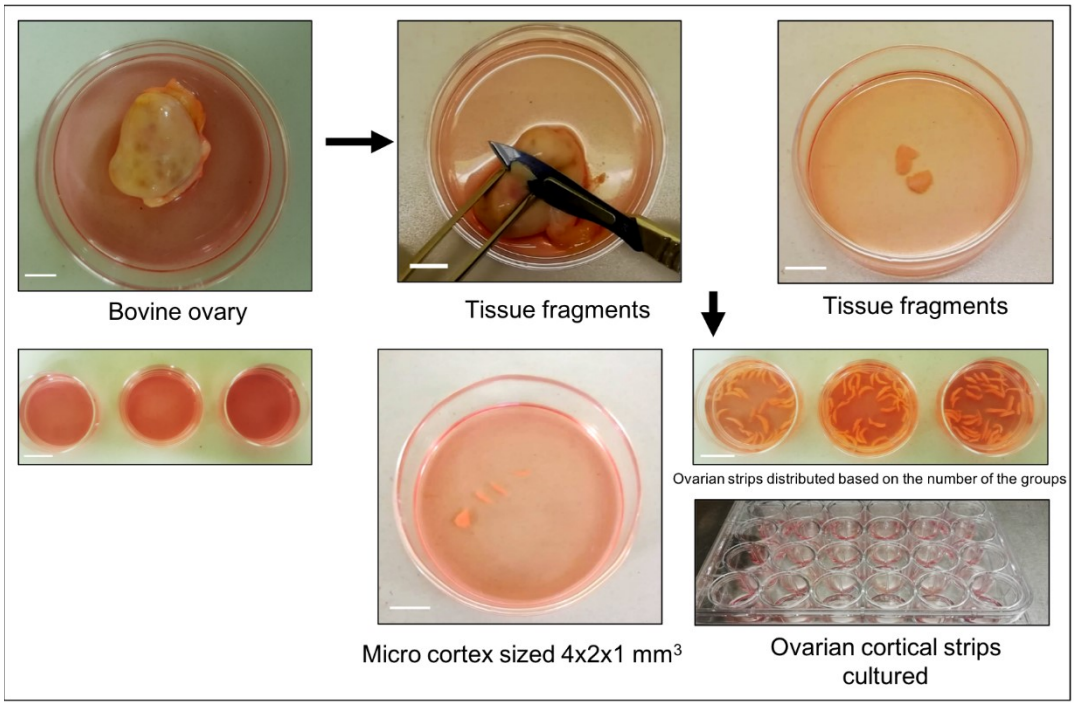

Figure 2.1. Ovarian cortical tissue dissection and culture. Scale bar = 1 cm.

2.3. Preantral Follicle Isolation and Culture

2.3.1. Preantral Follicle Dissection

Preantral follicle isolation was performed after 6 days of culture. On completion of the culture period, tissue fragments were placed in dissection medium and examined under a dissecting microscope. Preantral follicles were dissected using 25-gauge needles, scalpel blade no 15 and fine forceps (Terumo Europe, Belgium) under a dissecting microscope (Olympus, UK) with a calibrated eyepiece graticule (Graticules Ltd, Tonbridge, Kent, UK). To investigate whether the treatments could improve the growth of the follicles, all preantral follicles sized more than 66 μm (Telfer *et al.*, 2008) in diameter were included in the culture system. The reasoning behind the diameter of follicles dissected and selected for culture was that the diameter of preantral follicles size ranging from 66 – 139 μm cultured in the presence of activin A was able to increase to 58% after 4 days of culture (Telfer *et al.*, 2008).

2.3.2. Individual Preantral Follicle Culture

Preantral bovine follicles were cultured individually in 96-well V-bottomed culture plates (Corning Costar Europe, Badhoevedorp, The Netherlands) with 150 μl of pre-warmed culture medium (section 2.2.1) for 6 to 8 days within an incubator in a humidified air atmosphere with 5% CO_2 at 37ºC. Half the volume of medium per well was changed with fresh culture medium on alternate day during the culture period. On the day of isolation and on every 2 days thereafter, simultaneous with refreshing the culture media, the diameter of the follicles was measured. The average of two perpendicular measurements was used to determine a mean follicle diameter at these specific time points. After 6 to 8 days of culture, the follicles were fixed using 10% NBF overnight at 4ºC.

2.4. Histological Techniques

2.4.1. Tissue Fixation, Embedding, and Sectioning

Samples subjected to histology examination were fixed by being placed in 10% NBF solution for 24 hours at room temperature. Fixative was then removed, and the tissue was dehydrated through a series of graded ethanol baths (70, 90 and 100%) for one hour each to displace the water. Ethanol with eosin (coloured ethanol) was used to dehydrate the tissue when fixing individual follicles, thus allowing follicles visualisation during subsequent tissue processing. Absolute alcohol was cleared and replaced with cedarwood oil (BDH Laboratory Supplies, Poole, UK) for a minimum of 24 hours. Following dehydration, the tissue was then subsequently placed in toluene in a fume hood (Fisher Scientific UK Ltd, Loughborough, UK) for 30 minutes to achieve complete oil clearances. The tissue was embedded manually into paraffin wax

blocks at 60ºC for 4 hours with hourly changes of wax to ensure complete removal of toluene.

2.4.2. Sectioning and Mounting

Wax mounted ovarian cortical fragments and isolated follicles were serially sectioned at 5 μm using a microtome (Leica, model Jung RM2035, Nussloch, Germany), then floated on a water bath at 42ºC and then mounted on SuperFrost Plus slides (VWR International Ltd., Leicestershire, UK) and left to dry overnight at 37ºC in a slide oven.

2.4.3. Dewaxing and Tissue Rehydration

Sections were dewaxed by placing the slides in xylene (VWR International) for 30 minutes (2 x 15-minute immersions) and rehydrated by subsequent immersions in decreasing concentrations of alcohol (two washes in 100, then 90, 80 and 70% for 1 minute each). Slides were then washed in tap water prior to staining or antigen retrieval.

2.4.4. H & E Staining

Following dewaxing and rehydration and rinsing in tap water, the sections were placed in Harris' Haematoxylin (BDH Laboratory Supplies, Poole, UK) for 4 minutes then washed in tap water, immersed in Scott's tap water substitute (STWS; CellPath) for 2 minutes and placed back in tap water for at least 2 minutes. Slides were then dipped in 1% eosin (Sigma Chemicals, Poole, Dorset UK) solution for 2 minutes, washed in tap water and inspected under a light microscope to assess the quality of staining. Finally, they were placed in potassium aluminium solution for 2 minutes prior to a tap water rinse and dehydration through increasing concentrations of ethanol (70%, 90%, 95% and two washes of 100%) for 3 minutes each. Slides were then immersed in xylene for

15 minutes and subsequently mounted using Dibutylphthalate Polystyrene Xylene (DPX) mounting medium (BDH Laboratory Supplies, Poole, UK) and glass coverslips (BDH Laboratory Supplies, Poole, UK) and left to dry in a fume hood at room temperature.

2.5. Immunohistochemistry

2.5.1. Immunohistochemistry Protocol

Ovarian strips and follicles were processed and embedded as described in Section 2.4. Immunohistochemistry was performed to determine the localisation of antigens used in this study. Details of the primary and secondary antibodies used, incubation time, and the concentration of primary and secondary antibodies, antigen retrieval method, endogenous peroxidase quenching and visualisation techniques for specific antibody are detailed in the Methods and Materials sections of each chapter. All primary antibodies used to detect DNA damage and DNA repair proteins had never been tested in bovine, hence antibody optimisation was performed to determine the most appropriate antibody and concentration with maximum level of detection and minimum non-specific staining. Uncultured human ovarian cortical strips from caesarean section patients were utilised as a positive control, as all antibodies had previously been tested in human tissue.

In general, following dewaxing and rehydration in decreasing concentration of ethanol, slides were immersed in water for 5 minutes and then washed twice in Tris-buffered saline (TBS) 0.05 M with Tween 20 (TBST). Slides were then equilibrated for 5 minutes in 10 mM sodium citrate (pH 6.0) and antigen retrieval was performed

by heating the slides in sodium citrate using a microwave. The slides were allowed to cool in the buffer for approximately 20 minutes.

Following antigen retrieval, slides were washed in TBST (2 x 5 minutes) and then placed in 3% hydrogen peroxide (H_2O_2, Sigma-Aldrich) in methanol (VWR International) for 10 minutes to block endogenous peroxidase activity and then washed again in 2 x 5 minutes TBST. Sections were then incubated with appropriate blocking (Vectastain® ABC Kit, Vector Laboratories, Peterborough, UK) diluted in TBST (3 drops of serum (150 µl in 10 ml TBST) for 1 hour. The slides were then incubated overnight with the diluted primary antibodies (diluted in serum blocking solution) at 4ºC. Primary antibody was replaced with blocking solution for negative control. Following incubation with the primary antibody, slides were washed in TBST (2 x 5 minutes) and sections were incubated for 30 minutes with biotinylated secondary antibody at room temperature (Vectastain Elite ABC kit, Vector Laboratories, Peterborough, UK) and then washed in TBST (2 x 5 minutes). The secondary antibodies were selected based on the primary antibody of choice. Slides were then incubated with Streptavidin Horseradish Peroxidase (Streptavidin HRP) (made up as per the manufacturer's instructions; Vectastain® ABC Kit) for 30 minutes at room temperature. Following the TBST wash, DAB (3, 3′-diaminobenzidine) peroxidase substrate kit (Vector Laboratories, made up as per the manufacturer's instructions) solution was added to the sections for between 2 and 5 minutes. The slides were placed in tap water to stop the DAB reaction and then counterstained with haematoxylin and STSW and finally dehydrated in graded alcohol and mounted with DPX.

Analysis of follicles was made under the light microscope with a crossed micrometre under x40 magnification. The examiner was blinded to the treatment groups. The category of positive and negative staining was determined before the analysis and applied to all experiments (Figure 2.2).

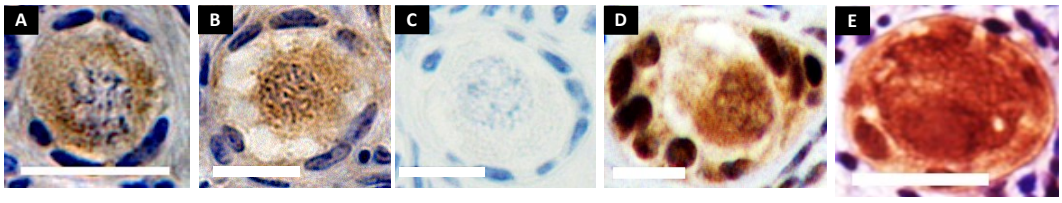

Figure 2.2. DAB category for immunohistochemistry analysis. A). Negative staining in oocyte (Negative staining in nucleus and positive in cytoplasm) and granulosa cells (Negative staining in nucleus and minimal in cytoplasm). B). Positive staining in oocyte (Positive staining in nucleus and minimal staining in cytoplasm. Negative staining in granulosa cells (Negative staining in nucleus and minimal staining in cytoplasm). C). Negative staining in oocyte (Negative staining in nucleus and negative in cytoplasm) and granulosa cells (Negative staining in nucleus and negative in cytoplasm). D). Positive staining in oocyte (Positive staining in nucleus and less staining in cytoplasm. Positive staining in granulosa cells (positive staining in nucleus and less staining in cytoplasm). E). Positive staining in oocyte (Equal staining in nucleus and cytoplasm. Positive staining in granulosa cells (equal staining in nucleus and cytoplasm or less staining in cytoplasm). Scale bar = 20 μm.

2.5.2. Immunofluorescence Protocol

As previously described mounted tissue sections were deparaffinised and rehydrated and then washed in in phosphate-buffered saline (PBS) with 0.1% triton X-100 (PBST) (pH 7.2 - 7.4) for 2 x 5 minutes. Slides were then equilibrated for 5 minutes in 10 mM sodium citrate prior to antigen retrieval, then left to cool for approximately 20 minutes and incubated for 1 hour at room temperature with blocking solution (5% goat serum in PBST). Tissue sections were then probed with primary antibody overnight at 4^{o}C. Blocking solution without primary antibody served as a negative control. After

washing with PBST (4 x 10 minutes), sections were incubated with appropriate secondary antibodies for 1 hour and then washed for 2 x 10 minutes. The slides were then mounted in vectashield hardset with 4′,6-diamidino-2-phenylindole (DAPI) (H-1500, Vector Laboratories).

2.5.3. Image Acquisition and Processing

Images were captured using confocal microscope (detailed in each chapter) with x20 magnification in the IMPACT imaging facility (Centre for Discovery Brain Sciences, The University of Edinburgh) with identical laser, gain, contrast, offset, pinhole, resolution and frame (focus) setting to all samples. Images were analysed using ImageJ, and γH2AX expression in oocytes and granulosa cells was determined. The number of oocytes with positive expression per total number of follicles was calculated. The protein expression in granulosa cells was quantitatively analysed by calculating the proportion of positive granulosa cells per total number of granulosa cells per follicle. Immunofluorescence analysis of isolated follicle culture detailed in chapter 5.

2.5.4. Collection and Analysis of Histological Results

Analysis of follicles within cortical pieces was made under the light microscope with a crossed micrometre under x40 magnification. For all morphological and numerical analyses, the examiner was blinded to the treatment groups. Analysis of follicles within tissue fragments was elaborated in each chapter. Pyknotic granulosa cells were identified as misshapen and had much darker staining than others. Follicle development was examined and classified based on the modification of Pederson classification (Pedersen and Peters, 1968):

(1) Primordial follicles: oocyte surrounded by a complete or incomplete single layer of a flattened granulosa cell.

(2) Transitory follicles: oocyte surrounded by a mixed layer of flattened and cuboidal granulosa cell.

(3) Primary follicles: oocyte surrounded by a single layer of cuboidal granulosa cells.

(4) Secondary stage: oocyte surrounded by two or more complete layers of cuboidal granulosa cells.

(5) Antral follicles: oocyte surrounded by two or more complete layers of cuboidal granulosa cells and the presence of the antral cavity.

Primordial and transitory follicle were grouped and classified as non-growing follicle due to the evidence suggesting that in the bovine ovary, these follicles remain in a quiescent state (van Wezel and Rodgers, 1996). The number of follicles at each stage of growth was recorded, for day 0 (D0) and day 6 (D6) of each treatment. The classification of healthy follicles was based on the same criteria as Telfer *et al*. (2008) with modifications (McLaughlin and Telfer, 2010, Telfer *et al.*, 2008). For follicles to be categorised as morphologically normal the oocyte must be grossly circular, surrounded by a zona pellucida, have a visible germinal vesicle and defined nucleolus and have less than 10% of pyknotic granulosa cells present.

The proportion of follicles at different developmental stages was defined as a percentage of follicle type over the total follicle count (Brunet *et al.*, 1999). Immunohistochemistry analysis in every chapter was divided into oocytes and granulosa cells. The protein expression in granulosa cells was quantitatively analysed by calculating the proportion of positive granulosa cells per total number of granulosa cells per follicle.

2.6. Western Blotting

2.6.1 Protein Extraction and Measurement

The number of replicates, tissue analysed, primary and secondary antibodies used were detailed in each chapter. Protein expression was only analysed in cultured tissue. Ovarian cortical strips were placed in gentle MACS M tubes (Miltenyi Biotec Ltd, Surrey, UK) and suspended in Radioimmunoprecipitation assay (RIPA) extraction buffer (Fisher Scientific, Loughborough, UK) supplemented with 1% Halt Protease and Phosphatase Inhibitor Cocktail (PI) (Thermo Scientific, Loughborough, UK). The tissue was dissected with clean scissors on ice as quickly as possible to prevent degradation by proteases and then homogenised using a GentleMacs dissociator program protein 0101. Then the sample was centrifuged at 3400 x *g* for 5 minutes at 4ºC.

2.6.1.1. Protein Concentration using Coomassie Blue

The protein concentration of each sample was quantified using Coomassie-Plus Reagent (Thermo Scientific Pierce, Northumberland, UK). Coomassie Blue, 1 ml, was pipetted into a cuvette to equilibrate at room temperature for 15 - 20 minutes. Samples were compared with BSA concentration standards using Spectrophotometry. Sample, 1 µl, was added to 1ml Coomassie Blue. Next, it was pipetted up and down to distribute and leave to incubate at room temperature for 10 minutes. The UV/Visible Spectrophotometer (Ultrospec 3100 pro, Amersham Biosciences) was set to read at 595 nm, and the reference was set using Coomassie Blue with no added protein. BSA was used in increasing concentrations to obtain absorbance readings, which were then plotted against their known concentrations to create a standard curve. The absorbance

was then read from unknown samples and plotted them against the standard curve to determine protein concentration.

2.6.2. Protein Purification Method

Preliminary experiments showed that different protein concentrations between 20 and 30 μg either failed to detect the phosphorylated antibodies. Protein purification was performed to allow a sufficient sample to be loaded onto the gels. Following centrifugation and protein measurements, lysates were transferred to Vivaspin tubes (Sartorius Mechatronics Ltd, Epsom, UK) with filter capacity adjusted to the molecular weight of protein of interest. The sample was loaded into Vivaspin tube from the round end, the top was secured, then centrifuged at 300 x *g* for 5 minutes. Filtrate with molecular weight less than the protein of interest in the pointed end was then removed. The tube was then inverted with the round end pointing downwards. The pointed end was then attached to the round end, then centrifuged again at 300 x *g* for 5 minutes. Lysates with molecular weight more than protein of interest molecular weight were than collected in the rounded end of the tube and protein concentration was measured again using Coomassie-Plus reagent (Thermo Scientific Pierce).

2.6.3. Protein Separation and Transfer

Protein samples were added to an equal volume sample buffer (detailed in each chapter) and denatured at 95 - 100^{o}C for 5 - 10 minutes. Depending on the experiments, equal amounts of lysates (between 20 - 30 μg) was loaded onto the wells of the sodium dodecyl sulphate (SDS) polyacrylamide gel electrophoresis (SDS-PAGE), along with molecular weight marker (PageRuler^{TM} Plus; Thermo Scientific). Gels were run at 125 V for 1 hour or until the loading dye had reached the bottom of the gel. Gels were rinsed in distilled water (dH_2O) prior to use. Nitrocellulose membranes (Amersham

Pharmacia) and 4 pieces of filter papers were cut to size and soaked in transfer buffer for at least 2 minutes. The transfer sandwich was then assembled, and the roller was utilised to ensure there were no air bubbles trapped underneath the gels. The gels were run in chilled transfer buffer with the time and voltage adjusted to the protein molecular weight.

2.6.4. Antibody Incubations, Chemiluminescence Detection

After transfer, the nitrocellulose membranes were blocked in BSA (5%) in TBST for 1 hour at room temperature with gentle agitation. The membranes were then probed with appropriate dilutions of primary antibody in blocking buffer overnight at 4^{o}C with gentle agitation. The following day, blots were washed in 0.1% TBST 5 times for 5 minutes each and then incubated with appropriate secondary antibodies in 5% BSA for 1 hour at room temperature. After 5 x 5 minutes washes in TBST, the signal was developed. To enhance chemiluminescence detection, nitrocellulose membranes were placed in Amersham (ECL) prime western blotting detection reagent (GE health care) for 1 minute, and exposed to autoradiographic film for different lengths of time in the darkroom and then paced in the developer until bands appeared, briefly rinsed with water and then placed in fixer. Western blots were digitally scanned and analysed using ImageJ. All analysis was normalised to alpha tubulin.

2.7. Commonly Used Solutions

2.7.1. Sodium Citrate

The stock solution of 0.1 M sodium citrate was made by dissolving 29.4 g dihydrate tri-sodium citrate in 1000 ml of dH_2O. The pH was altered to 6.0 with sodium hydroxide (all Sigma-Aldrich). When used, 900 ml of dH_2O was added to 100 ml stock solution to reach a final concentration of 10 mM.

2.7.2. PBS and PBST

PBS used was prepared by dissolving 5 PBS tablets (Sigma-Aldrich) into 1000 ml of distilled water. PBST was made by adding 1 ml of triton X-100 to 1000 ml of PBS.

2.7.3. TBS and TBST

A stock of 10x TBS was made by adding 2 tablets of TBS (Sigma-Aldrich) to 1000 ml of dH_2O. TBS x 1 was used in experiments by diluting 100 ml of stock solution in 1000 ml dH_2O. TBST was prepared by dissolving 0.5 ml -1 ml of tween 20 (Sigma Aldrich) to 1000 ml TBS.

2.7.4. Transfer Buffer

Transfer buffer for western blotting was prepared by adding 6 g tris buffer, 28.6 g glycine, 400 ml methanol to 1.6 l dH_2O (All Fisher scientific, UK Ltd).

2.8. Statistical Analysis

Statistical Package for the Social Sciences (SPSS) version 22 (SPSS, Inc., Chicago, USA) and Graph Pad version 7 (chapter 3) and version 8 (chapter 4) (GraphPad Inc., San Diego, California, USA) Statistical Software were used to analyse the data. The analysis of qualitative data was run by Chi-square or Fisher exact test as appropriate. Quantitative data were analysed either by one-way ANOVA for normally distributed data or by the Kruskal Wallis test with Dunn's Bonferroni test (post hoc test for Kruskal Wallis provided by SPSS) for data that was not normally distributed. Quantitative data were presented as mean ± SEM and as percentage for qualitative. Statistical significance was assigned at $p < 0.05$.

Chapter 3

Effects of PTEN Inhibition on DNA Damage and DNA Damage Repair Capacity of Oocytes and Granulosa Cells *In vitro*

3.1. Introduction

The data in this chapter have been published in the journal Human Reproduction 2019 Feb 1;34(2):297-307. doi: 10.1093/humrep/dey354.

Since it was demonstrated that rodent immature oocytes could be developed to maturity *in vitro* (Eppig and Schroeder, 1989, Eppig and O'Brien, 1996), efforts have been made to apply this to larger mammalian species such as human (Telfer *et al.*, 2008) and bovine (McLaughlin *et al.*, 2010a, McLaughlin *et al.*, 2018). A great deal of research has concentrated on trying to increase oocyte yield and improve oocyte quality by enhancing primordial follicle activation and the subsequent development of growing follicles. However, the safety and efficacy of this accelerated follicle activation and growth is still questionable. This process may lead to a deterioration in the quality of oocytes as they undergo further development and has been associated with ovarian pathology in mice (Kim *et al.*, 2015, Kim *et al.*, 2016). Further investigations into how manipulating activation of primordial follicles affects oocyte development are essential to improve oocyte quality *in vitro* (Van den Hurk *et al.*, 2000).

As explained in chapter 1, a limited control of primordial follicle growth and activation is the main difference between *in vitro* and *in vivo* follicle growth system (Smitz and Cortvrindt, 2002). Within *in vitro* culture systems, rapid and precocious growth of several primordial follicles is more likely to occur (Bertoldo *et al.*, 2018). Attempts to increase primordial follicle activation *in vitro* may lead to a disintegration of oocyte and granulosa cells coordination (Bertoldo *et al.*, 2018) that might be linked to poor oocyte yield and quality.

It has been demonstrated that the PI3K signalling pathway has an important role in regulating the activation of primordial follicles (Adhikari and Liu, 2009, Liu *et al.*, 2006) as well as being a primary pathway in cancer cell pathology (Lee and Chang, 2019). Activation of this pathway has been shown to induce malignancy, is associated with poor disease prognosis, and increases drug resistance (Lee and Chang, 2019). Akt activation during cell cycles in normal cell proliferation upregulates numerous substrates at the G1/S and G2/M transition, some of which are involved in DNA damage repair pathway. Several publications involving Akt activation in cancer cell pathology (Plo *et al.*, 2008, Puc and Parsons, 2005, Thacker, 2005) support the idea that oocytes lacking PTEN may accumulate DNA damage, with reduced DNA damage repair capacity. Unrepaired DNA DSBs may potentially impact upon the quality of oocytes (Carroll and Marangos, 2013, Oktay *et al.*, 2015, Winship *et al.*, 2018).

It is, however, worth noting that analysis of follicle survival in studies involving the IVG system has been limited to morphologically healthy follicles and apoptosis markers (Bezerra *et al.*, 2018a, Bezerra *et al.*, 2018b, Dubey *et al.*, 2011, Santos *et al.*, 2014). Additional insights into DDR defects may provide a better understanding of how to support oocyte development *in vitro,* given that they are the starting events of apoptosis and can be detected even in the absence of morphological changes. The overall aim of the experiments described in this chapter was to determine whether PTEN inhibition affected DNA damage and repair mechanisms in bovine ovarian follicles activated *in vitro*, using a serum-free culture system.

3.2. Materials and Methods

3.2.1. Ovarian Cortical Tissue Collection and Preparation

Bovine ovaries were collected and transported to the lab as described in chapter 2 section 2.1.1. Then the tissue was cut and prepared as described in section 2.1.3.

3.2.2. Ovarian Tissue Fragments Culture

Basic culture medium was prepared as described in section 2.1. Following tissue preparation and cutting, 10 to 12 fragments per culture were randomly selected as 0-hour control for histological examination. The remaining tissue fragments were cultured in flat-bottomed 24-well culture plates containing 300 µl basic culture medium or culture medium supplemented with the PTEN inhibitor, (bpv(HOpic) (Merck Millipore chemicals Ltd, UK), at 1 or 10 µM. After 24 hours, all media was removed and replaced with fresh basic culture medium. At this point 6 - 9 tissue fragments from each group were snap-frozen and stored at -80ºC for western blot analysis of Akt phosphorylation. Remaining tissue fragments were incubated for a further 5 days, with half the media removed and replaced with fresh every 2 days. On completion of the culture period, all remaining tissue fragments were fixed in 10% NBF for histological examination to determine the effect of PTEN inhibitor on follicle development (Figure 3.1).

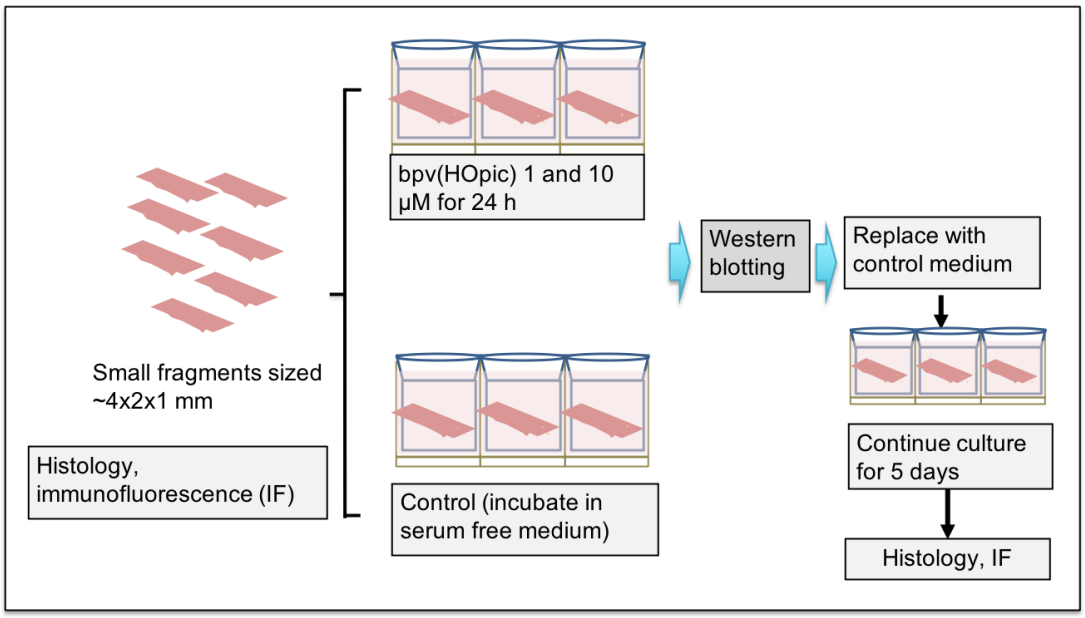

Figure 3.1. Experimental design. Small ovarian cortical fragments were cultured individually in 24 cultured plate in culture medium and medium containing either 1 or 10 µM bpv(HOpic), *in vitro* for 24 hours. A sub-group of tissue fragments were collected for western blot analysis after bpv(HOpic) exposure. The remainder were incubated in control medium for a further 5 days and then analysed histologically and by immunohistochemistry to detect DNA damage and repair pathways.

3.2.3. Histological Methods and Tissue Analysis

Details of histological analysis was as in chapter 2 section 2.4. In brief, after fixation in NBF for 24 hours, tissue fragments were further processed and embedded individually into paraffin wax blocks and serially sectioned at 5 µm thickness. At least four adjacent sections from each tissue sample from the start and end of the tissue were used for H & E staining, and six sections in the middle were used for immunohistochemistry and immunofluorescence. For all morphological and numerical analyses, the examiner was blinded to the treatment groups. The follicles were analysed on every section under the light microscope with a crossed micrometre under x40 magnification. Follicle developmental stage was categorised using a modification of an established system (Pedersen and Peters, 1968). Primordial and

transitory follicles were classified as non-growing follicles. The number of follicles within each stage of development was recorded, for D0 and D6 of each treatment. The proportion of follicles at different developmental stages was defined as a percentage of morphologically healthy follicles over the total follicle count.

3.2.3.1. Immunohistochemistry

Quantitative analysis of DNA damage was performed using immunofluorescence. DNA damage repair proteins were localised in tissue sections using antibodies against γH2AX, MRE11, ATM, BRCA1, BRCA2, and Rad51 (Table 3.1). Immunohistochemistry protocol was run as described in chapter 2 section 2.5.1. Antigen retrieval was performed by microwaving the slides in 10 mM sodium citrate (pH 6.0) at simmer setting for 20 minutes. The endogenous peroxidase activity was then quenched. Sections were then incubated with appropriate blocking solution (Table 3.1) for 1 hour at room temperature. Excess serum was shaken off the slides and primary antibody applied. Primary antibodies were omitted in the slides for negative control and replaced with blocking solution. On the following day, primary antibody was washed off, and sections were incubated for 30 minutes with biotinylated secondary antibody (Table 3.2). Slides were then incubated with Streptavidin Horseradish Peroxidase (Streptavidin horse-radish peroxidase (HRP)) for 30 minutes at room temperature. Following a TBST wash DAB peroxidase substrate kit solution was applied and counterstained with haematoxylin.

Immunohistochemical analysis was made in both oocytes and granulosa cells, as these two types of cells have a different response to DDR and every stage of follicular development has a distinct surveillance mechanism. The proportion of oocytes positive

for DNA repair protein was the number of follicles with oocytes positive for DNA repair protein expression in the nucleus over a total number of follicles at the same stage. While granulosa cells positive for DNA repair protein defined as the average proportion of the number of granulosa cells positive for DNA repair protein expression in the nucleus per the total number of granulosa cells per follicle. Non-nuclear detection for FOXO3 as a marker of activation defined as the number of follicles with negative staining for FOXO3 in the nucleus of the oocytes per total number of follicles.

3.2.3.2. Immunofluorescence

Localisation of γH2AX (a marker of DNA damage) was detected and quantify by immunofluorescence. Immunofluorescence pAkt Ser473 was performed only to show the pAkt Ser473 localisation within the follicles (Figure 3.3 B 1-5), whilst the quantification was made by western blot analysis.

As previously described, mounted tissue sections were deparaffinised and rehydrated and then washed in 0.1% PBST. Slides were then subjected to high-temperature antigen retrieval for 20 minutes using a microwave. After 20 minutes, the slides were let to cool for at least 20 minutes in room temperature. After several washes in PBS, slides were incubated for 1 hour at room temperature with blocking solution (5% goat serum in PBST). Tissue sections were then probed with primary antibody (Table 3.1) overnight at 4ºC. Blocking solution without primary antibody served as a negative control. Sections were then incubated with appropriate secondary antibodies (Table 3.2) for 1 hour on the following day, and then washed and mounted in vectashield hardset with DAPI.

Images were captured using a Zeiss LSM 800 confocal microscope with x20

magnification in the IMPACT imaging facility (Centre for Discovery Brain Sciences, The University of Edinburgh). A tiling that focused on the area with the presence of follicles was set to obtain a full image of every section. Images were analysed using ImageJ and γH2AX expression in oocytes and granulosa cells was determined. The number of oocytes with γH2AX foci per total number of follicles was calculated. The γH2AX expression in granulosa cells was quantitatively analysed by manually calculating (using ImageJ) the number of γH2AX positive granulosa cells per total number of granulosa cells per follicle and expressed as percentage.

Table 3.1. Primary antibodies used for immunohistochemistry analysis

Blocking serum	Primary antibody	Product number	Species raised	Final concentration (stock solution)	Source
Goat serum (Sigma Aldrich)	γH2AX	NB100-384	Rabbit polyclonal	1 µg/ml (1 mg/ml)	Novusbio
Goat serum (Sigma Aldrich)	pAkt Ser473	ab81283	Rabbit monoclonal	1.30 µg/ml (0.259 mg/ml)	Abcam
Goat Serum Vectastain Elite Kit PK-6101, Vector Laboratories, California, USA. 150 µl horse serum+ 10 ml TBST	Rad51	137323	Rabbit monoclonal	2.22 µg/ml (1.11 mg/ml)	Abcam
	MRE-11	NB100-142	Rabbit polyclonal	1.89 µg/ml (1.89 mg/ml)	Novusbio
	BRCA1	Ab16781	Rabbit polyclonal	0.5 µg/ml (0.1 mg/ml)	Abcam
	BRCA2	Ab27976	Rabbit polyclonal	2.5 µg/ml (0.5 mg/ml)	Abcam
Horse Serum Vectastain Elite Kit PK-6102, Vector Laboratories, California, USA. 150 µl horse serum+ 10 ml TBST	ATM	ab78	Mouse monoclonal	3.70 µg/ml (1.85 mg/ml)	Abcam
Goat Serum Vectastain Elite Kit PK-6101, Vector Laboratories, California, USA. 150 µl horse serum+ 10 ml TBST	FOXO3	NBP2-24579	Rabbit polyclonal	1 µg/ml (0.5 mg/ml)	Novusbio

Table 3.2. Secondary antibodies used for immunohistochemistry analysis

Secondary antibody	Product number	Final concentration (stock solution)	Source
VECTASTAIN Elite ABC HRP Kit (peroxidase, mouse IgG)	PK 6101	50 µl biotinylated secondary antibody+ 150 µl goat serum+ 10 ml TBST	Vector Laboratories
VECTASTAIN ABC-Elite ABC HRP Kit (peroxidase, mouse IgG)	PK 6102	50 µl biotinylated secondary antibody+ 150 µl horse serum+ 10 ml TBST	Vector Laboratories
Cy3 AffiniPure Donkey Anti-Rabbit IgG (H+L)	711-165-152	5.98 µg/ml (1.5 mg/ml)	Jackson Laboratories

3.2.4. Western Blotting

Six to nine ovarian cortical strips per group per experiment (4 replicates) were used for western blotting. Protein extraction and purification have been outlined in chapter 2 section 2.6.1 and 2.6.2. Vivaspin tubes with 50 kDa filters was utilised to obtain only protein with molecular weight more than 50 kDa included in the analysis. Protein samples were added to the same amount of a 2x sample buffer (Table 3.3). Lysates then denatured at 100ºC for 10 minutes. After brief centrifugation, 20 µg protein was loaded onto 4 - 20% gradient gels (Table 3.3) and run at 125 V for 1 hour. Proteins were transferred to nitrocellulose membranes (Amersham Pharmacia). BSA (5%) in TBST was used to block the nitrocellulose membranes. Blots were incubated, with primary antibodies (Table 3.4) and with a mouse monoclonal antibody against alpha-tubulin as a loading control, overnight at 4ºC with gentle agitation. On the following day, blots were washed and then incubated with appropriate secondary antibodies (Table 3.5) in 5% BSA for 1 hour at room temperature. Chemiluminescence detection was performed as described in chapter 2 section 2.6.4. Western blots were digitally scanned and analysed using ImageJ. All analysis was normalised to alpha tubulin.

Table 3.3. Gel and running buffer used for each antibody

Antibody	Molecular weight	Gel used	Sample buffer	Running buffer
Akt	60 kDa	NuPAGE Novex 4-12% Bis-tris Protein Gels (NP0321BOX)	Sample Buffer, laemli Concentrate (S3401-10VL)	Nupage MES SDS running buffer (NP0002)
pAkt Ser473	56 kDa			
pAkt Thr308	55 kDa			
Alpha tubulin	50 kDa			

Table 3.4. Primary antibodies used for western blotting

Primary antibody	Product number	Species raised	Final concentration (stock solution)	Source
Akt	9272	Rabbit polyclonal	0.01 µg/ml (34 µg/ml)	Cell Signalling
pAkt Ser473	ab81283	Rabbit monoclonal	0.52 µg/ml (0.259 mg/ml)	Abcam
pAkt Thr308	ab 105731	Mouse monoclonal	5 µg/ml (1 mg/ml)	Abcam
Alpha tubulin	ab7291	Mouse monoclonal	0.20 µg/ml (1 mg/ml)	Abcam

Table 3.5. Secondary antibodies used for western blotting

Secondary antibody	Product number	Final concentration (stock solution)	Source
Goat polyclonal antibody raised against mouse IgG (heavy and light chain)	115-035-146	0.16 µg/ml (0.8 mg/ml)	Jackson laboratory
Goat polyclonal antibody raised against rabbit IgG (H+L)	111-035-003	0.16 µg/ml (0.8 mg/ml)	Jackson laboratory

3.2.5. Statistical Analyses

All data were analysed using SPSS statistical software version 22 (SPSS, Inc., Chicago, USA) and the graph was generated by GraphPad Software version 7 Inc., San Diego, California, USA. Quantitative data were presented as mean ± SEM. Chi-square test was used to analyse the proportion of healthy and unhealthy follicles, the distribution of follicle stages and the proportion of oocytes expressing proteins related to DNA damage and DNA DSB repair. Granulosa cell expression of γH2AX, MRE11, ATM, Rad51, BRCA1, and BRCA2 and nuclear exclusion of FOXO3 were

determined using one-way ANOVA test followed by Bonferroni post hoc test. Western blotting was analysed using Kruskal Wallis. Statistical significance was assigned at $p < 0.05$.

3.4. Results

3.4.1. Analysis of Follicle Distribution

Histological sections of freshly fixed cortical fragments were analysed to determine the distribution of follicle proportion and developmental stage on D0. A total of 8833 follicles from 32 fragments (10 to 12 fragments per culture) were analysed. The most common type of follicle counted on D0 was non-growing follicles, which constituted 79.6 % of total follicle number, whereas the remainders were at the primary stage (19.0%) and secondary stage (1.4%) (Table 3.6). Additionally, more than 80.0% of the follicles at all stages on day 0 within the ovarian cortical strips were healthy (Figure 3.2). No antral follicles were observed at D0 in any tissue fragments.

3.4.2. Assessment of Follicle Distribution, Activation and Survival

Follicular activation was determined in all groups after 6 days of culture. Microscopic examination of 20,717 follicles from a total of 147 ovarian cortical tissue fragments (n = 15 - 18 fragments per group per culture) after 6 days of culture showed that the proportion of non-growing follicles reduced significantly in all groups compared to uncultured control (Table 3.6).

This reduction was balanced by a significant increase in the proportion of growing follicles either in cultured control or in bpv(HOpic) exposed tissue (primary and secondary follicles in D0: 20.4%, control: 70.5%, 1 μM bpv(HOpic): 78.6% and 10 μM bpv(HOpic): 88.7%) ($p \leq 0.001$). A higher proportion of growing follicles was observed in 10 μM bpv(HOpic) compared to control and 1 μM bpv(HOpic) ($p \leq 0.001$). Secondary follicles were the most mature growing follicle stage found in control and either of the treatments. The proportion of follicles progressing to the

secondary stage in the presence of bpv(HOpic) was significantly higher in 1 μM (9.7%, $p \leq 0.001$) and 10 μM (10.6%, $p \leq 0.001$) compared to control (6.2%). Nonetheless, it was similar in 1 and 10 μM bpv(HOpic) ($p = 0.530$) (Table 3.6).

Table 3.6. Total number of follicles in each treatment group, at day 0 and after 6 days of culture.

Group		Non-growing follicle n (%)	Primary follicle n (%)	Secondary follicle n (%)	Total
Day-0		7,029 (79.6) [a]	1,681 (19.0) [a]	123 (1.4) [a]	8,833
Control	6 days of culture	1,896 (29.5) [b]	4,129 (64.3) [b]	401 (6.2) [b]	6,426
1 μM bpv(HOpic)	6 days of culture	1,400 (21.4) [c]	4,513 (68.9) [c]	633 (9.7) [c]	6,546
10 μM bpv(HOpic)	6 days of culture	880 (11.4) [d]	6,047 (78.1) [d]	818 (10.6) [c]	7,745
			Total		**29,550**

(a), (b), (c) and (d) denote a significant difference between treatment groups. A significantly greater proportion of primary and secondary follicles were observed in treatment groups compared to control ($p < 0.05$), Chi test square test. p-value < 0.05 was considered significant.

Despite more growing follicles observed in bpv(HOpic) 10 μM group, a significant reduction in the proportion of morphologically healthy follicles was found in higher concentration bpv(HOpic) (non-growing: 67.8%, primary: 47.9%, secondary: 41.0%) compared to lower concentration (non-growing: 80.2 %, primary: 77.6 %, secondary: 74.9 %) and control group (non-growing: 81.6 %, primary: 76.4 %, secondary: 77.1%) ($p < 0.05$). The lower concentration of bpv(HOpic) had no significant effect vs control group for all follicle types (non-growing, $p = 0.960$, primary, $p = 0.181$, secondary, $p = 0.133$) (Figure 3.2).

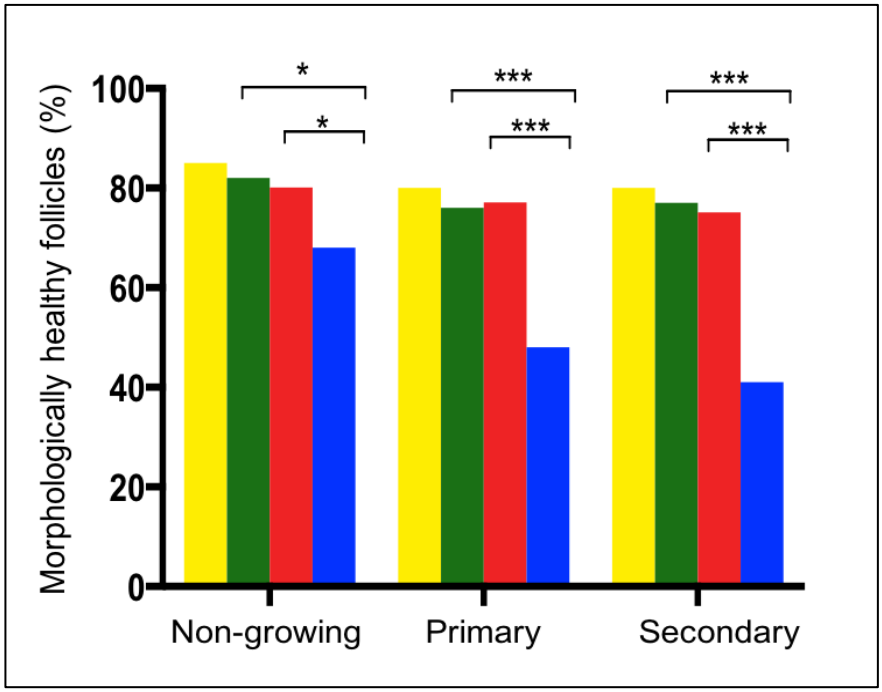

Figure 3.2. Proportion of morphologically healthy follicles at each stage of development. D0 (yellow), control medium (green), 1 μM bpv(HOpic) (red), and 10 μM bpv(HOpic) (blue). Chi square test, p-value < 0.05 was considered significant, asterisk (***) ≤ 0.001, (**) ≤ 0.01, (*) < 0.05. The total number of follicles analysed for each stage and treatment is shown in Table 1. Data here represent the proportion that were classified as healthy.

3.4.3. The Effects of bpv(HOpic) on PI3K Downstream Pathway Activation

3.4.3.1. Initiation of Akt

We used immunofluorescence microscopy to visualise phosphorylation of pAkt Ser473 within the follicles. Once phosphorylated, Akt transport from cytoplasm to the inner membrane of oocytes and granulosa cells. However, as is shown in Figure 3.3, pAkt Ser473 expression was not detected in oocytes, but expression can be clearly seen in granulosa cells, particularly in activated follicles following 24 hours exposure to bpv(HOpic) (Figure 3.3 B 4-5).

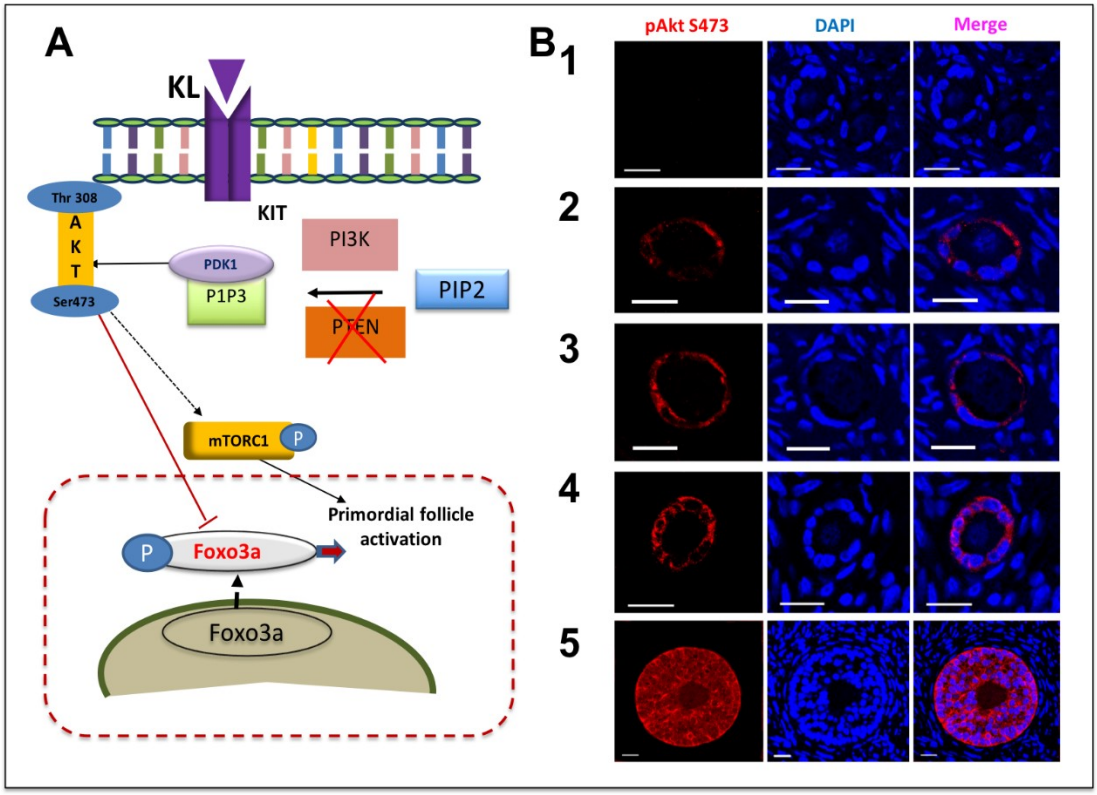

Figure 3.3. Akt activation as an effect of PI3K downstream pathway. A. A schematic Figure of PI3K/PTEN activation in the absence of PTEN. Full Akt activation is achieved after both sites are phosphorylated (Ser473 and Thr308). B. Immunofluorescence microscopy showing pAkt Ser473 localisation in follicles of (1) negative control, (2-3) non activated follicle in control group, (4-5) pAkt Ser473 location in activated follicles of (4) 1 µM bpv(HOpic) and (5) 10 µM bpv(HOpic). pAkt Ser473 expression is not seen in oocytes, but expression can be clearly observed in granulosa cells, particularly in activated follicles following 24 hours exposure to bpv(HOpic) Scale bar = 20 µm.

Western blot analysis of two Akt phosphorylation sites was conducted to quantify the effects of treatments in either higher or lower dose bpv(HOpic) on the activity of Akt as a downstream target of PTEN inhibition/PI3K activation. The western blot analysis was compared to control group (n = 4 replicates). Western blot analysis showed an increase in the ratio of pAkt Ser473 to Akt in bpv(HOpic) exposed tissue compared to control (2.25 ± 0.3 and 6.23 ± 1.1-fold higher in 1 and 10 µM bpv(HOpic) respectively ($p < 0.05$) (Figure 3.4 A, B 1). Full Akt activation is achieved after both

phosphorylation sites are activated. The relative expression of phosphorylated Akt at Thr308 increased 2.9 ± 0.16 and 5.8 ± 0.14-fold in tissue exposed to bpv(HOpic) 1 µM and 10 µM respectively compared to control ($p < 0.05$) (Figure 3.4 A, B 2).

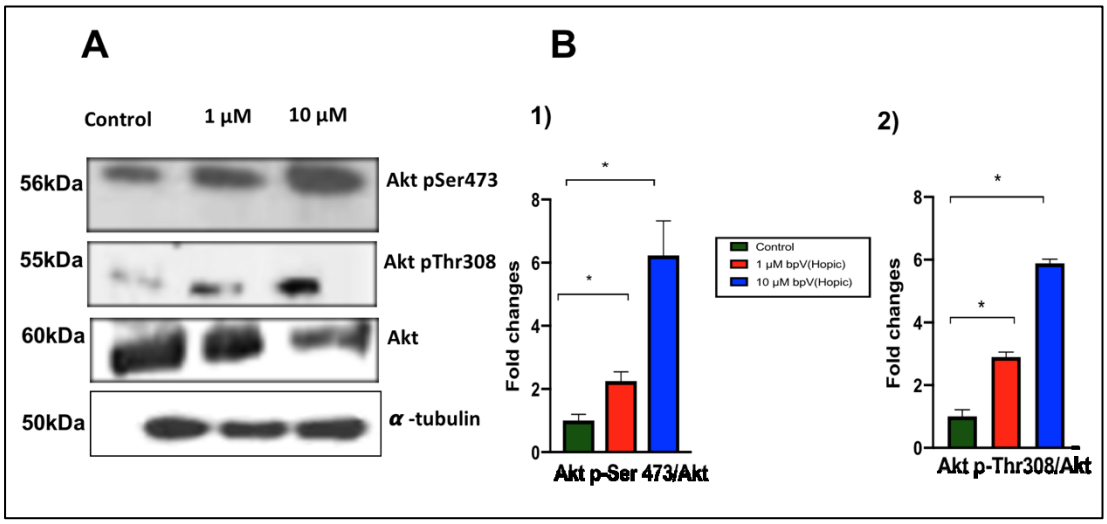

Figure 3.4. The ratio of pAkt Ser473 and Thr308 and Akt in control and bpv(HOpic) treated tissue. (A) Western blot showing phosphorylated Akt (pAkt) at both sites and total Akt expressions in all groups. (B) A significant increase in expression of (1) pAkt Ser473 and (2) Thr308 and Akt ratio in bpv(HOpic) groups compared to control. Kruskal Wallis, p-value was assigned at < 0.05. Green: control, red: 1 µM bpv(HOpic), blue: 10 µM bpv(HOpic).

3.4.3.2. Nuclear Exclusion of FOXO3

To examine the nuclear exclusion of FOXO3 as a downstream effect of PTEN inhibitor, FOXO3 localisation was determined by immunohistochemistry (Figure 3.5). A total of 1704 follicles were analysed over 3 separate cultures and the mean percentage ± SEM of oocytes showing non-nuclear detection of FOXO3 per total number of follicles was counted. Data were expressed as a proportion of follicles with non-nuclear detection of FOXO3 per total number of follicles of each ovarian fragment. A significant increase of follicles with nuclear exclusion of FOXO3 was perceived in tissue exposed to bpv(HOpic) 1 µM (69.1% ± 11.7) and 10 µM (81.2% ±

12.4) compared to controls (38.3% ± 9.2) ($p < 0.05$). Furthermore, the proportion of follicles with nuclear exclusion of FOXO3 was significantly higher in 10 µM bpv(HOpic) compared to 1 µM ($p = 0.02$) (Figure 3.5 D).

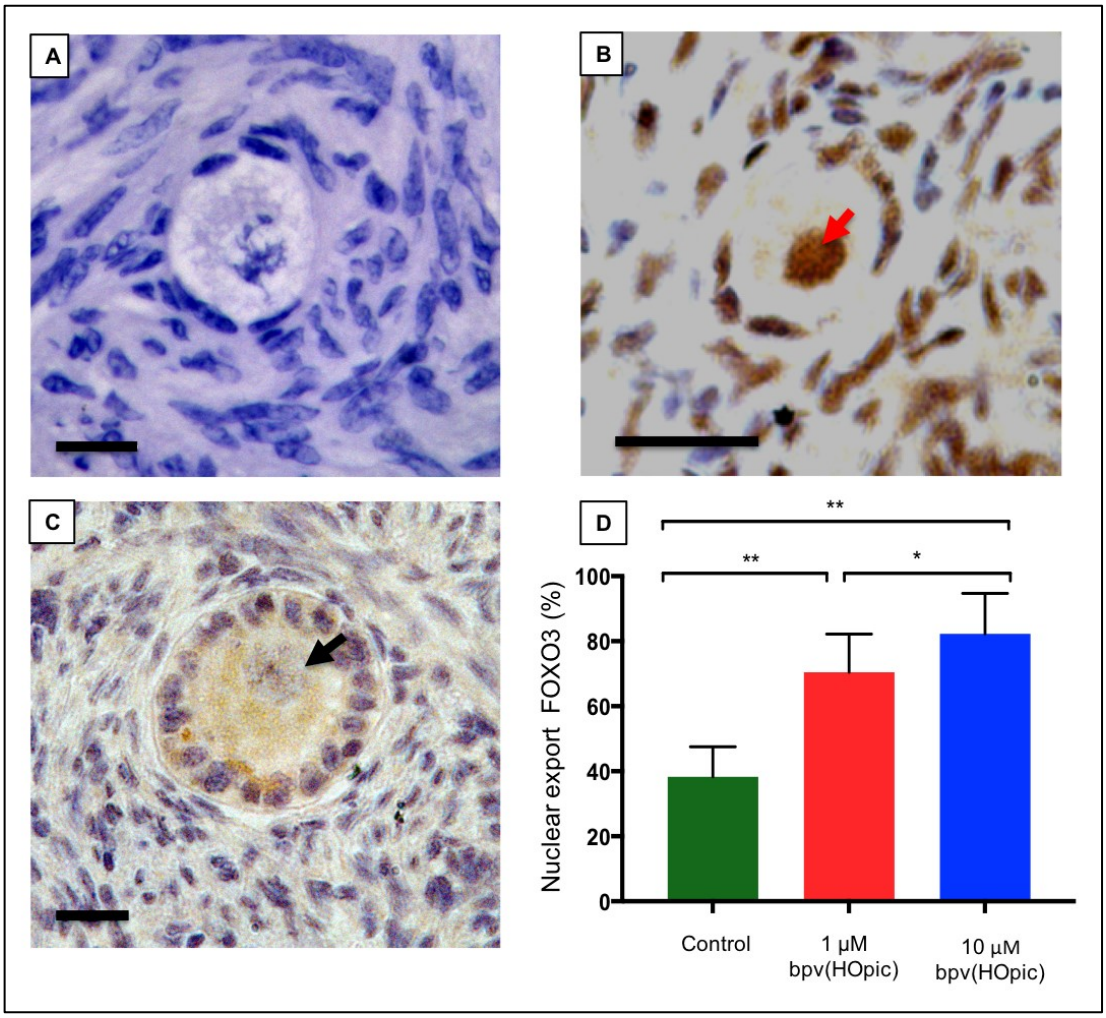

Figure 3.5. Analysis of FOXO3 localisation by immunohistochemistry. (A) Negative control, (B) FOXO3 was specifically expressed by oocytes of non-activated follicles indicated by brown staining in the nucleus (red arrow), (C) Once the follicle is activated, FOXO3 is shuttled from nucleus to cytoplasm (black arrow) as was seen in primary follicles in bpv(HOpic) group. Scale bar = 20 µm. (D) Comparison of oocyte nuclear export of FOXO3 in control and bpv(HOpic) groups. ANOVA and Bonferroni post hoc analysis, data show mean percentage ± SEM from 3 cultures per treatment. Asterisk (***) ≤ 0.001, (**) ≤ 0.01, (*) < 0.05.

3.4.4. The Effects of PTEN Inhibitor on DNA Damage

Immunohistochemistry and immunofluorescence were performed to characterise the effect of PTEN inhibitor on DNA damage and DSBs repair capacity of the oocytes of all ovarian section in all groups with antibodies against γH2AX, MRE11, ATM, BRCA1, BRCA2, and Rad51. All antibodies had never been tested in bovine, thus human ovarian biopsies of obstetric patients aged 23 and 24 years old and post cisplatin exposure adult mouse testis were used as positive controls for DSBs repair and γH2AX antigen. MRE11 was used as a representative marker for MRN complex activation (Figure 3.6). Mouse testis exposed to cisplatin was used as a positive control for γH2AX expression as cisplatin treatment induces DNA damage in testis (unpublished data). It cannot be predicted whether healthy ovarian tissue from obstetric patients can be used as a positive control for DNA repairs (MRE11, ATM, Rad51, BRCA1 and BRCA2) as they will be activated once cells are exposed to DNA damage. However, it has been shown that patients of a young age exhibit a functional DDR, thus oocytes will contain the relevant repair proteins (Lin *et al.*, 2017, Titus *et al.*, 2013). Primordial follicles that are expected to be high in young obstetric patients, are known to be sensitive to DNA induced damage. Primordial follicles also display a well preserve DNA repair mechanism (Winship *et al.*, 2018). It has been reported that DNA repair proteins significantly increase in ovarian tissue of young patients. In addition, during reproductive life, DNA repair proteins help cells to survive damage that may arise as a normal by product of cell activity (Jackson and Bartek, 2009). This is the basis for choosing ovarian tissue from young obstetric patients as a positive control.

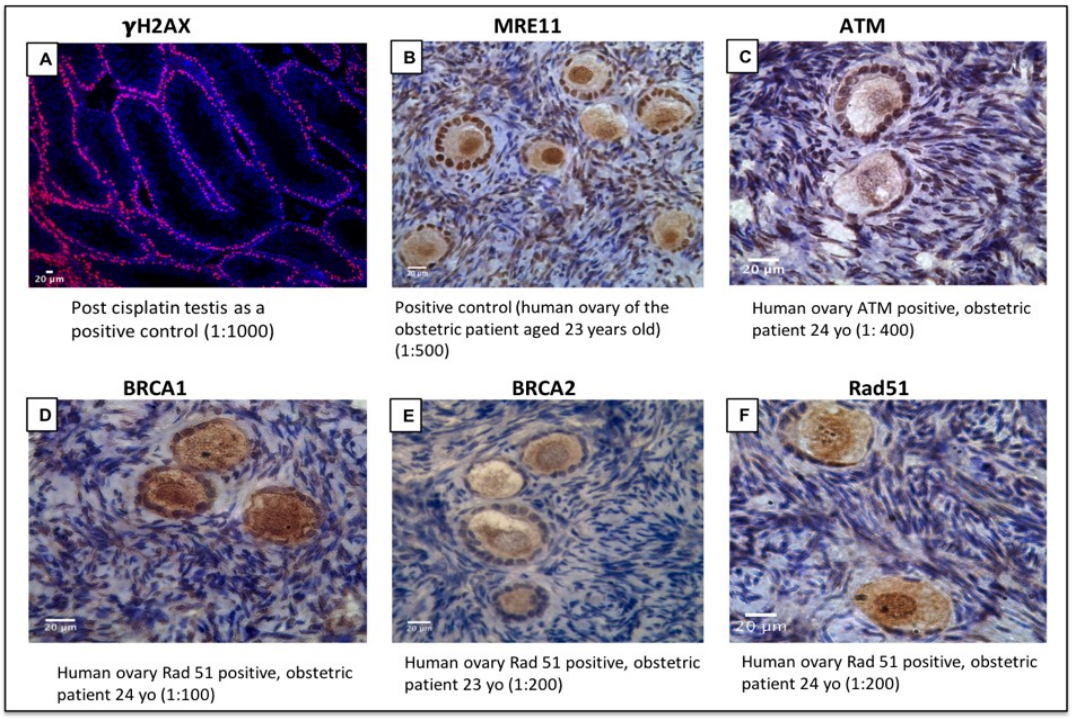

Figure 3.6. Positive control of antibodies used to examine DNA damage and DNA repair proteins. (A) Mouse testis following cisplatin exposure was utilised as a positive control of γH2AX antibody. Human ovaries from obstetric patients were used as a positive control for (B) MRE11, (C) ATM, (D) BRCA1, (E) BRCA2 and (F) Rad51.

γH2AX co-localisation in each group was analysed in oocytes (Figure 3.7 A-E) and granulosa cells (Figure 3.7 F-H). Analysis of 567 follicles from 3 independent experiments after six days of culture showed that the proportion of oocytes positive for γH2AX was markedly reduced from 79.0% (D0) to 30.0% and 59.0% in non-growing and primary follicles respectively ($p < 0.001$) (Figure 3.7 I). Culture did not affect γH2AX expression in oocytes of secondary follicles. However, bpv(HOpic) increased γH2AX expression in oocytes of all follicle types at both concentrations of bpv(HO)pic (1 μM: non-growing, 83.0%; primary, 76.0%; secondary, 77%; 10 μM: non-growing, 77.0%; primary, 84.0%; secondary, 89.0%) ($p < 0.05$), with no alteration between doses (Figure 3.7 I). While in the most mature follicles, DNA damage was

lower on D0 (25.0%) compared to control (50.0%) ($p < 0.001$). Nonetheless, an increase was seen in both treatment groups (77 vs 89%) compared to control (bpv(HOpic 1 μM, $p < 0.05$; bpv(HOpic) 10 μM, $p < 0.001$).

In granulosa cells, γH2AX expression in non-growing follicles did not significantly differ between groups (Figure 3.6 J). Similarly, no significant differences were observed between D0, control and the lower concentration of bpv(HOpic) in primary follicles (Figure 3.7 J). A significant increase was observed in primary follicles in the higher (36.9 ± 4.2%) compared to the lower concentration (11.8 ± 3.39%) and control (16.9 ± 2.9%) ($p \leq 0.001$) (Figure 3.7 J). γH2AX expression in granulosa cells of secondary follicles were similar between D0 and control. A significant increases were found in both bpv(HOpic) groups (1 μM: 76.9 ± 12.2%, $p = 0.024$; 10 μM bpv(HOpic): 77.8 ± 14.0%, $p = 0.011$) compared to control (16.7 ± 16.7%). There was no significant difference between the two doses (Figure 3.7 F-J).

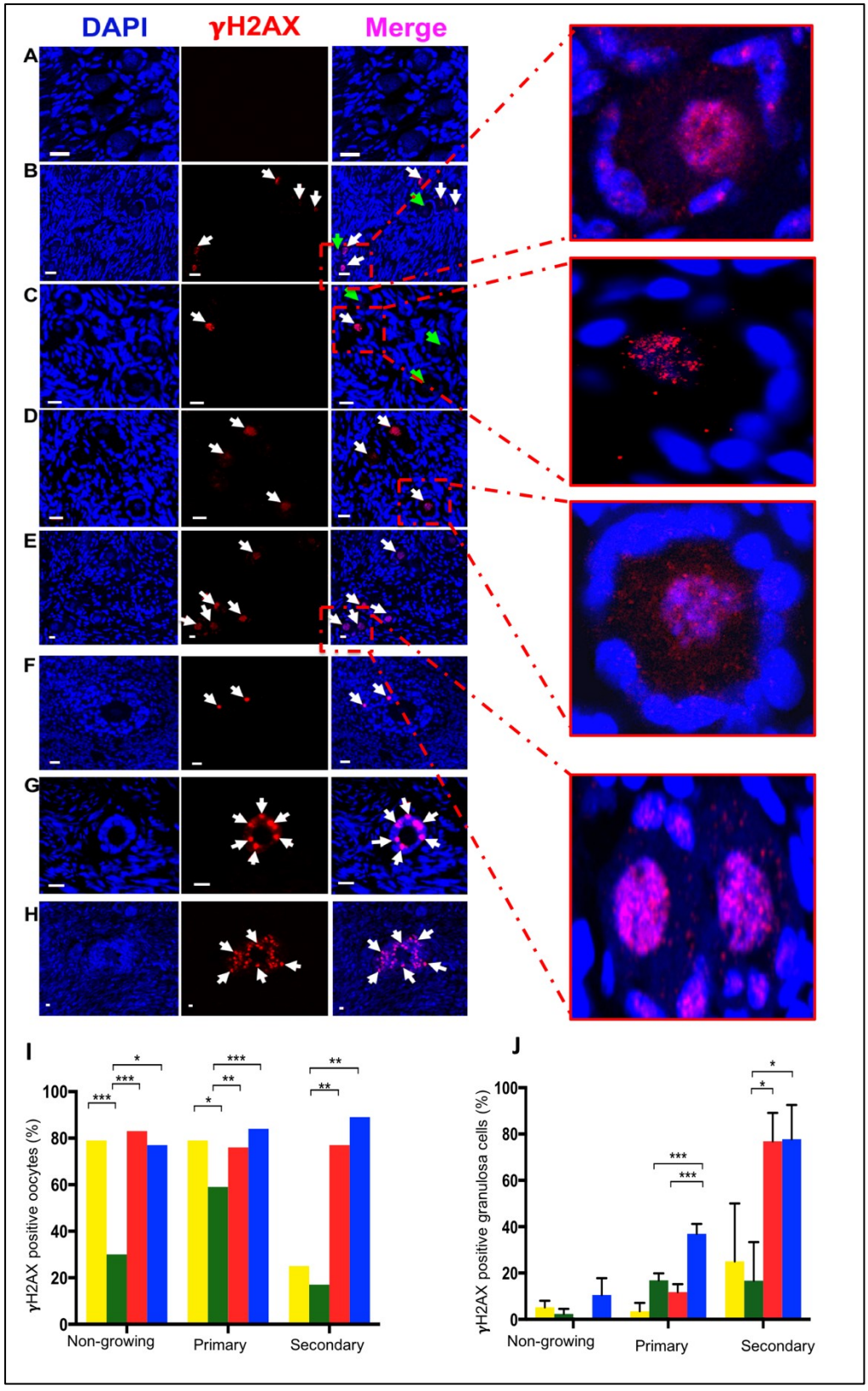

Figure 3.7. Representative images showing localisation by immunofluorescence of γH2AX bovine ovarian tissue in each treatment group. γH2AX (red) and DAPI (blue) staining in oocyte and

granulosa cells (A-H). γH2AX staining appeared as bright points (foci) within nuclei (white arrows) in oocytes (A-E). The green arrows indicate areas where there is no γH2AX expression. (A) Negative control, (B) γH2AX positive and negative in the oocytes of D0, (C) Positive and negative staining in cultured control, (D) Positive staining in 1 μM bpv(HOpic) and (E) 10 μM bpv(HOpic). Localisation of γH2AX expression (white arrows) in granulosa cells (F-H). (F) Control, (G) 1 μM and (H) 10 μM bpv(HOpic). Scale bar = 20 μm. Comparison of proportion of follicles showing γH2AX positive staining in the oocytes (I) and granulosa cells (J) in all groups. γH2AX expression was analysed using chi square test (oocytes) and ANOVA-Bonferroni post hoc test (granulosa cells). Data shows mean percentage ± SEM from 3 replicates. Asterisk (***) $p \leq 0.001$, (**) $p \leq 0.01$, (*) $p < 0.05$. Yellow, D0; green, cultured control; red, 1 μM bpv(HOpic) and blue, 10 μM bpv(HOpic).

3.4.5. The Effects of PTEN Inhibitor on DNA DSBs Repair Capacity in Follicles

To further investigate the effects of PTEN inhibitor on DNA DSBs repair capacity of both oocytes and granulosa cells, protein expression of each stage of key DNA repair pathway was analysed in all stages of follicle development after 6 days of culture. In contrast to γH2AX, MRE11 expression in oocytes within primary follicles in 1 μM (42.0%) and 10 μM (47.0%) declined significantly compared to control (68.0%) ($p \leq 0.001$) (Figure 3.8 A 1-5 and 3.9 A). The expression decreased significantly in oocytes of non-growing follicles in 10 μM bpv(HOPic) (44.1%) compared to control group (56.7%) ($p = 0.029$), and no significant changes observed between 1 μM bpv(HOPic) (57.6%) and control group ($p = 0.834$). Similarly, a significant reduction of MRE11 was observed in granulosa cells exposed to bpv(HOpic) in non-growing (1 μM: 41.2 ± 2.9%; 10 μM: 52.3 ± 3.9%) and primary follicles (1 μM: 56.2 ± 1.9%; 10 μM: 58.3 ± 2.5%), compared to control (non-growing: 75.9 ± 1.4% and primary follicles: 79.0 ± 1.8%) ($p < 0.05$ for all groups). It appeared that bpv(HOpic) did not affect MRE11

expression in granulosa cells of secondary follicles (Figure 3.9 B).

On the other hand, ATM expression was low in all treatment groups regardless of follicle types. bpv(HOpic) 1 and 10 µM reduced ATM expression in oocytes of non-growing from 41.6% in control group to 23.8% and 19.4% in 1 µM and 10 µM respectively ($p \leq 0.001$). Furthermore, the expression in primary and secondary follicles was reduced from 46.9% and 58.7 in control group to 26.0 and 10.0% in 1 µM bpv(HOpic) and 18.0 and 15.3 % in 10 µM bpv(HOpic) ($p \leq 0.001$) (Figure 3.8 B 1-5; Figure 3.9 C). In granulosa cells, ATM expression in bpv(HOpic) groups of non-growing and primary follicles was significantly lower compared to control ($p < 0.05$) (Figure 3.8 B and 3.9 D).

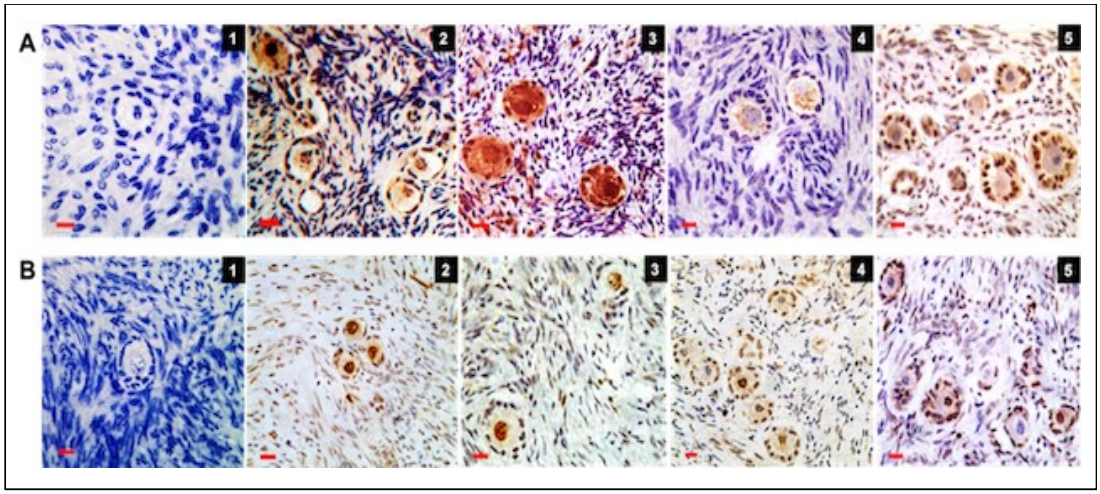

Figure 3.8. Immunohistochemical detection of MRE11 and ATM in oocytes and granulosa cells of follicles in all groups. Photomicrographs of (A) MRE11 localisation in oocytes and granulosa cells. (B) ATM expression in oocytes and granulosa cells. Negative control (1); positive staining (brown) in the oocytes and granulosa cells of D0 (2), control (3); 1 µM (4) and 10 µM bpv(HOpic) (5). Scale bar = 20 µm.

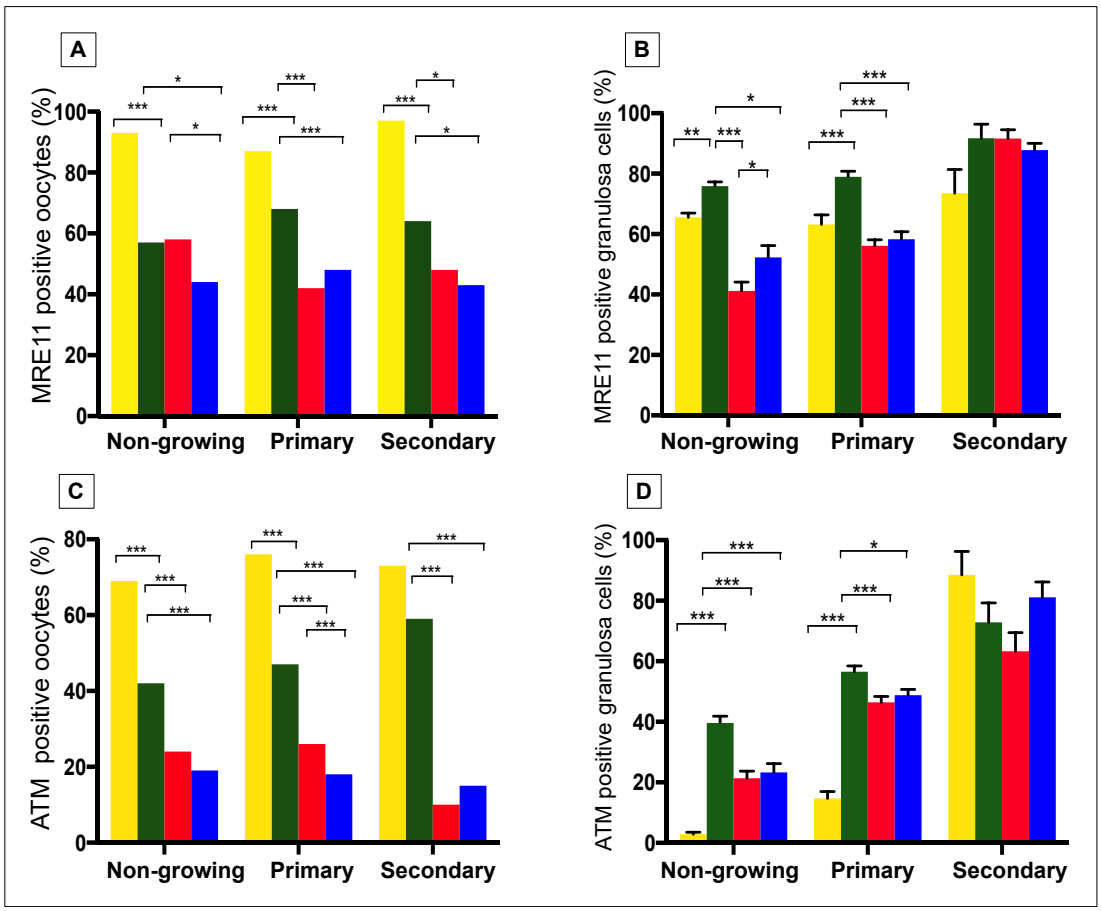

Figure 3.9. Immunohistochemistry analysis of MRE11 and ATM expression in oocytes and granulosa cells. (A) The proportion of MRE11 in oocytes and (B) granulosa cells, (C) ATM positive oocytes per total number of follicles in each stage of follicle development and (D) ATM positive in granulosa cells. MRE11 and ATM expression were analysed using chi square test (oocytes) and ANOVA-Bonferroni post hoc test (granulosa cells). Error bars show mean percentage ± SEM. Yellow bars, D0; green bars, cultured control; red bars, bpv(HOpic) 1 μM and blue bars, bpv(HOpic) 10 μM. The total number of follicles analysed: 4,659 (MRE) and 5,309 (ATM). Asterisk (***) ≤ 0.001, (**) ≤ 0.01, (*) < 0.05. p-value was assigned at < 0.05.

The impact of treatment on BRCA1, BRCA2, and RAD51 was also tested both in oocytes and granulosa cells (Figure 3.10 A-C). BRCA1 expression was upregulated in oocytes of non-growing and primary follicles in control group (19.0 vs 13.0% and 22.0 vs 14.0% in non-growing and primary follicles respectively) ($p < 0.05$). Lower dose

bpv(HOpic) did not significantly affect BRCA1 activity in oocytes all follicle types ($p > 0.05$). However, increasing the dose of bpv(HOpic) was sufficient to decrease the expression in 10 μM compared to 1 μM bpv(HOpic) and control group ($p < 0.001$) (Figure 3.10 A 1-5, 3.11 A). Similarly, BRCA1 expression was rarely expressed in granulosa cells of secondary follicles exposed to 10 μM bpv(HOpic) (Figure 3.11 B). However, primary follicles showed a different response to BRCA2 as culture condition did not significantly improve its expression in the oocytes (20.0%) compared to day 0 ($p < 0.001$). Surprisingly, it rose significantly in bpv(HOpic) 1 μM (36.0%, $p = 0.01$) but declined in bpv(HOpic) 10 μM ($p < 0.001$) (Figure 3.11 C). There was no significant difference in the expression within granulosa cells among all groups in growing follicles (Figure 3.10 B 1-5, 3.11 D).

It is intriguing that Rad51 activity was lower in oocytes of non-growing follicles following exposure to low dose (22.3%, $p = 0.002$)) but not to high dose (37.2%, $p > 0.05$) bpv(HOpic) compared to control (37.5%). In contrast, Rad51 expression in oocytes of primary follicles was significantly reduced in both bpv(HOpic) groups (control vs 1 and 10 μM bpv(HOpic): 48.0% vs 34.0% vs 24.0%) ($p < 0.05$), without significant changes in secondary follicles (Figure 3.10 C1-5, 3.11 E). Rad51 expression was observed infrequently (< 10%) in granulosa cells, mainly in secondary follicles with no significant changes observed among the groups ($p > 0.05$) (Figure 3.10 C1-5, 3.11 F).

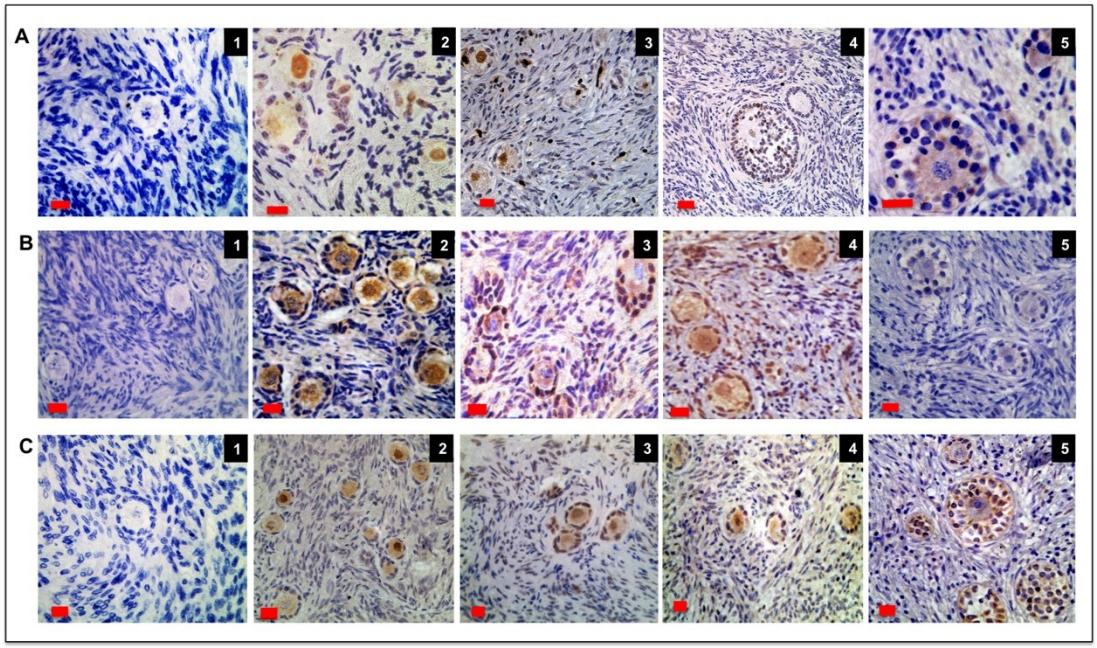

Figure 3.10. Immunohistochemical detection of BRCA1, BRCA2, and Rad51. Photomicrographs of BRCA1 (A1-5), BRCA2 (B1-5) and Rad51 (C1-5) expression in oocytes and granulosa cells. Negative control (A1, B1, C1); positive staining (brown) in the oocytes and granulosa cells of D0 (A2, B2, C2), control (A3, B3, C3); 1 µM (A4, B4, C4) and 10 µM bpv(HOpic) (A5, B5, C5). Scale bar = 20 µm.

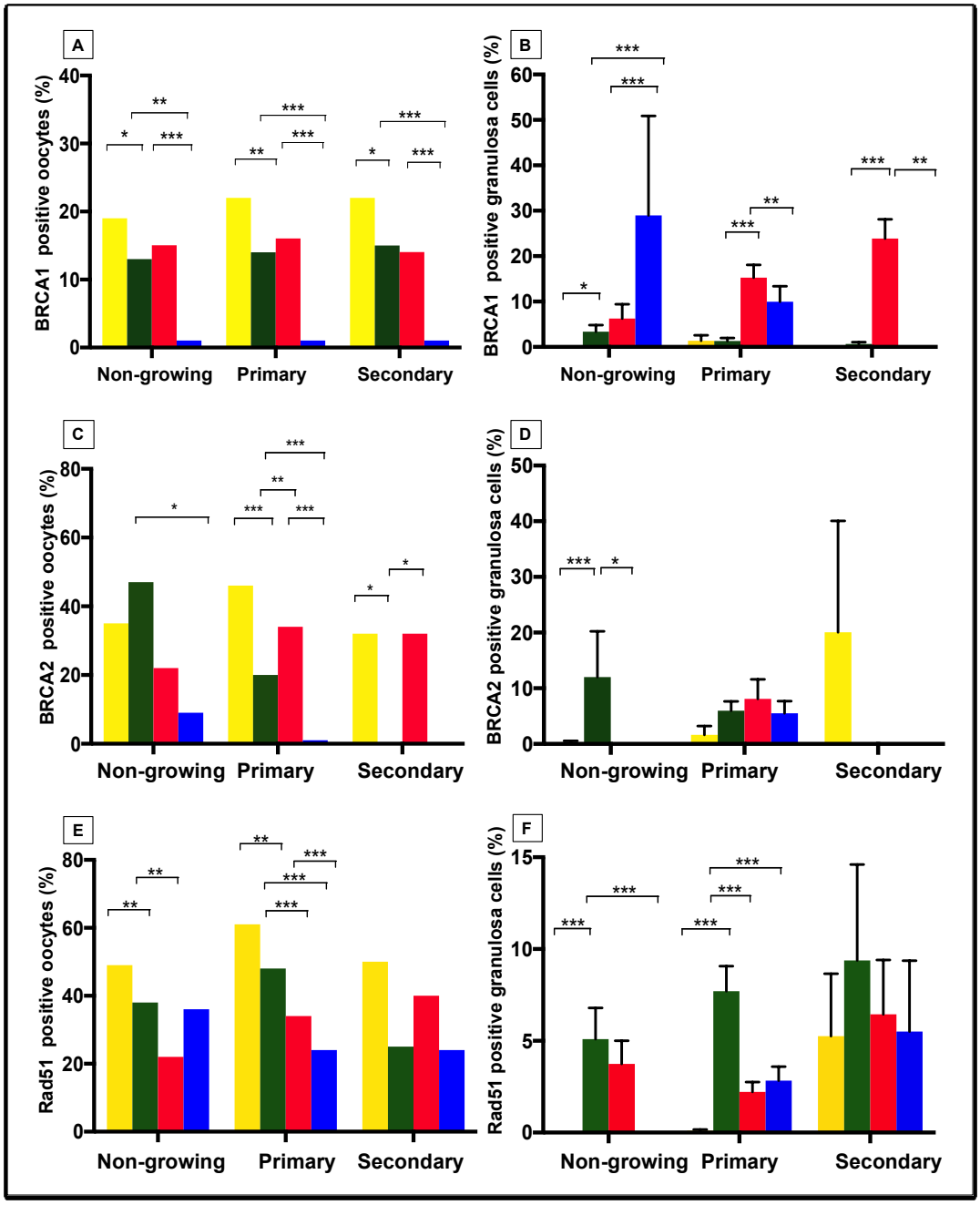

Figure 3.11. Immunohistochemistry analysis of BRCA1, BRCA2, and Rad51 in oocytes and granulosa cells. The proportion of oocytes (A, C and E) and granulosa cells (B, D and F) expressing BRCA1, BRCA2 and Rad51 in each treatment group. DNA repair protein eexpression was analysed using chi square test (oocytes) and ANOVA-Bonferroni post hoc test (granulosa cells). (Yellow bars, D0; green bars, control; red bars, bpv(HOpic) 1 μM and blue bars, bpv(HOpic) 10 μM). Analysis of 1,315 (BRCA1) 1,134 BRCA2) and 4,148 (Rad51) follicles. Asterisk (***) ≤ 0.001, (**) ≤ 0.01, (*) < 0.05).

3.5. Discussion

Bovine ovarian tissue fragments exposed to 1 and 10 μM bpv(HOpic) for 24 hours showed increased primordial follicle activation, consistent with our previous findings in human tissue (McLaughlin *et al.*, 2014). PI3K initiation as a downstream pathway of PTEN inhibition was confirmed by increased phosphorylated Akt at both phosphorylation sites in western blot analysis and non-nuclear detection of FOXO3 in the oocytes. However, the immunofluorescence staining to localise the pAkt Ser473 did not indicate the location in oocytes with most of the expression being observed in the membrane of granulosa cells, specifically within activated follicles. Negative expression in oocytes might indicate a weak pAkt expression or it could be due to the natural behaviour of the phosphorylated antibody particularly in immunohistochemistry (reviewed by (Mandell, 2008)). In addition, protein phosphorylation is recognised to alter the protein affinity toward its interacting partner and enzymatic activity (Goto and Inagaki, 2007). The weakness of western blot analysis is that it fails to localise the site of antigen expression in the tissue. In this context, the expression can be either in oocytes or granulosa cells. The quantification of pAkt using western blot analysis revealed an increase in bpv(HOpic) group and it has been previously demonstrated in mice that PI3K activation increases Akt phosphorylation in both granulosa cells and oocytes (Fan *et al.*, 2008, Reddy *et al.*, 2008).

An adverse effect on follicle morphological health was observed with the higher dose bpv(HOpic), in parallel with data from human ovary (Lerer-Serfaty *et al.*, 2013, McLaughlin *et al.*, 2014). The present data extended the observations from previous studies by demonstrating that enhanced activation coincided with increased DNA

damage and diminished DNA repair in ovarian follicles and oocytes in particular. The outcomes of the experiments in this chapter support the view that the PTEN/Akt/PI3K pathway implicates other intracellular pathways (Blanco-Aparicio *et al.*, 2007) that may have damaging effects on follicle growth. The initiation of PTEN/PI3K/Akt activity impacts on DNA damage and repair (Hunt *et al.*, 2012, Ming and He, 2012) and has a fundamental role in controlling the apoptosis cascade activity (Lu *et al.*, 2016, Weng *et al.*, 2001). As DNA damage precedes the apoptotic process and can exist without any significant morphological changes, we determined the effect of PTEN inhibition on DNA damage and DNA repair capacity of oocytes and granulosa cells. The cell's fate depends on the capability of cells to repair damage, as sufficient DNA damage repair function permits cells to resist apoptosis initiated by DNA damage (Kujjo *et al.*, 2010). It was shown that low concentrations bpv(HOpic) was sufficient to induce DNA damage and compromised DNA repair capacity of the follicles.

The DNA damage repair pathway encompasses γH2AX that binds exclusively to the site of damage and controls recruitment of DNA repair proteins to the locations of damage. We discovered that γH2AX expression was considerably higher in uncultured D0 tissue compared to control. Nevertheless, it was concomitant with increased expression of MRE11, ATM, Rad51 at all stages of follicle development. These data could indicate latent damage owing to mild injury during tissue preparation and transport that seems to be briskly resolved and may not trigger severe consequences. This type of damage can be restored without cell cycle arrest (Menezo *et al.*, 2010), as was denoted by the attenuation in γH2AX expression following tissue culture and there being fewer morphologically unhealthy follicles in the cultured control tissue. All

types of follicles in control cultures generated ample DNA repair capacity compared to treatment groups which may suggest a culture medium with a nutrient-rich milieu is valuable to cell metabolism (Paynter *et al.*, 1999).

DNA damage in the oocytes of both bpv(HOpic) treatment groups was not accompanied by increased DNA repair protein expression. In the DNA damage repair pathway, BRCA2 is essential in controlling the action of Rad51. Increased BRCA2 expression in oocytes was in parallel with the expression of Rad51 except in the higher dose of bpv(HOpic) of non-growing follicles wherein low level of BRCA2 was not associated with a change in Rad51 expression. In contrast, BRCA2 expression was elevated in 1 μM bpv(HOpic) exposed primary follicles, but was not related with enhanced Rad51 expression. This may imply compromised HR and designate Akt activation perturbs DNA damage repair protein interactions. This similar finding has previously been linked to ovarian ageing in human and mouse studies (Titus *et al.*, 2013). Nevertheless, BRCA1, BRCA2 and Rad51 expression reduced significantly in parallel with increased concentration of bpv(HOpic). It is worth noting that a reduction in DNA repair proteins can be an indication of reduced DNA damage, but in this study, DNA damage in the higher dose group was significantly increased. This data may suggest that DNA damage in follicles exposed to higher concentration bpv(HOpic) is severe resulting in limited repair capacity.

High γH2AX expression was detected in granulosa cells of growing follicles in the bpv(HOpic) treated groups. Nonetheless, DNA DSBs repair capacity of secondary follicles was not affected, except in BRCA1, which declined with higher dose bpv(HOpic). This finding may be related to the nature of granulosa cells in growing

follicles which are mitotically and metabolically very active that might substantially increase with Akt activity. In this regard, granulosa cells of secondary follicles are more susceptible to DNA induced damage. A reduction in granulosa cell DNA repair function seemed to arise more slowly than DNA damage, in parallel to the process occurred with ageing (Zhang *et al.*, 2015). However, a reduction in DNA repair capacity in the oocytes and granulosa cells may also indicate that the minimal impacts of the treatment on DNA damage.

It is intriguing that the proportion of morphologically normal follicles was similar between 1 μM bpv(HOpic) and control group regardless of the presence of DNA damage and lack of DNA repair capacity. However, as it has been reported that the growth of apparently healthy preantral follicles isolated from bpv(HOpic) group was eventually compromised following a further six days of culture (McLaughlin *et al.*, 2014). This finding may suggest that the dose of bpv(HOpic) also affects the time frame between the occurrence of DNA damage and apoptotic events.

It is worth considering the wider implication of these findings since PTEN inhibition has been utilised to stimulate primordial follicles in POI patients by incubating the tissue in medium containing Akt activators prior to grafting (Suzuki *et al.*, 2015). The present data imply that further investigation is required to determine whether the *in vivo* environment may overcome the DNA damage following ovarian tissue replacement after 48 hours incubation in PTEN inhibition. The impact of DNA damage on oocytes may range from meiotic dysfunction to cell death (Oktay *et al.*, 2015), possibly leading to reduced fertility (Adriaens *et al.*, 2009, Kirk and Lyon, 1982, Meirow *et al.*, 2001, Menezo *et al.*, 2007). It is reported that despite more than 50% of

oocytes with severe DNA DSBs ultimately resume meiosis, but none of these oocytes progress to M2 (Lin *et al.*, 2014). This implies that intact oocytes DNA DSBs repair capacity is vital to achieve mature and competent oocytes.

This study has depended upon the use of immunohistochemistry and of course there are limitations with this technique. It is important to consider the controls that are used, and it is worth noting that omitting the primary antibody to represent the negative control in the present study may be less appropriate for specificity of the primary antibody. It is important to substitute the primary antibody for a pre-immunised serum, ideally from the same animal or normal serum from the same species (Ivell *et al.*, 2014). Another method that would be appropriate is the use of immunoglobulin G (IgG) (Burry, 2011).

In summary (Figure 3.12), the experiments in this chapter demonstrate that increasing activity of the PI3/AKT pathway via a short exposure to bovine ovarian tissue fragments to bpv(HOpic) results in increased primordial follicle activation. However, this was accompanied by increased DNA damage and compromised DNA DSBs repair capacity, in both oocytes and granulosa cells. These findings highlight the complexities and interactions between the regulation of initiation of follicle growth and the maintenance of follicle health and indicate the need for caution in developing pharmacological approaches to manipulation of this pathway for clinical use.

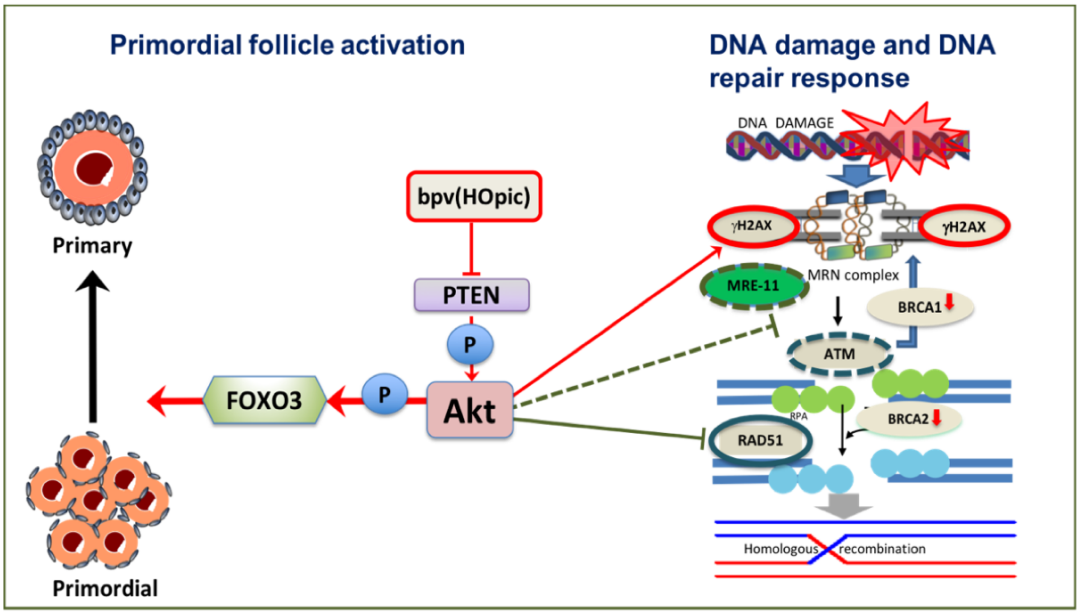

Figure 3.12. Summary of findings of the experiments in chapter 3. The presence of bpv(HOpic) in culture medium to inhibit PTEN is sufficient to induce primordial follicle activation, but it increases DNA damage and decreases DNA repair protein expression of MRE11, ATM and compromise HR indicated by low Rad51 expression. But it did not affect BRCA1 and BRCA2 expression. The increasing of BRCA2 expression in bpv(HOpic) of primary follicles that is not followed by increased Rad 51 expression may indicate compromised HR. These observations may suggest the association between Akt activation and defects in DNA damage repair protein interactions (Maidarti *et al.*, 2020).

Chapter 4

Modulation of PTEN and mTOR pathway: impact on primordial follicle activation and DDR of oocytes and granulosa cells *in vitro*

4.1. Introduction

As demonstrated in chapter 3, PTEN inhibition to trigger primordial follicle activation adversely affected the DDR of oocytes and granulosa cells in bovine ovarian cortical fragments. A reduction in DNA repair proteins and a resultant increase in DNA damage was observed. Whilst the influence of the Hippo signalling pathway in fragmenting the ovarian cortex was not fully explored, it is now well recognised that cutting the tissue into strips is associated with Hippo signalling pathway disruption and further augments follicle growth activation (Kawamura *et al.*, 2013). Activation of primordial follicles observed in tissue exposed to PTEN inhibition may reflect synergistic effects of Akt activation and Hippo signalling pathway disruption. Most importantly, massive disruption of Hippo signalling has been linked to cancer pathology (Fan *et al.*, 2017b) suggesting that DNA damage with limited repair may be due to mutual effects of both PI3K/Akt activation and Hippo pathway disruption.

Targeting the benefits of the fine balance between follicle growth acceleration and deceleration (Zhou *et al.*, 2017) through the PI3K/PTEN/Akt/mTORC pathway, substrates to inhibit mTORC have been investigated to protect ovaries against the damaging effects of chemotherapy, and to maintain ovarian function and fertility in mice (Goldman *et al.*, 2017). Inhibition of mTOR has been proven to reduce excessive primordial follicle activation and to maintain the primordial follicle pool (Adhikari *et al.*, 2013, Zhang *et al.*, 2013, Zhou *et al.*, 2017). Short exposure to a specific inhibitor of mTORC1 partially hindered follicular activation while improving follicle survival and steroidogenesis (Grosbois and Demeestere, 2018). However, it is still unclear whether the modulation of PI3K/Akt/mTOR substrate including either inhibition or activation of a part of this pathway affects DDR in oocytes and/or granulosa cells. The

aim of this chapter was to investigate whether the combination of modulation of PTEN inhibitor to activate primordial follicles and mTOR inhibitor to attenuate activation affected the DNA damage and DNA repair capacity of bovine ovarian follicles activated *in vitro*.

4.2. Material and Methods

4.2.1. Ovarian Cortical Fragments Collection and Preparation

Bovine ovaries were obtained from the abattoir and collected in culture medium as previously detailed in the material and methods section of Chapter 2 and 3.

4.2.2. The Screening Process to Determine Drug Concentrations

The bpv(HOpic) concentration selected in these experiments was based on the results presented in chapter 3. Only the lower concentration of bpv(HOpic), 1 μM, was used in the experiments of this chapter since the higher dose of bpv(HOpic) compromised follicle health. The rapamycin concentration was selected based on unpublished findings from the Telfer lab examining the effects of rapamycin on bovine primordial follicle activation. Several doses were included to find the lowest rapamycin concentration that might result in increased activation while minimising effects on DNA damage in oocytes *in vitro*. The doses of 0.01 pM and 0.1 nM rapamycin were included in the screening process to find the appropriate concentration. Screening was performed with analysis of morphologically activated primordial follicles and γH2AX expression from 2 independent experiments. The final concentration of Dimethyl sulfoxide (DMSO) used was 0.02%. The dose selection method, in detail, is presented in Figure 4.1.

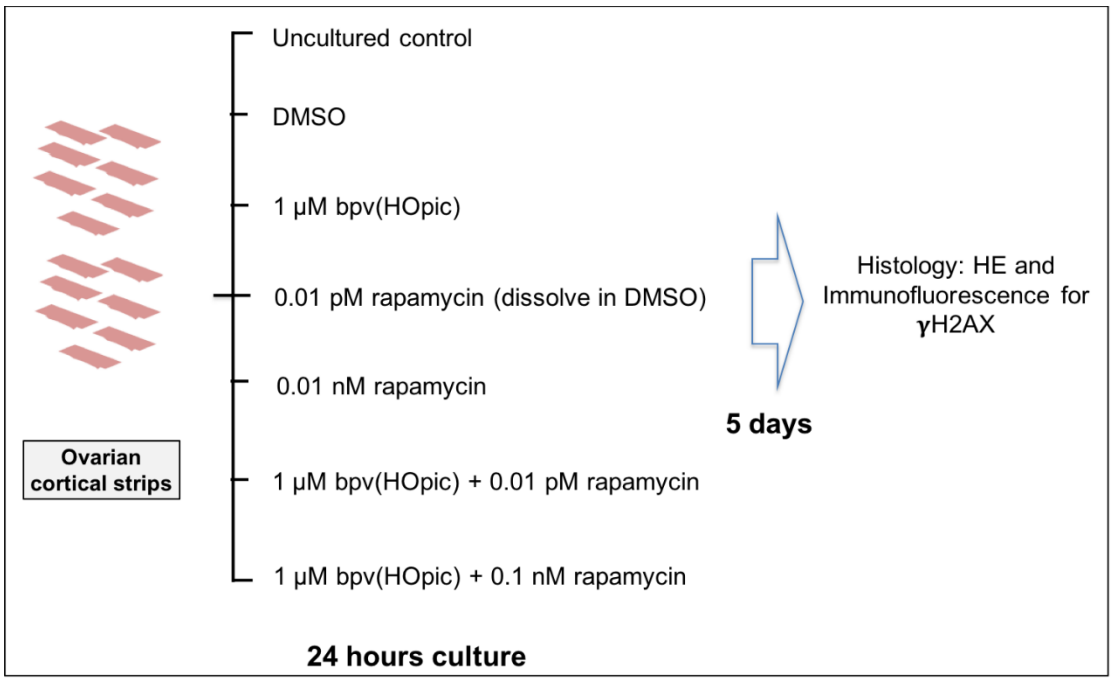

Figure 4.1. The screening process to determine the concentration used as the treatments.

4.2.3. Treatment and Culture

Four to six fragments per culture were selected as 0-hour controls for histological examination. The remaining tissue fragments were cultured in flat-bottomed 24-well culture plates containing 300 µl of DMSO as vehicle control, bpv(HOpic) and rapamycin either on their own or in combination, at 37°C in a humidified air atmosphere with 5% CO_2. After 24 hours, all media was removed from tissue fragments and replaced with fresh culture medium. Some tissue fragments from each group were subjected to western blot analysis. The remaining tissue fragments were cultured for an additional five days, with half the medium being removed and replaced every two days. After six days of culture, all fragments were fixed for histology and immunohistochemistry (Figure 4.2).

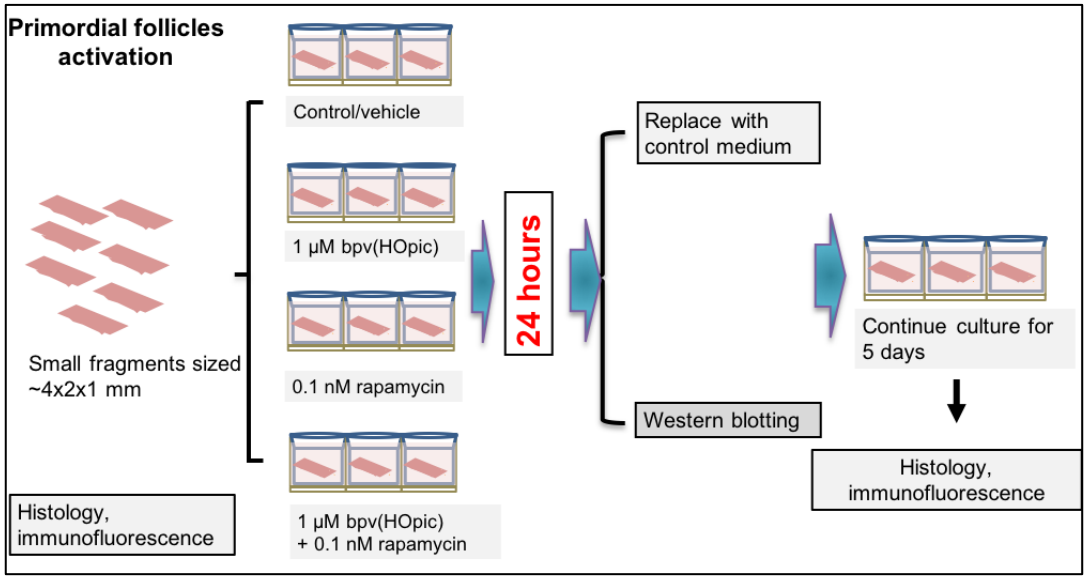

Figure 4.2. Experimental design to investigate the effects of the final treatment on DDR of follicles *in vitro*.

4.2.4. Histological Methods and Tissue Analysis

Follicle developmental stage was categorised using the same system as described in chapter 3. Oocytes and granulosa cells morphology were assessed by the same criteria as previously published with modifications (McLaughlin and Telfer, 2010, Telfer *et al.*, 2008). Immunohistochemistry and immunofluorescence microscopy protocols, including primary and secondary antibodies used, are as described in the material and methods section in chapter 2 and 3. Immunofluorescence images were captured using a Nikon A1R confocal microscope with x20 magnification. A tiling that focused on the area with the presence of follicles was set to obtain a full image of every section. Images were analysed using ImageJ as described in chapter 3 Section 3.2.3.2.

4.2.5. Western Blotting

Ovarian cortical strips (16 - 20 per group per experiment) were suspended in RIPA extraction buffer supplemented with 1% PI with the final concentration was 3x (30 ml/ml). The tissue was cut with scissors and homogenised using a GentleMacs

dissociator. The sample was centrifuged at 3400 x g for 5 minutes, and protein was purified using Vivaspin tubes with 10 kDa filters. Protein samples were denatured at 95ºC for 5 minutes, and 25 to 30 µg of protein sample was loaded onto gels (Table 4.1) and run at 125 V for 1 hour. Proteins were transferred to nitrocellulose membranes (Amersham Pharmacia). BSA (5%) in TBST was used to block the nitrocellulose membranes for 1 hour at room temperature. Blots were then incubated in antibodies against Akt, pAkt Ser473, pAkt Thr308, rpS6, phosphorylated (prpS6), 4EBP1 and phosphorylated 4EBP1 (p4EBP1) (Table 3.3 and 4.2) overnight at 4ºC. Antibody against alpha-tubulin was used as a loading control. The blots were then washed in TBST and incubated with secondary antibodies (Table 4.2) diluted in 5% BSA for 30 minutes at room temperature. Nitrocellulose membranes were then placed in Amersham (ECL) prime western blotting detection reagent for 1 minute and exposed to autoradiographic film. The relative intensity was calculated using ImageJ. All analysis was normalised to loading control.

Table 4.1. Gel and running buffer used for each antibody

Antibody	Molecular weight	Gel used	Sample buffer	Running buffer
Akt	60 kDa	NuPAGE Novex 4-12% Bis-tris Protein Gels (NP0321BOX)	Sample Buffer, laemli Concentrate (S3401-10VL)	Nupage MES SDS running buffer (NP0002)
pAkt Ser473	56 kDa	Novex Tricine 16% gel (EC6695BOX)	Novex Tricine SDS Sample Buffer (2x) (LC 1676)	Tricine SDS running buffer (LC 1675)
pAkt Thr308	55 kDa	NuPAGE Novex 4-12% Bis-tris Protein Gels (NP0321BOX)	Sample Buffer, laemli Concentrate (S3401-10VL)	Nupage MES SDS running buffer (NP0002)
prpS6 Ser 235/236)	32 kDa	NuPAGE Novex 4-12% Bis-tris Protein Gels (NP0321BOX)	Sample Buffer, laemli Concentrate (S3401-10VL)	Nupage MES SDS running buffer (NP0002)
rpS6	32 kDa	NuPAGE Novex 4-12% Bis-tris Protein Gels (NP0321BOX)	Sample Buffer, laemli Concentrate (S3401-10VL)	Nupage MES SDS running buffer (NP0002)
p4E-BP1 Thr37/46	15-20 kDa	Novex Tricine 16% gel (EC6695BOX)	Novex Tricine SDS Sample Buffer (2x) (LC 1676)	Tricine SDS running buffer (LC 1675)
4E-BP1	15-20 kDa	Novex Tricine 16% gel (EC6695BOX)	Novex Tricine SDS Sample Buffer (2x) (LC 1676)	Tricine SDS running buffer (LC 1675)
Alpha tubulin	50 kDa	Novex Tricine 16% gel (EC6695BOX)	Novex Tricine SDS Sample Buffer (2x) (LC 1676)	Tricine SDS running buffer (LC 1675)

Table 4.2. Additional antibodies used for western blotting

Primary antibody	Product number	Species raised	Final concentration (stock solution)	Source
prpS6 Ser 235/236)	4858	Rabbit monoclonal	0.12 µg/ml (59 µg/ml)	Cell Signalling
rpS6	2217	Rabbit monoclonal	0.01 µg/ml (37 µg/ml)	Cell Signalling
p4E-BP1 Thr37/46	9459	Rabbit monoclonal	0.89 µg/ml (219.0 µg/ml)	Cell Signalling
4E-BP1	9644	Rabbit monoclonal	0.17 µg/ml (169 µg/ml)	Cell Signalling

4.2.6. Statistical Analysis

SPSS version 22 (SPSS, Inc., Chicago, USA) was used to analyse the data. Graph Pad version 8 (Inc., San Diego, California, USA) was utilised to generate the graphs. Qualitative data, including the proportion of follicles morphological health, follicle stages distribution and the proportion of oocytes with DNA damage and DNA DSB repair protein expression, were presented as a percentage. The analysis was run by Chi-square or Fisher exact test as appropriate. Quantitative data of nuclear exclusion of FOXO3, western blotting, granulosa cells expression of γH2AX, MRE11, ATM, Rad51, BRCA1, BRCA2 were analysed either by the Kruskal Wallis test followed by Dunn's Bonferroni test for data that were not normally distributed or by using one-way ANOVA followed by Bonferroni post hoc test for normally distributed data. Quantitative data were presented as mean ± SEM. p-value < 0.05 were considered significant.

4.3. Results

4.3.1. Determination of Rapamycin Concentration to Use

Preliminary experiments were conducted to determine the concentration of rapamycin used in this chapter. A total of 2870 follicles were analysed after 6 days of culture to determine the proportion of activated follicles. A significant increase in the proportion of activated follicles was observed in 1 μM bpv(HOpic) (62.3%, $p \leq 0.001$), 1 μM bpv(HOpic) + 0.01 pM rapamycin (54.7%, $p \leq 0.001$), 1 μM bpv(HOpic) + 0.1 nM rapamycin (46.6%, $p = 0.009$) compared to control (36.2%). Whilst 0.01 pM (39.7%), and 0.1 nM rapamycin (30.0%) ($p = 0.065$) did not reveal a significant reduction.

The activated rate in tissue fragments exposed to 1 μM bpv(HOpic) + 0.01 pM rapamycin (54.7%) was similar to 1 μM bpv(HOpic) group (62.3%) ($p = 0.055$). On the other hand, the proportion of activated follicles was much lower in 1μM bpv(HOpic) + 0.1 nM rapamycin ($p \leq 0.001$) compared to 1 μM bpv(HOpic) group. In this context the addition of 0.1 nM rapamycin to medium containing 1 μM bpv(HOpic) was sufficient to increase the activation compared to control but with a much lower rate than that in bpv(HOpic) group (Figure 4.3 A).

The number of follicles included for γH2AX analysis was 520 follicles from 2 independent experiments. Primary and secondary stage follicles were categorised as growing follicles. A marked increase in γH2AX expression was observed in oocytes of non-growing and growing follicles in 1 μM bpv(HOpic) (64.4% and 59.6%) compared to control (17.9%, $p \leq 0.001$ and 22.9%, $p = 0.001$), 0.1 nM rapamycin (35.8% and 23.5%, $p = 0.005$), and 1 μM bpv(HOpic) + 0.1 nM rapamycin (16.9%, $p \leq 0.001$ and 18.8%, $p \leq 0.001$). However, the addition of a low dose rapamycin either

on its own (0.01 pM rapamycin: 45.8%, p = 0.271) or in combination with bpv(HOpic) did not significantly change the expression in oocytes of activated follicles (1µM bpv(HOpic) + 0.01 pM rapamycin: 52.4%, p > 0.05) with only non-growing follicles were affected (26.9%, p=0.002 and 41.1%, p = 0.017). Based on these findings, we included 0.1 nM rapamycin alone and with 1µM bpv(HOpic) as the final concentration used in this chapter (Figure 4.3 B).

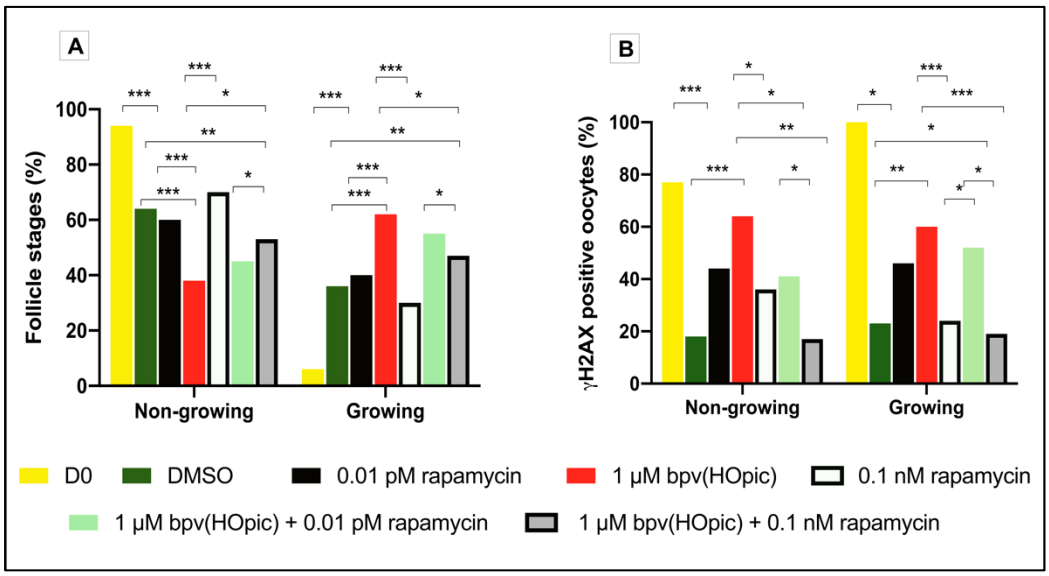

Figure 4.3. Analysis of follicle distribution in all treatment groups included in the screening. (A) Follicle distribution after six days of culture. (B). γH2AX expression in oocytes. A significant increase of growing follicles can be seen in 1 µM bpv(HOpic) and 1 µM bpv(HOpic) + 0.1 nM rapamycin (A). However, the bar graph shows an increased in γH2AX expression in the oocytes of 1 µM bpv(HOpic) group. Chi square test, p-value < 0.05 was considered significant. Asterisk (***) ≤ 0.001, (**) ≤ 0.01, (*) < 0.05.

4.3.2. The Effect of PTEN and mTOR Inhibition on Follicle Growth

A total of 116 ovarian cortical strips and 13,033 follicles from four independent experiments were analysed, and 2,845 follicles from 20 ovarian cortical strips were examined on D0. Non-growing follicles were the most prevalent, constituting 89.9.0%

of total follicle count on D0 (freshly fixed tissue). The remaining were primary (8.6%) and secondary (1.5%) with no antral follicles present on D0 (Table 4.3 and Figure 4.4). In addition, all follicle types in control and treatment groups had similar proportion of healthy follicles throughout the culture period.

Ovarian cortical sections exposed to 1 μM bpv(HOpic) (27.4%) and combined 1 μM bpv(HOpic) and 0.1 nM rapamycin (38.7%) displayed a significant reduction in the proportion of non-growing follicles compared to control (48.9%), reflecting an increased in the growing follicle proportion (control: 51.2%; 1 μM bpv(HOpic): 73.7%; 1 μM bpv(HOpic) +1 nM rapamycin: 60.5%) ($p < 0.05$). Secondary follicles were the most mature stage observed in all groups. There was no significant influence of any the treatments on the proportion of secondary follicles, with the highest proportion observed in the combined group (6.0%) ($p > 0.05$) (Table 4.3).

Table 4.3. The total number of follicles in each treatment group, at day 0 and after 6 days of culture

Group	Non-growing n (%)	Primary n (%)	Secondary n (%)	Total
D0 (freshly fixed)	2,558 (89.9) [a]	244 (8.6) [a]	43 (1.5) [a]	2,845
Control	1,952 (48.9) [b]	1,916 (48.0) [b]	127(3.2) [a]	3,995
1 μM bpv(HOpic)	455 (27.4) [c]	1,126 (67.9) [c]	98 (5.8) [a]	1,659
1 μM bpv(HOpic) + 1 nM rapamycin	942 (38.7) [d]	1,327 (54.5) [e]	145 (6.0) [a]	2,434
1 nM rapamycin	1083 (51.6) [e]	956 (45.5) [b, f]	61 (2.9) [a]	2,100
Total				13,033

(a), (b), (c), (d), (e), and (f) denote a significant difference between treatment groups. A significantly higher proportion of primary and secondary follicles were observed in treatment groups compared to control ($p < 0.05$). Chi square test, p-value < 0.05 was considered significant.

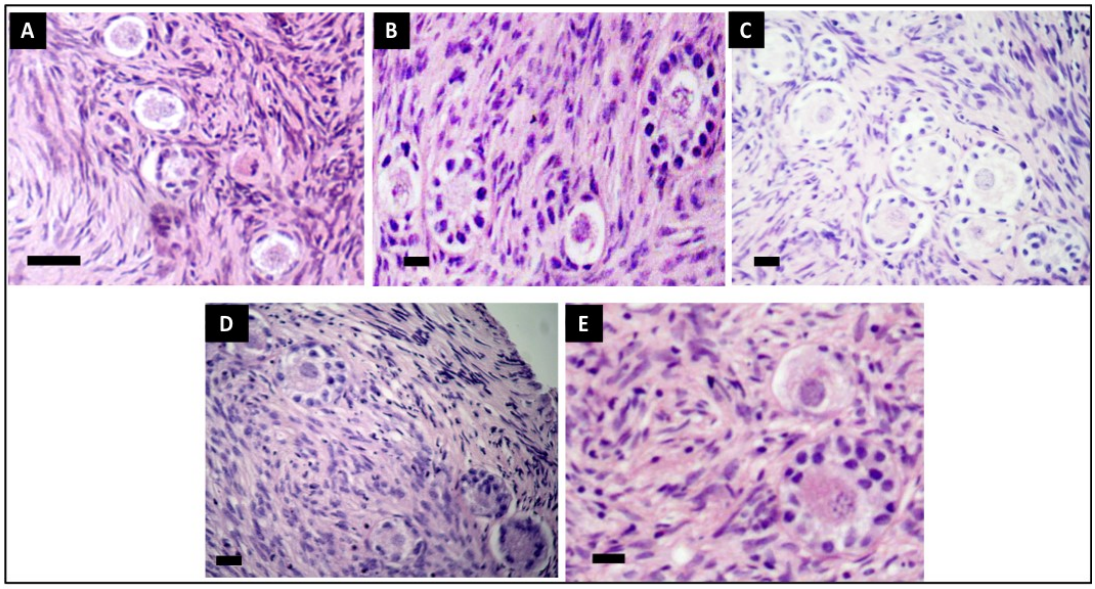

Figure 4.4. Photomicrographs H & E staining of ovarian cortical strips after 6 days of culture. The appearance of follicles in ovarian cortical fragments in freshly fixed and after 6 days of culture. (1) Freshly fixed ovarian tissue fragment, (2) Control, (3) bpv(HOpic), and (4) combined bpv(HOpic) and rapamycin, and (5) rapamycin group. Scale bar = 20 μm.

4.3.3. Effects of PTEN and mTOR Inhibition on PI3K/Akt Downstream Pathway

Western blot analysis was utilised to evaluate the effects of treatments with PTEN or mTOR suppression to disrupt the PI3K/Akt/mTOR downstream pathway. All experiments were conducted on fresh tissue precisely 24 hours after exposure and repeated 2 - 3 times. For each experiment, material from 16 to 20 ovarian fragments per group was used per lane. In each lane, 25 - 30 μg of protein sample was loaded. Western blot analysis revealed an increase in ratio of pAkt Ser473 and Thr308 to Akt and in bpv(HOpic) (3.24 ± 0.58 and 2.65 ± 0.75-fold higher) and combined bpv(HOpic) and rapamycin group (2.52 ± 0.50 and 2.06 ± 0.35-fold changes) compared to control ($p < 0.05$) (Figure 4.5 B and C 1, 2).

The ratio did not change with rapamycin alone (0.65 ± 0.10 and 0.96 ± 0.19-fold, $p > 0.05$). Activation of Akt consequently increased the expression of the downstream effector prpS6 to rpS6 ratio in bpv(HOpic) ((3.4 ± 0.72-fold higher) and the combined bpv(HOpic) and rapamycin group (2.4 ± 0.58-fold higher) compared to control ($p < 0.05$) (Figure 4.2 B and C 3), whereas a reduction in the rapamycin group did not reach significance (0.49 ± 0.14-fold lower-fold lower) compared to control ($p > 0.05$). No significant changes in p4EBP1 to 4EBP1 ratio were detected, regardless of the treatments (Figure 4.5 B and C 4).

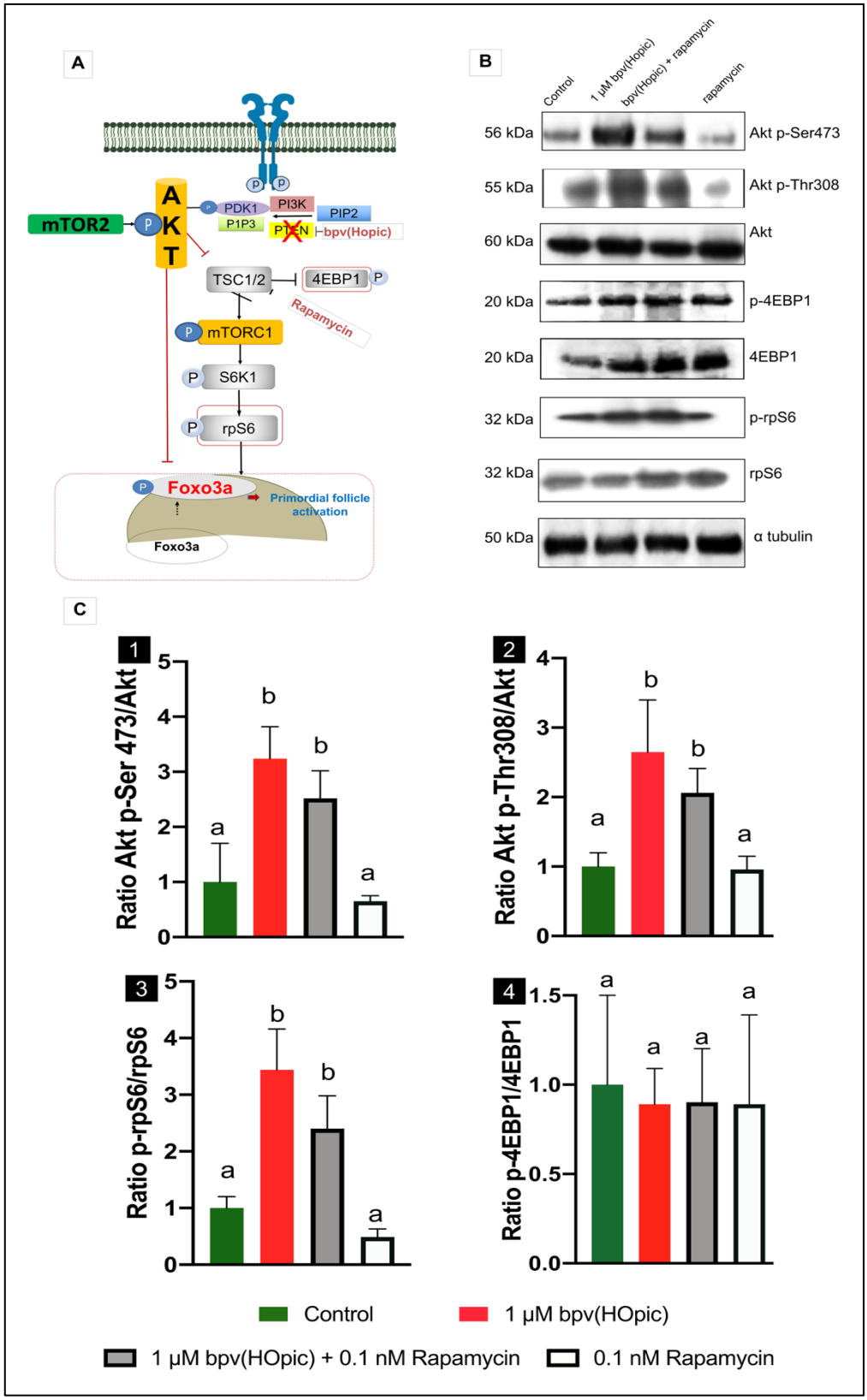

Figure 4.5. PTEN and mTOR inhibition impacts on primordial follicle activation through the modulation of PI3K/Akt/mTOR downstream pathway. (A) A reflection of PTEN and mTOR

inhibition effects on PI3K/Akt/mTOR downstream substrate. (B, C) Short term exposure to PTEN and mTOR inhibition effects on PI3K/Akt/mTOR downstream substrates of (1) pAkt S473 to total Akt ratio, (2) pAkt Thr308 to total Akt, (3) prpS6 to rpS6 ratio and (4) p4EBP1 to 4EPB1 ratio in all groups. Kruskal Wallis, p-value < 0.05 was considered significant. Different letters indicate $p < 0.05$.

Nuclear export of FOXO3 as an effect of PTEN inhibition on PI3K downstream pathway was determined by immunohistochemistry. A total of 656 follicles were analysed. Nuclear exclusion of FOXO3 was detected in a higher proportion of oocytes in the bpv(HOpic) alone (78.7 ± 2.3%) and bpv(HOpic) and rapamycin groups (59.1 ± 4.8%) compared to control (38.5 ± 5.2%, $p \leq 0.001$ and $p = 0.016$) and the rapamycin only groups (34.0 ± 3.6, $p \leq 0.001$ and $p = 0.001$ respectively) (Figure 4.6).

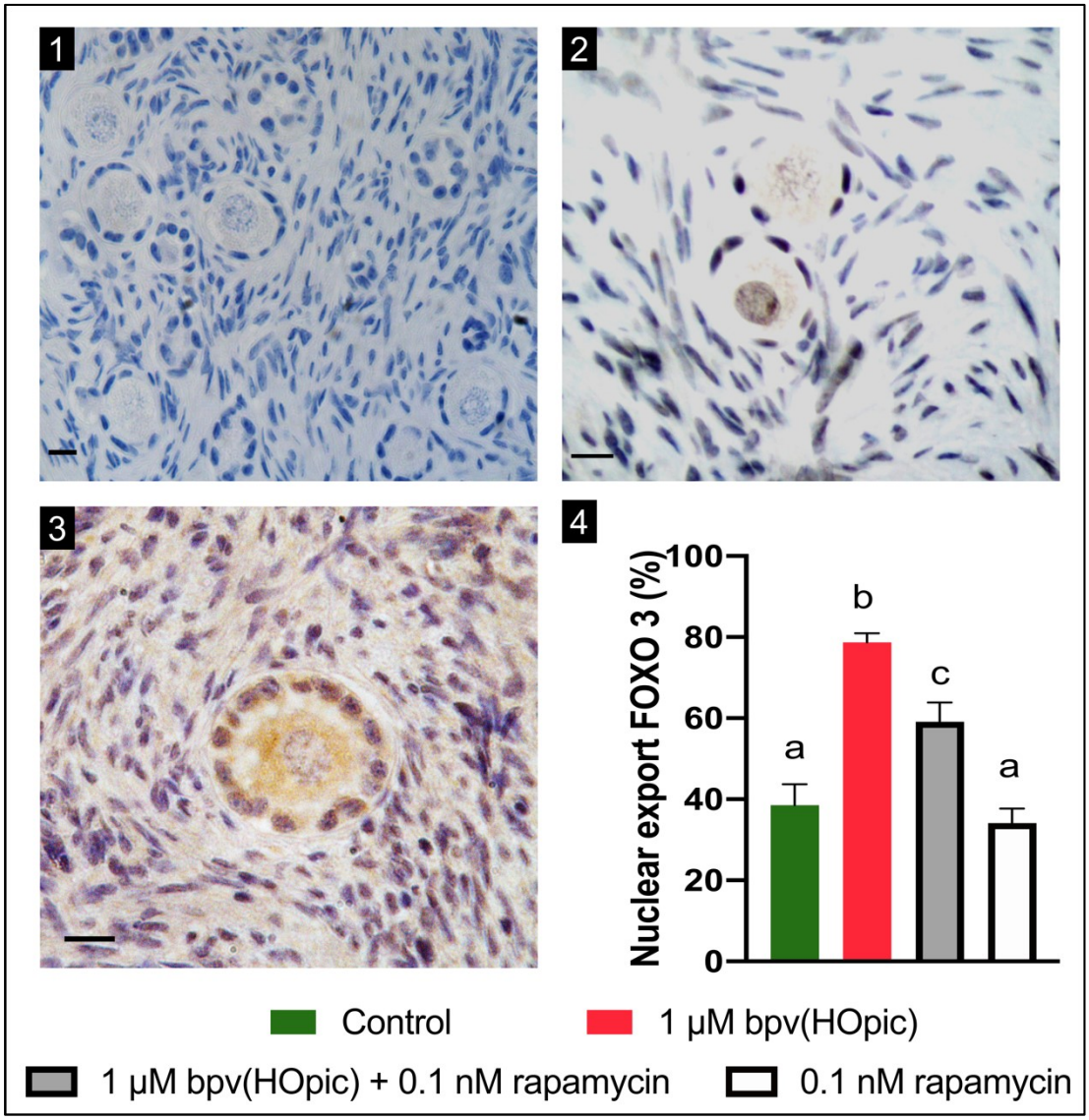

Figure 4.6. Nuclear export of FOXO3 in control and treatment groups. The graph shows an average proportion of oocytes showing non-nuclear detection of FOXO3 in every section. (1-3) Representative photomicrographs showing localisation of FOXO3 in bovine follicles. (1) Negative control, (2) Non-nuclear exclusion of FOXO3 in non-growing follicles with brown staining in the nucleus, and (3) Nuclear export of FOXO3 from the nucleus of the activated follicles indicated by brown staining in the ooplasm and negative staining within the nucleus. (4) The graph shows a significant increase in nuclear export of FOXO3 in bpv(HOpic) and combined bpv(HOpic) and rapamycin group. Data shows mean percentage ± SEM from 4 replicates. ANOVA and Bonferroni post hoc test, p-value was assigned at < 0.05. Different letters indicate $p < 0.05$. Scale bar = 20 µm.

4.3.4. PTEN/Akt/mTOR Modulation Pathway Impacts on DNA Damage within Oocytes and Granulosa Cells of Each Follicle stage

Non-growing and primary follicles of freshly fixed tissue exhibited a high γH2AX level (68.2% and 80.0%) compared to controls (20.5% and 16.7%) ($p < 0.05$). Its expression rose significantly in bpv(HOpic) (80.0% and 64.5%) compared to control groups ($p < 0.05$). Furthermore, the presence of rapamycin either on its own (18.3% and 33.7%) or in combination with bpv(HOpic) reduced γH2AX expression compared to bpv(Hopic) group. Importantly, the combined effects of bpv(HOpic) and rapamycin was still sufficient to induce growth activation (Although it was not as high as in bpv(HOpic) group) but with decreased γH2AX expression ($p < 0.05$). Nevertheless, in oocytes of secondary follicles, a marked difference was only observed between bpv(HOpic) (66.7%) and control group (22.7%) ($p < 0.05$) (Figure 4.7 A, B). Meanwhile, γH2AX expression in granulosa cells was higher in bpv(HOpic) (16.0 ± 1.2%) of growing follicles compared to control (0.48 ± 0.19%) and significantly reduced with the addition of rapamycin (1.4 ± 1.3%) ($p < 0.05$). Notwithstanding, the highest expression in the secondary stage was seen in bpv(HOpic) group, but it did not reach significance (Figure 4.7 A, C).

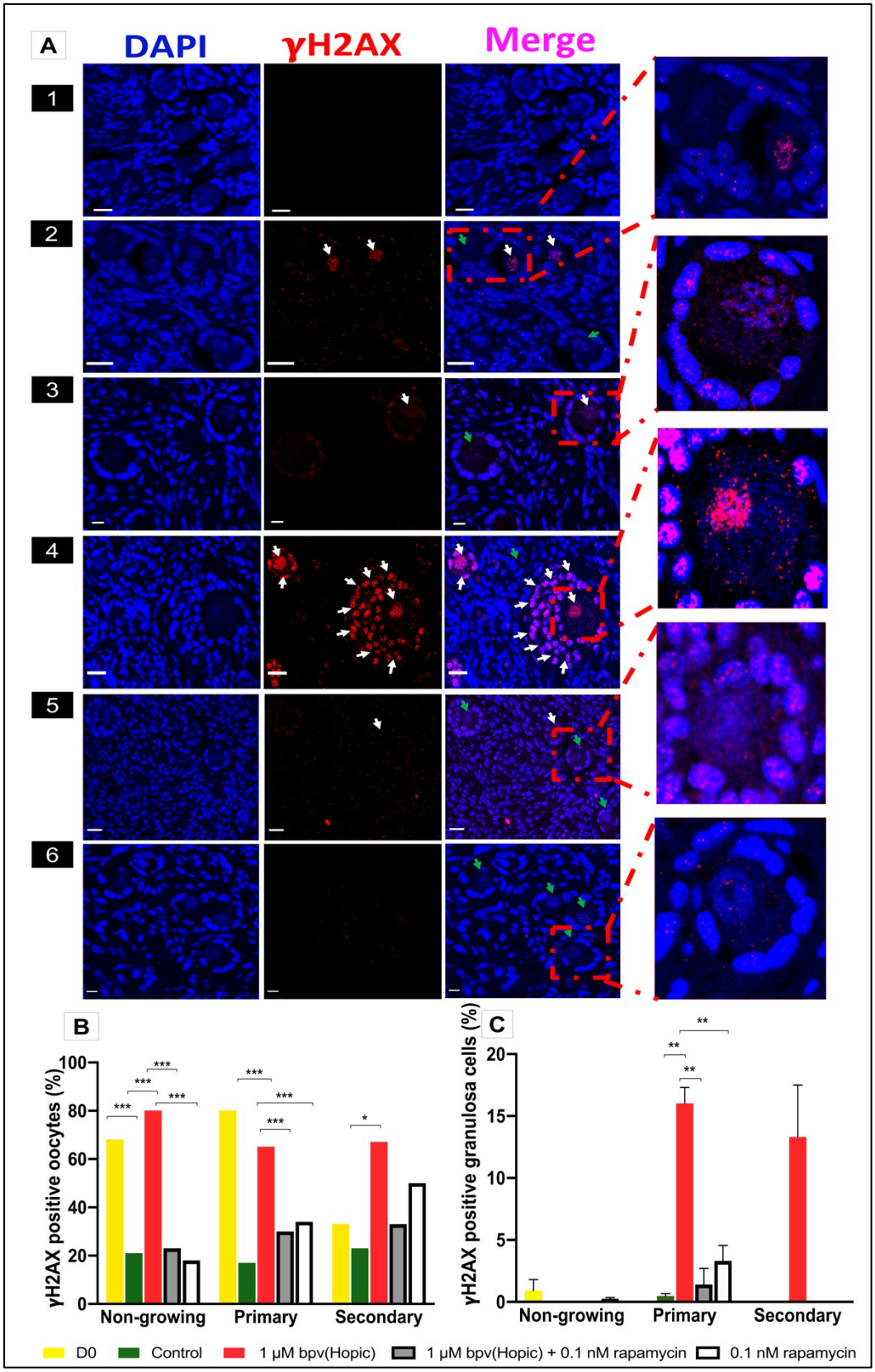

Figure 4.7. γH2AX localisation by immunofluorescence in control and treatment groups. (A) Photomicrograph of immunofluorescence microscopy represent γH2AX positive staining displayed as

bright red points (foci) (white arrows) and negative staining DAPI (blue) indicated by green arrows within the nucleus of oocytes and granulosa cells. (1) Negative control, (2) Freshly fixed tissue, (3) Control with negative and weak γH2AX expression within oocytes of primary follicles, (4) γH2AX positive within the nucleus of oocytes and granulosa cells in 1μM bpv(HOpic) group, (5) Combined bpv(HOpic) and rapamycin, (6) Negative expression of γH2AX in rapamycin group. Scale bar = 20μm. (B) Bar graphs show an increase in the proportion of γH2AX-positive oocytes and (C) Expression of γH2AX in granulosa cells showing the proportion of granulosa cells positive staining in nucleus over a total number of granulosa cells. Analysis of 130-220 follicles per group from 4 independent experiments. Chi square test (oocytes) and ANOVA (granulosa cells), p-value was assigned at < 0.05. Data are presented in mean ± SEM. Asterisk (***): $p \leq 0.001$, (**): $p \leq 0.01$, (*): $p < 0.05$.

4.3.5. Impact of PTEN and mTOR Inhibition on DNA DSB Repair Capacity of Oocytes and Granulosa cells

We performed immunohistochemistry for key DNA repair proteins MRE11, ATM, BRCA1, Rad51 and BRCA2, to determine the DNA repair capacity of both oocytes and granulosa cells at all stages of follicle development. MRE11 expression declined in oocytes of more growing follicles in bpv(HOpic) group (primary: 69.5%; secondary: 72.7%) compared to control (primary: 88.2%; secondary: 94.7%) ($p < 0.05$). The presence of rapamycin either in combination with bpv(HOpic) (93.2% and 85.7%) or on its own (86.4% and 76.5%) upregulated MRE11expression in non-growing and primary but not secondary follicles compared to bpv(HOpic) group ($p < 0.05$). A decrease in MRE11 expression was also observed in granulosa cells of non-growing (75.3 ± 2.24%) and primary follicle (76.2 ± 2.97%) in bpv(HOpic) compared to control group (88.9 ± 1.77%) ($p = 0.012$) and (86.4 ± 2.60%) ($p = 0.039$). The addition of rapamycin did not significantly alter the expression in all follicle types ($p > 0.05$) (Figure 4.8 A 1-6 and 4.9 A, B).

Similarly, ATM expression in non-growing (16.7%) and primary follicles (30.1%) showed a significant decline in oocytes in bpv(HOpic) treated tissue compared to control (63.0%, and 65.5%) ($p < 0.05$) (Figure 4.8 B 1-7 and 4.9 C). A marked increase was observed with combined bpv(HOpic) and rapamycin treatment (57.8%, $p = 0.001$ and 65.0%, $p \leq 0.001$). However, a significant increase in rapamycin group observed in primary follicles (66.7%, $p \leq 0.001$) (Figure 4.9 C). In granulosa cells, ATM was expressed at lower level in non-growing (45.8 ± 10.4%), and primary follicles (72.1 ± 4.4%) of bpv(HOpic) group compared to controls (90.6 ± 4.5% and 91.8 ± 2.6%, $p < 0.05$) (Figure 4.9 D). Unlike MRE11, the presence of rapamycin alone (88.5 ± 3.9% and 87.5 ± 3.1%, $p < 0.05$) or together with bpv(HOpic) (91.1± 4.3% and 90.4 ± 2.4%, $p < 0.05$) seemed to diminish the negative effects of bpv(HOpic) on lower ATM expression. Nonetheless, no changes were observed in secondary stage follicles with either treatment (Figure 4.9 D).

Rad51 is required to complete the DNA repair process and has an essential role in HR. It is evident from the results presented in Figure 4.9 E that Rad51 was reduced in non-growing (21.1%) and primary follicles (31.3%) of bpv(HOpic) group compared to control (83.8%, $p \leq 0.001$ and 72.2%, $p \leq 0.001$), rapamycin (49.2% and 59.6%, $p < 0.05$) and combined bpv(HOpic) and rapamycin group (61.4%, $p = 0.002$; 49.3, $p = 0.007$). Furthermore, we previously demonstrated that Rad51 was rarely expressed in granulosa cells. In the present study, treatments did not alter Rad51 expression in granulosa cells with the highest level observed in the control group (Figure 4.8 C1-7 and 4.9 F).

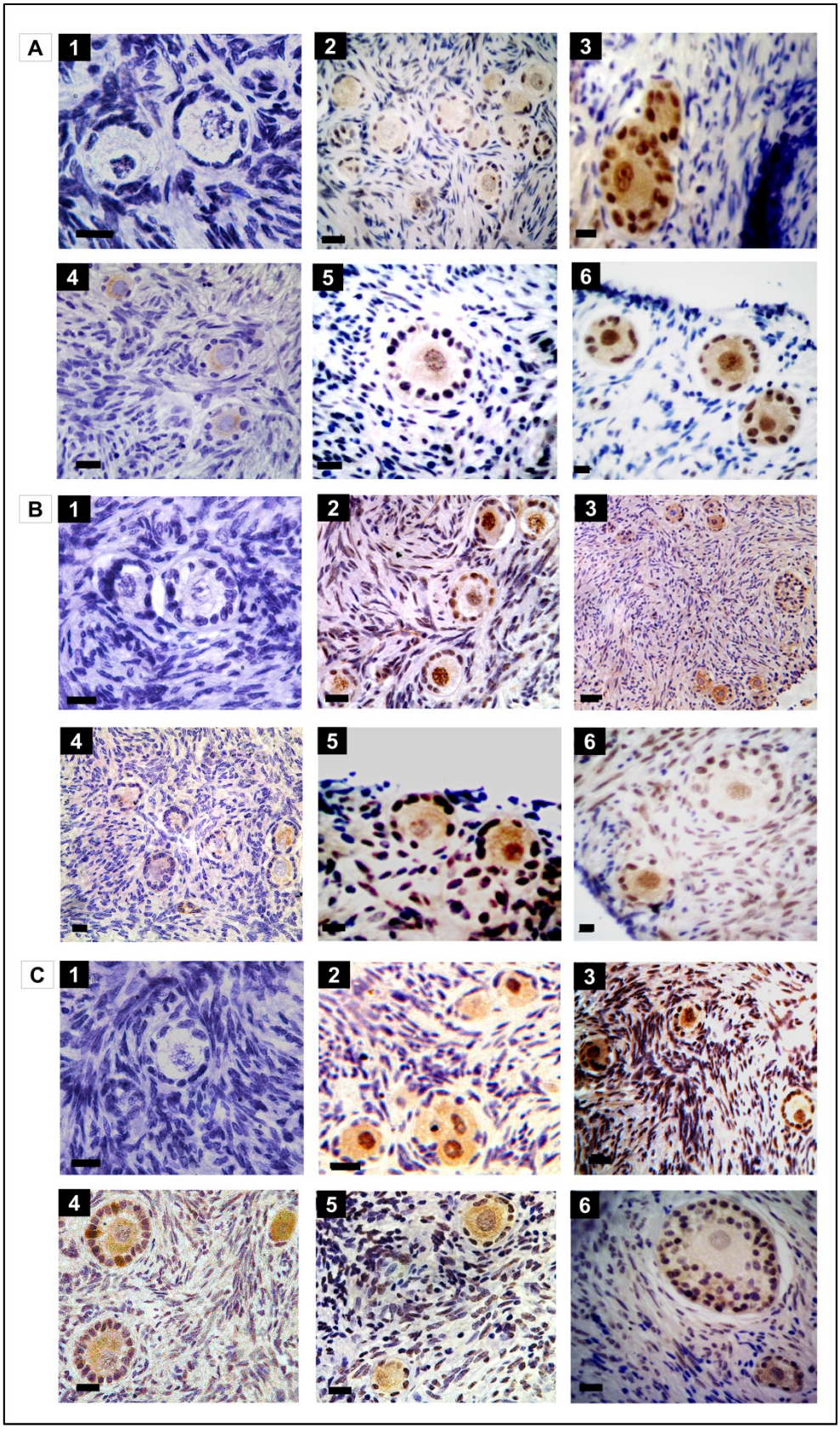

Figure 4.8. Localisation of DNA repair protein MRE11, ATM, and Rad51 in oocytes and

granulosa cells of follicles in all groups. Representative images of MRE11 localisation (A1-6), ATM (B1-6) and (C1-6) expression in oocytes and granulosa cells. (1) Negative control; positive staining (brown) in the oocytes and granulosa cells of (2) D0, (3) Control, (4) 1 µM bpv(HOpic) (5) 1 µM bpv(HOpic) and 0.1 nM rapamycin and (6) 0.1 nM rapamycin. Scale bar = 20 µm.

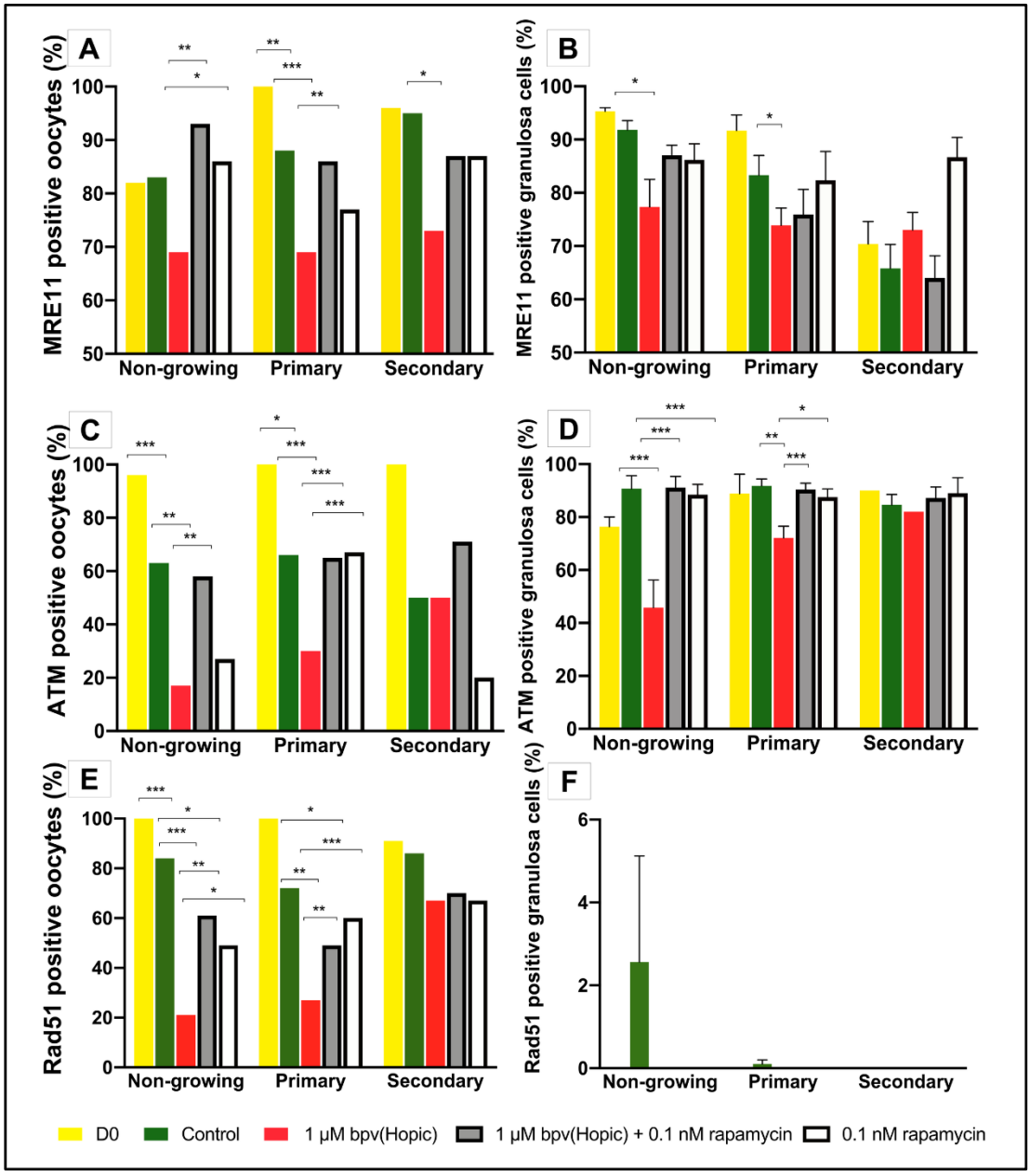

Figure 4.9. Analysis of markers for DSBs: MRE11, ATM, and Rad51 in oocytes and granulosa cells of follicles in all groups. The proportion of (A) MRE11, (C) ATM and (E) Rad51 in oocytes (shown as percentage) and granulosa cells (B, D, and F) (shown as mean percentage ± SEM). Oocytes:

Chi square; granulosa cells: ANOVA, except for Rad51: Kruskal Wallis test, asterisk (***) ≤ 0.001, (**) ≤ 0.01, (*) < 0.05. p-value was assigned at < 0.05.

In contrast to MRE11, ATM and Rad51, the DNA DSBs key proteins BRCA1 and BRCA2 rose significantly in oocytes of activated follicles (13.5 and 63.5%) in bpv(HOpic) group compared to control (4.8 and 43.7%) ($p < 0.05$). However, BRCA1 or BRCA2 levels in both non-growing and secondary follicles were not affected. Interestingly, rapamycin (16.7%) and combined bpv(HOpic) and rapamycin (13.6%) enhanced BRCA1 expression in oocytes of non-activated follicles ($p < 0.05$) (Figure 4.10 A B and 4.11 A and C). We also analysed these two DNA repair proteins in granulosa cells. We found that bpv(HOpic) seemed to increase BRCA1 expression in granulosa cells in non-growing (12.8 ± 1.2%) and primary follicles (4.1 ± 1.1) of bpv(HOpic) group compared to the control (8.4 ± 0.9%) and (0.8 ± 0.4%) ($p < 0.05$) (Figure 4.10 A1-7 and 4.11 B). BRCA2 activity was downregulated in non-growing follicles of bpv(HOpic) (10.7 ± 3.3%) compared to control group (26.8 ± 4.1%) ($p < 0.05$) without any significant changes observed in primary follicles. Expression was increased in the presence of rapamycin in culture media (62.7 ± 6.3%) ($p < 0.05$) (Figure 4.10 B 1-7). No significant differences were detected between any treatments in the expression of BRCA1 and BRCA2 in granulosa cells of growing secondary follicles ($p > 0.05$) (Figure 4.10 A, B 1-7 and 4.11 B, D).

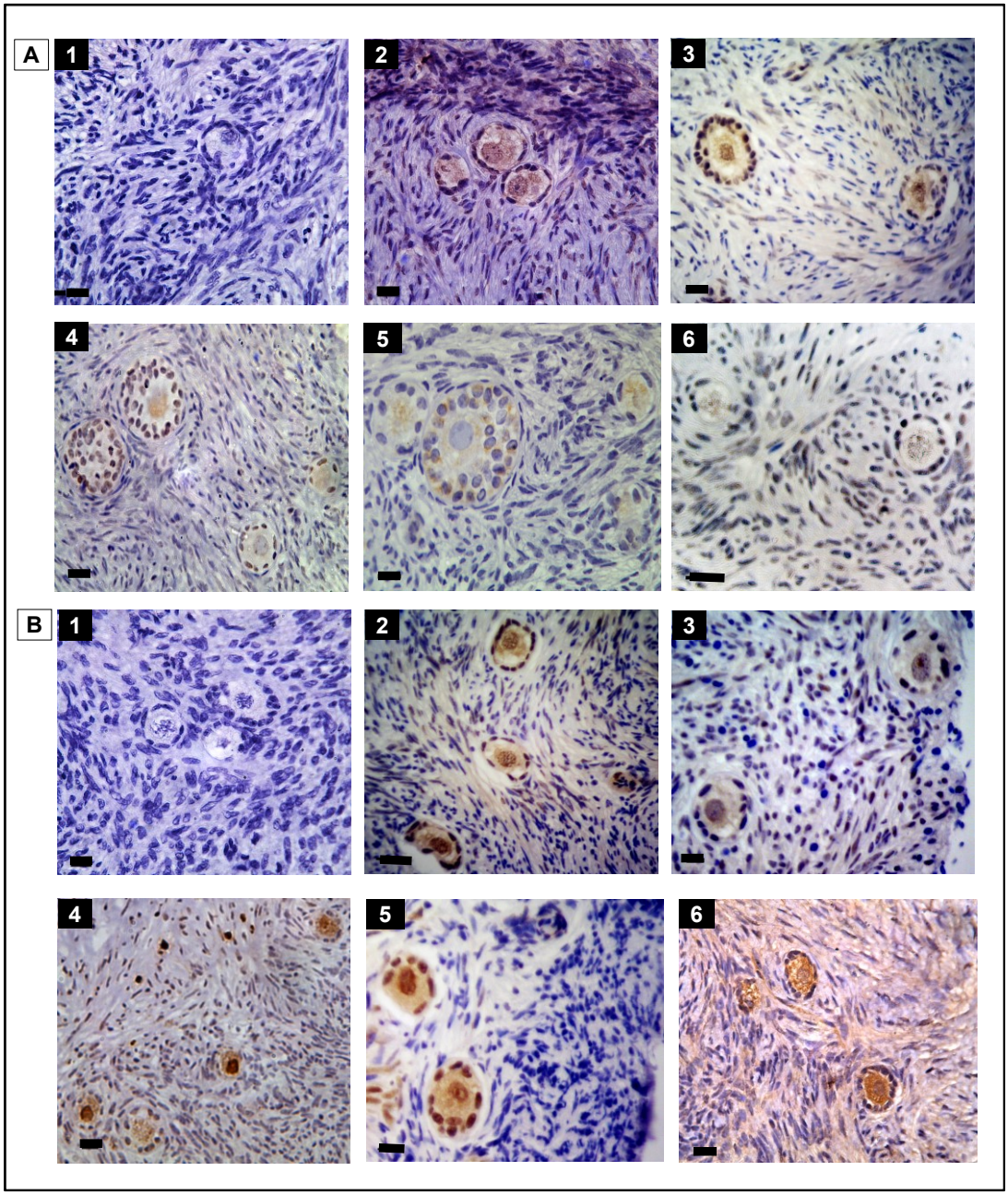

Figure 4.10. Photomicrograph of immunohistochemical detection of BRCA1 and BRCA2 in oocytes and granulosa cells of follicles in all groups. Representative image of BRCA1 localisation (A1-6) and BRCA2 (B1-6) expression in oocytes and granulosa cells. (1) Negative control; positive staining (brown) in the oocytes and granulosa cells of (2) D0, (3) Control, (4) 1 µM bpv(HOpic) (5) 1 µM bpv(HOpic) and 0.1 nM rapamycin and (6) 0.1 nM rapamycin. Scale bar = 20 µm.

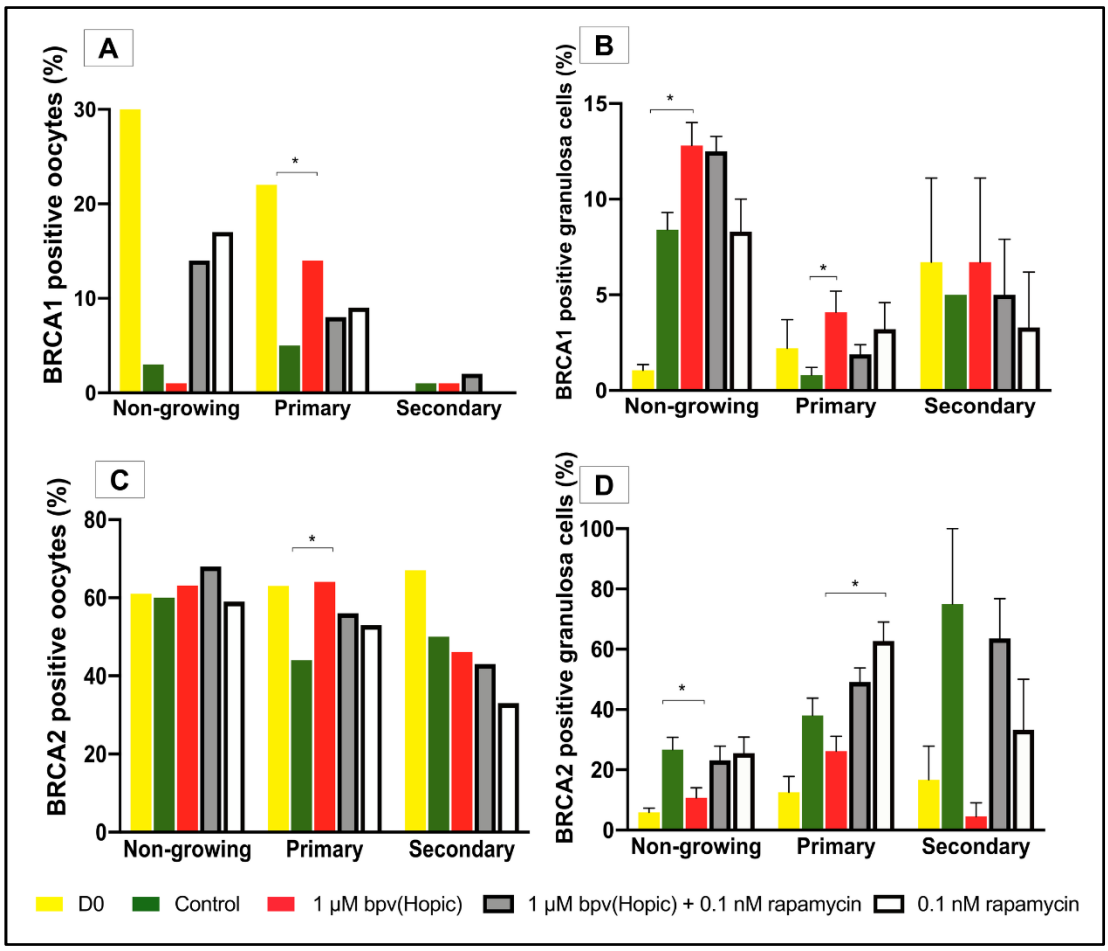

Figure 4.11. Immunohistochemical detection of BRCA1 and BRCA2 in oocytes and granulosa cells of follicles in all groups. The proportion of BRCA1 and BRCA2 in oocytes (A7, B7, and C7) and granulosa cells (A8, B8, and C8) shown as mean percentage ± SEM. Chi square and ANOVA. Asterisk (***) ≤ 0.001, (**) ≤ 0.01, (*) < 0.05.

4.4. Discussion

The findings in chapter 3 indicated that accelerated growth in the presence of PTEN inhibition in culture media was associated with increased DNA damage with limited repair. These results have led to the question of how lowering the activation rate would impact on DDR. In these experiments rapamycin was used to inhibit mTOR and therefore decrease activation, and bpv(HOpic) was used to inhibit PTEN to increase the activation. By utilising both of these treatments, it can be determined whether modulation of one or both of these pathways to alter the activation rate improves the DDR of oocytes and/or granulosa cells.

The results in this chapter confirm the previous findings, that demonstrated an increase in primordial follicle activation after exposure to bpv(HOpic), which was concordant with an increased DDR, exclusively in oocytes. Enhanced activation was observed in all treatment groups after 6 days of culture without affecting follicle health. Increased primordial follicle activation with bpv(HOpic) alone or in combination with rapamycin was in accordance with increased pAkt to Akt ratio, at both phosphorylation sites. The addition of rapamycin alone did not change the pAkt to total Akt ratio. It is commonly accepted that in the PI3K/Akt/mTORC signalling pathway, primordial follicle activation is the result of FOXO3 nucleocytoplasmic shuttling following Akt phosphorylation and mTOR-induced protein translation. The primary action of mTOR is governing the translation of protein synthesis, cell cycle progression, apoptosis and metabolic regulation through upregulation of Akt (Adhikari *et al.*, 2010). In our case, it seems likely that FOXO3 phosphorylation as a downstream substrate of Akt was functionally more dominant than reduced protein translation in the presence of bpv(HOpic) and rapamycin. Mutual effects of modulation of these pathways resulted

in increased activation compared to control. It is, however, important to note that five rpS6 phosphorylation sites have been recorded, including serine 235, serine 236, serine 240, serine 244 and serine 247 (reviewed by (Ruvinsky and Meyuhas, 2006)).

A decrease in DNA damage alongside the reduced activation rate might suggest the importance of preventing an accelerated and precocious growth. Recent publications provide evidence that mTORC1 inhibitor could retain the follicle in a functionally integrated state, preserve follicle ultrastructure and promote the continuance of oocyte and granulosa cells communication throughout culture period that is in parallel with delayed follicular growth (Grosbois *et al.*, 2019). Those outcomes supports the notion that precocious growth *in vitro* contributes to uncoordinated growth of oocytes and granulosa cells (Smitz and Cortvrindt, 2002), and that reducing the rate of activation may sustain oocyte and granulosa cell coordination.

However, in contrast to our findings, porcine granulosa cells isolated from antral follicles exposed to high dose organophosphorus insecticide diazinon (DZN), recognised to inhibit PI3K/Akt activation and induce DNA damage in a dose-dependent manner. It appeared that damaged granulosa cells reacted by generating DNA repair proteins ATM, Rad51, and BRCA1 but not MRE11. Although the DDR response is pertinent, a significant increase in p53 expression was detected, and most cells eventually underwent apoptosis (Wang *et al.*, 2019a). Nevertheless, this study was focused on granulosa cells of growing follicles and performed in a different species. It is generally accepted that oocytes and granulosa cells exhibit different reactions to DNA induced damage (Hanoux *et al.*, 2007, Roos and Kaina, 2006, Winship *et al.*, 2018). It has been reported that despite increased expression of γH2AX

in oocytes and granulosa cells with age in the rhesus monkey, BRCA1 is not affected, which may help to repair DSBs accumulated with age (Zhang *et al.*, 2015).

Moreover, each species reacts differently to DNA damage and exhibit a unique DNA repair mechanism (Kujjo *et al.*, 2010, Kujjo *et al.*, 2012, Perez *et al.*, 2007, Wang *et al.*, 2017b). Likewise, human ovarian cortical strips cultured in a higher dose than that used in the present experiment resulted in empty follicles, which may be a result of granulosa cell phagocytosis of oocytes (McLaughlin *et al.*, 2011). This finding together with the data in porcine granulosa cells may suggest that profound mTORC inhibition can interfere with the delicate balance of PI3K/Akt/mTOR pathway leading to cell death mediated by either apoptosis or autophagy.

In addition, follicles exposed to Akt activators showed decreased estradiol production, perhaps due to uncoordinated growth of oocyte and granulosa cells (Grosbois and Demeestere, 2018). In contrast, short exposure to another mTORC1 inhibitor, everolimus, was able to mitigate the negative effect of Akt activators on estradiol production (Grosbois and Demeestere, 2018). In the present study, we used a much lower dose of rapamycin, and this low dose and short exposure significantly reduced DNA damage and increased DNA repair protein expression. By using either rapamycin alone or in combination with bpv(HOpic), we could demonstrate a gradual decrease in the activation rate together with reduced DNA damage. These findings highlight the importance of maintaining the physiological balance of the PI3K/Akt/mTOR pathway in oocytes.

The results with combined bpv(HOpic) and rapamycin treatment may reflect the mechanism by which rapamycin or other type of mTOR inhibitors protects the ovary

against chemotherapy. In a mouse model, the mTOR inhibitor was able to counteract the primordial follicle activation and follicle loss induced by CP (Goldman *et al.*, 2017, Zhou *et al.*, 2017) and cisplatin (Tanaka *et al.*, 2018). However, Akt phosphorylation following CP exposure did not reflect CP-induced PI3K/Akt activation with only prpS6 affected implying that excessive primordial follicle activation is mediated by upregulation of mTORC1 signalling pathway (Goldman *et al.*, 2017, Zhou *et al.*, 2017).

In a study investigating the mechanism by which cisplatin provoked ovarian failure, reduced PTEN expression in oocytes gave rise to primordial follicle activation. Once follicles were activated to grow, they became more vulnerable to apoptosis and showed loss of LHR expression. This condition may contribute to reduced oocyte meiotic competence and ovulation failure (Chang *et al.*, 2015). Granulosa cells of secondary follicles were also the most adversely affected, as indicated by high levels of cleaved (Adenosine Diphosphate)-Ribose Polymerase (PARP) (Chang *et al.*, 2015). Furthermore, the PI3K/Akt inhibitor was sufficient to reduce follicle loss in an endometriosis mice model (Takeuchi *et al.*, 2019). It is known that the presence of endometriosis (Choi *et al.*, 2018, Kitajima *et al.*, 2014) or chemotherapy treatments (Chang *et al.*, 2015, Kerr *et al.*, 2012a, Kerr *et al.*, 2012b, Nguyen *et al.*, 2018) treatments are associated with increased DNA damage, suggesting that rapamycin might be beneficial to ameliorate the negative impact of PI3K/Akt activation in those situations, which is concomitant with our findings.

In conclusion, the addition of a low dose of rapamycin to ovarian tissue treated with bpv(HOpic) reduced DNA damage and improved DNA repair capacity of the oocytes, whilst maintaining increased follicle activation (Figure 4.12).

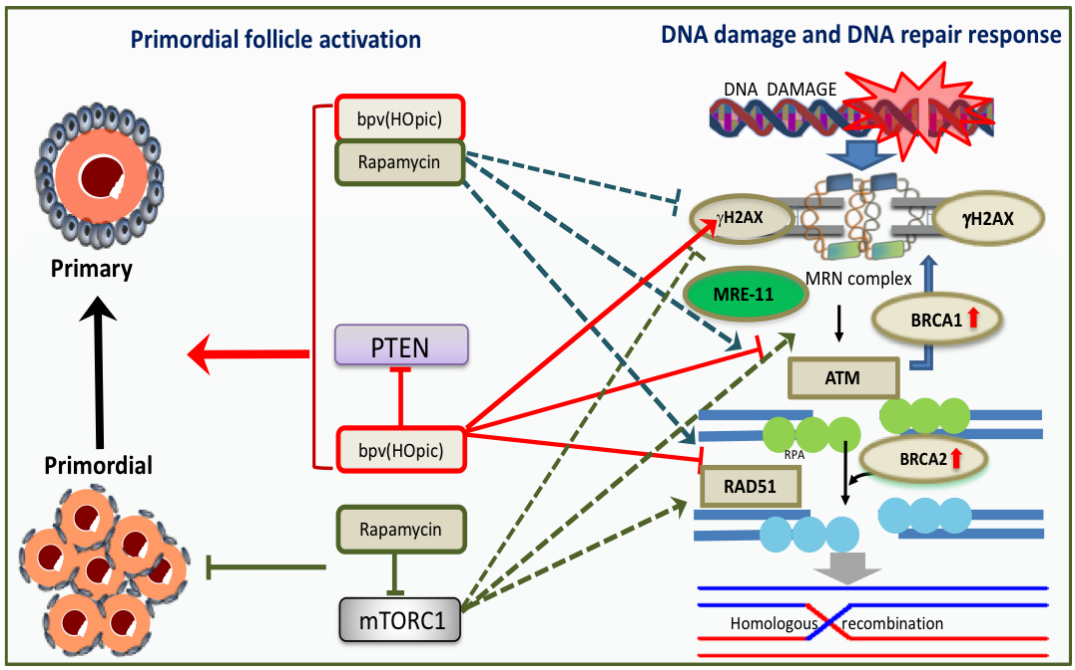

Figure 4.12. Summary of findings of the experiments in chapter 4. The presence of rapamycin and bpv(HOpic) in the culture medium is sufficient to induce primordial follicle activation, attenuate γH2AX activity and improve DNA repair proteins, MRE11, ATM and Rad51 in oocytes.

Chapter 5
Modulation of PTEN and mTOR Impact on the Growth of Isolated Preantral Follicles

5.1. Introduction

The experiments described in chapter 3 and 4 have confirmed that the use of PTEN inhibition to activate primordial follicles may have a detrimental effect on the DDR of oocytes and granulosa cells *in vitro.* Bovine ovarian cortical strips cultured in the presence of bpv(HOpic) resulted in more than 70% of follicles being activated within six days of culture. These findings confirmed that the culture system supported the spontaneous recruitment of dormant follicles into the growing pool and that this was enhanced by PTEN inhibition, in agreement with earlier studies in the human and bovine model (McLaughlin and Telfer, 2010, McLaughlin *et al.*, 2018, Telfer *et al.*, 2008). However, follicular growth in this IVG system is in contrast to physiological *in vivo* conditions where activation occurs gradually and it may take several months to reach the antral stage in larger animals and humans (Gougeon, 1998, Smitz and Cortvrindt, 2002). The evidence presented in chapter 3 brings into question the benefit and safety of this massive activation for supporting further follicular growth and follicle quality. These observations highlight the importance of amending the direction of managing *in vitro* follicular growth, as demonstrated in chapter 4.

The results presented in chapter 4, showed that the addition of rapamycin to inhibit mTORC1 on its own or in combination with bpv(HOpic) improved DDR of oocytes and granulosa cells whilst still supporting increased activation of primordial follicles. The experiments in the previous two chapters were limited to primordial follicle activation and any implications for later stages of follicle development were not assessed. It should be pointed out that previously published findings from our lab showed that despite more growing follicles being observed after exposure to bpv(HOpic), the subsequent growth of these follicles was compromised following a

further 6 days of culture (McLaughlin *et al.*, 2014). These data emphasised the need to extend the experiments to the subsequent stage of the follicle development in this study.

The prime issue in all stages of the IVG system is how to maintain oocyte and granulosa cell connections, as the exceptional growth of the follicle is vulnerable to compromised cell interaction throughout the culture period (Smitz and Cortvrindt, 2002). Upon activation, follicles grow and develop to large multi-laminar structures. These follicles will not survive within the cortical environment and they need to be removed from the cortical stromal and be cultured individually in order to avoid the influence of follicle interactions (Telfer *et al.*, 2008, Telfer and McLaughlin, 2012). Preantral follicles are primarily characterised by oocyte growth and development that is in line with increased production of GDF9 and pronounced junctional connexin expression within the follicles (Elvin *et al.*, 2000). The rapid growth of follicles observed *in vitro* may be related to a deficit in intercellular communication that may decrease oocyte quality (Smitz and Cortvrindt, 2002). Preantral follicle growth is also typified by increased basal lamina expansion (Rodgers *et al.*, 2003). The major problem is how to substitute the *in vivo* environment to support preantral follicle growth *in vitro*. The results illustrated in chapter 4 challenged us to investigate further whether modifying follicular recruitment might provide an environment that is closer to physiological conditions.

The endpoints of the experiments in this chapter were to investigate the effect of PTEN and mTOR inhibition on subsequent isolated preantral follicular growth, survival and development *in vitro* and whether the size of isolated follicles at the starting point would determine their growth potential. The same approach employed in previous

chapters was used i.e. a two-step culture system designed to enhance the activation of primordial follicles within ovarian cortical strips (step one) and then growth and development of isolated secondary follicles (step two).

5.2. Material and Methods

5.2.1. Ovarian Cortical Fragments Culture

Ovarian cortical fragments collection, preparation, the treatment and cultured were as described in chapter 4. In brief, the tissue fragments were cultured in 24-well culture plates containing basic culture medium comprising DMSO as vehicle control, bpv(HOpic) and rapamycin either on its own or in combination with bpv(HOpic) at 37^{o}C in a humidified air atmosphere with 5% CO_2.

5.2.2. Follicle Isolation and Culture

After six days of culture, ovarian cortical fragments were subjected to follicle isolation as detailed in chapter 2 section 2.3.1 and 2.3.2. In brief, the tissue fragments were placed in dissection medium and assessed under light microscopy. Follicles measuring ≥ 66 μm in diameter (Telfer *et al.*, 2008) were isolated mechanically using 25 gauge needles, scalpel blade and fine forceps (section 2.3.1). Isolated follicles were then placed individually in 96-well V-bottomed culture plates in 150 μl of culture medium (Section 2.2.1) supplemented with 100 ng/ml recombinant activin A (rhAct A) (R & D Systems, Abingdon, UK). Isolated follicles were cultured for a further 6 to 8 days at 37^{o}C in humidified air with 5% CO_2. Half of the culture medium was removed and replaced and at the same time follicle diameter was measured in two perpendicular dimensions using a dissecting microscope with a crossed micrometer and the mean value recorded on the day of isolation (D6) and every alternate day (Figure

5.1). Measurements were taken from basement membrane from one side to the other. Theca was excluded from the measurements.

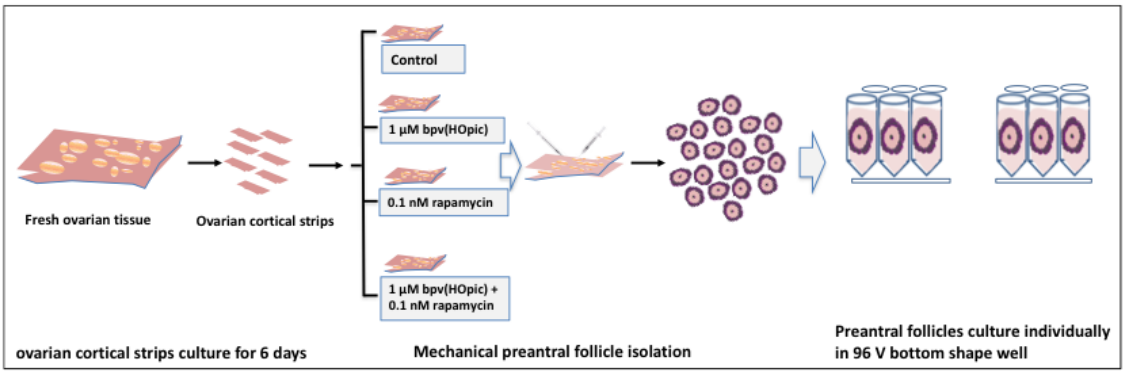

Figure 5.1. Experimental design to investigate the effects of the treatments on the subsequent follicular growth and survival.

5.2.3. Histological Analysis

H & E staining was performed to analyse morphology of follicles. Analysis of isolated follicle was performed under the light microscope with a crossed micrometre under x40 magnification. The analysis was made on the section with the presence of a nucleolus, except when defining the presence of an antrum where all sections of the follicle were observed. Mean follicle and oocyte diameter were recorded for each isolated follicle. In this chapter, we categorised the isolated preantral follicles into 2 groups based on the follicle size (Araujo *et al.*, 2014, Braw-Tal and Yossefi, 1997, Wandji *et al.*, 1996b), which were < 100 and ≥ 100 µm.

5.2.4. Detection of γH2AX, ATM, Cx43, GDF9 and Laminin Antigen by Immunofluorescence Microscopy.

Double staining with immunofluorescence for γH2AX and ATM was performed to provide information on whether DNA damage and repair occurred at the same time point. Immunofluorescence method was as described in chapter 2, 3 and 4. Details of

antibodies used are shown in Table 5.1. In brief: slides were subjected to high-temperature antigen retrieval for 20 minutes using a microwave. Following incubation in blocking solution for 1 hour, slides were then probed with primary antibody against γH2AX and ATM (Table 5.1) overnight at 4ºC. Blocking solution without primary antibody served as a negative control. Sections were then incubated with appropriate secondary antibodies (Table 5.2) for 1 hour on the following day, and then washed and mounted in vectashield hardset with DAPI. Images were captured using a Zeiss LSM 800 confocal microscope with x20 magnification with identical setting for all samples. Images were analysed using ImageJ and protein expression was determined both in oocytes and granulosa cells, except for Cx43 and laminin which were analysed in granulosa cells only. Tissue permeabilisation with 0.1% triton was applied to all samples, including laminin, to investigate laminin expression in basal lamina and membrana granulosa of the follicle.

Table 5.1. Primary antibodies used for immunohistochemistry analysis

Blocking serum	Primary antibody	Product number	Species raised	Final concentration (stock solution)	Source
Goat serum (Sigma Aldrich)	γH2AX	NB100-384	Rabbit polyclonal	1 μg/ml (1 mg/ml)	Novusbio
Goat serum (Sigma Aldrich)	ATM	ab78	Mouse monoclonal	7.4 μg/ml (1.85 mg/ml)	Abcam
Goat serum (Sigma Aldrich)	Connexin 43	ab79010	Mouse monoclonal	4.98 μg/ml (1 mg/ml)	Abcam
Goat serum (Sigma Aldrich)	GDF9	ab93892	Rabbit polyclonal	4.5 μg/ml (0.9 mg/ml)	Abcam
Goat serum (Sigma Aldrich)	Laminin	ab11575	Rabbit polyclonal	2.5 μg/ml (0.5 mg/ml)	Abcam

Table 5.2. Additional secondary antibodies used for immunohistochemistry analysis

Secondary antibody	Product number	Final concentration (stock solution)	Source
VECTASTAIN Elite ABC HRP Kit (peroxidase, mouse IgG)	PK 6101	50 µl biotinylated secondary antibody + 150 µl goat serum+ 10 ml TBST.	Vector Laboratories
VECTASTAIN ABC-Elite ABC HRP Kit (peroxidase, mouse IgG)	PK 6102	50 µl biotinylated secondary antibody+ 150 µl horse serum+ 10 ml TBST.	Vector Laboratories
Cy3 AffiniPure Donkey Anti-Rabbit IgG (H+L)	711-165-152	5.98 µg/ml (1.5 mg/ml)	Jackson Laboratories
Cy2 AffiniPure Goat Anti-Mouse IgG (H+L)	115-225-146	5.98 µg/ml (1.5 mg/ml)	Jackson Laboratories

5.2.5. Quantitative Analysis of γH2AX, ATM, Cx43, GDF9 and Laminin

ImageJ was used to quantify the immunofluorescence intensity or the area with positive staining for γH2AX, ATM, Cx43 and GDF9. The level of fluorescence in the nucleus of oocytes was calculated using mean gray value. The area of cells with positive antibody staining was calculated by setting a threshold value on the fluorescence intensity. This is achieved by manually adjusting the intensity value to cover the positively stained area. We then normalised the measured area by dividing it with the total area of the granulosa cells compartment and expressed as percentage (Figure 5.2). Data are presented as mean ± SEM.

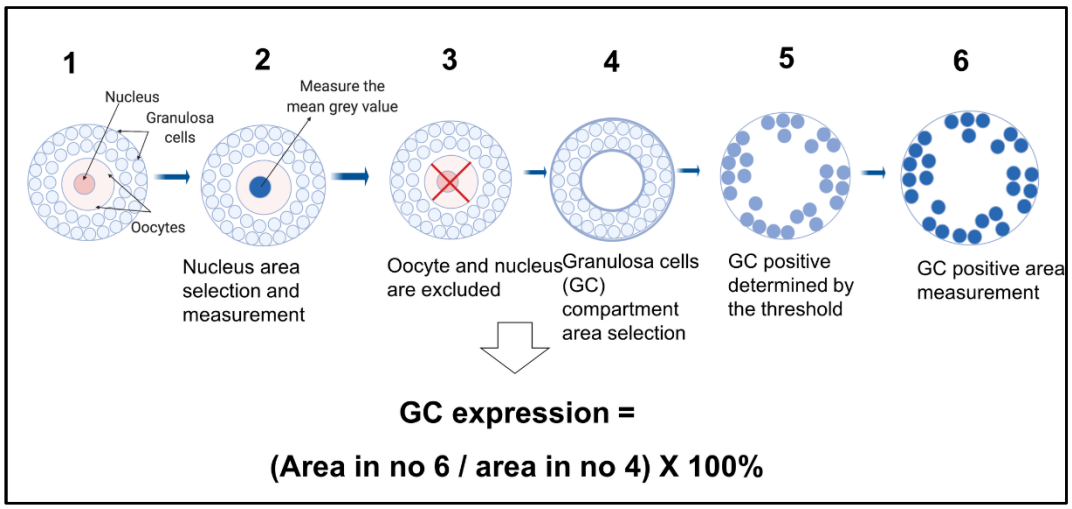

Figure 5.2. Diagram showing the method to analysis the γH2AX and ATM expression in (1) oocyte (nucleus) and (2-5) granulosa cells.

The expression of Cx43 and intrafollicular laminin was determined by measuring the area of positive expression as described above. This measurement was then averaged over the values obtained in the section with the largest oocyte diameter (middle section), two sections in between the first and middle section and between the last and middle section (Figure 5.3).

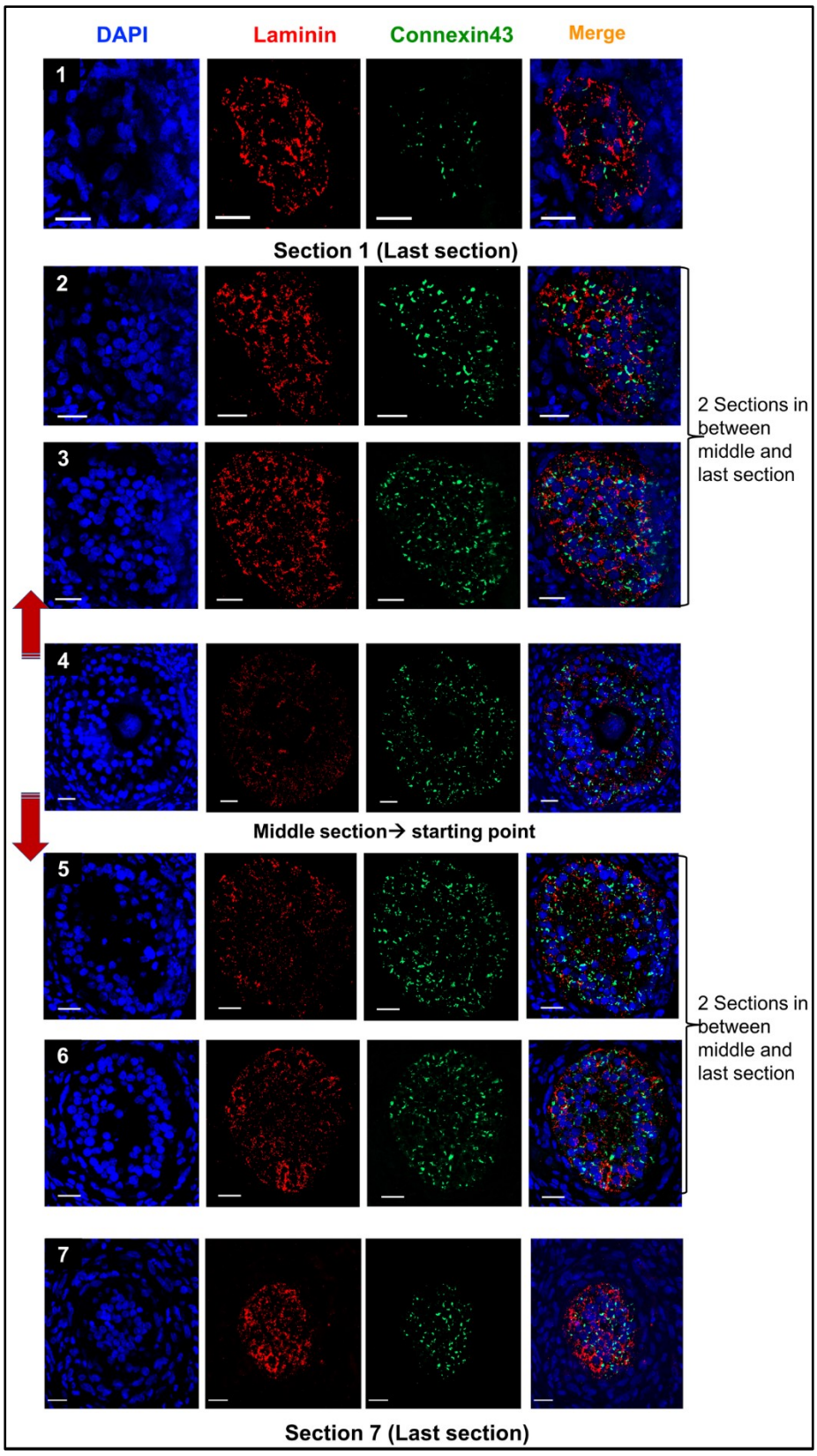

Figure 5.3. Representative images of a serial section to determine laminin and connexin43 expression within granulosa cells. Permeabilisation of the membrane was performed to determine the

laminin expression surrounding the granulosa cells and basal lamina of the follicles. Depending on the size of the follicle, approximately 3 to 7 sections were analysed in each follicle per group. The section containing the oocyte nucleus and therefore the point of the largest diameter was considered the middle section, The analysis started from this middle section, then moved to sections in both directions. Two sections between the middle section and the last section either on the left or the right side were included into the analysis. Scale bar = 50 μm.

5.2.6. Immunohistochemistry

DNA damage repair protein Rad51 was localised in tissue sections using antibodies against Rad51 (Table 3.1). Immunohistochemistry protocol was run as described in chapter 2 section 2.5.1. The expression of Rad51 was determined in oocytes and granulosa cells. The proportion of oocytes positive for Rad51 was defined as the number of follicles with positive expression in oocytes per total number of follicles in each group. The mean proportion of granulosa cells was determined as the number of granulosa cells positive for Rad51 over a total number of granulosa cells in each follicle. The expression was presented as mean ± SEM.

5.2.7. Statistical Analysis

SPSS version 22 was used to analyse the data. GraphPad version 8 was utilised to generate the graphs. Qualitative data were presented as a percentage. The analysis was run by either Chi-square or Fisher exact test. Quantitative data were analysed either by the Kruskal Wallis followed by the Dunn's Bonferroni test for the data that was not normally distributed or one-way ANOVA followed by Fisher least significant differences (LSD) post hoc test for normally distributed data. The follicle and oocyte diameter were compared among treatment groups at D6 and every second day of the culture period using ANOVA and LSD post hoc test. The difference of growth rate

from D6, D8, D10 and D12 was assessed using general linear model repeated measure. The pairwise comparison t-test was simultaneously generated within the analysis. p-value < 0.05 was considered significant. Quantitative data are presented as mean ± SEM.

5.3. Results

5.3.1. Isolated Follicle Growth and Survival

The amount of stromal tissue surrounding isolated follicles varied due to the dissimilarity in stromal density in tissue fragments. During isolation, care was taken to ensure basal lamina was intact and adequate theca cells was presented as they are fundamental to preserve follicle growth and development. In this experiment, we included 9 replicates of ovarian strip cultures. After 6 days, growing follicles were mechanically isolated from all strips. A total of 578 follicles were isolated from all groups after six days of ovarian strip culture. The follicles isolated ranged in size from 66.1 to 144.6 μm, of which a total of 237 (41%) follicles were greater than 100 μm.

A significant increase in the mean proportion of isolated follicles (regardless of diameter at isolation) from every culture was observed in bpv(HOpic) group (35.7 ± 18.5%) compared to control (21.1 ± 2.6%) and rapamycin (11.9 ± 3.2%) on its own ($p < 0.05$). The combined bpv(HOpic) and rapamycin group (30.6 ± 3.0%) did not exhibit a significant difference from bpv(HOpic) alone ($p > 0.05$) (Figure 5.4 1-5).

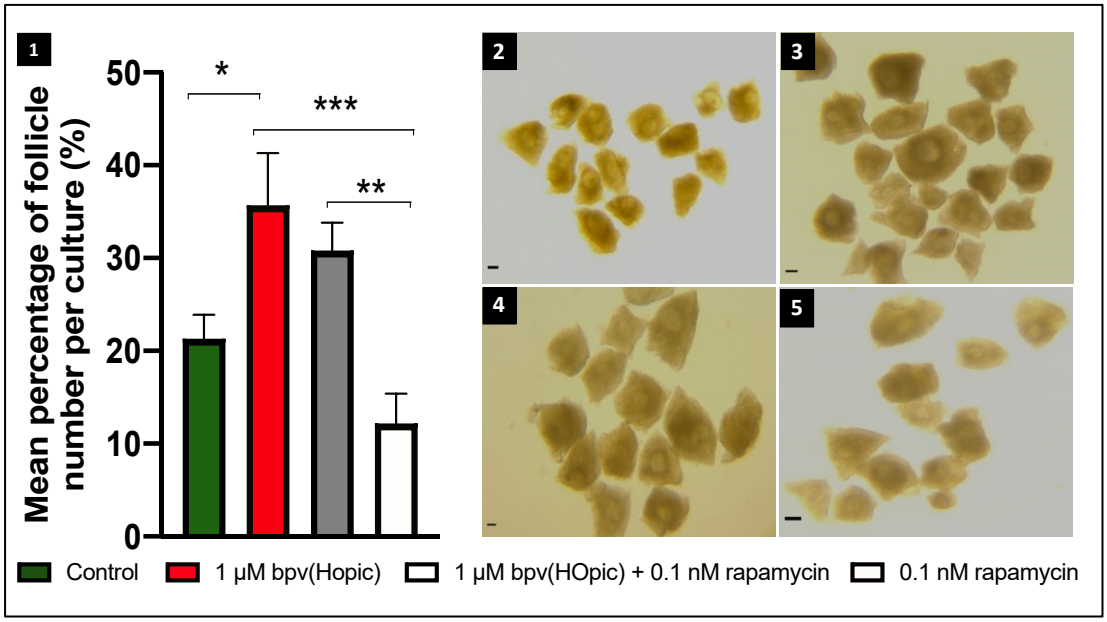

Figure 5.4. The average proportion of isolated follicle number per each group. 1) The average percentage of follicles isolated from ovarian cortical strips in each group after 6 days of culture. A total of 578 follicles were isolated from 9 separate cultures. Asterisk (***) ≤ 0.001, (**) ≤ 0.01, (*) < 0.05. Kruskal Wallis test, p-value was assigned at < 0.05. Data shows mean percentage ± SEM from 9 replicates. Photomicrograph of isolated follicles from each group. 2) Control, 3) 1 µM bpv(HOpic), 4) Combined 1 µM bpv(HOpic) and 0.1 nM rapamycin and 5) 0.1 nM rapamycin. Scale bar = 100 µm.

The proportion of isolated follicles in each group based on the diameter at isolation (more or < 100 µm) was calculated. Follicles sized ≥ 100 µm in diameter (at isolation) was significantly higher in bpv(HOpic) (56.8%) compared to control (35.9, p ≤ 0.001), rapamycin (19.4%, p ≤ 0.001) and combined bpv(HOpic) and rapamycin group (36.1%, p = 0.001) (Table 5.3). The number of follicles isolated from combined bpv(HOpic) and rapamycin group tended to be similar to control group (p > 0.05).

Table 5.3. The distribution of isolated follicles sized more and < 100 μm in each group of ovarian fragments after 6 days of culture.

Group	Follicle size		Total
	< 100 μm (n, %)	≥ 100 μm (n, %)	
Control	82 (64.1) [a]	46 (35.9) [a]	128
1μM bpv(HOpic)	83(43.2) [b]	109 (56.8) [b]	192
1 μM bpv(HOpic) + 0.1 nM rapamycin	122 (63.9) [a]	69 (36.1) [a]	191
0.1 nM rapamycin	54 (80.6) [d]	13 (19.4) [d]	67
Total	341 (59.0)	237 (41.0)	578

(a), (b), (c) and (d) denote a significant difference between treatment groups. Different letters indicate $p < 0.05$. Chi square test, p-value < 0.05 was considered significant.

The mean follicle diameter measured < 100 μm at isolation was 84.9 ± 0.5 μm, and 116.4 ± 0.7 μm for the follicles ≥ 100 μm in diameter. However, overall, the follicle isolated from rapamycin group were tended to be smaller compared to other groups (110.7 ± 3.6 μm). Analysis within the group showed that the diameter of the follicles isolated from the control group (sized ≥ 100 μm at isolation) rose from 118.4 ± 1.8 on D6 to 220.5 ± 11.0 μm on D12 with a significant increase in the measurement during the subsequent 6 days of culture period ($p \leq 0.001$). Likewise, in combined bpv(HOpic) and rapamycin and rapamycin alone group, follicle size increased significantly from D6 (118.3 ± 1.3 and 110 ± 3.6 μm) to D12 (196.9 ± 9.9 and 178.6 ± 15.2 μm) ($p \leq 0.001$) (Figure 5. 5 A, C, D, E, F). On the other hand, follicles isolated from the tissue exposed to bpv(HOpic) exhibited an increase in diameter, with limited, nonsignificant growth from D10 (134.9 ± 4.2 μm) to D12 (136.5 ± 6.9 μm ($p > 0.752$). Eventually, the follicle diameter in bpv(HOpic) was significantly reduced compared to control group on the completion of culture period (136.5 ± 6.9 vs 220.5 ± 11.0 μm,

p ≤ 0.001). No changes were observed in combined bpv(HOpic) and rapamycin and rapamycin alone (p > 0.05) (Figure 5.5 A).

Meanwhile, the treatment did not affect the growth of follicles < 100 µm (Figure 5.5 B), and it appeared to be very slow, though a significant increase was still observed from D6 to D12 in all groups. The proportion of isolated follicles (sized < 100 µm) that was able to grow and reach the diameter > 50% of the original size at the start of culture (D6) after 6 days of culture was similar across the groups ranging from 23.6 to 28.1%. Nevertheless, it only occurred when the diameter of the follicles on D6 was 88.9 ± 0.9 µm (p ≤ 0.001) regardless of the initial treatment in ovarian cortical fragments.

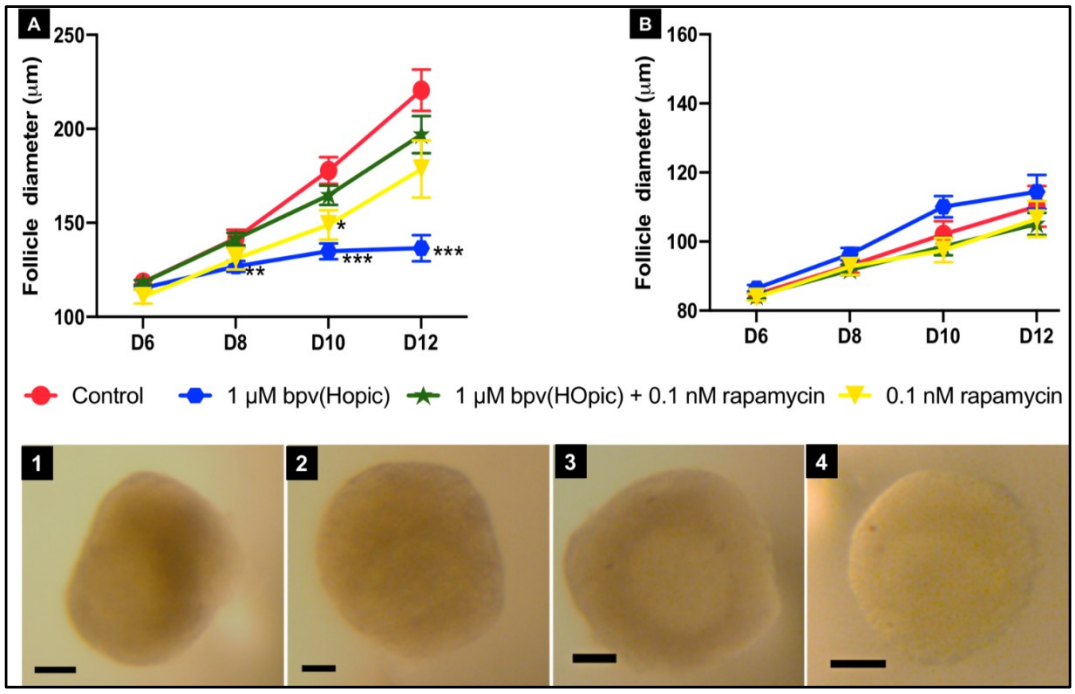

Figure 5.5. The follicular growth charts. (A) The growth of follicles sized ≥ 100 µm (B) < 100 µm at isolation. Follicle growth sized ≥ 100 µm at isolation increased significantly after 6 days of culture in control group. While follicles in bpv(HOpic) group displayed a limited and non-significant growth. The follicle growth was tended to be similar in the follicles sized <100 µm at isolation. Statistical analyses

were performed in comparison with the control group. ANOVA, the p-value was assigned at < 0.05. The difference of growth rate from D6, 8, 10 and 12 was assessed using general linear model repeated measure. Asterisk (***) ≤ 0.001, (**) ≤ 0.01, (*) < 0.05. Data shows mean percentage ± SEM from 9 replicates. (1- 4) Photomicrographs of isolated follicles after a total of 12 days in culture. (1) Control, (2) bpv(HOpic), (3) combined bpv(HOpic) and rapamycin, and (4) rapamycin group. Scale bar = 100 μm.

The variability in the stromal density surrounding the isolated follicles led to difficulties in precisely assessing the growth of the oocyte during the culture system. In this respect, the oocyte diameter was determined on the D12 of culture by evaluating the growth of the oocytes within histological sections. In parallel with follicle growth, oocyte diameter within the follicles sized ≥ 100 μm at isolation was significantly smaller in bpv(HOpic) (39.2 ± 1.6 μm) compared to control group (60.1 ± 2.8 μm, $p \leq 0.001$) (Figure 5.6 A). Likewise, rapamycin either on its own or in combination with bpv(HOpic) did not significantly affect the oocyte diameter. Furthermore, in parallel to follicle growth there was no significant difference in the mean oocyte diameter (within follicles sized < 100 μm) at isolation across all groups on completion of the culture period ($p > 0.05$) (Figure 5.6 B).

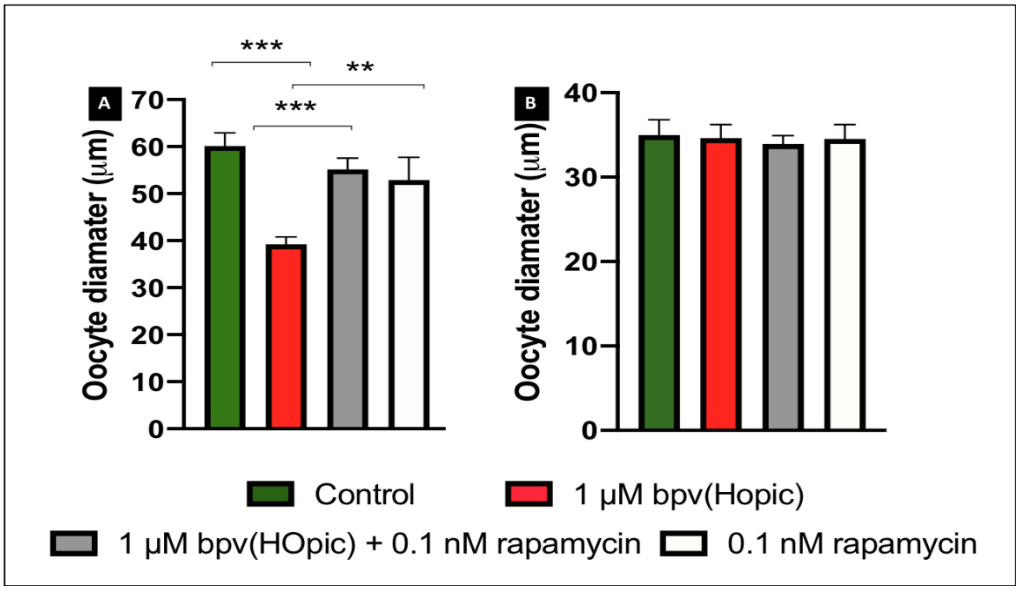

Figure 5.6. Oocytes growth after six days of culture. (A) Oocyte diameter in the follicles with a diameter ≥ 100 µm and (B) < 100 µm at isolation show an increase in oocyte diameter in control compared to bpv(HOpic) group when the size of the follicles at the start was ≥ 100 µm. Oocyte diameter tended to be similar across the groups in follicles < 100 µm. Analysis of 341 and 237 follicles respectively. ANOVA, the p-value was assigned at ≤ 0.05. Asterisk (***) ≤ 0.001, (**) ≤ 0.01, (*) < 0.05. Data shows mean percentage ± SEM from 9 cultures replicates.

Most of the follicles were morphologically unhealthy after 6 days of culture. Further analysis showed that all follicles regardless of the diameter at isolation demonstrated a decline in morphological health in bpv(HOpic) (1.6% healthy) compared to control group (7.0%, $p < 0.05$) (Figure 5.7 A). The presence of rapamycin either alone or in combination with bpv(HOpic) did not alter the proportion of morphologically healthy follicles ($p > 0.05$) (Figure 5.7 A). The analysis was then separated based on follicle diameter at isolation and a similar observation was found in follicles ≥ 100 µm in diameter (at isolation) in bpv(HOpic) group (1.8%) compared to control (11.6%, $p < 0.05$) (Figure 5.7 B). Rapamycin alone (12.5%, $p > 0.05$) or in combination with bpv(HOpic) (5.8%, $p > 0.05$) did not change the proportion compared to bpv(HOpic)

group. However, all treatments showed no difference in follicles < 100 µm (at isolation) ($p > 0.05$, Figure 5.7 C).

Meanwhile, antral follicles were only observed in control (1.7%) and rapamycin group (1.3%) and no significant difference observed among the groups ($p > 0.05$, Figure 5.7 D). Nevertheless, no antral follicles were healthy irrespective of the treatments and, none of the follicles < 100 µm (at isolation) reached the antral stage (Figure 5.7 4).

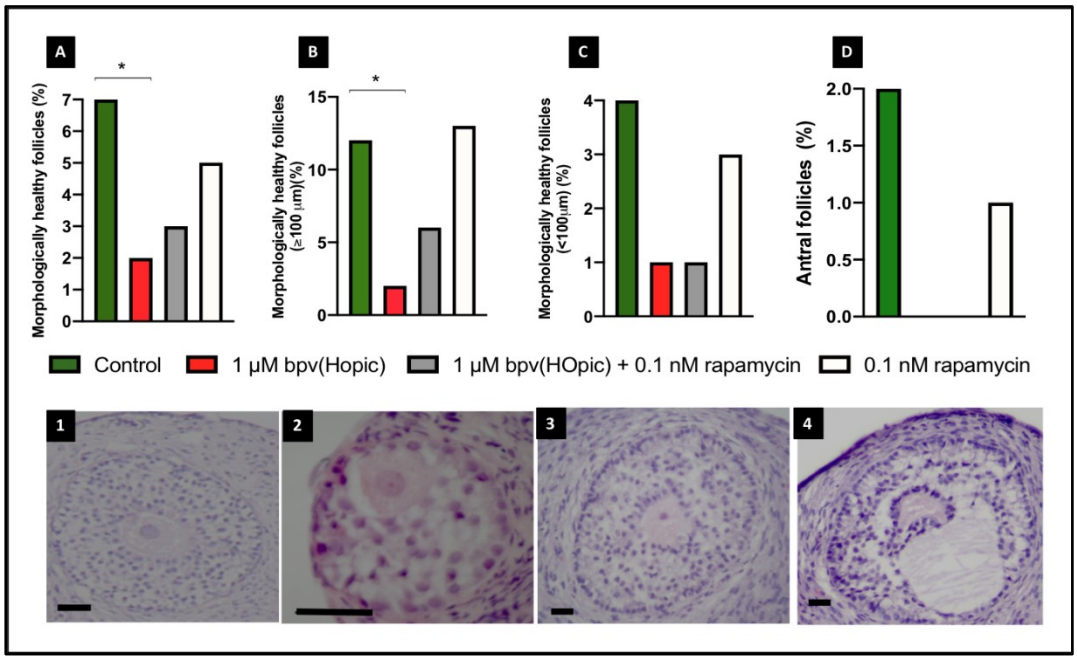

Figure 5.7. Morphologically healthy follicles analysis in all groups. (A) Proportion of morphologically healthy follicles regardless of follicles diameter when the culture was initiated, (B) Follicles diameter was ≥ 100 µm and (C) < 100 µm at isolation. Data are presented as a proportion (%) from 9 replicates (analysis of 578 follicles). Fisher exact test, p-value was assigned at < 0.05. Asterisk (***) ≤ 0.001, (**) ≤ 0.01, (*) < 0.05. Adjacent photomicrographs of isolated follicles in (1) control, (2) bpv(HOpic) with limited follicle growth, (3) bpv(HOpic) and rapamycin showing follicle increased in size with the misshapen oocyte, and (4) Antral follicle in rapamycin group. Scale bar = 50 µm.

5.3.2. Effects of the Treatment in Tissue Fragments on DDR in Isolated Follicles.

Only follicles with initial diameter ≥ 100 μm at isolation were included for analysis of DDR markers using immunofluorescence microscopy. The follicles subjected to analysis were randomly chosen from each culture group. After 6 days of culture, γH2AX expression within oocytes and granulosa cells was similar across the groups regardless of treatment ($p > 0.05$) (Figure 5.8 A and B, 5.9 A-E). However, ATM expression in both oocytes (40.5 ± 10.5) and granulosa cells (11.8 ± 0.9%) of bpv(HOpic) group was significantly lower compared to control (90.5 ± 14.3 and 18.4 ± 2.9%, $p < 0.05$) (Figure 5.8 C and D and 5.9 A-E). The expression was upregulated in the combined bpv(HOpic) and rapamycin group compared to bpv(HOpic) alone, both in oocytes (77.3 ± 14.7) and granulosa cells (14.7 ± 1.5%) ($p < 0.05$). While rapamycin on its own did not alter the expression in oocytes (69.4 ± 13.9, $p > 0.05$), it decreased significantly in granulosa cells (15.7 ± 1.5) compared to bpv(HOpic) group $p < 0.05$) (Figure 5.8 C, D and 5.9 A-E).

The γH2AX to ATM ratio was calculated to further analyse whether DNA damage occurred concurrently with ATM expression. Oocyte γH2AX to ATM ratio was defined as oocyte mean gray value of γH2AX divided by ATM. Whilst in granulosa cells, the ratio was obtained by dividing the proportion of γH2AX expression by ATM. The ratio was markedly increased in oocytes of bpv(HOpic) (1.99 ± 0.27) group compared to control (1.04 ± 0.2, $p < 0.05$). No significant differences were observed either in the rapamycin (1.2 ± 0.3) or in combined bpv(HOpic) and rapamycin groups (1.06 ± 0.15) ($p > 0.05$) compared to control, but significant differences were observed

when these two groups were compared to the bpv(HOpic) group ($p < 0.05$). On the other hand, the ratio in granulosa cells was higher in bpv(HOpic) (1.5 ± 0.2) ($p < 0.05$) and there were no significant changes in combined bpv(HOpic) and rapamycin or rapamycin on its own compared to control group (Figure 5.8 E and F).

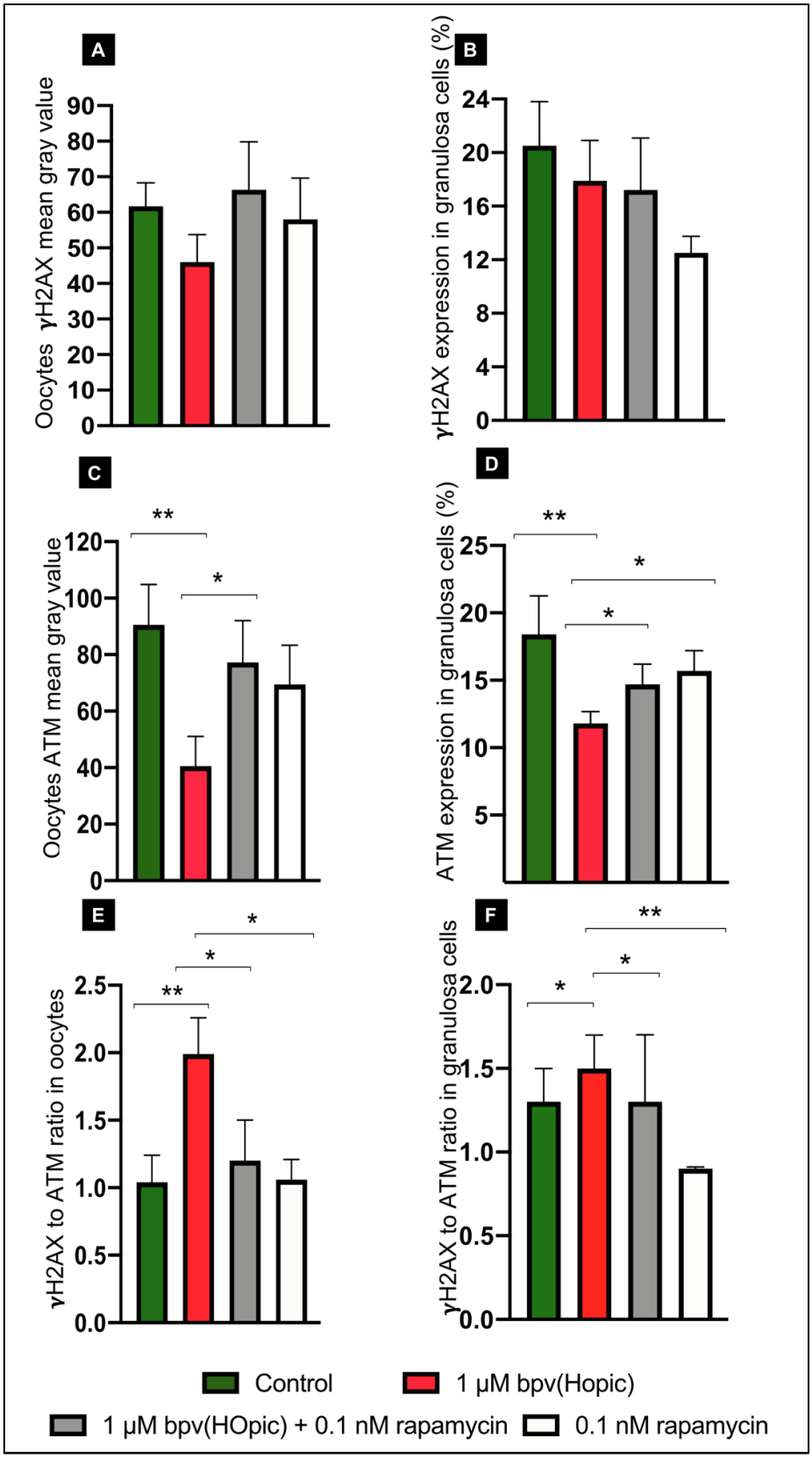

Figure 5.8. γH2AX and ATM localisation by immunofluorescence in the control and treatment groups. (A) γH2AX expression in the nucleus within oocytes and (B) granulosa cells did not reveal

significant differences across the groups. While DNA repair protein, ATM, was downregulated in (C) oocytes and (D) granulosa cells in bpv(HOpic) group. (E) The ratio of γH2AX to ATM indicated an increase in bpv(HOpic) compared to control in oocytes and (F) granulosa cells. Kruskal Wallis test. Asterisk (***): $p \leq 0.001$, (**): $p \leq 0.01$, (*): $p < 0.05$. Analysis of 62 follicles.

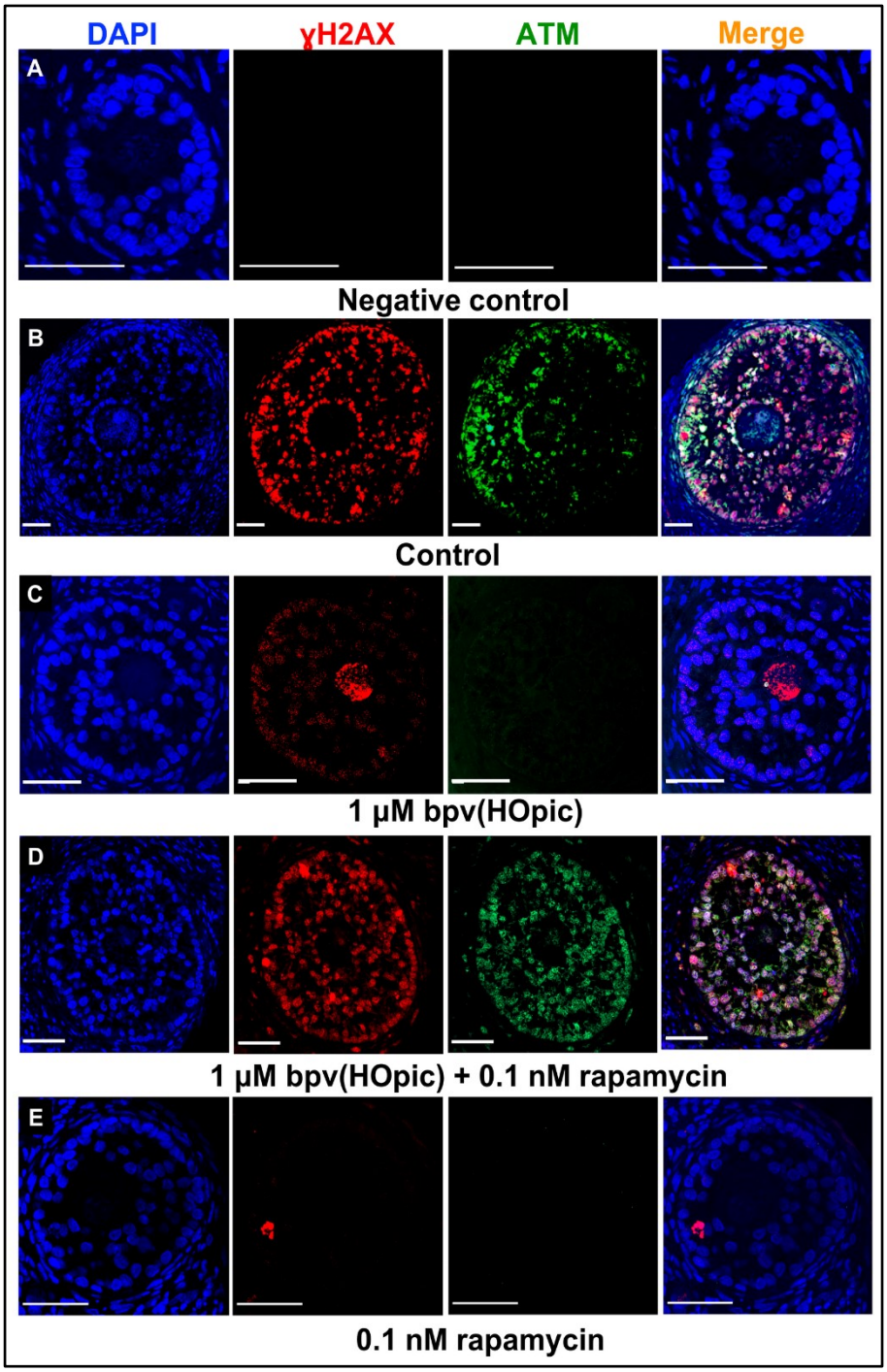

Figure 5.9. Photomicrographs of immunofluorescence microscopy of γH2AX and ATM expression in all groups. (A) Negative control, (B) Control, with positive γH2AX and ATM expression

both in oocytes and granulosa cells, (C) γH2AX and less ATM expression within oocytes and granulosa cells in bpv(HOpic) group, (D) Positive γH2AX and ATM expression in bpv(HOpic) and rapamycin, and (E) Negative γH2AX and ATM expression in oocytes with limited expression in granulosa cells in rapamycin group. Negative staining of γH2AX and ATM in oocyte and minimal staining in granulosa cells in rapamycin group could reflect minimal effect of rapamycin on DNA damage. In this context, both γH2AX and ATM were not upregulated. Scale bar = 50 µm.

Follicular capacity to repair damage was assessed by analysing Rad51. It was shown that Rad51 expression in oocytes was downregulated in bpv(HOpic) (22.2%) compared to control (58.3%) ($p = 0.008$). The addition of rapamycin either in combination with bpv(HOpic) (46.4%, $p = 0.059$) or rapamycin alone (28.6%, $p = 0.166$) did not significantly alter the expression (Figure 5.10 A). Rad51 expression within granulosa cells was similar across groups ($p > 0.05$) (Figure 5.10 B).

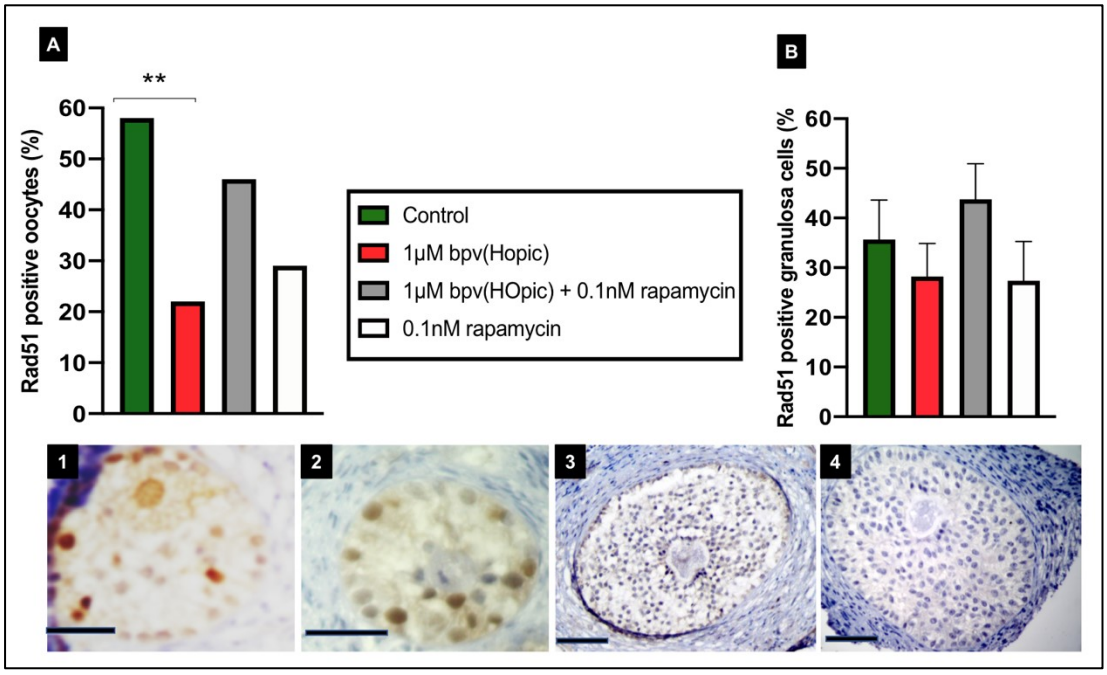

Figure 5.10. Immunohistochemistry analysis of Rad51 expression in oocytes and granulosa cells. (A) The proportion of Rad51 in oocytes showing a decline in the oocyte of bpv(HOpic) group. (B) Granulosa cells expression of Rad51 showing a similar Rad51 expression across the groups. Error bars show mean percentage ± SEM. Kruskal Wallis test. Asterisk (***) ≤ 0.001, (**) ≤ 0.01, (*) < 0.05. p-

value was assigned at < 0.05. Adjacent photomicrographs of Rad51 expression within oocytes and granulosa cells of isolated follicles in (1) control, antral follicle with positive staining in oocytes, (2) Negative staining in oocytes in bpv(HOpic) group, (3) bpv(HOpic) and rapamycin and (4) rapamycin group. Scale bar = 50 μm.

5.3.3. Effects of the Treatment on Cx43, Laminin and GDF9 Expression

Cx43, GDF9 and laminin expression was determined within the follicles after 6 to 8 days of the culture period. Cx43 expression was assessed in isolated follicles after 6 days of culture to determine whether culture condition affected cell communication. Cx43 and laminin were only expressed within the granulosa cell area, while GDF9 protein was also detected in the granulosa cells area (Figure 5.11 B, C, D. E). GDF9 expression was similar across the groups ($p > 0.05$) (Figure 5.11 A). Cx43 and laminin were calculated as an area in the granulosa cell compartment that expressed Cx43 and laminin above the threshold set at the same level across the follicle (before the analysis) to a total granulosa cells area per follicles. Depending on the follicle size, 173 sections from 57 follicles were included in the analysis. Cx43 expression in granulosa cells was markedly decreased in bpv(HOpic) (14.8 ± 0.9%) compared to control (17.01 ± 0.70%) ($p = 0.006$), and no significant alterations were found either in rapamycin or combined bpv(HOpic) and rapamycin group ($p > 0.05$) (Figure 5.12 B). Laminin expression was determined to assess basal lamina expansion and whether the culture conditions were able to preserve membrana granulosa throughout the culture period. There was no significant effect of either the treatment or the isolation techniques on laminin expression (Figure 5.12 C, 5.13 A-E).

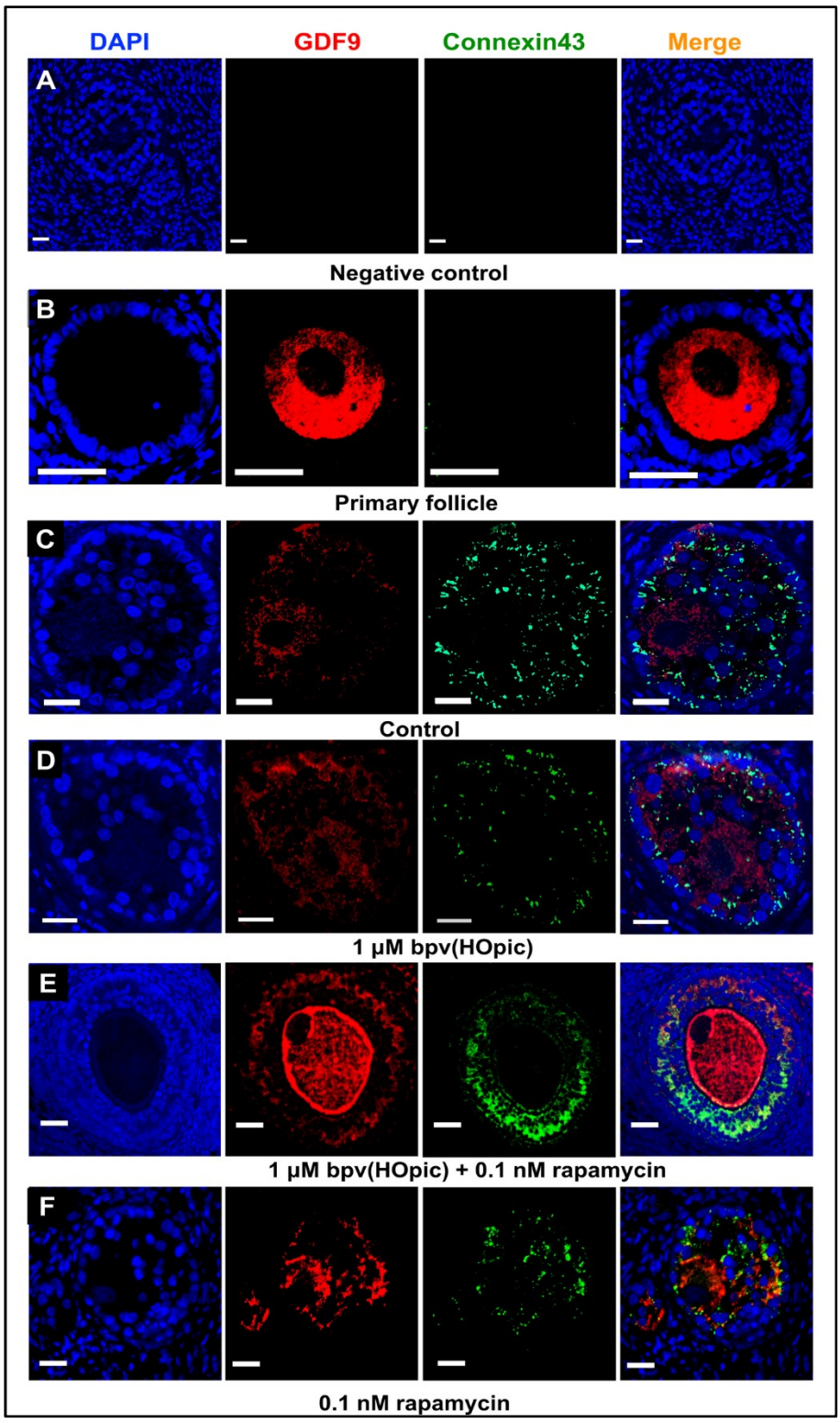

Figure 5.11. The localisation of GDF9 (red) and Cx43 (green) protein within ovarian follicles following six days of the culture period. (A) Negative control (B) GDF9 (red) and Cx43 (green) expression within primary follicles indicate a limited Cx43 expression within granulosa cells compartment and intense GDF9 expression within the oocyte. (C) GDF9 and Cx43 expression in

control. (D) bpv(HOpic) group shows a weak Cx43 expression within granulosa cells with GDF9 expressed in the oocyte. (E) bpv(HOpic) and rapamycin and (F) rapamycin group. GDF9 is not detected in granulosa cells of the primary follicle. GDF9 expression seems to be low both in oocyte and granulosa cells in control and bpv(HOpic) groups. However, quantitative analysis showed no significant difference in GDF9 expression across the groups. Scale bar = 50 µm.

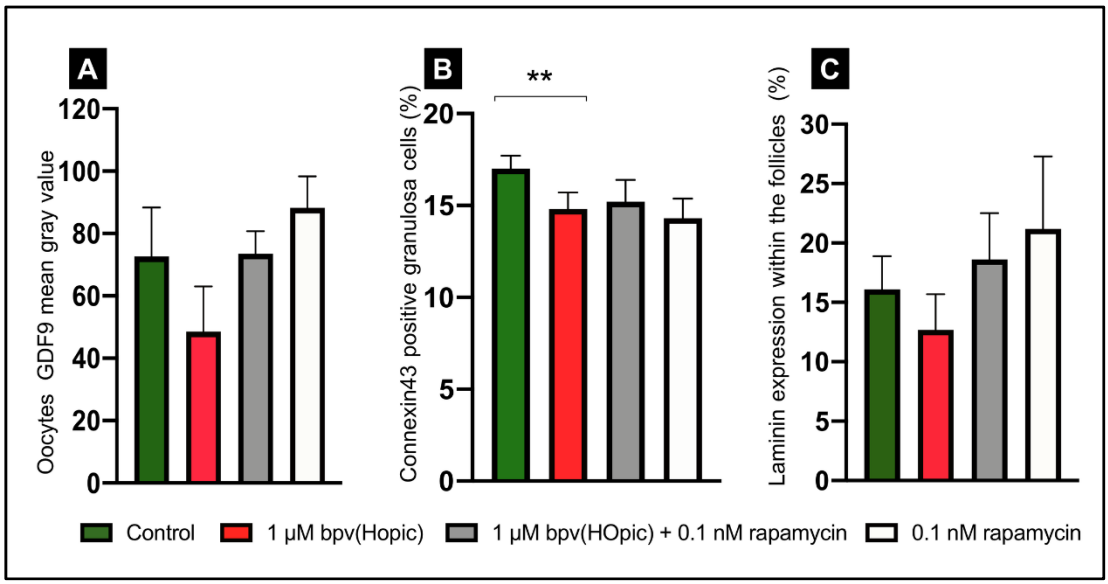

Figure 5.12. Oocytes of *in vitro* grown follicles expression of GDF9, granulosa cells expression of Cx43 and follicular expression of laminin. (A) Oocytes expression of GDF9 indicates no significant differences observed among the groups. (B) Cx43 expression was lower in bpv(HOpic) group (C) Laminin expressed in a similar fashion across the groups. Kruskal Wallis test. Asterisk (***) ≤ 0.001, (**) ≤ 0.01, (*) < 0.05. Data shows mean percentage ± SEM.

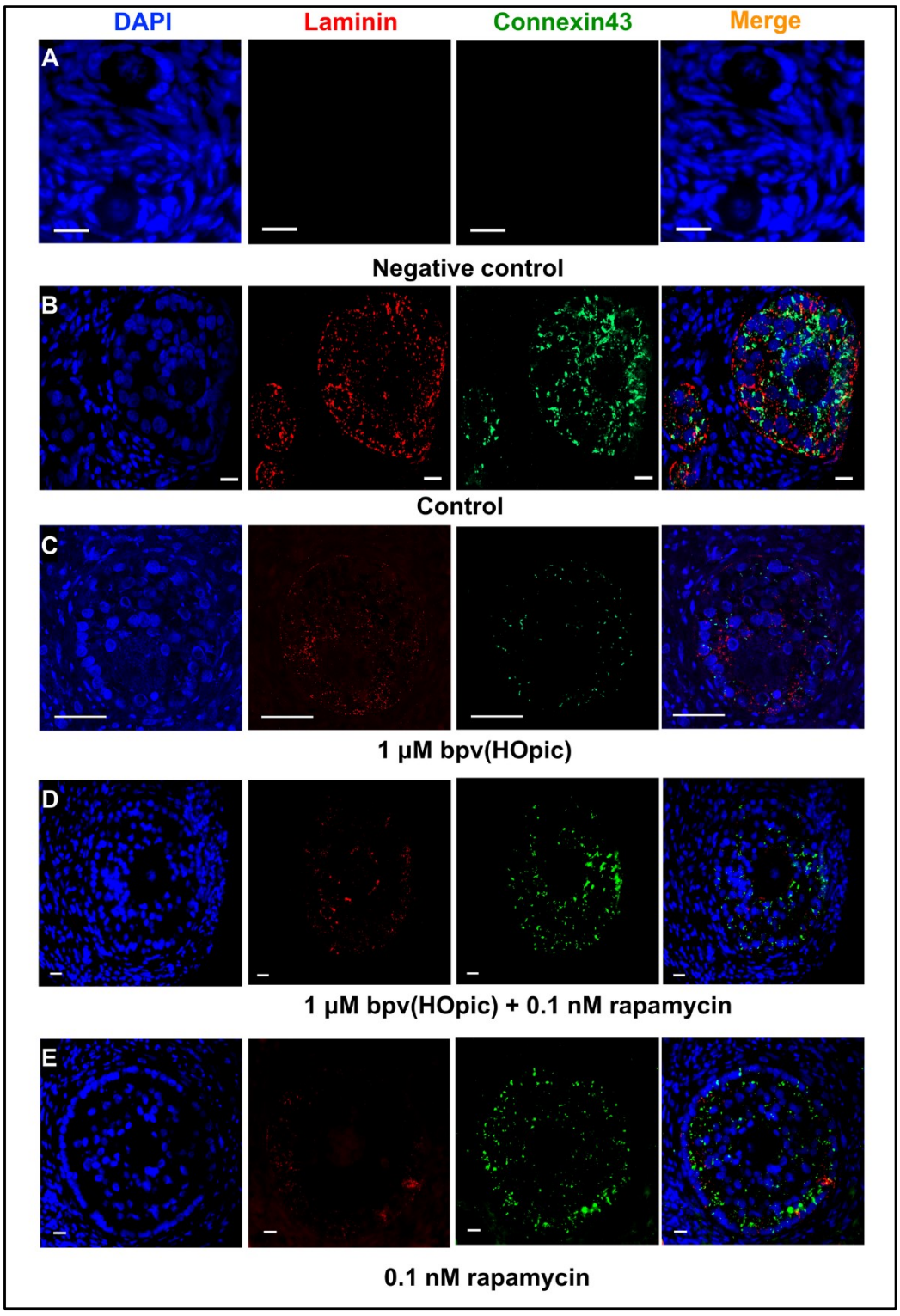

Figure 5.13. Photomicrographs of immunofluorescence microscopy of laminin and Cx43 within the granulosa cells compartment. (A) Freshly fixed tissue used as a negative control, (B) Control, with positive Cx43 (green) and laminin (red) expression in granulosa cells, (C) bpv(HOpic) group, (D) bpv(HOpic) and rapamycin, and (E) rapamycin group. Scale bar = 50 µm.

5.4. Discussion

In this chapter, the investigation on whether isolated preantral follicles from the tissue fragments treated with rapamycin or bpv(HOPic) could restore DDR following 6 days of culture was extended. The results demonstrated that the addition of bpv(HOpic) alone in culture media decreased preantral follicle growth compared to control in agreement with our previous published findings (McLaughlin *et al.*, 2014). It appeared that culture of preantral follicles isolated from either rapamycin on its own or in combination with bpv(HOpic) did not alter the proportion of morphologically healthy follicles. It is interesting to note that, overall morphological health in the control group was considerably lower compared to our previous study in bovine (McLaughlin and Telfer, 2010) and human (McLaughlin *et al.*, 2018). The primary features of morphologically unhealthy follicles in all groups were disorganised or granulosa cell loss, loopy basal lamina and shrunken oocytes (Abdel-Khalek *et al.*, 2010). Eventually, the growth of preantral follicles throughout the culture period only reached the antral stage in control and rapamycin group and all antral follicles obtained were morphologically unhealthy.

In this chapter, we investigated further whether the treatment in ovarian cortical fragments was sufficient to obviate DNA damage and restore DNA repair functions in isolated preantral follicles cultured for another 6 to 8 days. Despite a significant increase in morphologically unhealthy follicles in bpv(HOpic) group, γH2AX expression did not differ across the group. In contrast, at the same time point, DNA repair protein expression of ATM and Rad51 in bpv(HOpic) group was attenuated compared to control suggesting a lack of DNA repair protein interaction. Likewise, both the rapamycin and combined bpv(HOpic) and rapamycin groups did not show a

significantly enhanced ATM expression. However, morphologically healthy follicles in these groups did not differ from control and bpv(HOpic) group. Whilst there appeared to be a trend that morphologically healthy follicles were more evident in rapamycin compared to the bpv(HOpic) group, it did not reach statistical significance. These findings indicated that DNA damage occurrence in all treatment groups was either severe with limited repair or DNA repair mechanism did not function appropriately that might trigger the pro-apoptotic gene activation and subsequently apoptosis (Livera *et al.*, 2008, Suh *et al.*, 2006).

ATM phosphorylation has been reported as the first step in the G2 checkpoint activation in the DNA damage repair pathway (Carroll and Marangos, 2013). We demonstrated that ATM was downregulated in bpv(HOpic) group. As was shown in chapter 4, granulosa cells of secondary follicles exhibited a low DNA damage in all groups and generally DNA repair capacity was not affected. However, it seemed likely that follicles in bpv(HOpic) group were not able to survive as the highest morphologically unhealthy follicle were observed in this group. In line with this finding, widespread granulosa cells of secondary follicle apoptosis have been reported following cisplatin exposure and is associated with upregulation of PI3K/Akt signaling pathway (Chang *et al.*, 2015). In surviving follicles, DNA repair protein activity was able to repair DNA damage as was shown by Rad51 activity in response to doxorubicin induced DNA damage in mouse oocytes (Kujjo *et al.*, 2010).

During preantral follicle development, increased expression of GFD9 is observed but this was not found in this study. Despite an increase in follicle growth, in control group, GDF9 expression did not differ across the group. Photomicrographs in Figure 5.11 C and D show that GDF9 expression appears to be low both in oocyte and granulosa

cells in control and bpv(HOpic) groups. However, the images used in the photomicrographs have been randomly selected and any perceived differences are not necessarily reflected in the quantitative analysis. Indeed, the analysis showed no significant difference in GDF9 expression across the groups. GDF9 protein was detected within oocytes and granulosa cells as previously reported in a range of species (Fernandez *et al.*, 2016, Kona *et al.*, 2016, Palomino and De Los Reyes, 2016), including in bovine (Hosoe *et al.*, 2011) and human cumulus cells (Li *et al.*, 2014). Increases in GDF9 expression can be an indication of oocyte growth and granulosa cells differentiation. It is well established that maintenance of oocyte-granulosa cell connections is fundamental for healthy follicle development (Albertini *et al.*, 2001, Eppig, 2001, McLaughlin *et al.*, 2010a). However, in the present study no significant changes in GDF9 and Cx43 expression in the treatment groups compared to control.

Granulosa cell interaction appeared well preserved in control group but a decline in Cx43 expression was observed in the bpv(HOpic) group. It is worth noting that in vitro culture may interfere with the intercellular interactions as evident by the existence of granulosa cell loosening and intercellular spaces (Nottola *et al.*, 2011) suggesting the similar situation possibly applied in granulosa cells of control group as only 7% of the follicles in this group exhibited morphologically healthy after 6 days of culture. However, more evidence is required to support this outcome, including the presence of uncultured preantral and antral follicles as a comparison. The investigation of Cx37 or other markers such as rhodamine-phalloidin expression could also provide comprehensive information pertaining to follicles grown *in vitro*.

It has been reported that the formation of an antral cavity is commonly established when the diameter of the follicle reaches 200 μm (McLaughlin *et al.*, 2010a). We previously demonstrated that the presence of activin in media during the multi-step IVG system was associated with an increased number of antral follicles compared to medium without activin (McLaughlin *et al.*, 2010a). In contrast, in the present study, despite the mean follicle diameter in control group being able to reach 200 μm or larger after 6 days of culture, only 1.7% of follicles in the control group formed antral cavities. These outcomes reflect variation between cultures and perhaps with more experience and a greater number of replicates, a higher proportion of follicles would be achieved.

The use of mechanical isolation has been established in our group as the most appropriate method to isolate preantral follicles from cattle and human as the use of enzymes can be deleterious. However, this method is laborious and is associated with low follicle yield (Kim *et al.*, 2018). In domestic animals or human, these techniques become more time consuming and difficult to achieve since the ovary is more fibrous than the mouse ovary. The time needed for isolation might influence follicular health and survival and this of course is operator dependent (Kim *et al.*, 2018). Nonetheless, outcomes are significantly poorer after enzyme digestion as the basement membrane and thecal cell layer are affected resulting in poor follicle morphology (Demeestere *et al.*, 2002, Kim *et al.*, 2018, Telfer *et al.*, 2000, Telfer and Zelinski, 2013). The presence of adequate theca layers is required in growing follicles to retain the 3D structure of the isolated follicle. Collagenase treatment may lead to destruction of theca layers, though this damage can be eluded by the addition of new purified enzyme such as liberase (reviewed by (Telfer and Zelinski, 2013)).

Mechanical isolation has an advantage in that the theca cells can be conserved, and this may support follicle growth and development through steroid biosynthesis and the production of matrix metalloproteinases (MMPs) and tissue inhibitors of metalloproteinases (TIMPs) that are critical for tissue remodelling and basal lamina turnover (Thomas *et al.*, 2001). However, follicular growth is hampered by a large number of stromal cells, therefore it is essential to ensure a balance to preserve adequate theca cells that support follicle development but does not prevent growth. In this respect, technical skill is essential to achieve this condition. Insufficient and ineffective isolation techniques may lead to the presence of a large amount of stroma and theca cells leading to poor morphological health of follicles in this experiment..

Basal lamina expansion is used as a marker of follicular growth (Hatzirodos *et al.*, 2014, Hummitzsch *et al.*, 2013a, Irving-Rodgers *et al.*, 2009). Expansion of basal lamina could not be analysed in the present study since the methodology used in this study involved permeabilisation during immunohistochemistry. Therefore, this is not a reflection of the basal lamina morphology as most of the laminin expression was observed in membrana granulosa cells rather than in basal lamina. In this context, laminin expression might not be useful in determining the impact of technical isolation on isolated preantral follicles.

Recent findings analysing the ultrastructure of ovarian follicles isolated from tissue exposed to mTOR inhibitor suggested that granulosa cell intercellular spaces and vacuolisation were more noticeable in the control group compared to the mTOR inhibitor group (Grosbois *et al.*, 2019). The defects were more likely as a consequence of culture conditions as they were more common following six days of culture period

both in control and mTOR inhibitor group (Grosbois *et al.*, 2019). It is intriguing that, despite more follicles showing morphologically poor health, the effects of mTOR inhibitor in isolated follicle culture was still present after 6 days of culture, which might be due to a higher dose of mTOR inhibitor compared to that used in our present study. Although there was a trend for more morphologically healthy follicles to be present in the rapamycin group in the experiments of this chapter, it did not achieve significance. This observation could be due to there being fewer follicles sized ≥ 100 µm in this group. Alternatively, the low dose rapamycin used in this study was perhaps not sufficient to deliver continuous effects on the isolated follicle growth. We were not able to identify whether rapamycin could provide a better follicle growth outcome compared to control as was shown in another recent study (Grosbois *et al.*, 2019).

Our investigations have not been able to definitively demonstrate the effects of treatment on isolated preantral follicles. The low sample size and poor survival rate are principal limitations of this study. For these reasons LSD was used as a post-hoc test following ANOVA rather than Bonferroni that was used in previous chapters. The aim of changing the post hoc analysis type was that in Bonferroni there is an increased risk of having a type 2 error (false negative) when sample size is low. Given the low sample size compared to the data presented in chapter 3 and 4, type 2 errors are less likely using LSD. However, the risk of having type 1 errors (false positive) become more likely (Williams and Abdi, 2010). Whilst the use of LSD analysis might not be ideal, it provides information on the trend of the results. If the number of follicles in each group can be increased, then Bonferroni's would be used with greater confidence to ensure the validity of the results.

In conclusion, preantral follicles isolated from bpv(HOpic) exposed tissue displayed decreased morphological health in parallel with diminished DNA repair protein. The effect of rapamycin administration in culture media during ovarian fragments culture did not significantly increase preantral follicle survival. Likewise, Cx43 expression as the main connexins forming gap junctions between granulosa cells did not significantly improve with rapamycin.

Chapter 6
General Discussion

6.1. General Discussion

Developing culture systems to support the earliest stage of follicle/oocyte development to maturity in women is an optimistic but challenging strategy to preserve fertility when ovarian tissue transplantation is contraindicated. Each cell component that makes up the follicle (oocyte, granulosa cells and stromal cells) makes significant contributions to regulating follicle growth and in regulating the quality of follicles at all stages. Given that the majority of follicles within the ovarian cortex are at the dormant, primordial follicle stage, any IVG system must begin with the activation of this stage (Telfer and Zelinski, 2013). However, uninhibited growth *in vitro* at this stage has become a significant concern as it could lead to perturbation of tightly regulated growth patterns and possibly intercellular communication throughout the culture period and ultimately the development of poor-quality oocytes.

The process of follicle development is species-specific with each having a specific timescale *in vivo* (Smitz and Cortvrindt, 2002). The approximate length of follicular growth from primordial to primary follicle is at least 120 days in the human, and it takes about 65 days for primary follicles to reach the early antral stage (Gougeon, 1986) although it is not known if this is continuous growth or a start-stop process. Meanwhile, it requires several months in large domestic animals (Smitz and Cortvrindt, 2002). Despite the risk of precocious growth during *in vitro* follicle culture, a multi-step IVG system established in our group has demonstrated the capacity to produce mature human oocytes developed from primordial follicles entirely *in vitro* (McLaughlin *et al.*, 2018). This has provided proof of principle, but the outcomes need to be improved in terms of optimising oocyte quality and yield. The work presented in this thesis focused on the first two stages of the IVG system which are 1) primordial

follicle activation and 2) preantral follicle isolation with growth to antral stage of development. Experiments were designed to alter the rate of activation and to determine how this affected subsequent development. The overall aim of this thesis was to further investigate and determine the effects of pharmacological activation utilising the PI3K/Akt/mTOR signalling pathway on follicle growth and DDR of both oocytes and granulosa cells *in vitro.* A primary focus was to explore the DDR function in oocytes and granulosa cells with the aim of gaining a better understanding of follicle quality and to provide indications on how to improve the IVG system. The bovine ovary shares the same characteristics as humans, in term of morphology and function (Adams *et al.*, 2012). In addition, because the bovine tissue was more readily available, it was used in all of the experiments carried out in this thesis.

6.1.1. The Impact of PI3K/Akt Pathway Modulation on Follicular Growth, Survival and DDR

The PI3K/Akt/mTOR pathway within the oocyte is the primary pathway controlling primordial follicle activation. The activation rate is an accumulative effect of all substrates involved in this pathway and determined by the delicate balance between stimulatory and inhibitory signals (Adhikari and Liu, 2009). The work reported in this thesis has revealed that bovine ovarian cortical strips exposed to an inhibitor of PTEN (bpv(HOpic)) leads to increased primordial follicle activation but that this is associated with increased DNA damage and attenuated DNA repair capacity of both oocytes and granulosa cells *in vitro*. PTEN is an essential factor in normal cell growth in oocytes and in proliferation of granulosa cells (Jagarlamudi *et al.*, 2009, Reddy *et al.*, 2008). An excessive increase of Akt, caused by PTEN inhibition, may compromise HR activity leading to genomic instability. This condition also plays a pivotal role in the

pathology of cancer as Akt inhibits apoptosis and increases cell proliferation (Plo *et al.*, 2008).

The role of the Hippo signalling pathway was not directly investigated in this study, nevertheless, the way the tissue was prepared by cutting the cortex into pieces of 1 mm thick, removing excess stroma and then gently stretching fragments would be expected to induce Hippo pathway activity within the tissue, as has been previously demonstrated in the mouse and human ovary (Kawamura *et al.*, 2013). Disrupting the Hippo pathway may be the underlying mechanism of primordial follicle activation in the absence of PTEN inhibition (control group) as was shown by increased the proportion of activated follicles more than 50% after 6 days of culture. This finding confirmed that the culture system is capable of supporting primordial follicle activation. The presence of PTEN inhibition in the culture media further augments the activation. Ultimately, an increase in primordial follicle activation in the PTEN inhibition group is an accumulative consequence of both PI3K modulation and Hippo pathway disruption (Grosbois and Demeestere, 2018, Kawamura *et al.*, 2013, Li *et al.*, 2010a). However, it should be pointed out that disrupting the Hippo pathway has also been linked to cancer pathology (Fan *et al.*, 2017a). Inactivation of the Hippo pathway has been delineated to confine cancer cells transformation in response to DNA damage. In response to DNA damage, the Hippo pathway may trigger either cell death or preserved genome integrity (Pefani and O'Neill, 2016).

The involvement of PI3K/Akt activation in our experiments could be the cause of impaired DDR in oocytes and granulosa cells. Excessive PI3K/Akt activity leads to an increase in DNA damage with limited DNA repair. This increase in activity has been connected to the rapid loss of the primordial follicle pool and accelerated ovarian

ageing (Reddy *et al.*, 2008, Reddy *et al.*, 2009), whether it be age related (Govindaraj *et al.*, 2015, Oktay *et al.*, 2015, Titus *et al.*, 2013, Zhang *et al.*, 2015) or following genotoxic insults to DNA(Chang *et al.*, 2015, Kerr *et al.*, 2012b, Lin *et al.*, 2017, Nguyen *et al.*, 2018, Rinaldi *et al.*, 2017, Wang *et al.*, 2019b).

Likewise, there are some interesting data showing an association between increased PI3K/Akt activity and endometriosis (Barra *et al.*, 2018, Govatati *et al.*, 2014, Madanes *et al.*, 2019, Makker *et al.*, 2012, Takeuchi *et al.*, 2019, Yin *et al.*, 2012). Primordial follicle loss in endometriosis has been hypothesised as a cause of PI3K/Akt upregulation in mice and human (Takeuchi *et al.*, 2019) and is suggested to be responsible for ovarian ageing in women with endometriosis (Kitajima *et al.*, 2014). Diminished ovarian reserved in endometriosis patients occurs concomitantly with compromised DSB repair mechanism (Choi *et al.*, 2018).

Considering that PI3K/Akt signalling pathway upregulation enhances resting follicle growth *in vitro*, but with increased DNA damage and impaired DNA repair, we extended the investigation by lowering the activation rate. Rapamycin, an mTOR inhibitor, has been shown to prolong cell lifespan and enhance metabolic function (Kennedy and Lamming, 2016). The use of an mTOR inhibitor has been beneficial to prevent excessive primordial follicle activation and maintain the primordial follicle pool (Zhou *et al.*, 2017). A series of publications have investigated the impact of chemotherapy on DDR of both oocytes and granulosa cells in a range of species. The fact that rapamycin prevents primordial follicle loss against chemotherapy is due to its mechanism to inhibit PI3K/Akt/mTOR activation (Goldman *et al.*, 2017, Zhou *et al.*, 2017), supporting utilisation of this substrate to lower the activation rate as was designed in the experiments in chapter 4. We tested the hypothesis that the presence

of rapamycin in the culture media could ameliorate the effects of PI3K induced excessive activation and improve DDR of both oocytes and granulosa cells during ovarian fragment culture. We further investigated whether rapamycin alone, by reducing follicle activation, might promote similar effects on DDR as the control group or even better.

The results presented in chapter 4 demonstrated that the addition of rapamycin in culture media combined with a low dose of bpv(HOpic) enhanced follicle activation but at a significantly lower rate compared to PTEN inhibition alone. However, DNA damage decreased, with increased expression of the DNA repair proteins MRE11, ATM and Rad51 in mainly non-growing and primary follicles. DNA damage was significantly lower in granulosa cells of primary follicles in the presence of rapamycin either on its own or in combination with bpv(Hopic) compared to the PTEN inhibition group. In parallel with our findings, the administration of rapamycin as a co-treatment with CP was able to amend the follicle loss and decreased AMH level caused by CP in a mouse model (Zhou *et al.*, 2017). Similarly, everolimus, another mTOR inhibitor, has been shown to be capable of preventing follicle loss following cisplatin treatment. Similar outcomes are also revealed when both mTORC1 and 2 are inhibited in mice (Goldman *et al.*, 2017).

The efficacy of mTOR inhibition to attenuate PI3K/Akt activity has been implicated in preclinical studies to reduce the growth of endometriosis implants (Kacan *et al.*, 2017, Lee and Kim, 2014, Matsuzaki *et al.*, 2018). Recently, a study in mice demonstrated that PI3K/Akt inhibition was sufficient to reduce follicle loss caused by endometriosis (Takeuchi *et al.*, 2019). It is known that both of these situations have been associated with increased DNA damage and compromised DSB repair

mechanism (Choi *et al.*, 2018, Kim and Suh, 2014, Kujjo *et al.*, 2010, Kujjo *et al.*, 2012, Nguyen *et al.*, 2019, Soleimani *et al.*, 2011) suggesting that rapamycin might be beneficial to mitigate the negative impact of PI3K/Akt activation on DDR of follicular growth *in vitro.* This is consistent with our findings. It has been reported that γH2AX expression is upregulated both in endometrium and ovarian tissue of patients with endometriosis. DNA repair proteins ATM, Rad51 and BRCA1 are significantly attenuated in parallel with decreased ovarian reserve indicated by low AMH serum concentration (Choi *et al.*, 2018). Hence, the mechanism underpinning follicle loss, ovarian ageing and DNA damage in endometriosis may be similar to chemotherapy-induced damage to oocytes. It is intriguing to note that oocytes and granulosa cells within the follicles in endometriotic ovarian tissue may be more vulnerable to genotoxic exposure, as is shown by increased DNA damage propensity (Choi *et al.*, 2018).

6.1.2. The Impact of PI3K/Akt Pathway Modulation on Preantral Follicle Growth and DDR

In contrast to primordial follicles that can be grown within ovarian cortical fragments, growth beyond the preantral stage is inhibited within the dense human and bovine ovarian stromal. In this respect, preantral follicles must be removed and then cultured individually in V-bottom 96 well plates (McLaughlin *et al.*, 2010a, McLaughlin *et al.*, 2010b, McLaughlin *et al.*, 2018). Human (Telfer *et al.*, 2008) and bovine (McLaughlin and Telfer, 2010) primordial follicle activation and development to secondary stage follicles within ovarian cortical fragments has been achieved by utilising the first 2 stages of this IVG system. In chapter 5, the impact of the treatments on growth, survival, and DDR response of isolated follicles cultured for another 6 to 8 days

following primordial follicle activation was explored. The results demonstrated that the overall morphological health of follicles was reduced, and a low number of antral follicles was obtained, suggesting the ability of follicles to grow beyond 6 days in culture merits further study. The observed antral follicle formation is an indication that the isolated follicles can be grown *in vitro*. However, the presence of PTEN inhibition during culture of ovarian cortex is associated with impaired growth of isolated preantral follicles, which is in line with the observed compromised DNA repair proteins ATM and Rad51.

The impact of treatments on granulosa cell communication was further studied by monitoring Cx43 expression. This study demonstrated that Cx43 expression was significantly increased in the control group, concomitant with a higher proportion of follicles surviving in this group. Loss of cellular connections has been a recurring feature in IVG systems and is linked to accelerated follicular growth *in vitro* (Smitz and Cortvrindt, 2002). Cx43 plays an essential role in granulosa cell communication as has been highlighted in a null mouse model. Cx43 ablation in mice delayed oocyte development (Ackert *et al.*, 2001). Follicles lacking Cx43 fail to become multilaminar with reduced intercellular connections (Ackert *et al.*, 2001).

6.3. Concluding Remarks

The work in this thesis has demonstrated that increased primordial follicle activation due to PI3K/Akt signalling activity induces DNA damage and compromises DNA repair proteins within both oocytes and granulosa cells *in vitro.* The outcomes presented in this thesis also provide some new insights into the effect of downregulating the PI3K/Akt pathway and its impact on follicular development as well as on DDR of oocytes and granulosa cells *in vitro.* It has been identified that

increased DNA damage with limited DNA repair in oocytes and granulosa cells is ameliorated by the presence of rapamycin in culture media. Data presented here suggests the interaction between substrates involved in the PI3K/Akt/mTOR pathway affects follicular growth *in vitro*. The presence of rapamycin in ovarian cortical strip culture reduces the adverse effects of PI3K/Akt on DDR of both oocytes and granulosa cells *in vitro*. Nevertheless, cumulative effects of interactions between all DNA damage and DNA repair proteins in the presence of rapamycin, do not mitigate the negative impacts of PI3K/Akt on DDR in isolated preantral follicle growth cultured individually for another 6 days. The overall findings in this thesis suggest that an mTORC1 inhibitor can be a functional pharmacological agent to reduce the activation rate and may be beneficial to improve follicle growth and survival. This positive effect at step 1 was not maintained in isolated growing follicles. Before the use of these factors can be applied clinically, further research on human tissue is required.

6.4. Future Direction

The outcomes presented in this thesis could form the basis of a new approach to improve IVG systems. These findings raised issues that remain to be addressed and should be further investigated, including the long-term impacts and implication of manipulating the PI3K/Akt/mTOR and the Hippo signalling pathways. Given that the canonical PI3K/Akt signalling pathway controls a myriad of cellular functions, further studies on how PI3K/Akt triggers DNA damage are required.

From a clinical perspective, the development of IVG systems for endometriosis patients is another intriguing direction for future research. An increase in growing follicles alongside reduced primordial follicles in endometriosis may represent a persistent process of follicle activation and loss leading to a global decrease in ovarian

reserve (Carrillo *et al.*, 2016). The use of agents to limit activation may be constructive to improve DDR in endometriosis patients. Since the study has been limited to mice (Takeuchi *et al.*, 2019), IVG system in endometriosis patients with mTOR inhibition treatments could be considered to counteract impaired DDR associated PI3K/Akt activation. This approach in developing IVG systems in endometriosis patients could provide a new opportunity for fertility enhancement or preservation for these patients.

IVA methods have raised controversy regarding efficacy and safety with *in vitro* studies indicating that manipulating activation by pharmacological methods has an impact on subsequent quality of oocytes (Grosbois and Demeestere, 2018, Lerer-Serfaty *et al.*, 2013, McLaughlin *et al.*, 2014). It should be pointed out that the PI3K/Akt signalling pathway has also been linked to primordial follicle loss following ovarian tissue transplantation. Attempts to prevent follicle loss following tissue transplantation have been considered. It has been shown recently that an IVA protocol utilising both PI3K/Akt and Hippo signalling pathways prior to ovarian tissue transplantation may have disastrous consequences on follicle health (Dolmans *et al.*, 2007, Gavish *et al.*, 2018, Roness *et al.*, 2013). It remains uncertain whether IVA procedure prior to ovarian tissue transplantation was truly effective emphasising the necessity for further in-depth investigations focused on clinical implication, technical improvement, long term safety, and efficacy. Future research on whether the administration of a substrate to limit follicle activation prior to ovarian tissue transplantation will be more beneficial to counteract follicle loss after transplantation.

Many studies have been carried out by targeting DNA damage and DNA damage repair capacity of oocytes and granulosa cells, including prevention of ovarian damage against chemotherapy, radiation or environmental toxicants. The future direction

should be focused on whether it is feasible to increase DNA repair capacity in oocytes. DNA repair mechanisms targeting ATM have been used to protect the ovary against Phosphoramide mustard (PM). ATM inhibition increases the number of large primary follicles following exposure to PM, suggesting the potential use of ATM inhibition to increase the viability and maturation of ovarian follicles exposed to PM (Ganesan and Keating, 2016a).

It is worth considering that DNA damage heralds apoptotic events and may exist without any significant morphological alterations. Moreover, the cell's aptitude to mend the damage determines the balance between cell survival and apoptosis. In this perspective, attempts to optimise the DDR efficiency may be beneficial to improve oocyte quality either *in vivo* or *in vitro*. However, all of these studies have been conducted experimentally and merit further investigation prior to considering any clinical application. In this context, further research emphasising either the most appropriate timing or the dose of mTOR administration are required.

The work presented in this thesis demonstrates that the presence of rapamycin in the culture media is not sufficient to improve the growth and survival of isolated preantral follicles. Interestingly, the overall follicle survival is low. Future studies are required to investigate all aspects involved in the culture system that might influence outcomes, including the impact of stromal thickness on isolated follicular growth and survival.

References

Aaltonen J, Laitinen M P, Vuojolainen K, Jaatinen R, Horelli-Kuitunen N, Seppa L, Louhio H, Tuuri T, Sjoberg J, Butzow R, Hovata O, Dale L*, et al.* (1999). Human growth differentiation factor 9 (GDF-9) and its novel homolog GDF-9B are expressed in oocytes during early folliculogenesis. *J Clin Endocrinol Metab.* 84 (8): 2744-50.

Abdel-Khalek E A, El-Harairy M A, Shamiah Sh M & Khalil W A (2010). Effect of ovary preservation period on recovery rate and categories of dromedary camel oocytes. *Saudi journal of biological sciences.* 17 (3): 231-5.

Abel M H, Wootton A N, Wilkins V, Huhtaniemi I, Knight P G & Charlton H M (2000). The effect of a null mutation in the follicle-stimulating hormone receptor gene on mouse reproduction. *Endocrinology.* 141 (5): 1795-803.

Abir R, Nitke S, Ben-Haroush A & Fisch B (2006). In vitro maturation of human primordial ovarian follicles: clinical significance, progress in mammals, and methods for growth evaluation. *Histol Histopathol.* 21 (8): 887-98.

Abir R, Franks S, Mobberley M A, Moore P A, Margara R A & Winston R M (1997). Mechanical isolation and in vitro growth of preantral and small antral human follicles. *Fertil Steril.* 68 (4): 682-8.

Ackert C L, Gittens J E, O'Brien M J, Eppig J J & Kidder G M (2001). Intercellular communication via connexin43 gap junctions is required for ovarian folliculogenesis in the mouse. *Developmental biology.* 233 (2): 258-70.

Adams G P, Singh J & Baerwald A R (2012). Large animal models for the study of ovarian follicular dynamics in women. *Theriogenology.* 78 (8): 1733-48.

Adhikari D & Liu K (2009). Molecular mechanisms underlying the activation of mammalian primordial follicles. *Endocrine reviews.* 30 (5): 438-64.

Adhikari D & Liu K (2010). mTOR signaling in the control of activation of primordial follicles. *Cell cycle (Georgetown, Tex.).* 9 (9): 1673-4.

Adhikari D, Risal S, Liu K & Shen Y (2013). Pharmacological inhibition of mTORC1 prevents over-activation of the primordial follicle pool in response to elevated PI3K signaling. *PloS one.* 8 (1): e53810.

Adhikari D, Gorre N, Risal S, Zhao Z, Zhang H, Shen Y & Liu K (2012). The safe use of a PTEN inhibitor for the activation of dormant mouse primordial follicles and generation of fertilizable eggs. *PloS one.* 7 (6): e39034.

Adhikari D, Flohr G, Gorre N, Shen Y, Yang H, Lundin E, Lan Z, Gambello M J & Liu K (2009). Disruption of Tsc2 in oocytes leads to overactivation of the entire pool of primordial follicles. *Molecular human reproduction.* 15 (12): 765-70.

Adhikari D, Zheng W, Shen Y, Gorre N, Hamalainen T, Cooney A J, Huhtaniemi I, Lan Z J & Liu K (2010). Tsc/mTORC1 signaling in oocytes governs the quiescence and activation of primordial follicles. *Human molecular genetics.* 19 (3): 397-410.

Adriaens I, Smitz J & Jacquet P (2009). The current knowledge on radiosensitivity of ovarian follicle development stages. *Hum Reprod Update.* 15 (3): 359-77.

Aerts J M & Bols P E (2010). Ovarian follicular dynamics: a review with emphasis on the bovine species. Part I: Folliculogenesis and pre-antral follicle development. *Reprod Domest Anim.* 45 (1): 171-9.

Albertini D F (2015), 'The Mammalian Oogenesis', in Tony M Plant and Anthony J Zeleznik (eds.), *Knobil and Neill's Physiology of Reproduction* (Academic Press), 59-97.

Albertini D F, Combelles C M, Benecchi E & Carabatsos M J (2001). Cellular basis for paracrine regulation of ovarian follicle development. *Reproduction.* 121 (5): 647-53.

Altieri F, Grillo C, Maceroni M & Chichiarelli S (2008). DNA damage and repair: from molecular mechanisms to health implications. *Antioxid Redox Signal.* 10 (5): 891-937.

Altiok S, Batt D, Altiok N, Papautsky A, Downward J, Roberts T M & Avraham H (1999). Heregulin induces phosphorylation of BRCA1 through phosphatidylinositol 3-Kinase/AKT in breast cancer cells. *The Journal of biological chemistry.* 274 (45): 32274-8.

Amelio I, Grespi F, Annicchiarico-Petruzzelli M & Melino G (2012). p63 the guardian of human reproduction. *Cell cycle (Georgetown, Tex.).* 11 (24): 4545-51.

Araujo V R, Gastal M O, Figueiredo J R & Gastal E L (2014). In vitro culture of bovine preantral follicles: a review. *Reprod Biol Endocrinol.* 1278.

Astle M V, Hannan K M, Ng P Y, Lee R S, George A J, Hsu A K, Haupt Y, Hannan R D & Pearson R B (2012). AKT induces senescence in human cells via mTORC1 and p53 in the absence of DNA damage: implications for targeting mTOR during malignancy. *Oncogene.* 31 (15): 1949-62.

Baker T G (1963). A Quantitative and cytological study of germ cells in human ovaries. *Proc R Soc Lond B Biol Sci.* 158417-33.

Barnes F L, Kausche A, Tiglias J, Wood C, Wilton L & Trounson A (1996). Production of embryos from in vitro-matured primary human oocytes. *Fertil Steril.* 65 (6): 1151-6.

Barra F, Ferro Desideri L & Ferrero S (2018). Inhibition of PI3K/AKT/mTOR pathway for the treatment of endometriosis. *Br J Pharmacol.* 175 (17): 3626-7.

Bastings L, Beerendonk C C, Westphal J R, Massuger L F, Kaal S E, van Leeuwen F E, Braat D D & Peek R (2013). Autotransplantation of cryopreserved ovarian tissue in cancer survivors and the risk of reintroducing malignancy: a systematic review. *Hum Reprod Update.* 19 (5): 483-506.

Basu A & Haldar S (1998). The relationship between BcI2, Bax and p53: consequences for cell cycle progression and cell death. *Molecular human reproduction.* 4 (12): 1099-109.

Bayne R A, Kinnell H L, Coutts S M, He J, Childs A J & Anderson R A (2015). GDF9 is transiently expressed in oocytes before follicle formation in the human fetal ovary and is regulated by a novel NOBOX transcript. *PLoS One.* 10 (3): e0119819.

Bekker-Jensen S & Mailand N (2010). Assembly and function of DNA double-strand break repair foci in mammalian cells. *DNA repair.* 9 (12): 1219-28.

Bendsen E, Byskov A G, Andersen C Y & Westergaard L G (2006). Number of germ cells and somatic cells in human fetal ovaries during the first weeks after sex differentiation. *Hum Reprod.* 21 (1): 30-5.

Bertoldo M J, Walters K A, Ledger W L, Gilchrist R B, Mermillod P & Locatelli Y (2018). In-vitro regulation of primordial follicle activation: challenges for

fertility preservation strategies. *Reproductive biomedicine online.* 36 (5): 491-9.

Bezerra M E S, Barberino R S, Menezes V G, Gouveia B B, Macedo T J S, Santos J M S, Monte A P O, Barros V R P & Matos M H T (2018a). Insulin-like growth factor-1 (IGF-1) promotes primordial follicle growth and reduces DNA fragmentation through the phosphatidylinositol 3-kinase/protein kinase B (PI3K/AKT) signalling pathway. *Reprod Fertil Dev.* 30 (11): 1503-13.

Bezerra M E S, Gouveia B B, Barberino R S, Menezes V G, Macedo T J S, Cavalcante A Y P, Monte A P O, Santos J M S & Matos M H T (2018b). Resveratrol promotes in vitro activation of ovine primordial follicles by reducing DNA damage and enhancing granulosa cell proliferation via phosphatidylinositol 3-kinase pathway. *Reproduction in domestic animals = Zuchthygiene.* 53 (6): 1298-305.

Bissell M J, Rizki A & Mian I S (2003). Tissue architecture: the ultimate regulator of breast epithelial function. *Curr Opin Cell Biol.* 15 (6): 753-62.

Blanco-Aparicio C, Renner O, Leal J F & Carnero A (2007). PTEN, more than the AKT pathway. *Carcinogenesis.* 28 (7): 1379-86.

Branzei D & Foiani M (2008). Regulation of DNA repair throughout the cell cycle. *Nat Rev Mol Cell Biol.* 9 (4): 297-308.

Braw-Tal R & Yossefi S (1997). Studies in vivo and in vitro on the initiation of follicle growth in the bovine ovary. *J Reprod Fertil.* 109 (1): 165-71.

Brito I R, Lima I M, Xu M, Shea L D, Woodruff T K & Figueiredo J R (2014). Three-dimensional systems for in vitro follicular culture: overview of alginate-based matrices. *Reprod Fertil Dev.* 26 (7): 915-30.

Broekmans F J, Soules M R & Fauser B C (2009). Ovarian aging: mechanisms and clinical consequences. *Endocrine reviews.* 30 (5): 465-93.

Brunet A, Bonni A, Zigmond M J, Lin M Z, Juo P, Hu L S, Anderson M J, Arden K C, Blenis J & Greenberg M E (1999). Akt promotes cell survival by phosphorylating and inhibiting a Forkhead transcription factor. *Cell.* 96 (6): 857-68.

Bruzzone R, White T W & Paul D L (1996). Connections with connexins: the molecular basis of direct intercellular signaling. *Eur J Biochem.* 238 (1): 1-27.

Burry R W (2011). Controls for immunocytochemistry: an update. *The journal of histochemistry and cytochemistry : official journal of the Histochemistry Society.* 59 (1): 6-12.

Bzymek M, Thayer N H, Oh S D, Kleckner N & Hunter N (2010). Double Holliday junctions are intermediates of DNA break repair. *Nature.* 464 (7290): 937-41.

Carrillo L, Seidman D S, Cittadini E & Meirow D (2016). The role of fertility preservation in patients with endometriosis. *J Assist Reprod Genet.* 33 (3): 317-23.

Carroll J & Marangos P (2013). The DNA damage response in mammalian oocytes. *Front Genet.* 4117.

Castrillon D H, Miao L, Kollipara R, Horner J W & DePinho R A (2003). Suppression of ovarian follicle activation in mice by the transcription factor Foxo3a. *Science (New York, N.Y.).* 301 (5630): 215-8.

Chang E M, Lim E, Yoon S, Jeong K, Bae S, Lee D R, Yoon T K, Choi Y & Lee W S (2015). Cisplatin Induces Overactivation of the Dormant Primordial Follicle

through PTEN/AKT/FOXO3a Pathway which Leads to Loss of Ovarian Reserve in Mice. *PloS one.* 10 (12): e0144245.

Chang H H Y, Pannunzio N R, Adachi N & Lieber M R (2017). Non-homologous DNA end joining and alternative pathways to double-strand break repair. *Nat Rev Mol Cell Biol.* 18 (8): 495-506.

Choi Y & Rajkovic A (2006). Characterization of NOBOX DNA binding specificity and its regulation of Gdf9 and Pou5f1 promoters. *J Biol Chem.* 281 (47): 35747-56.

Choi Y S, Park J H, Lee J H, Yoon J K, Yun B H, Park J H, Seo S K, Sung H J, Kim H S, Cho S & Lee B S (2018). Association Between Impairment of DNA Double Strand Break Repair and Decreased Ovarian Reserve in Patients With Endometriosis. *Front Endocrinol (Lausanne).* 9772.

Collins J K & Jones K T (2016). DNA damage responses in mammalian oocytes. *Reproduction.* 152 (1): R15-22.

Collins J K, Lane S I, Merriman J A & Jones K T (2015). DNA damage induces a meiotic arrest in mouse oocytes mediated by the spindle assembly checkpoint. *Nature communications.* 68553.

Cortez D, Guntuku S, Qin J & Elledge S J (2001). ATR and ATRIP: partners in checkpoint signaling. *Science (New York, N.Y.).* 294 (5547): 1713-6.

Coutandin D, Osterburg C, Srivastav R K, Sumyk M, Kehrloesser S, Gebel J, Tuppi M, Hannewald J, Schafer B, Salah E, Mathea S, Muller-Kuller U*, et al.* (2016). Quality control in oocytes by p63 is based on a spring-loaded activation mechanism on the molecular and cellular level. *eLife.* 5.

Da Silva-Buttkus P, Marcelli G, Franks S, Stark J & Hardy K (2009). Inferring biological mechanisms from spatial analysis: prediction of a local inhibitor in the ovary. *Proc Natl Acad Sci U S A.* 106 (2): 456-61.

Day F R , Ruth K S , Thompson D J , Lunetta K L , Pervjakova N , Chasman D I , Stolk L , Finucane H K , Sulem P , Bulik-Sullivan B , Esko T , Johnson A D*, et al.* (2015). Large-scale genomic analyses link reproductive aging to hypothalamic signaling, breast cancer susceptibility and BRCA1-mediated DNA repair. *Nat Genet.* 47 (11): 1294-303.

de Bruin J P, Dorland M, Spek E R, Posthuma G, van Haaften M, Looman C W & te Velde E R (2004). Age-related changes in the ultrastructure of the resting follicle pool in human ovaries. *Biology of reproduction.* 70 (2): 419-24.

Demeestere I, Delbaere A, Gervy C, Van Den Bergh M, Devreker F & Englert Y (2002). Effect of preantral follicle isolation technique on in-vitro follicular growth, oocyte maturation and embryo development in mice. *Hum Reprod.* 17 (8): 2152-9.

Deutsch G B, Zielonka E M, Coutandin D & Dotsch V (2011a). Quality control in oocytes: domain-domain interactions regulate the activity of p63. *Cell cycle (Georgetown, Tex.).* 10 (12): 1884-5.

Deutsch G B, Zielonka E M, Coutandin D, Weber T A, Schafer B, Hannewald J, Luh L M, Durst F G, Ibrahim M, Hoffmann J, Niesen F H, Senturk A*, et al.* (2011b). DNA damage in oocytes induces a switch of the quality control factor TAp63alpha from dimer to tetramer. *Cell.* 144 (4): 566-76.

Diaz F J, Wigglesworth K & Eppig J J (2007). Oocytes are required for the preantral granulosa cell to cumulus cell transition in mice. *Dev Biol.* 305 (1): 300-11.

Dolmans M M & Masciangelo R (2018). Risk of transplanting malignant cells in cryopreserved ovarian tissue. *Minerva ginecologica.* 70 (4): 436-43.

Dolmans M M, Luyckx V, Donnez J, Andersen C Y & Greve T (2013). Risk of transferring malignant cells with transplanted frozen-thawed ovarian tissue. *Fertility and sterility.* 99 (6): 1514-22.

Dolmans M M, Marinescu C, Saussoy P, Van Langendonckt A, Amorim C & Donnez J (2010). Reimplantation of cryopreserved ovarian tissue from patients with acute lymphoblastic leukemia is potentially unsafe. *Blood.* 116 (16): 2908-14.

Dolmans M M, Martinez-Madrid B, Gadisseux E, Guiot Y, Yuan W Y, Torre A, Camboni A, Van Langendonckt A & Donnez J (2007). Short-term transplantation of isolated human ovarian follicles and cortical tissue into nude mice. *Reproduction (Cambridge, England).* 134 (2): 253-62.

Dong J, Albertini D F, Nishimori K, Kumar T R, Lu N & Matzuk M M (1996). Growth differentiation factor-9 is required during early ovarian folliculogenesis. *Nature.* 383 (6600): 531-5.

Dubey P K, Tripathi V, Singh R P & Sharma G T (2011). Influence of nitric oxide on in vitro growth, survival, steroidogenesis, and apoptosis of follicle stimulating hormone stimulated buffalo (Bubalus bubalis) preantral follicles. *Journal of veterinary science.* 12 (3): 257-65.

Dupont J & Scaramuzzi R J (2016). Insulin signalling and glucose transport in the ovary and ovarian function during the ovarian cycle. *The Biochemical journal.* 473 (11): 1483-501.

Durlinger A L, Kramer P, Karels B, de Jong F H, Uilenbroek J T, Grootegoed J A & Themmen A P (1999). Control of Primordial Follicle Recruitment by Anti-Mullerian Hormone in the Mouse Ovary1. *Endocrinology.* 140 (12): 5789-96.

Edson M A, Nagaraja A K & Matzuk M M (2009). The mammalian ovary from genesis to revelation. *Endocr Rev.* 30 (6): 624-712.

Eggan K, Jurga S, Gosden R, Min I M & Wagers A J (2006). Ovulated oocytes in adult mice derive from non-circulating germ cells. *Nature.* 441 (7097): 1109-14.

Elvin J A & Matzuk M M (1998). Mouse models of ovarian failure. *Rev Reprod.* 3 (3): 183-95.

Elvin J A, Yan C & Matzuk M M (2000). Oocyte-expressed TGF-beta superfamily members in female fertility. *Mol Cell Endocrinol.* 159 (1-2): 1-5.

Eppig J J (1991). Intercommunication between mammalian oocytes and companion somatic cells. *Bioessays.* 13 (11): 569-74.

Eppig J J (2001). Oocyte control of ovarian follicular development and function in mammals. *Reproduction.* 122 (6): 829-38.

Eppig J J & Schroeder A C (1989). Capacity of mouse oocytes from preantral follicles to undergo embryogenesis and development to live young after growth, maturation, and fertilization in vitro. *Biol Reprod.* 41 (2): 268-76.

Eppig J J & O'Brien M J (1996). Development in vitro of mouse oocytes from primordial follicles. *Biol Reprod.* 54 (1): 197-207.

Eppig J J, Schultz R M, O'Brien M & Chesnel F (1994). Relationship between the developmental programs controlling nuclear and cytoplasmic maturation of mouse oocytes. *Dev Biol.* 164 (1): 1-9.

Eppig J J, Pendola F L, Wigglesworth K & Pendola J K (2005). Mouse oocytes regulate metabolic cooperativity between granulosa cells and oocytes: amino acid transport. *Biol Reprod.* 73 (2): 351-7.

Faddy M J & Gosden R G (1995). A mathematical model of follicle dynamics in the human ovary. *Human reproduction (Oxford, England).* 10 (4): 770-5.

Faddy M J, Gosden R G, Gougeon A, Richardson S J & Nelson J F (1992). Accelerated disappearance of ovarian follicles in mid-life: implications for forecasting menopause. *Human reproduction (Oxford, England).* 7 (10): 1342-6.

Falck J, Coates J & Jackson S P (2005). Conserved modes of recruitment of ATM, ATR and DNA-PKcs to sites of DNA damage. *Nature.* 434 (7033): 605-11.

Fan H-Y & Sun Q-Y (2019), 'Oocyte Meiotic Maturation', *The Ovary* (3 edn.: Academic Press), 181-203.

Fan H Y, Liu Z, Cahill N & Richards J S (2008). Targeted disruption of Pten in ovarian granulosa cells enhances ovulation and extends the life span of luteal cells. *Molecular endocrinology (Baltimore, Md.).* 22 (9): 2128-40.

Fan Q, Cheng Y, Chang H M, Deguchi M, Hsueh A J & Leung P C K (2017a). Sphingosine-1-phosphate promotes ovarian cancer cell proliferation by disrupting Hippo signaling. *Oncotarget.* 8 (16): 27166-76.

Fan Q, Cheng Y, Chang H M, Deguchi M, Hsueh A J & Leung P C (2017b). Sphingosine-1-phosphate promotes ovarian cancer cell proliferation by disrupting Hippo signaling. *Oncotarget.* 8 (16): 27166-76.

Fenwick M A, Mora J M, Mansour Y T, Baithun C, Franks S & Hardy K (2013). Investigations of TGF-beta signaling in preantral follicles of female mice

reveal differential roles for bone morphogenetic protein 15. *Endocrinology.* 154 (9): 3423-36.

Fernandez T, Palomino J, Parraguez V H, Peralta O A & De los Reyes M (2016). Differential expression of GDF-9 and BMP- 15 during follicular development in canine ovaries evaluated by flow cytometry. *Anim Reprod Sci.* 16759-67.

Findlay J K (1993). An update on the roles of inhibin, activin, and follistatin as local regulators of folliculogenesis. *Biol Reprod.* 48 (1): 15-23.

Findlay J K, Drummond A E, Dyson M L, Baillie A J, Robertson D M & Ethier J F (2002). Recruitment and development of the follicle; the roles of the transforming growth factor-beta superfamily. *Mol Cell Endocrinol.* 191 (1): 35-43.

Findlay J K, Dunning K R, Gilchrist R B, Hutt K J, Russell D & Walters K A (2019), 'Follicle Selection in Mammalian Ovaries', *The Ovary* (Elsevier), 1-21.

Fortune J E (1994). Ovarian follicular growth and development in mammals. *Biol Reprod.* 50 (2): 225-32.

Fortune J E (2003). The early stages of follicular development: activation of primordial follicles and growth of preantral follicles. *Animal reproduction science.* 78 (3-4): 135-63.

Fortune J E, Cushman R A, Wahl C M & Kito S (2000). The primordial to primary follicle transition. *Molecular and cellular endocrinology.* 163 (1-2): 53-60.

Fraser M, Zhao H, Luoto K R, Lundin C, Coackley C, Chan N, Joshua A M, Bismar T A, Evans A, Helleday T & Bristow R G (2012). PTEN deletion in prostate cancer cells does not associate with loss of RAD51 function: implications for radiotherapy and chemotherapy. *Clin Cancer Res.* 18 (4): 1015-27.

Fujita Y, Mori T, Suzuki A, Nihnobu K & Nishimura T (1981). Functional and structural relationships in steroidogenesis in vitro by human corpora lutea during development and regression. *J Clin Endocrinol Metab.* 53 (4): 744-51.

Galloway S M, McNatty K P, Cambridge L M, Laitinen M P, Juengel J L, Jokiranta T S, McLaren R J, Luiro K, Dodds K G, Montgomery G W, Beattie A E, Davis G H*, et al.* (2000). Mutations in an oocyte-derived growth factor gene (BMP15) cause increased ovulation rate and infertility in a dosage-sensitive manner. *Nat Genet.* 25 (3): 279-83.

Ganesan S & Keating A F (2016a). The ovarian DNA damage repair response is induced prior to phosphoramide mustard-induced follicle depletion, and ataxia telangiectasia mutated inhibition prevents PM-induced follicle depletion. *Toxicol Appl Pharmacol.* 29265-74.

Ganesan S & Keating A F (2016b). Bisphenol A-Induced Ovotoxicity Involves DNA Damage Induction to Which the Ovary Mounts a Protective Response Indicated by Increased Expression of Proteins Involved in DNA Repair and Xenobiotic Biotransformation. *Toxicological sciences : an official journal of the Society of Toxicology.* 152 (1): 169-80.

Gavish Z, Peer G, Roness H, Cohen Y & Meirow D (2014). Follicle activation and 'burn-out' contribute to post-transplantation follicle loss in ovarian tissue grafts: the effect of graft thickness. *Hum Reprod.* 29 (5): 989-96.

Gavish Z, Spector I, Peer G, Schlatt S, Wistuba J, Roness H & Meirow D (2018). Follicle activation is a significant and immediate cause of follicle loss after ovarian tissue transplantation. *J Assist Reprod Genet.* 35 (1): 61-9.

Gebel J, Tuppi M, Krauskopf K, Coutandin D, Pitzius S, Kehrloesser S, Osterburg C & Dotsch V (2017). Control mechanisms in germ cells mediated by p53 family proteins. *Journal of cell science.*130: 2663-70.

Geber S, Megale R, Vale F, Lanna A M A & Cabral A C V (2012). Variation in ovarian follicle density during human fetal development. *J Assist Reprod Genet.* 29 (9): 969-72.

Goldenberg R L, Powell R D, Rosen S W, Marshall J R & Ross G T (1976). Ovarian morphology in women with anosmia and hypogonadotropic hypogonadism. *Am J Obstet Gynecol.* 126 (1): 91-4.

Goldman K N, Chenette D, Arju R, Duncan F E, Keefe D L, Grifo J A & Schneider R J (2017). mTORC1/2 inhibition preserves ovarian function and fertility during genotoxic chemotherapy. *Proceedings of the National Academy of Sciences of the United States of America.* 114 (12): 3186-91.

Gong S P, Lee S T, Lee E J, Kim D Y, Lee G, Chi S G, Ryu B K, Lee C H, Yum K E, Lee H J, Han J Y, Tilly J L*, et al.* (2010). Embryonic stem cell-like cells established by culture of adult ovarian cells in mice. *Fertil Steril.* 93 (8): 2594-601, 601 e1-9.

Gonzalez-Robayna I J, Falender A E, Ochsner S, Firestone G L & Richards J S (2000). Follicle-Stimulating hormone (FSH) stimulates phosphorylation and activation of protein kinase B (PKB/Akt) and serum and glucocorticoid-lnduced kinase (Sgk): evidence for A kinase-independent signaling by FSH in granulosa cells. *Mol Endocrinol.* 14 (8): 1283-300.

Gosden R G (2000). Low temperature storage and grafting of human ovarian tissue. *Mol Cell Endocrinol.* 163 (1-2): 125-9.

Gosden R G (2004). Germline stem cells in the postnatal ovary: is the ovary more like a testis? *Hum Reprod Update.* 10 (3): 193-5.

Goto H & Inagaki M (2007). Production of a site- and phosphorylation state-specific antibody. *Nature protocols.* 2 (10): 2574-81.

Gougeon A (1986). Dynamics of follicular growth in the human: a model from preliminary results. *Hum Reprod.* 1 (2): 81-7.

Gougeon A (1996). Regulation of ovarian follicular development in primates: facts and hypotheses. *Endocrine reviews.* 17 (2): 121-55.

Gougeon A (1998). Ovarian follicular growth in humans: ovarian ageing and population of growing follicles. *Maturitas.* 30 (2): 137-42.

Gougeon A & Busso D (2000). Morphologic and functional determinants of primordial and primary follicles in the monkey ovary. *Mol Cell Endocrinol.* 163 (1-2): 33-42.

Govatati S, Kodati V L, Deenadayal M, Chakravarty B, Shivaji S, Bhanoori M, Yin X, Pavone M E, Lu Z, Wei J & Kim J J (2014). Mutations in the PTEN tumor gene and risk of endometriosis: a case-control study. *Hum Reprod.* 29 (2): 324-36.

Govindaraj V, Keralapura Basavaraju R & Rao A J (2015). Changes in the expression of DNA double strand break repair genes in primordial follicles from immature and aged rats. *Reproductive biomedicine online.* 30 (3): 303-10.

Govindaraj V, Krishnagiri H, Chauhan M S & Rao A J (2017). BRCA-1 Gene Expression and Comparative Proteomic Profile of Primordial Follicles from Young and Adult Buffalo (Bubalus bubalis) Ovaries. *Animal biotechnology.* 28 (2): 94-103.

Granot I & Dekel N (1998). Cell-to-cell communication in the ovarian follicle: developmental and hormonal regulation of the expression of connexin43. *Hum Reprod.* 13 Suppl 485-97.

Green L J, Zhou H, Padmanabhan V & Shikanov A (2019). Adipose-derived stem cells promote survival, growth, and maturation of early-stage murine follicles. *Stem Cell Res Ther.* 10 (1): 102.

Griffith L G & Swartz M A (2006). Capturing complex 3D tissue physiology in vitro. *Nat Rev Mol Cell Biol.* 7 (3): 211-24.

Grosbois J & Demeestere I (2018). Dynamics of PI3K and Hippo signaling pathways during in vitro human follicle activation. *Hum Reprod.* 33 (9): 1705-14.

Grosbois J, Vermeersch M, Devos M, Clarke H & Demeestere I (2019). Ultrastructure and inter-cellular contact-mediated communication in cultured human early stage follicles exposed to mTORC1 inhibitor. *Mol Hum Reprod.*

Grynberg M, Mayeur Le Bras A, Hesters L, Gallot V & Frydman N (2020). First birth achieved after fertility preservation using vitrification of in vitro matured oocytes in a woman with breast cancer. *Annals of Oncology.* 301-2.

Hanoux V, Pairault C, Bakalska M, Habert R & Livera G (2007). Caspase-2 involvement during ionizing radiation-induced oocyte death in the mouse ovary. *Cell death and differentiation.* 14 (4): 671-81.

Hatzirodos N, Hummitzsch K, Irving-Rodgers H F, Harland M L, Morris S E & Rodgers R J (2014). Transcriptome profiling of granulosa cells from bovine ovarian follicles during atresia. *BMC genomics.* 1540.

Heijink A M, Krajewska M & van Vugt M A (2013). The DNA damage response during mitosis. *Mutation research.* 750 (1-2): 45-55.

Hernandez Gifford J A (2015). The role of WNT signaling in adult ovarian folliculogenesis. *Reproduction.* 150 (4): R137-48.

Hikabe O, Hamazaki N, Nagamatsu G, Obata Y, Hirao Y, Hamada N, Shimamoto S, Imamura T, Nakashima K, Saitou M & Hayashi K (2016). Reconstitution in vitro of the entire cycle of the mouse female germ line. *Nature.* 539 (7628): 299-303.

Hirshfield A N (1991). Development of follicles in the mammalian ovary. *Int Rev Cytol.* 12443-101.

Hobeika E, Armouti M, Kala H, Fierro M A, Winston N J, Scoccia B, Zamah A M & Stocco C (2019). Oocyte-Secreted Factors Synergize With FSH to Promote Aromatase Expression in Primary Human Cumulus Cells. *J Clin Endocrinol Metab.* 104 (5): 1667-76.

Holt J E, Jackson A, Roman S D, Aitken R J, Koopman P & McLaughlin E A (2006). CXCR4/SDF1 interaction inhibits the primordial to primary follicle transition in the neonatal mouse ovary. *Dev Biol.* 293 (2): 449-60.

Hong S, Sung Y, Yu M, Lee M, Kleckner N & Kim K P (2013). The logic and mechanism of homologous recombination partner choice. *Molecular cell.* 51 (4): 440-53.

Hosoe M, Kaneyama K, Ushizawa K, Hayashi K G & Takahashi T (2011). Quantitative analysis of bone morphogenetic protein 15 (BMP15) and growth differentiation factor 9 (GDF9) gene expression in calf and adult bovine ovaries. *Reprod Biol Endocrinol.* 933.

Hovatta O, Silye R, Abir R, Krausz T & Winston R M (1997). Extracellular matrix improves survival of both stored and fresh human primordial and primary ovarian follicles in long-term culture. *Hum Reprod.* 12 (5): 1032-6.

Hovatta O, Wright C, Krausz T, Hardy K & Winston R M (1999). Human primordial, primary and secondary ovarian follicles in long-term culture: effect of partial isolation. *Hum Reprod.* 14 (10): 2519-24.

Hsueh A J, Kawamura K, Cheng Y & Fauser B C (2015). Intraovarian control of early folliculogenesis. *Endocr Rev.* 36 (1): 1-24.

Hummitzsch K, Irving-Rodgers H F, Hatzirodos N, Bonner W, Sabatier L, Reinhardt D P, Sado Y, Ninomiya Y, Wilhelm D & Rodgers R J (2013a). A New Model of Development of the Mammalian Ovary and Follicles. *PLoS One.* 8 (2).

Hummitzsch K, Irving-Rodgers H F, Hatzirodos N, Bonner W, Sabatier L, Reinhardt D P, Sado Y, Ninomiya Y, Wilhelm D & Rodgers R J (2013b). A new model of development of the mammalian ovary and follicles. *PLoS One.* 8 (2): e55578.

Hunt C R, Gupta A, Horikoshi N & Pandita T K (2012). Does PTEN loss impair DNA double-strand break repair by homologous recombination? *Clin Cancer Res.* 18 (4): 920-2.

Hutt K J, McLaughlin E A, Holland M K, Hutt K J, McLaughlin E A & Holland M K (2006). KIT/KIT ligand in mammalian oogenesis and folliculogenesis: roles in rabbit and murine ovarian follicle activation and oocyte growth. *Biol Reprod.* 75 (3): 421-33.

Hwa A J, Fry R C, Sivaraman A, So P T, Samson L D, Stolz D B & Griffith L G (2007). Rat liver sinusoidal endothelial cells survive without exogenous VEGF in 3D perfused co-cultures with hepatocytes. *FASEB J.* 21 (10): 2564-79.

Irving-Rodgers H F, Morris S, Collett R A, Peura T T, Davy M, Thompson J G, Mason H D & Rodgers R J (2009). Phenotypes of the ovarian follicular basal lamina predict developmental competence of oocytes. *Hum Reprod.* 24 (4): 936-44.

Ivell R, Teerds K & Hoffman G E (2014). Proper application of antibodies for immunohistochemical detection: antibody crimes and how to prevent them. *Endocrinology.* 155 (3): 676-87.

Jackson S P & Bartek J (2009). The DNA-damage response in human biology and disease. *Nature.* 461 (7267): 1071-8.

Jagarlamudi K, Reddy P, Adhikari D & Liu K (2010). Genetically modified mouse models for premature ovarian failure (POF). *Molecular and cellular endocrinology.* 315 (1-2): 1-10.

Jagarlamudi K, Liu L, Adhikari D, Reddy P, Idahl A, Ottander U, Lundin E & Liu K (2009). Oocyte-specific deletion of Pten in mice reveals a stage-specific function of PTEN/PI3K signaling in oocytes in controlling follicular activation. *PLoS One.* 4 (7): e6186.

Jazayeri A, Falck J, Lukas C, Bartek J, Smith G C, Lukas J & Jackson S P (2006). ATM- and cell cycle-dependent regulation of ATR in response to DNA double-strand breaks. *Nature cell biology.* 8 (1): 37-45.

Jefferson W, Newbold R, Padilla-Banks E & Pepling M (2006). Neonatal genistein treatment alters ovarian differentiation in the mouse: inhibition of oocyte nest breakdown and increased oocyte survival. *Biol Reprod.* 74 (1): 161-8.

Jia Y, Song W, Zhang F, Yan J & Yang Q (2013). Akt1 inhibits homologous recombination in Brca1-deficient cells by blocking the Chk1-Rad51 pathway. *Oncogene.* 32 (15): 1943-9.

John G B, Shirley L J, Gallardo T D & Castrillon D H (2007). Specificity of the requirement for Foxo3 in primordial follicle activation. *Reproduction (Cambridge, England).* 133 (5): 855-63.

Johnson J, Canning J, Kaneko T, Pru J K & Tilly J L (2004). Germline stem cells and follicular renewal in the postnatal mammalian ovary. *Nature.* 428 (6979): 145-50.

Johnson J, Bagley J, Skaznik-Wikiel M, Lee H J, Adams G B, Niikura Y, Tschudy K S, Tilly J C, Cortes M L, Forkert R, Spitzer T, Iacomini J*, et al.* (2005). Oocyte generation in adult mammalian ovaries by putative germ cells in bone marrow and peripheral blood. *Cell.* 122 (2): 303-15.

Joyce I M, Pendola F L, Wigglesworth K & Eppig J J (1999). Oocyte regulation of kit ligand expression in mouse ovarian follicles. *Dev Biol.* 214 (2): 342-53.

Joyce I M, Clark A T, Pendola F L & Eppig J J (2000). Comparison of recombinant growth differentiation factor-9 and oocyte regulation of KIT ligand messenger ribonucleic acid expression in mouse ovarian follicles. *Biol Reprod.* 63 (6): 1669-75.

Juneja S C, Barr K J, Enders G C & Kidder G M (1999). Defects in the germ line and gonads of mice lacking connexin43. *Biol Reprod.* 60 (5): 1263-70.

Jungmichel S & Stucki M (2010). MDC1: The art of keeping things in focus. *Chromosoma.* 119 (4): 337-49.

Kacan T, Yildiz C, Baloglu Kacan S, Seker M, Ozer H & Cetin A (2017). Everolimus as an mTOR Inhibitor Suppresses Endometriotic Implants: an Experimental Rat Study. *Geburtshilfe Frauenheilkd.* 77 (1): 66-72.

Kaipia A & Hsueh A J (1997). Regulation of ovarian follicle atresia. *Annu Rev Physiol.* 59349-63.

Kao G D, Jiang Z, Fernandes A M, Gupta A K & Maity A (2007). Inhibition of phosphatidylinositol-3-OH kinase/Akt signaling impairs DNA repair in glioblastoma cells following ionizing radiation. *The Journal of biological chemistry.* 282 (29): 21206-12.

Katayama T, Shiota K & Takahashi M (1990). Activin A increases the number of follicle-stimulating hormone cells in anterior pituitary cultures. *Mol Cell Endocrinol.* 69 (2-3): 179-85.

Kawamura K, Kawamura N & Hsueh A J (2016). Activation of dormant follicles: a new treatment for premature ovarian failure? *Current opinion in obstetrics & gynecology.* 28 (3): 217-22.

Kawamura K, Cheng Y, Suzuki N, Deguchi M, Sato Y, Takae S, Ho C H, Kawamura N, Tamura M, Hashimoto S, Sugishita Y, Morimoto Y*, et al.* (2013). Hippo signaling disruption and Akt stimulation of ovarian follicles for infertility treatment. *Proceedings of the National Academy of Sciences of the United States of America.* 110 (43): 17474-9.

Kayampilly P P & Menon K M (2007). Follicle-stimulating hormone increases tuberin phosphorylation and mammalian target of rapamycin signaling through an extracellular signal-regulated kinase-dependent pathway in rat granulosa cells. *Endocrinology.* 148 (8): 3950-7.

Keefe D L, Niven-Fairchild T, Powell S & Buradagunta S (1995). Mitochondrial deoxyribonucleic acid deletions in oocytes and reproductive aging in women. *Fertil Steril.* 64 (3): 577-83.

Kennedy B K & Lamming D W (2016). The Mechanistic Target of Rapamycin: The Grand ConducTOR of Metabolism and Aging. *Cell Metab.* 23 (6): 990-1003.

Kerr J B, Hutt K J, Cook M, Speed T P, Strasser A, Findlay J K & Scott C L (2012a). Cisplatin-induced primordial follicle oocyte killing and loss of fertility are not prevented by imatinib. *Nature medicine.* 18 (8): 1170-2; author reply 2-4.

Kerr J B, Hutt K J, Michalak E M, Cook M, Vandenberg C J, Liew S H, Bouillet P, Mills A, Scott C L, Findlay J K & Strasser A (2012b). DNA damage-induced primordial follicle oocyte apoptosis and loss of fertility require TAp63-mediated induction of Puma and Noxa. *Molecular cell.* 48 (3): 343-52.

Kezele P & Skinner M K (2003). Regulation of ovarian primordial follicle assembly and development by estrogen and progesterone: endocrine model of follicle assembly. *Endocrinology.* 144 (8): 3329-37.

Kezele P, Nilsson E E & Skinner M K (2005). Keratinocyte growth factor acts as a mesenchymal factor that promotes ovarian primordial to primary follicle transition. *Biol Reprod.* 73 (5): 967-73.

Kezele P R, Nilsson E E & Skinner M K (2002). Insulin but not insulin-like growth factor-1 promotes the primordial to primary follicle transition. *Mol Cell Endocrinol.* 192 (1-2): 37-43.

Khan D R, Fournier E, Dufort I, Richard F J, Singh J & Sirard M A (2016). Meta-analysis of gene expression profiles in granulosa cells during folliculogenesis. *Reproduction.* 151 (6): R103-10.

Khanna K K & Jackson S P (2001). DNA double-strand breaks: signaling, repair and the cancer connection. *Nature genetics.* 27 (3): 247-54.

Kidder G M & Vanderhyden B C (2010). Bidirectional communication between oocytes and follicle cells: ensuring oocyte developmental competence. *Can J Physiol Pharmacol.* 88 (4): 399-413.

Kim D A & Suh E K (2014). Defying DNA double-strand break-induced death during prophase I meiosis by temporal TAp63alpha phosphorylation regulation in developing mouse oocytes. *Molecular and cellular biology.* 34 (8): 1460-73.

Kim E J, Lee J, Youm H W, Kim S K, Lee J R, Suh C S & Kim S H (2018). Comparison of Follicle Isolation Methods for Mouse Ovarian Follicle Culture In Vitro. *Reprod Sci.* 25 (8): 1270-8.

Kim S Y, Ebbert K, Cordeiro M H, Romero M M, Whelan K A, Suarez A A, Woodruff T K & Kurita T (2016). Constitutive Activation of PI3K in Oocyte Induces Ovarian Granulosa Cell Tumors. *Cancer research.* 76 (13): 3851-61.

Kim S Y, Ebbert K, Cordeiro M H, Romero M, Zhu J, Serna V A, Whelan K A, Woodruff T K & Kurita T (2015). Cell autonomous phosphoinositide 3-kinase activation in oocytes disrupts normal ovarian function through promoting survival and overgrowth of ovarian follicles. *Endocrinology.* 156 (4): 1464-76.

Kirk M & Lyon M F (1982). Induction of congenital anomalies in offspring of female mice exposed to varying doses of X-rays. *Mutat Res.* 106 (1): 73-83.

Kitagawa T, Suganuma N, Nawa A, Kikkawa F, Tanaka M, Ozawa T & Tomoda Y (1993). Rapid accumulation of deleted mitochondrial deoxyribonucleic acid in postmenopausal ovaries. *Biol Reprod.* 49 (4): 730-6.

Kitagishi Y & Matsuda S (2013). Redox regulation of tumor suppressor PTEN in cancer and aging (Review). *Int J Mol Med.* 31 (3): 511-5.

Kitajima M, Dolmans M M, Donnez O, Masuzaki H, Soares M & Donnez J (2014). Enhanced follicular recruitment and atresia in cortex derived from ovaries with endometriomas. *Fertil Steril.* 101 (4): 1031-7.

Knight P G & Glister C (2001). Potential local regulatory functions of inhibins, activins and follistatin in the ovary. *Reproduction.* 121 (4): 503-12.

Kona S S, Praveen Chakravarthi V, Siva Kumar A V, Srividya D, Padmaja K & Rao V H (2016). Quantitative expression patterns of GDF9 and BMP15 genes in sheep ovarian follicles grown in vivo or cultured in vitro. *Theriogenology.* 85 (2): 315-22.

Kujjo L L, Laine T, Pereira R J, Kagawa W, Kurumizaka H, Yokoyama S & Perez G I (2010). Enhancing survival of mouse oocytes following chemotherapy or aging by targeting Bax and Rad51. *PloS one.* 5 (2): e9204.

Kujjo L L, Ronningen R, Ross P, Pereira R J, Rodriguez R, Beyhan Z, Goissis M D, Baumann T, Kagawa W, Camsari C, Smith G W, Kurumizaka H*, et al.* (2012). RAD51 plays a crucial role in halting cell death program induced by ionizing radiation in bovine oocytes. *Biology of reproduction.* 86 (3): 76.

Kumar T R, Wang Y, Lu N & Matzuk M M (1997). Follicle stimulating hormone is required for ovarian follicle maturation but not male fertility. *Nat Genet.* 15 (2): 201-4.

Laitinen M, Vuojolainen K, Jaatinen R, Ketola I, Aaltonen J, Lehtonen E, Heikinheimo M & Ritvos O (1998). A novel growth differentiation factor-9

(GDF-9) related factor is co-expressed with GDF-9 in mouse oocytes during folliculogenesis. *Mech Dev.* 78 (1-2): 135-40.

Laplante M & Sabatini D M (2012). mTOR Signaling. *Cold Spring Harb Perspect Biol.* 4 (2).

Le Bouffant R, Guerquin M J, Duquenne C, Frydman N, Coffigny H, Rouiller-Fabre V, Frydman R, Habert R & Livera G (2010). Meiosis initiation in the human ovary requires intrinsic retinoic acid synthesis. *Hum Reprod.* 25 (10): 2579-90.

Lee, II & Kim J J (2014). Influence of AKT on progesterone action in endometrial diseases. *Biol Reprod.* 91 (3): 63.

Lee H N & Chang E M (2019). Primordial follicle activation as new treatment for primary ovarian insufficiency. *Clin Exp Reprod Med.* 46 (2): 43-9.

Lee J H & Paull T T (2005). ATM activation by DNA double-strand breaks through the Mre11-Rad50-Nbs1 complex. *Science (New York, N.Y.).* 308 (5721): 551-4.

Lee W S, Otsuka F, Moore R K & Shimasaki S (2001). Effect of bone morphogenetic protein-7 on folliculogenesis and ovulation in the rat. *Biol Reprod.* 65 (4): 994-9.

Lee W S, Yoon S J, Yoon T K, Cha K Y, Lee S H, Shimasaki S, Lee S & Lee K A (2004). Effects of bone morphogenetic protein-7 (BMP-7) on primordial follicular growth in the mouse ovary. *Mol Reprod Dev.* 69 (2): 159-63.

Lei L, Jin S, Mayo K E & Woodruff T K (2010). The interactions between the stimulatory effect of follicle-stimulating hormone and the inhibitory effect of estrogen on mouse primordial folliculogenesis. *Biol Reprod.* 82 (1): 13-22.

Lerer-Serfaty G, Samara N, Fisch B, Shachar M, Kossover O, Seliktar D, Ben-Haroush A & Abir R (2013). Attempted application of bioengineered/biosynthetic supporting matrices with phosphatidylinositol-trisphosphate-enhancing substances to organ culture of human primordial follicles. *Journal of assisted reproduction and genetics.* 30 (10): 1279-88.

Levine A J, Tomasini R, McKeon F D, Mak T W & Melino G (2011). The p53 family: guardians of maternal reproduction. *Nat Rev Mol Cell Biol.* 12 (4): 259-65.

Li J, Kawamura K, Cheng Y, Liu S, Klein C, Duan E K & Hsueh A J (2010a). Activation of dormant ovarian follicles to generate mature eggs. *Proc Natl Acad Sci U S A.* 107 (22): 10280-4.

Li J, Kawamura K, Cheng Y, Liu S, Klein C, Liu S, Duan E K & Hsueh A J (2010b). Activation of dormant ovarian follicles to generate mature eggs. *Proceedings of the National Academy of Sciences of the United States of America.* 107 (22): 10280-4.

Li Q, Geng X, Zheng W, Tang J, Xu B & Shi Q (2012). Current understanding of ovarian aging. *Science China. Life sciences.* 55 (8): 659-69.

Li Y, Li R Q, Ou S B, Zhang N F, Ren L, Wei L N, Zhang Q X & Yang D Z (2014). Increased GDF9 and BMP15 mRNA levels in cumulus granulosa cells correlate with oocyte maturation, fertilization, and embryo quality in humans. *Reprod Biol Endocrinol.* 1281.

Lighten A D, Hardy K, Winston R M & Moore G E (1997). Expression of mRNA for the insulin-like growth factors and their receptors in human preimplantation embryos. *Mol Reprod Dev.* 47 (2): 134-9.

Lin F, Ma X S, Wang Z B, Wang Z W, Luo Y B, Huang L, Jiang Z Z, Hu M W, Schatten H & Sun Q Y (2014). Different fates of oocytes with DNA double-strand breaks in vitro and in vivo. *Cell cycle (Georgetown, Tex.).* 13 (17): 2674-80.

Lin W, Titus S, Moy F, Ginsburg E S & Oktay K (2017). Ovarian Aging in Women With BRCA Germline Mutations. *J Clin Endocrinol Metab.* 102 (10): 3839-47.

Lindahl T & Barnes D E (2000). Repair of endogenous DNA damage. *Cold Spring Harb Symp Quant Biol.* 65127-33.

Liu K, Rajareddy S, Liu L, Jagarlamudi K, Boman K, Selstam G & Reddy P (2006). Control of mammalian oocyte growth and early follicular development by the oocyte PI3 kinase pathway: new roles for an old timer. *Dev Biol.* 299 (1): 1-11.

Liu L, Rajareddy S, Reddy P, Du C, Jagarlamudi K, Shen Y, Gunnarsson D, Selstam G, Boman K & Liu K (2007). Infertility caused by retardation of follicular development in mice with oocyte-specific expression of Foxo3a. *Development.* 134 (1): 199-209.

Livera G, Petre-Lazar B, Guerquin M J, Trautmann E, Coffigny H & Habert R (2008). p63 null mutation protects mouse oocytes from radio-induced apoptosis. *Reproduction (Cambridge, England).* 135 (1): 3-12.

Lu X X, Cao L Y, Chen X, Xiao J, Zou Y & Chen Q (2016). PTEN Inhibits Cell Proliferation, Promotes Cell Apoptosis, and Induces Cell Cycle Arrest via Downregulating the PI3K/AKT/hTERT Pathway in Lung Adenocarcinoma A549 Cells. *Biomed Res Int.* 20162476842.

Madanes D, Bilotas M A, Baston J I, Singla J J, Meresman G F, Baranao R I, Ricci A G, Takeuchi A, Koga K, Satake E, Makabe T, Taguchi A, *et al.* (2019). PI3K/AKT pathway is altered in the endometriosis patient's endometrium and presents differences according to severity stage. *Gynecol Endocrinol.* 104 (11): 1-5.

Maidarti M, Anderson R A & Telfer E E (2020). Crosstalk between PTEN/PI3K/Akt Signalling and DNA Damage in the Oocyte: Implications for Primordial Follicle Activation, Oocyte Quality and Ageing. *Cells.* 9 (1).

Maidarti M, Clarkson Y L, McLaughlin M, Anderson R A & Telfer E E (2019). Inhibition of PTEN activates bovine non-growing follicles in vitro but increases DNA damage and reduces DNA repair response. *Hum Reprod.* 34 (2): 297-307.

Makker A, Goel M M, Das V & Agarwal A (2012). PI3K-Akt-mTOR and MAPK signaling pathways in polycystic ovarian syndrome, uterine leiomyomas and endometriosis: an update. *Gynecol Endocrinol.* 28 (3): 175-81.

Mandell J W (2008). Immunohistochemical assessment of protein phosphorylation state: the dream and the reality. *Histochemistry and cell biology.* 130 (3): 465-71.

Mandl A M & Zuckerman S (1951). The relation of age to numbers of oocytes. *J Endocrinol.* 7 (2): 190-3.

Manning B D, Tee A R, Logsdon M N, Blenis J & Cantley L C (2002). Identification of the tuberous sclerosis complex-2 tumor suppressor gene product tuberin as a target of the phosphoinositide 3-kinase/akt pathway. *Mol Cell.* 10 (1): 151-62.

Marangos P & Carroll J (2012). Oocytes progress beyond prophase in the presence of DNA damage. *Current biology : CB.* 22 (11): 989-94.

Marangos P, Verschuren E W, Chen R, Jackson P K & Carroll J (2007). Prophase I arrest and progression to metaphase I in mouse oocytes are controlled by Emi1-dependent regulation of APC(Cdh1). *J Cell Biol.* 176 (1): 65-75.

Marangos P, Stevense M, Niaka K, Lagoudaki M, Nabti I, Jessberger R & Carroll J (2015). DNA damage-induced metaphase I arrest is mediated by the spindle assembly checkpoint and maternal age. *Nature communications.* 68706.

Martin J H, Bromfield E G, Aitken R J, Lord T & Nixon B (2018). Double Strand Break DNA Repair occurs via Non-Homologous End-Joining in Mouse MII Oocytes. *Scientific reports.* 8 (1): 9685.

Matsuzaki S, Pouly J L & Canis M (2018). In vitro and in vivo effects of MK2206 and chloroquine combination therapy on endometriosis: autophagy may be required for regrowth of endometriosis. *Br J Pharmacol.* 175 (10): 1637-53.

Matzuk M M, Burns K H, Viveiros M M & Eppig J J (2002). Intercellular communication in the mammalian ovary: oocytes carry the conversation. *Science (New York, N.Y.).* 296 (5576): 2178-80.

Mayer A, Baran V, Sakakibara Y, Brzakova A, Ferencova I, Motlik J, Kitajima T S, Schultz R M & Solc P (2016). DNA damage response during mouse oocyte maturation. *Cell cycle (Georgetown, Tex.).* 15 (4): 546-58.

McCaffery F H, Leask R, Riley S C & Telfer E E (2000). Culture of bovine preantral follicles in a serum-free system: markers for assessment of growth and development. *Biol Reprod.* 63 (1): 267-73.

McGee E A & Hsueh A J (2000). Initial and cyclic recruitment of ovarian follicles. *Endocrine reviews.* 21 (2): 200-14.

McLaughlin E A & McIver S C (2009). Awakening the oocyte: controlling primordial follicle development. *Reproduction (Cambridge, England).* 137 (1): 1-11.

McLaughlin M & Telfer E E (2010). Oocyte development in bovine primordial follicles is promoted by activin and FSH within a two-step serum-free culture system. *Reproduction.* 139 (6): 971-8.

McLaughlin M, Bromfield J J, Albertini D F & Telfer E E (2010a). Activin promotes follicular integrity and oogenesis in cultured pre-antral bovine follicles. *Mol Hum Reprod.* 16 (9): 644-53.

McLaughlin M, Kinnell H L, Anderson R A & Telfer E E (2014). Inhibition of phosphatase and tensin homologue (PTEN) in human ovary in vitro results in increased activation of primordial follicles but compromises development of growing follicles. *Molecular human reproduction.* 20 (8): 736-44.

McLaughlin M, Albertini D F, Wallace W H B, Anderson R A, Telfer E E, McLaughlin M & Telfer E E (2018). Metaphase II oocytes from human unilaminar follicles grown in a multi-step culture system. *Mol Hum Reprod.* 24 (3): 135-42.

McLaughlin M, Patrizio P, Kayisli U, Luk J, Thomson T C, Anderson R A, Telfer E E & Johnson J (2011). mTOR kinase inhibition results in oocyte loss characterized by empty follicles in human ovarian cortical strips cultured in vitro. *Fertility and sterility.* 96 (5): 1154-9 e1.

Meirow D, Epstein M, Lewis H, Nugent D & Gosden R G (2001). Administration of cyclophosphamide at different stages of follicular maturation in mice: effects

on reproductive performance and fetal malformations. *Hum Reprod.* 16 (4): 632-7.

Meirow D, Ben Yehuda D, Prus D, Poliack A, Schenker J G, Rachmilewitz E A & Lewin A (1998). Ovarian tissue banking in patients with Hodgkin's disease: is it safe? *Fertil Steril.* 69 (6): 996-8.

Menezo Y, Dale B & Cohen M (2010). DNA damage and repair in human oocytes and embryos: a review. *Zygote (Cambridge, England).* 18 (4): 357-65.

Menezo Y, Jr., Russo G, Tosti E, El Mouatassim S & Benkhalifa M (2007). Expression profile of genes coding for DNA repair in human oocytes using pangenomic microarrays, with a special focus on ROS linked decays. *Journal of assisted reproduction and genetics.* 24 (11): 513-20.

Ming M & He Y Y (2012). PTEN in DNA damage repair. *Cancer Lett.* 319 (2): 125-9.

Mizunuma H, Liu X, Andoh K, Abe Y, Kobayashi J, Yamada K, Yokota H, Ibuki Y & Hasegawa Y (1999). Activin from secondary follicles causes small preantral follicles to remain dormant at the resting stage. *Endocrinology.* 140 (1): 37-42.

Moher D, Shamseer L, Clarke M, Ghersi D, Liberati A, Petticrew M, Shekelle P, Stewart L A & Group P-P (2015). Preferred reporting items for systematic review and meta-analysis protocols (PRISMA-P) 2015 statement. *Syst Rev.* 41.

Mollgard K, Jespersen A, Lutterodt M C, Yding Andersen C, Hoyer P E & Byskov A G (2010). Human primordial germ cells migrate along nerve fibers and Schwann cells from the dorsal hind gut mesentery to the gonadal ridge. *Mol Hum Reprod.* 16 (9): 621-31.

Monniaux D (2016). Driving folliculogenesis by the oocyte-somatic cell dialog: Lessons from genetic models. *Theriogenology.* 86 (1): 41-53.

Monniaux D, Clement F, Dalbies-Tran R, Estienne A, Fabre S, Mansanet C & Monget P (2014). The ovarian reserve of primordial follicles and the dynamic reserve of antral growing follicles: what is the link? *Biol Reprod.* 90 (4): 85.

Mori T (2016), 'Regulatory Principles of Follicular Development', in Allahbadia G and Morimoto Y (eds.), *Ovarian Stimulation Protocols* (New Delhi: Springer).

Morohaku K, Tanimoto R, Sasaki K, Kawahara-Miki R, Kono T, Hayashi K, Hirao Y & Obata Y (2016). Complete in vitro generation of fertile oocytes from mouse primordial germ cells. *Proc Natl Acad Sci U S A.* 113 (32): 9021-6.

Motta P M, Makabe S, Motta P M & Makabe S (1986). Elimination of germ cells during differentiation of the human ovary: an electron microscopic study. *Eur J Obstet Gynecol Reprod Biol.* 22 (5-6): 271-86.

Murray A & Spears N (2000). Follicular development in vitro. *Semin Reprod Med.* 18 (2): 109-22.

Nazarov I B, Smirnova A N, Krutilina R I, Svetlova M P, Solovjeva L V, Nikiforov A A, Oei S L, Zalenskaya I A, Yau P M, Bradbury E M & Tomilin N V (2003). Dephosphorylation of histone gamma-H2AX during repair of DNA double-strand breaks in mammalian cells and its inhibition by calyculin A. *Radiation research.* 160 (3): 309-17.

Nguyen Q N, Zerafa N, Liew S H, Morgan F H, Strasser A, Scott C L, Findlay J K, Hickey M & Hutt K J (2018). Loss of PUMA protects the ovarian reserve during DNA-damaging chemotherapy and preserves fertility. *Cell death & disease.* 9 (6): 618.

Nguyen Q N, Zerafa N, Liew S H, Findlay J K, Hickey M, Hutt K J, Bezerra M E S, Gouveia B B, Barberino R S, Menezes V G, Macedo T J S, Cavalcante A Y P*, et al.* (2019). Cisplatin- and cyclophosphamide-induced primordial follicle depletion is caused by direct damage to oocytes. *Mol Hum Reprod.* 53 (6): 1298-305.

Nilsson E, Parrott J A & Skinner M K (2001). Basic fibroblast growth factor induces primordial follicle development and initiates folliculogenesis. *Molecular and cellular endocrinology.* 175 (1-2): 123-30.

Nilsson E E & Skinner M K (2003). Bone morphogenetic protein-4 acts as an ovarian follicle survival factor and promotes primordial follicle development. *Biol Reprod.* 69 (4): 1265-72.

Nilsson E E, Kezele P & Skinner M K (2002). Leukemia inhibitory factor (LIF) promotes the primordial to primary follicle transition in rat ovaries. *Molecular and cellular endocrinology.* 188 (1-2): 65-73.

Nilsson E E, Detzel C & Skinner M K (2006). Platelet-derived growth factor modulates the primordial to primary follicle transition. *Reproduction.* 131 (6): 1007-15.

Nogueira V & Hay N (2013). Molecular pathways: reactive oxygen species homeostasis in cancer cells and implications for cancer therapy. *Clin Cancer Res.* 19 (16): 4309-14.

Norris R P, Freudzon M, Mehlmann L M, Cowan A E, Simon A M, Paul D L, Lampe P D & Jaffe L A (2008). Luteinizing hormone causes MAP kinase-dependent phosphorylation and closure of connexin 43 gap junctions in mouse ovarian

follicles: one of two paths to meiotic resumption. *Development.* 135 (19): 3229-38.

Nottola S A, Cecconi S, Bianchi S, Motta C, Rossi G, Continenza M A & Macchiarelli G (2011). Ultrastructure of isolated mouse ovarian follicles cultured in vitro. *Reproductive biology and endocrinology : RB&E.* 93.

Novella-Maestre E, Herraiz S, Rodriguez-Iglesias B, Diaz-Garcia C & Pellicer A (2015). Short-Term PTEN Inhibition Improves In Vitro Activation of Primordial Follicles, Preserves Follicular Viability, and Restores AMH Levels in Cryopreserved Ovarian Tissue From Cancer Patients. *PloS one.* 10 (5): e0127786.

Nuttinck F, Peynot N, Humblot P, Massip A, Dessy F & Flechon J E (2000). Comparative immunohistochemical distribution of connexin 37 and connexin 43 throughout folliculogenesis in the bovine ovary. *Mol Reprod Dev.* 57 (1): 60-6.

O'Brien M J, Pendola J K & Eppig J J (2003). A revised protocol for in vitro development of mouse oocytes from primordial follicles dramatically improves their developmental competence. *Biol Reprod.* 68 (5): 1682-6.

Oktay K, Briggs D & Gosden R G (1997). Ontogeny of follicle-stimulating hormone receptor gene expression in isolated human ovarian follicles. *J Clin Endocrinol Metab.* 82 (11): 3748-51.

Oktay K, Newton H, Mullan J & Gosden R G (1998). Development of human primordial follicles to antral stages in SCID/hpg mice stimulated with follicle stimulating hormone. *Hum Reprod.* 13 (5): 1133-8.

Oktay K, Kim J Y, Barad D & Babayev S N (2010). Association of BRCA1 mutations with occult primary ovarian insufficiency: a possible explanation for the link between infertility and breast/ovarian cancer risks. *Journal of clinical oncology : official journal of the American Society of Clinical Oncology.* 28 (2): 240-4.

Oktay K, Turan V, Titus S, Stobezki R & Liu L (2015). BRCA Mutations, DNA Repair Deficiency, and Ovarian Aging. *Biology of reproduction.* 93 (3): 67.

Pacchiarotti J, Maki C, Ramos T, Marh J, Howerton K, Wong J, Pham J, Anorve S, Chow Y C & Izadyar F (2010). Differentiation potential of germ line stem cells derived from the postnatal mouse ovary. *Differentiation.* 79 (3): 159-70.

Palomino J & De Los Reyes M (2016). Temporal expression of GDF-9 and BMP-15 mRNAs in canine ovarian follicles. *Theriogenology.* 86 (6): 1541-9.

Pan Z, Sun M, Liang X, Li J, Zhou F, Zhong Z & Zheng Y (2016). The Controversy, Challenges, and Potential Benefits of Putative Female Germline Stem Cells Research in Mammals. *Stem Cells Int.* 20161728278.

Pangas S A & Rajkovic A (2006). Transcriptional regulation of early oogenesis: in search of masters. *Hum Reprod Update.* 12 (1): 65-76.

Pangas S A & Rajkovic A (2015), 'Follicular Development: Mouse, Sheep, and Human Models', in Tony M Plant and Anthony J Zeleznik (eds.), *Knobil and Neill's Physiology of Reproduction* (4 edn.: Academic Press).

Parrott J A & Skinner M K (1999). Kit-ligand/stem cell factor induces primordial follicle development and initiates folliculogenesis. *Endocrinology.* 140 (9): 4262-71.

Paynter S J, Cooper A, Fuller B J & Shaw R W (1999). Cryopreservation of bovine ovarian tissue: structural normality of follicles after thawing and culture in vitro. *Cryobiology.* 38 (4): 301-9.

Pedersen T & Peters H (1968). Proposal for a classification of oocytes and follicles in the mouse ovary. *J Reprod Fertil.* 17 (3): 555-7.

Pefani D E & O'Neill E (2016). Hippo pathway and protection of genome stability in response to DNA damage. *The FEBS journal.* 283 (8): 1392-403.

Pelosi E, Omari S, Michel M, Ding J, Amano T, Forabosco A, Schlessinger D & Ottolenghi C (2013). Constitutively active Foxo3 in oocytes preserves ovarian reserve in mice. *Nature communications.* 41843.

Pepling M E (2012). Follicular assembly: mechanisms of action. *Reproduction.* 143 (2): 139-49.

Pepling M E & Spradling A C (2001). Mouse ovarian germ cell cysts undergo programmed breakdown to form primordial follicles. *Dev Biol.* 234 (2): 339-51.

Perez G I, Acton B M, Jurisicova A, Perkins G A, White A, Brown J, Trbovich A M, Kim M R, Fissore R, Xu J, Ahmady A, D'Estaing S G*, et al.* (2007). Genetic variance modifies apoptosis susceptibility in mature oocytes via alterations in DNA repair capacity and mitochondrial ultrastructure. *Cell Death Differ.* 14 (3): 524-33.

Peters H, Byskov A G, Lintern-Moore S, Faber M & Andersen M (1973). The effect of gonadotrophin on follicle growth initiation in the neonatal mouse ovary. *J Reprod Fertil.* 35 (1): 139-41.

Phillips K A, Collins I M, Milne R L, McLachlan S A, Friedlander M, Hickey M, Stern C, Hopper J L, Fisher R, Kannemeyer G, Picken S, Smith C D*, et al.* (2016). Anti-Mullerian hormone serum concentrations of women with germline BRCA1 or BRCA2 mutations. *Human reproduction (Oxford, England).* 31 (5): 1126-32.

Picton & Gosden R G (2000). In vitro growth of human primordial follicles from frozen-banked ovarian tissue. *Mol Cell Endocrinol.* 166 (1): 27-35.

Picton H, Briggs D & Gosden R (1998). The molecular basis of oocyte growth and development. *Molecular and cellular endocrinology.* 145 (1-2): 27-37.

Plo I, Laulier C, Gauthier L, Lebrun F, Calvo F & Lopez B S (2008). AKT1 inhibits homologous recombination by inducing cytoplasmic retention of BRCA1 and RAD51. *Cancer Res.* 68 (22): 9404-12.

Praxedes E C G, Lima G L, Bezerra L G P, Santos F A, Bezerra M B, Guerreiro D D, Rodrigues A P R, Domingues S F S & Silva A R (2018). Development of fresh and vitrified agouti ovarian tissue after xenografting to ovariectomised severe combined immunodeficiency (SCID) mice. *Reprod Fertil Dev.* 30 (3): 459-68.

Puc J & Parsons R (2005). PTEN loss inhibits CHK1 to cause double stranded-DNA breaks in cells. *Cell Cycle.* 4 (7): 927-9.

Puc J, Keniry M, Li H S, Pandita T K, Choudhury A D, Memeo L, Mansukhani M, Murty V V, Gaciong Z, Meek S E, Piwnica-Worms H, Hibshoosh H*, et al.* (2005). Lack of PTEN sequesters CHK1 and initiates genetic instability. *Cancer Cell.* 7 (2): 193-204.

Rajareddy S, Reddy P, Du C, Liu L, Jagarlamudi K, Tang W, Shen Y, Berthet C, Peng S L, Kaldis P & Liu K (2007). p27kip1 (cyclin-dependent kinase inhibitor 1B)

controls ovarian development by suppressing follicle endowment and activation and promoting follicle atresia in mice. *Molecular endocrinology (Baltimore, Md.).* 21 (9): 2189-202.

Rajkovic A, Pangas S A, Ballow D, Suzumori N & Matzuk M M (2004). NOBOX deficiency disrupts early folliculogenesis and oocyte-specific gene expression. *Science.* 305 (5687): 1157-9.

Reddy P, Shen L, Ren C, Boman K, Lundin E, Ottander U, Lindgren P, Liu Y X, Sun Q Y & Liu K (2005). Activation of Akt (PKB) and suppression of FKHRL1 in mouse and rat oocytes by stem cell factor during follicular activation and development. *Developmental biology.* 281 (2): 160-70.

Reddy P, Adhikari D, Zheng W, Liang S, Hamalainen T, Tohonen V, Ogawa W, Noda T, Volarevic S, Huhtaniemi I & Liu K (2009). PDK1 signaling in oocytes controls reproductive aging and lifespan by manipulating the survival of primordial follicles. *Human molecular genetics.* 18 (15): 2813-24.

Reddy P, Liu L, Adhikari D, Jagarlamudi K, Rajareddy S, Shen Y, Du C, Tang W, Hamalainen T, Peng S L, Lan Z J, Cooney A J*, et al.* (2008). Oocyte-specific deletion of Pten causes premature activation of the primordial follicle pool. *Science (New York, N.Y.).* 319 (5863): 611-3.

Rein K & Stracker T H (2014). The MRE11 complex: an important source of stress relief. *Experimental cell research.* 329 (1): 162-9.

Ribeiro R P, Portela A M, Silva A W, Costa J J, Passos J R, Cunha E V, Souza G B, Saraiva M V, Donato M A, Peixoto C A, van den Hurk R & Silva J R (2015). Effects of jacalin and follicle-stimulating hormone on in vitro goat primordial follicle activation, survival and gene expression. *Zygote.* 23 (4): 537-49.

Richards J S (1980). Maturation of ovarian follicles: actions and interactions of pituitary and ovarian hormones on follicular cell differentiation. *Physiol Rev.* 60 (1): 51-89.

Richards J S & Pangas S A (2010). The ovary: basic biology and clinical implications. *J Clin Invest.* 120 (4): 963-72.

Rinaldi V D, Hsieh K, Munroe R, Bolcun-Filas E & Schimenti J C (2017). Pharmacological Inhibition of the DNA Damage Checkpoint Prevents Radiation-Induced Oocyte Death. *Genetics.* 206 (4): 1823-8.

Rodgers R J, Irving-Rodgers H F & Russell D L (2003). Extracellular matrix of the developing ovarian follicle. *Reproduction.* 126 (4): 415-24.

Rogakou E P, Pilch D R, Orr A H, Ivanova V S & Bonner W M (1998). DNA double-stranded breaks induce histone H2AX phosphorylation on serine 139. *The Journal of biological chemistry.* 273 (10): 5858-68.

Roness H, Gavish Z, Cohen Y & Meirow D (2013). Ovarian follicle burnout: a universal phenomenon? *Cell Cycle.* 12 (20): 3245-6.

Roos W P & Kaina B (2006). DNA damage-induced cell death by apoptosis. *Trends in molecular medicine.* 12 (9): 440-50.

Rosendahl M, Timmermans Wielenga V, Nedergaard L, Kristensen S G, Ernst E, Rasmussen P E, Anderson M, Schmidt K T & Andersen C Y (2011). Cryopreservation of ovarian tissue for fertility preservation: no evidence of malignant cell contamination in ovarian tissue from patients with breast cancer. *Fertil Steril.* 95 (6): 2158-61.

Ruvinsky I & Meyuhas O (2006). Ribosomal protein S6 phosphorylation: from protein synthesis to cell size. *Trends Biochem Sci.* 31 (6): 342-8.

Sadeu JC M C, Smitz J (2008), 'Human follicle culture in vitro', in Velasco JG Rizk B, Salam H, Makrigiannakis A (ed.), *Infertility and assisted reproduction* (1 edn.; New York: Cambridge university press).

Samoto T, Maruo T, Ladines-Llave C A, Matsuo H, Deguchi J, Barnea E R & Mochizuki M (1993). Insulin receptor expression in follicular and stromal compartments of the human ovary over the course of follicular growth, regression and atresia. *Endocr J.* 40 (6): 715-26.

Sanchez F & Smitz J (2012). Molecular control of oogenesis. *Biochim Biophys Acta.* 1822 (12): 1896-912.

Santos J M, Menezes V G, Barberino R S, Macedo T J, Lins T L, Gouveia B B, Barros V R, Santos L P, Goncalves R J & Matos M H (2014). Immunohistochemical localization of fibroblast growth factor-2 in the sheep ovary and its effects on pre-antral follicle apoptosis and development in vitro. *Reprod Domest Anim.* 49 (3): 522-8.

Schindler R, Nilsson E & Skinner M K (2010). Induction of ovarian primordial follicle assembly by connective tissue growth factor CTGF. *PLoS One.* 5 (9): e12979.

Schmidt D, Ovitt C E, Anlag K, Fehsenfeld S, Gredsted L, Treier A C & Treier M (2004). The murine winged-helix transcription factor Foxl2 is required for granulosa cell differentiation and ovary maintenance. *Development.* 131 (4): 933-42.

Schubert B S J (2010), 'In vitro culture of human primordial follicles.', in Quinn P Chian RC (ed.), *Fertility cryopreservation* (Philadephia: Cambridge university press), 200-11.

Scott J E, Carlsson I B, Bavister B D & Hovatta O (2004). Human ovarian tissue cultures: extracellular matrix composition, coating density and tissue dimensions. *Reprod Biomed Online.* 9 (3): 287-93.

Sharan S K, Pyle A, Coppola V, Babus J, Swaminathan S, Benedict J, Swing D, Martin B K, Tessarollo L, Evans J P, Flaws J A & Handel M A (2004). BRCA2 deficiency in mice leads to meiotic impairment and infertility. *Development (Cambridge, England).* 131 (1): 131-42.

Shen W H, Balajee A S, Wang J, Wu H, Eng C, Pandolfi P P & Yin Y (2007). Essential role for nuclear PTEN in maintaining chromosomal integrity. *Cell.* 128 (1): 157-70.

Shi L, Zhang J, Lai Z, Tian Y, Fang L, Wu M, Xiong J, Qin X, Luo A & Wang S (2016). Long-Term Moderate Oxidative Stress Decreased Ovarian Reproductive Function by Reducing Follicle Quality and Progesterone Production. *PLoS One.* 11 (9): e0162194.

Shimasaki S, Moore R K, Otsuka F & Erickson G F (2004). The bone morphogenetic protein system in mammalian reproduction. *Endocr Rev.* 25 (1): 72-101.

Silva J R, van den Hurk R, de Matos M H, dos Santos R R, Pessoa C, de Moraes M O & de Figueiredo J R (2004). Influences of FSH and EGF on primordial follicles during in vitro culture of caprine ovarian cortical tissue. *Theriogenology.* 61 (9): 1691-704.

Silva J R, Tharasanit T, Taverne M A, van der Weijden G C, Santos R R, Figueiredo J R & van den Hurk R (2006). The activin-follistatin system and in vitro early follicle development in goats. *The Journal of endocrinology.* 189 (1): 113-25.

Simon A M, Goodenough D A, Li E & Paul D L (1997). Female infertility in mice lacking connexin 37. *Nature.* 385 (6616): 525-9.

Skinner M K (2005). Regulation of primordial follicle assembly and development. *Human reproduction update.* 11 (5): 461-71.

Smitz J E & Cortvrindt R G (2002). The earliest stages of folliculogenesis in vitro. *Reproduction (Cambridge, England).* 123 (2): 185-202.

Soleimani R, Heytens E, Darzynkiewicz Z & Oktay K (2011). Mechanisms of chemotherapy-induced human ovarian aging: double strand DNA breaks and microvascular compromise. *Aging.* 3 (8): 782-93.

Straub W E, Weber T A, Schafer B, Candi E, Durst F, Ou H D, Rajalingam K, Melino G & Dotsch V (2010). The C-terminus of p63 contains multiple regulatory elements with different functions. *Cell death & disease.* 1e5.

Su Y Q, Sugiura K & Eppig J J (2009). Mouse oocyte control of granulosa cell development and function: paracrine regulation of cumulus cell metabolism. *Semin Reprod Med.* 27 (1): 32-42.

Suh E K, Yang A, Kettenbach A, Bamberger C, Michaelis A H, Zhu Z, Elvin J A, Bronson R T, Crum C P & McKeon F (2006). p63 protects the female germ line during meiotic arrest. *Nature.* 444 (7119): 624-8.

Sun X, Su Y, He Y, Zhang J, Liu W, Zhang H, Hou Z, Liu J & Li J (2015). New strategy for in vitro activation of primordial follicles with mTOR and PI3K stimulators. *Cell cycle (Georgetown, Tex.).* 14 (5): 721-31.

Sung P & Klein H (2006). Mechanism of homologous recombination: mediators and helicases take on regulatory functions. *Nat Rev Mol Cell Biol.* 7 (10): 739-50.

Suzuki N, Yoshioka N, Takae S, Sugishita Y, Tamura M, Hashimoto S, Morimoto Y & Kawamura K (2015). Successful fertility preservation following ovarian tissue vitrification in patients with primary ovarian insufficiency. *Human reproduction (Oxford, England).* 30 (3): 608-15.

Tajima K, Orisaka M, Mori T & Kotsuji F (2007). Ovarian theca cells in follicular function. *Reprod Biomed Online.* 15 (5): 591-609.

Takeuchi A, Koga K, Satake E, Makabe T, Taguchi A, Miyashita M, Takamura M, Harada M, Hirata T, Hirota Y, Yoshino O, Wada-Hiraike O*, et al.* (2019). Endometriosis Triggers Excessive Activation of Primordial Follicles via PI3K-PTEN-Akt-Foxo3 Pathway. *J Clin Endocrinol Metab.* 104 (11): 5547-54.

Tanaka Y, Kimura F, Zheng L, Kaku S, Takebayashi A, Kasahara K, Tsuji S & Murakami T (2018). Protective effect of a mechanistic target of rapamycin inhibitor on an in vivo model ofcisplatin-induced ovarian gonadotoxicity. *Experimental animals.* 67 (4): 493-500.

Tatone C, Amicarelli F, Carbone M C, Monteleone P, Caserta D, Marci R, Artini P G, Piomboni P & Focarelli R (2008). Cellular and molecular aspects of ovarian follicle ageing. *Human reproduction update.* 14 (2): 131-42.

Tee A R, Fingar D C, Manning B D, Kwiatkowski D J, Cantley L C & Blenis J (2002). Tuberous sclerosis complex-1 and -2 gene products function together to inhibit mammalian target of rapamycin (mTOR)-mediated downstream signaling. *Proc Natl Acad Sci U S A.* 99 (21): 13571-6.

Telfer E E & McLaughlin M (2012). Strategies to support human oocyte development in vitro. *Int J Dev Biol.* 56 (10-12): 901-7.

Telfer E E & Zelinski M B (2013). Ovarian follicle culture: advances and challenges for human and nonhuman primates. *Fertility and sterility.* 99 (6): 1523-33.

Telfer E E, Binnie J P, McCaffery F H & Campbell B K (2000). In vitro development of oocytes from porcine and bovine primary follicles. *Mol Cell Endocrinol.* 163 (1-2): 117-23.

Telfer E E, McLaughlin M, Ding C & Thong K J (2008). A two-step serum-free culture system supports development of human oocytes from primordial follicles in the presence of activin. *Human reproduction (Oxford, England).* 23 (5): 1151-8.

Telfer E E, Gosden R G, Byskov A G, Spears N, Albertini D, Andersen C Y, Anderson R, Braw-Tal R, Clarke H, Gougeon A, McLaughlin E, McLaren A*, et al.* (2005). On regenerating the ovary and generating controversy. *Cell.* 122 (6): 821-2.

Thacker J (2005). The RAD51 gene family, genetic instability and cancer. *Cancer letters.* 219 (2): 125-35.

Thomas F H, Armstrong D G & Telfer E E (2003a). Activin promotes oocyte development in ovine preantral follicles in vitro. *Reprod Biol Endocrinol.* 176.

Thomas F H, Walters K A & Telfer E E (2003b). How to make a good oocyte: an update on in-vitro models to study follicle regulation. *Hum Reprod Update.* 9 (6): 541-55.

Thomas F H, Campbell B K, Armstrong D G & Telfer E E (2007). Effects of IGF-I bioavailability on bovine preantral follicular development in vitro. *Reproduction.* 133 (6): 1121-8.

Thomas F H, Leask R, Srsen V, Riley S C, Spears N & Telfer E E (2001). Effect of ascorbic acid on health and morphology of bovine preantral follicles during long-term culture. *Reproduction.* 122 (3): 487-95.

Titus S, Li F, Stobezki R, Akula K, Unsal E, Jeong K, Dickler M, Robson M, Moy F, Goswami S & Oktay K (2013). Impairment of BRCA1-related DNA double-strand break repair leads to ovarian aging in mice and humans. *Science translational medicine.* 5 (172): 172ra21.

Tomilin N V, Solovjeva L V, Svetlova M P, Pleskach N M, Zalenskaya I A, Yau P M & Bradbury E M (2001). Visualization of focal nuclear sites of DNA repair synthesis induced by bleomycin in human cells. *Radiation research.* 156 (4): 347-54.

Torgovnick A & Schumacher B (2015). DNA repair mechanisms in cancer development and therapy. *Frontiers in genetics.* 6157.

Van den Hurk R, Abir R, Telfer E E & Bevers M M (2000). Primate and bovine immature oocytes and follicles as sources of fertilizable oocytes. *Hum Reprod Update.* 6 (5): 457-74.

van Wezel I L & Rodgers R J (1996). Morphological characterization of bovine primordial follicles and their environment in vivo. *Biol Reprod.* 55 (5): 1003-11.

Vitt U A, Hayashi M, Klein C & Hsueh A J (2000). Growth differentiation factor-9 stimulates proliferation but suppresses the follicle-stimulating hormone-induced differentiation of cultured granulosa cells from small antral and preovulatory rat follicles. *Biol Reprod.* 62 (2): 370-7.

Wallace W H & Kelsey T W (2010). Human ovarian reserve from conception to the menopause. *PLoS One.* 5 (1): e8772.

Walters K A, Binnie J P, Campbell B K, Armstrong D G & Telfer E E (2006). The effects of IGF-I on bovine follicle development and IGFBP-2 expression are dose and stage dependent. *Reproduction.* 131 (3): 515-23.

Wandji S A, Eppig J J & Fortune J E (1996a). FSH and growth factors affect the growth and endocrine function in vitro of granulosa cells of bovine preantral follicles. *Theriogenology.* 45 (4): 817-32.

Wandji S A, Srsen V, Voss A K, Eppig J J & Fortune J E (1996b). Initiation in vitro of growth of bovine primordial follicles. *Biol Reprod.* 55 (5): 942-8.

Wang C, Zhou B & Xia G (2017a). Mechanisms controlling germline cyst breakdown and primordial follicle formation. *Cell Mol Life Sci.* 74 (14): 2547-66.

Wang W, Luo S M, Ma J Y, Shen W & Yin S (2019a). Cytotoxicity and DNA Damage Caused from Diazinon Exposure by Inhibiting the PI3K-AKT Pathway in Porcine Ovarian Granulosa Cells. *J Agric Food Chem.* 67 (1): 19-31.

Wang X, Liu D, He D, Suo S, Xia X, He X, Han J J & Zheng P (2017b). Transcriptome analyses of rhesus monkey preimplantation embryos reveal a reduced capacity for DNA double-strand break repair in primate oocytes and early embryos. *Genome research.* 27 (4): 567-79.

Wang Y, Hu Z, Liu Z, Chen R, Peng H, Guo J, Chen X & Zhang H (2013). MTOR inhibition attenuates DNA damage and apoptosis through autophagy-mediated suppression of CREB1. *Autophagy.* 9 (12): 2069-86.

Wang Y, Liu M, Johnson S B, Yuan G, Arriba A K, Zubizarreta M E, Chatterjee S, Nagarkatti M, Nagarkatti P & Xiao S (2019b). Doxorubicin obliterates mouse

ovarian reserve through both primordial follicle atresia and overactivation. *Toxicol Appl Pharmacol.* 381114714.

Wayne C M, Fan H Y, Cheng X & Richards J S (2007). Follicle-stimulating hormone induces multiple signaling cascades: evidence that activation of Rous sarcoma oncogene, RAS, and the epidermal growth factor receptor are critical for granulosa cell differentiation. *Mol Endocrinol.* 21 (8): 1940-57.

Weaver V M, Fischer A H, Peterson O W & Bissell M J (1996). The importance of the microenvironment in breast cancer progression: recapitulation of mammary tumorigenesis using a unique human mammary epithelial cell model and a three-dimensional culture assay. *Biochem Cell Biol.* 74 (6): 833-51.

Weinberg-Shukron A, Rachmiel M, Renbaum P, Gulsuner S, Walsh T, Lobel O, Dreifuss A, Ben-Moshe A, Zeligson S, Segel R, Shore T, Kalifa R*, et al.* (2018). Essential Role of BRCA2 in Ovarian Development and Function. *N Engl J Med.* 379 (11): 1042-9.

Weng L, Brown J & Eng C (2001). PTEN induces apoptosis and cell cycle arrest through phosphoinositol-3-kinase/Akt-dependent and -independent pathways. *Hum Mol Genet.* 10 (3): 237-42.

Williams C J & Erickson G F (2000), 'Morphology and Physiology of the Ovary', in K. R. Feingold, et al. (eds.), *Endotext* (South Dartmouth MA: MDText.com, Inc.).

Williams L & Abdi H (2010), 'Fisher's Least Significant Difference (LSD) Test', in N Salkind (ed.), *Encyclopedia of Research Design* (Thousand Oaks), 3-6.

Winship A L, Stringer J M, Liew S H & Hutt K J (2018). The importance of DNA repair for maintaining oocyte quality in response to anti-cancer treatments,

environmental toxins and maternal ageing. *Hum Reprod Update.*24 (2): 119-34

Woods D C, White Y A & Tilly J L (2013). Purification of oogonial stem cells from adult mouse and human ovaries: an assessment of the literature and a view toward the future. *Reprod Sci.* 20 (1): 7-15.

Xiang C, Li J, Hu L, Huang J, Luo T, Zhong Z, Zheng Y & Zheng L (2015). Hippo signaling pathway reveals a spatio-temporal correlation with the size of primordial follicle pool in mice. *Cellular physiology and biochemistry : international journal of experimental cellular physiology, biochemistry, and pharmacology.* 35 (3): 957-68.

Xiao S, Zhang J, Romero M M, Smith K N, Shea L D & Woodruff T K (2015). In vitro follicle growth supports human oocyte meiotic maturation. *Sci Rep.* 517323.

Xu M, Barrett S L, West-Farrell E, Kondapalli L A, Kiesewetter S E, Shea L D & Woodruff T K (2009). In vitro grown human ovarian follicles from cancer patients support oocyte growth. *Human reproduction (Oxford, England).* 24 (10): 2531-40.

Yang B, Oo T N & Rizzo V (2006). Lipid rafts mediate H2O2 prosurvival effects in cultured endothelial cells. *FASEB J.* 20 (9): 1501-3.

Yerushalmi G M, Salmon-Divon M, Yung Y, Maman E, Kedem A, Ophir L, Elemento O, Coticchio G, Dal Canto M, Mignini Renzinu M, Fadini R & Hourvitz A (2014). Characterization of the human cumulus cell transcriptome during final follicular maturation and ovulation. *Mol Hum Reprod.* 20 (8): 719-35.

Yin X, Pavone M E, Lu Z, Wei J & Kim J J (2012). Increased activation of the PI3K/AKT pathway compromises decidualization of stromal cells from endometriosis. *J Clin Endocrinol Metab.* 97 (1): E35-43.

Zeleznik A J (2001). Follicle selection in primates: "many are called but few are chosen". *Biology of reproduction.* 65 (3): 655-9.

Zhang D, Fouad H, Zoma W D, Salama S A, Wentz M J & Al-Hendy A (2008). Expression of stem and germ cell markers within nonfollicle structures in adult mouse ovary. *Reprod Sci.* 15 (2): 139-46.

Zhang D, Zhang X, Zeng M, Yuan J, Liu M, Yin Y, Wu X, Keefe D L & Liu L (2015). Increased DNA damage and repair deficiency in granulosa cells are associated with ovarian aging in rhesus monkey. *Journal of assisted reproduction and genetics.* 32 (7): 1069-78.

Zhang H & Liu K (2015). Cellular and molecular regulation of the activation of mammalian primordial follicles: somatic cells initiate follicle activation in adulthood. *Hum Reprod Update.* 21 (6): 779-86.

Zhang H, Risal S, Gorre N, Busayavalasa K, Li X, Shen Y, Bosbach B, Brannstrom M & Liu K (2014). Somatic cells initiate primordial follicle activation and govern the development of dormant oocytes in mice. *Current biology : CB.* 24 (21): 2501-8.

Zhang X M, Li L, Xu J J, Wang N, Liu W J, Lin X H, Fu Y C & Luo L L (2013). Rapamycin preserves the follicle pool reserve and prolongs the ovarian lifespan of female rats via modulating mTOR activation and sirtuin expression. *Gene.* 523 (1): 82-7.

Zhou L, Xie Y, Li S, Liang Y, Qiu Q, Lin H & Zhang Q (2017). Rapamycin Prevents cyclophosphamide-induced Over-activation of Primordial Follicle pool through PI3K/Akt/mTOR Signaling Pathway in vivo. *Journal of ovarian research.* 10 (1): 56.

Zhuo Y, Hua L, Feng B, Jiang X, Li J, Jiang D, Huang X, Zhu Y, Li Z, Yan L, Jin C, Che L*, et al.* (2019). Fibroblast growth factor 21 coordinates adiponectin to mediate the beneficial effects of low-protein diet on primordial follicle reserve. *EBioMedicine.* 41623-35.

Zou K, Yuan Z, Yang Z, Luo H, Sun K, Zhou L, Xiang J, Shi L, Yu Q, Zhang Y, Hou R & Wu J (2009). Production of offspring from a germline stem cell line derived from neonatal ovaries. *Nat Cell Biol.* 11 (5): 631-6.

Appendix

Published Papers

Human Reproduction, Vol.34, No.2 pp. 297–307, 2019
Advanced Access publication on December 6, 2018 doi:10.1093/humrep/dey354

human reproduction

ORIGINAL ARTICLE ***Reproductive biology***

Inhibition of PTEN activates bovine non-growing follicles *in vitro* but increases DNA damage and reduces DNA repair response

Mila Maidarti[1,2], Yvonne L. Clarkson[2], Marie McLaughlin[2], Richard A. Anderson[1], and Evelyn E. Telfer[2,*]

[1]MRC Centre for Reproductive Health, Queens Medical Research Institute, University of Edinburgh, Edinburgh EH16 4TJ, UK [2]Institute of Cell Biology and Genes and Development Group, CDBS Hugh Robson Building, University of Edinburgh, Edinburgh EH8 9XD, UK

*Correspondence address. Institute of Cell Biology and Genes and Development Group, CDBS Hugh Robson Building, University of Edinburgh, Edinburgh, EH8 9XD, UK. Tel: +44-131-650-5393; E-mail: evelyn.telfer@ed.ac.uk

Submitted on August 15, 2018; resubmitted on November 7, 2018; accepted on November 15, 2018

STUDY QUESTION: Does ovarian follicle activation by phosphatase homologue of chromosome-10 (PTEN) inhibition affect DNA damage and repair in bovine oocytes and granulosa cells?

SUMMARY ANSWER: PTEN inhibition promotes bovine non-growing follicle activation but results in increased DNA damage and impaired DNA repair capacity in ovarian follicles *in vitro*.

WHAT IS KNOWN ALREADY: Inhibition of PTEN is known to activate primordial follicles but may compromise further developmental potential. In breast cancer cells, PTEN inhibition represses nuclear translocation of breast cancer susceptibility 1 (BRCA1) and Rad51; this impairs DNA repair resulting in an accumulation of damaged DNA, which contributes to cell senescence.

STUDY DESIGN, SIZE, DURATION: Bovine ovarian tissue fragments were exposed to control medium alone or containing either 1 or 10 μM bpv(HOpic), a pharmacological inhibitor of PTEN, *in vitro* for 24 h. A sub-group of tissue fragments were collected for Western blot analysis after bpv(HOpic) exposure. The remainder were incubated in control medium for a further 5 days and then analysed histologically and by immunohistochemistry to detect DNA damage and repair pathways.

PARTICIPANTS/MATERIALS, SETTING, METHODS: Bovine ovaries were obtained from abattoir-slaughtered heifers. Tissue fragments were exposed to either control medium alone or medium containing either 1 μM or 10 μM bpv(HOpic) for 24 h. Tissue fragments collected after 24 h were subjected to Akt quantification by Western blotting (six to nine fragments per group per experiment). Follicle stage and morphology were classified in remaining fragments. Immunohistochemical analysis included nuclear exclusion of FOXO3 as a marker of follicle activation, γH2AX as a marker of DNA damage, meiotic recombination 11 (MRE11), ataxia telangiectasia mutated (ATM), Rad51, breast cancer susceptibility 1 (BRCA1) and breast cancer susceptibility 2 (BRCA2) as DNA repair factors. A total of 29 550 follicles from three independent experiments were analysed.

MAIN RESULTS AND THE ROLE OF CHANCE: Tissue fragments exposed to bpv(HOpic) had increased Akt phosphorylation at serine 473 (pAkt/Akt ratio, 2.25- and 6.23-fold higher in 1 and 10 μM bpv(HOpic) respectively compared to control, $P < 0.05$). These tissue fragments contained a significantly higher proportion of growing follicles compared to control (78.6% in 1 μM and 88.7% in 10 μM versus 70.5% in control; $P < 0.001$). The proportion of morphologically healthy follicles did not differ significantly between 1 μM bpv(HOpic) and control ($P < 0.001$) but follicle health was lower in 10 μM compared to 1 μM and control in all follicle types ($P < 0.05$). DNA damage in oocytes, indicated by expression of γH2AX, increased following exposure to 1 μM bpv(HOpic) (non-growing, 83%; primary follicles, 76%) and 10 μM (non-growing, 77%; primary, 84%) compared to control (non-growing, 30% and primary, 59%) ($P < 0.05$ for all groups). A significant reduction in expression of DNA repair proteins MRE11, ATM and Rad51 was observed in oocytes of non-growing and primary follicles of treatment groups (primary follicles in controls versus 10 μM bpv(HOpic): MRE, 68% versus 47%; ATM, 47% versus 18%; Rad51, 48%

versus 24%), $P < 0.05$ for all groups. Higher dose bpv(HOpic) also resulted in lower expression of BRCA1 compared to control and 1 μM bpv(HOpic) ($P < 0.001$) in non-growing and primary follicles. BRCA2 expression was increased in oocytes of primary follicles in 1 μM bpv (HOpic) (36%) compared to control (20%, $P = 0.010$) with a marked decrease in 10 μM (1%, $P \leq 0.001$). Granulosa cells of primary and secondary follicles in bpv(HOpic) groups showed more DNA damage compared to control ($P < 0.05$). However, bpv(HOpic) did not impact granulosa cell DNA repair capacity in secondary follicles, but BRCA1 declined significantly in higher dose bpv(HOpic).

LARGE-SCALE DATA: N/A.

LIMITATIONS, REASONS FOR CAUTION: This study focuses on non-growing follicle activation after 6 days culture and may not reflect DNA damage and repair capacity in later stages of oocyte and follicle growth.

WIDER IMPLICATIONS OF THE FINDINGS: *In vitro* activation of follicle growth may compromise the bidirectional signalling between oocyte and granulosa cells necessary for optimal oocyte and follicle health. This large animal model may be useful in optimising follicle activation protocols with a view to transfer for clinical application.

STUDY FUNDING/COMPETING INTEREST(S): This work was supported by Indonesia endowment fund for education. No competing interest.

TRIAL REGISTRATION NUMBER: Not applicable.

Key words: PTEN inhibition / non-growing follicle activation / DNA damage / DNA repair / bovine ovarian follicles / *in vitro*

Introduction

The phosphatidylinositol 3-kinase (PI3K) signalling pathway appears to be the primary non-gonadotrophic growth factor signalling pathway that regulates the growth and differentiation of ovarian follicles (Dupont and Scaramuzzi, 2016). The balance between PI3K/Akt substrates determines follicle growth acceleration, deceleration, survival and apoptosis (Liu *et al.*, 2006; Zhou *et al.*, 2017), and phosphatase homologue of chromosome-10 (PTEN) is a negative regulator of this pathway. Excessive PI3K activation in mice has been hypothesised to contribute to premature activation of primordial follicles which in turn results in depletion of the primordial follicle pool and ovarian aging (Reddy *et al.*, 2008; Sobinoff *et al.*, 2012). Inhibition of PTEN in cultured human ovarian cortex results in increased activation of primordial follicles and more secondary follicles, however the subsequent growth and survival of those apparently healthy isolated secondary follicles is compromised (McLaughlin *et al.*, 2014; Grosbois and Demeestere, 2018).

This finding might be related to the role of PTEN in maintaining genomic integrity (Shen *et al.*, 2007), promoting and regulating cell growth and survival (Reddy *et al.*, 2008; Jagarlamudi *et al.*, 2009). Akt activation during cell cycles in normal cell proliferation upregulates numerous substrates at the G1/S and G2/M transition, some of which are involved in DNA damage repair pathway. DNA damage is the starting event of apoptosis and can be detected even in the absence of morphological changes. It is suggested that the PI3K/Akt pathway initiates checkpoint kinase 1 (Chk1) phosphorylation during DNA damage response cascade at G2 arrest (Xu *et al.*, 2010), thus allowing time for DNA repair processing.

Effects of PTEN inhibition on DNA damage response have been reported in many different types of cancer (Altiok *et al.*, 1999; Plo *et al.*, 2008; Golding *et al.*, 2009; Fraser *et al.*, 2012) with varying outcomes. Endogenously high levels of Akt decreases homologous recombination repair capacity of DNA double-strand breaks (DSBs) (Brunet *et al.*, 1999; Thacker, 2005; Plo *et al.*, 2008; Jia *et al.*, 2013). In addition, a study using a breast cancer cell line showed that high intracellular levels of Akt repressed nuclear translocation of breast cancer susceptibility 1 (BRCA1) and Rad51, resulting in the lack of homologous recombination of DNA DSB repair (Plo *et al.*, 2008). Upregulation of the PI3K/Akt pathway can also generate spontaneous DNA breaks and pose a significant threat to genome stability by inhibition of Chk1 (Puc and Parsons, 2005). On the other hand, low protein kinase B (Akt) activity has been shown to impair the DNA damage repair mechanism by non-homologous end joining in human glioma cells (Kao *et al.*, 2007; Golding *et al.*, 2009).

Taken together, these findings support the idea that oocytes lacking PTEN may accumulate DNA damage, with reduced DNA damage repair capacity. DNA DSBs are the most detrimental type of damage, but they do not occur as frequently as other lesions. Persistent unrepaired DNA DSBs may lead to genomic instability (Khanna and Jackson, 2001; Jackson and Bartek, 2009; Menezo *et al.*, 2010; Titus *et al.*, 2013) and the capacity of the cell to repair the damage will influence the balance between cell survival and apoptosis (Bzymek *et al.*, 2010; Torgovnick and Schumacher, 2015). In oocytes and granulosa cells, unrepaired DNA DSBs may potentially impact upon the quality of oocytes (Carroll and Marangos, 2013; Oktay *et al.*, 2015; Winship *et al.*, 2018). In this study, our aim was to determine whether PTEN inhibition affected DNA damage and repair mechanisms in bovine ovarian follicles activated *in vitro*, using a serum-free culture system. We have shown that this system is able to maintain follicular growth and support oocyte development *in vitro* using bovine and human ovaries (Telfer *et al.*, 2008; McLaughlin and Telfer, 2010).

Materials and Methods

Ovarian cortical tissue collection, preparation

Bovine ovaries were obtained from the abattoir and collected in pre-warmed culture medium M199 (HEPES buffered) (Gibco BRL, Life Technologies Ltd., Paisley, Renfrewshire, UK) supplemented with sodium pyruvate (2 mM), glutamine (2 mM), bovine serum albumin (BSA) (3 mg/ml),

penicillin G (75 μg/ml), streptomycin (50 μg/ml) and amphotericin B (2.5 μg/ml) (all chemicals from Sigma-Aldrich Chemicals, Poole, Dorset, UK). At the laboratory, thin slices of ovarian cortex were removed from the ovaries using a scalpel blade no. 24 and then transferred into fresh dissection medium comprising preheated Leibovitz medium (Gibco BRL) supplemented with sodium pyruvate (2 mM), glutamine (2 mM), BSA (Fraction V. 3 mg/ml), penicillin G (75 μg/ml) and streptomycin (50 μg/ml). Excess stromal tissue was trimmed using forceps and a scalpel blade. The tissue was gently stretched using the blunt edge of a scalpel blade with the cortex uppermost and cut into small strips sized 4 mm × 2 mm × 1 mm. Any follicles measuring >40 μm were excised from the tissue fragments.

Ovarian tissue fragments culture

Basic culture medium was prepared from McCoy's 5a medium with bicarbonate and HEPES (20 mM) (GIbco BRL) supplemented with BSA (1 mg/ml), glutamine (3 mM), penicillin G (0.1 mg/ml), streptomycin (0.1 mg/ml), transferrin (2.5 μg/ml), sodium selenite (4 ng/ml), insulin (l0 ng/ml), hFSH (1 ng/ml) and ascorbic acid (50 μg/ml) (all obtained from Sigma-Aldrich Chemicals). Before use, the medium was equilibrated at 37°C in humidified air with 5% CO_2.

Following tissue preparation and cutting, 10–12 fragments per culture were randomly selected as 0 h controls for histological examination. The remaining tissue fragments were cultured in flat-bottomed 24-well culture plates (Corning Costar Europe, Badhoevedorp, The Netherlands) containing 300 μl of basic culture medium or culture medium supplemented with the PTEN inhibitor dipotassium bisperoxo(5-hydroxypyridine-2-carboxyl) oxovanadate (V) (bpv(HOpic) (Merck Millipore Chemicals Ltd, UK) at 1 or 10 μM at 37°C in humidified air with 5% CO_2. After 24 h, all media was removed from tissue fragments and replaced with fresh basic culture medium. At this point, 6–9 tissue fragments from each group were snap-frozen and stored at −80°C for Western blot analysis of Akt phosphorylation.

Remaining tissue fragments were incubated for a further 5 days, with half the media removed and replaced with fresh on alternate days. On completion of the culture period, all remaining tissue fragments were fixed in 10% normal buffered formalin (NBF) for histological examination to determine the effect of PTEN inhibitor on follicle and oocyte development.

Histological methods and tissue analysis

After fixation in NBF for 24 h, tissues were further processed and embedded individually into paraffin wax blocks and serially sectioned at 5 μm thickness. Sections were mounted on Super Frost Plus slides (VWR International Ltd., Leicestershire, UK). For all morphological and numerical analyses, the examiner was blinded to the treatment groups. Analysis of follicles within tissue fragments was performed on every section under the light microscope with a crossed micrometre under 40× magnification. Follicle developmental stage was categorised using a modification of an established system (Pedersen and Peters, 1968). Primordial and transitory follicles were classified as non-growing due to the evidence suggesting that in the bovine ovary these follicles are in quiescence (van Wezel and Rodgers, 1996). The number of follicles within each stage of development was recorded, for Day 0 and Day 6 of each treatment. The classification of healthy follicles was based on the same criteria as in Telfer *et al.* with modifications (Telfer *et al.*, 2008). For follicles to be categorised as morphologically normal the oocyte must be grossly circular, surrounded by a zona pellucida, have a visible germinal vesicle and defined nucleolus and have <10% of pyknotic granulosa cells present. The proportion of follicles at different developmental stages was defined as a percentage of morphologically healthy follicles over the total follicle count (Brunet *et al.*, 1999).

Immunohistochemistry

Quantitative analysis of DNA damage was performed using immunofluorescence. DNA damage repair proteins were localised in tissue sections using antibodies against Rad51 (137323; 1:500; Abcam), meiotic recombination (MRE) 11 (NB100-142; 1:1000; Novusbio), BRCA1 (Ab16781; 1:200; Abcam), ATM (ab78; 1:500; Abcam) and BRCA2 (Ab27976; 1:200; Abcam). Nuclear exclusion of FOXO3 was detected using immunohistochemistry (NBP2-24579; 1:500; Novusbio).

Tissue sections mounted on slides were dewaxed in xylene and rehydrated through decreasing concentrations of alcohol before being immersed in tris-buffered saline with 0.05% (v/v) Tween 20 (TBST). Antigen retrieval was performed by microwaving the slides in 10 mM sodium citrate (pH 6.0) at simmer setting for 20 min. Following antigen retrieval, the slides were washed in TBST (2 × 5 min) and then immersed in 3% (v/v) hydrogen peroxide to quench endogenous peroxidase activity. After 2 × 5 min washes in TBST, sections were incubated with appropriate blocking solution for 1 h (150 μl goat serum or horse serum in 10 ml TBST followed by overnight incubation with the diluted primary antibodies at 4°C. Primary antibody was replaced with blocking solution for negative controls.

Primary antibody was washed off, and sections were incubated for 30 min with biotinylated secondary antibody at room temperature (Vectastain Elite ABC kit; Vector Laboratories, Peterborough, UK) and then washed in TBST (2 × 5 min). Slides were then incubated with Streptavidin Horseradish Peroxidase (Streptavidin horse-radish peroxidase; HRP) for 30 min at room temperature. Following a TBST wash DAB (3,3′-diaminobenzidine) peroxidase substrate kit (Vector Laboratories) solution was added to the sections for between 2 and 5 min and counterstained with haematoxylin for 20 s, dehydrated in graded alcohol, cleared and then mounted with dibutylphthalate polystyrene xylene (DPX).

Immunofluorescence

Localisation of γH2AX (a marker of DNA damage) was detected by immunofluorescence. As previously described mounted tissue sections were deparaffinised and rehydrated and then washed in PBS with 0.1% (v/v) Triton X-100 (PBST) (pH 7.2–7.4) for 2 × 5 min. Then, the slides were subjected to high temperature antigen retrieval as described earlier and incubated for 1 h at RT with blocking solution (5%, v/v, goat serum in PBST). Tissue sections were then probed with primary antibody (1:1000) against γH2AX (NB100-384; Novusbio) overnight at 4°C. Blocking solution without primary antibody served as negative control. After washing with PBST (4 × 10 min), sections were incubated with appropriate secondary antibodies (Cy3-conjugated affinity pure donkey anti rabbit IgG [H + L], 1:250; Jackson Laboratories) for 2 hours and then washed for 2 × 10 min. The slides were then mounted in Vectashield hardset with 4′-6-diamidino-2-phenylindole (DAPI) (H-1500; Vector Laboratories).

Images were analysed using ImageJ and γH2AX expression in oocytes and granulosa cells determined. The number of oocytes with γH2AX foci per total number of follicles was calculated. The γH2AX expression in granulosa cells was quantitatively analysed by calculating the proportion of γH2AX positive granulosa cells per total number of granulosa cells per follicle. Images were captured using a Zeiss LSM 800 confocal microscope with X20 magnification in the IMPACT imaging facility (Centre for Discovery Brain Sciences, The University of Edinburgh).

Western blotting

Ovarian cortical strips (6–9 per group per experiment) were suspended in radio immunoprecipitation assay buffer (RIPA) extraction buffer (Fisher Scientific, Loughborough, UK) supplemented with 1% v/v Halt Protease and Phosphatase Inhibitor Cocktail (PI) (Thermo Scientific, Loughborough,

UK). The tissue was cut with scissors and homogenised. Proteins were detected using a slightly modified protocol as previously described (Clarkson et al., 2018). In brief, the sample was centrifuged at 3400 × g for 5 min and protein was purified using Vivaspin tubes (Sartorius Mechatronics Ltd, Epsom, UK) with 50 kDa filters. Protein concentration was measured using Coomassie-Plus Reagent (Thermo Scientific Pierce, Northumberland, UK). Protein samples were denatured at 100°C for 10 min, 20 µg was loaded onto 4–20% gradient gels (Life Technologies, Paisley, UK) in Tris-glycine/SDS running buffer (25 mM Tris-HCl, 52 mM glycine, 0.1% SDS) and run at 125 V for 1 h. Proteins were transferred to nitrocellulose membranes (Amersham Pharmacia). Bovine serum albumin (BSA) (5%, w/v) in TBST was used to block the nitrocellulose membranes for 1 h at room temperature with gentle agitation. Blots were then incubated, with a rabbit monoclonal antibody against Akt (9272, 1:5000; Cell Signaling) or rabbit polyclonal antibody against Akt phosphorylated at serine 473 (ab81283, 1:500; Abcam) and with a mouse monoclonal antibody against alpha tubulin (ab7291, 1:5000; Abcam) as a loading control, overnight at 4°C with gentle agitation. Blots were washed in 0.1% TBST and then incubated with appropriate secondary antibodies, a goat polyclonal antibody raised against mouse IgG (heavy and light chain) (115-035-146; Jackson Laboratory) or rabbit IgG (H + L) (111-035-003) 1:5000 in 5% BSA for 1 h at room temperature. To enhance chemiluminescence detection, nitrocellulose membranes were placed in Amersham (ECL) prime Western blotting detection reagent (GE Health Care) for 1 min and exposed to autoradiographic film. Western blots were digitally scanned and analysed using ImageJ. All analysis was normalised to alpha tubulin.

Statistical analyses

All data were analysed using the SPSS statistical software version 22 (SPSS, Inc., Chicago, USA) and GraphPad Software version 7 (GraphPad Software Inc., San Diego, CA, USA). Quantitative data are presented as mean ± SEM. Chi-squared test was used to analyse the percentage of healthy and unhealthy follicles, the distribution of follicle stages and the proportion of oocytes expressing proteins related to DNA damage and DNA DSB repair. Granulosa cell expression of γH2AX, MRE11, ATM, Rad51, BRCA1 and BRCA2 was determined using one-way ANOVA test followed by Bonferroni *post hoc* test. Statistical significance was assigned at $P \leq 0.05$.

Results

Analysis of follicle distribution

A total of 32 ovarian cortical fragments were obtained on Day 0 from three culture replicates, and a total of 8833 follicles were analysed. Non-growing follicles were the most prevalent on Day 0, constituting 79.6% of total follicle number. The majority of the remaining follicles were at the primary stage (19.0%) and a small percentage were at secondary stage (1.4%) (Table I). More than 80% of all follicles at Day 0 were healthy (Fig. 1). No antral follicles were observed at Day 0 (D0) in any tissue fragments.

Assessment of follicle activation and survival

Analysis of 20 717 follicles from a total of 147 ovarian cortical tissue fragments ($n = 15–18$ fragments per group per culture) after 6 days of culture showed that the proportion of non-growing follicles declined significantly in all groups compared to D0 (Table I). This decline was balanced by a significant increase in the percentage of growing follicles (primary and secondary follicles in D0: 20.4%, control: 70.5%, 1 µM bpv(HOpic): 78.6% and 10 µM bpv(HOpic): 88.7%) ($P < 0.001$ for all groups). A greater proportion of growing follicles was observed in 10 µM bpv(HOpic) compared to control and 1 µM bpv(HOpic) ($P < 0.001$ for all groups). Secondary follicles were the most mature growing follicle stage observed in all groups. The proportion of follicles progressing to the secondary stage in the presence of bpv(HOpic) was significantly higher compared to control (1 µM: 9.7%, 10 µM: 10.6%, control: 6.2%) ($P < 0.05$). No significant difference was observed between 1 and 10 µM bpv(HOpic) ($P = 0.530$). The higher concentration of bpv(HOpic) resulted in a reduction in the proportion of morphologically healthy follicles at all stages. This was seen for both non-growing ($P < 0.05$ for all groups) and growing follicles ($P < 0.001$ for primary and secondary follicles) compared to control and 1 µM bpv(HOpic) (Fig. 1).

The effects of bpv(HOpic) on PI3K downstream pathway activation

To assess the nuclear exclusion of FOXO3 as an effect of PTEN inhibitor on the PI3K pathway, FOXO3 localisation was determined by immunohistochemistry (Fig. 2A–D). A total of 1704 follicles were analysed over three separate cultures and the mean percentage ± SEM of oocytes showing nuclear exclusion of FOXO3 was calculated (Fig. 2A). A significant increase in nuclear exclusion of FOXO3 was observed in oocytes contained within tissue exposed to bpv(HOpic) 1 µM (69.1 ± 11.7%; $P = 0.008$) and 10 µM (81.2 ± 12.4%; $P = 0.003$) compared to controls (38.3 ± 9.2%). Furthermore, the proportion of follicles with nuclear exclusion of FOXO3 was significantly higher in 10 µM compared to 1 µM ($P = 0.020$) (Fig. 2A).

Western blot analysis showed an increase in the ratio of pAkt (Ser473) to Akt in bpv(HOpic) exposed tissue compared to control (2.25- and 6.23-fold higher in 1 and 10 µM bpv(HOpic) respectively, $P < 0.05$) (Fig. 2E and F). A significant increase was observed in the higher concentration of bpv(HOpic) compared to 1 µM ($P = 0.030$) (Fig. 2F).

The effects of PTEN inhibitor on DNA damage and DNA DSB repair capacity in follicles

γH2AX binds at DNA strand breaks and is a marker of DNA damage. Localisation of γH2AX in each of the groups was analysed in oocytes (Fig. 3A–E) and granulosa cells (Fig. 3F–H). After 6 days of culture, γH2AX expression was reduced from 79% (D0) to 30 and 59% in non-growing and primary follicles respectively ($P < 0.001$) (Fig. 3I). Culture did not significantly affect γH2AX expression in oocytes of secondary follicles. However, bpv(HOpic) increased γH2AX expression in oocytes of all follicle types at both concentrations of bpv(HO)pic (1 µM: non-growing, 83%; primary, 76%; secondary, 77%; 10 µM: non-growing, 77%; primary, 84%; secondary, 89%) ($P < 0.05$), with no difference between doses (Fig. 3I).

In granulosa cells, γH2AX expression in non-growing follicles did not significantly differ between groups (Fig. 3J). Similarly, no significant differences were observed between D0, control and the lower concentration of bpv(HOpic) in primary follicles (Fig. 3J). A significant increase in expression in primary follicles was observed in the higher (36.9 ± 4.2) compared to the lower concentration (11.8 ± 3.39) and control (16.9 ± 2.9) ($P \leq 0.001$) (Fig. 3J). No differences in γH2AX expression in granulosa cells of secondary follicles were observed

Table I Total number of follicles in each treatment group, at Day 0 and after 6 days of culture. (a), (b), (c) and (d) denote a significant difference between treatment groups. A significantly greater proportion of primary and secondary follicles were observed in treatment groups compared to control ($P < 0.05$).

Group	Non-growing follicle n (%)	Primary follicle n (%)	Secondary follicle n (%)	Total
Day-0	7029 (79.6)[a]	1681 (19.0)[a]	123 (1.4)[a]	8833
Control	1896 (29.5)[b]	4129 (64.3)[b]	401 (6.2)[b]	6426
1 μM bpv(HOpic) } 6 days of culture	1400 (21.4)[c]	4513 (68.9)[c]	633 (9.7)[c]	6546
10 μM bpv(HOpic) } 6 days of culture	880 (11.4)[d]	6047 (78.1)[d]	818 (10.6)[c]	7745
		Total		**29,550**

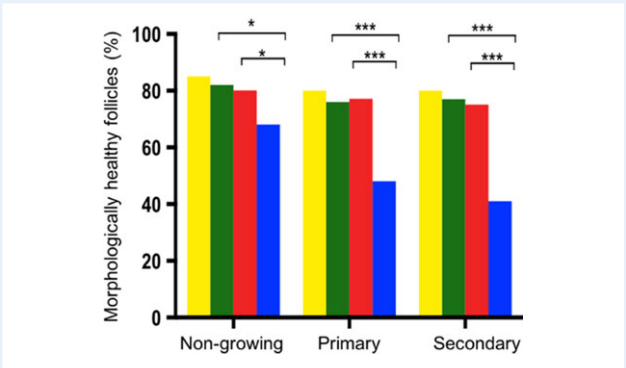

Figure 1 Proportion of morphologically healthy follicles at each stage of development. Day 0 (yellow), control medium (green), 1 μM bpv(HOpic) (red) and 10 μM bpv(HOpic) (blue). ***≤0.001, **≤0.01 and *≤0.05. The total number of follicles analysed for each stage and treatment is shown in Table I. Data here represent the proportion that were classified as healthy.

between D0 and control; however, significant increases were observed in both bpv(HOpic) treatment groups (1 μM: 76.9 ± 12.2, $P = 0.024$; 10 μM bpv[HOpic]: 77.8 ± 14.0, $P = 0.011$) compared to control (16.7 ± 16.7) (Fig. 3F–J). There was no significant difference between the two concentrations.

Expression of the DNA DSBs repair proteins MRE11 (Fig. 4A1–5) and ATM (Fig. 4B1–5) was observed in all stages of follicle development after 6 days of culture (Fig. 4A and B). MRE11 was decreased in oocytes in 1 μM (42%) and 10 μM bpv(HOpic) (47%) of primary follicles compared to control (68%) ($P < 0.001$) (Fig. 4 A6). Similarly, the expression of MRE11 in granulosa cells declined significantly in the presence of bpv(HOpic) in non-growing (1 μM: 41.2 ± 2.9%; 10 μM: 52.3 ± 3.9%) and primary follicles (1 μM: 56.2 ± 1.9%; 10 μM: 58.3 ± 2.5%), compared to control (non-growing: 75.9 ± 1.4% and primary follicles: 79.0 ± 1.8%) ($P < 0.05$ for all groups). No significant reduction was observed in secondary follicles with either dose (Fig. 4A7).

ATM, a regulator of the DNA repair downstream pathway, declined significantly in all types of follicles in bpv(HOpic) groups at Day 6 of culture. bpv(HOpic) reduced ATM expression in oocytes of primary follicles from 26% in 1 μM to 18% in 10 μM bpv(HOpic) ($P \leq 0.001$) (Fig. 4B6). In granulosa cells, ATM expression in bpv(HOpic) groups of non-growing and primary follicles was significantly lower compared to control ($P < 0.05$) (Fig. 4B7).

BRCA1, BRCA2 and RAD51 were localised within oocytes and granulosa cells (Fig. 5A–C). Analysis of 1315 follicles revealed that the proportion of BRCA1 positive oocytes of non-growing and primary follicles decreased significantly after 6 days of culture in control group (19 versus 13% and 22 versus 14% in non-growing and primary follicles, respectively) ($P < 0.05$) (Fig. 5A6). BRCA1 expression in all follicle types treated with 1 μM bpv(HOpic) did not change significantly compared to control ($P > 0.05$). However, there was very low expression of BRCA1 in all follicle groups treated with 10 μM bpv(HOpic) ($P < 0.001$) (Fig. 5A6). Similarly, low expression of BRCA1 was seen in granulosa cells of growing follicles treated with 10 μM bpv(HOpic) although granulosa cells of non-growing follicles showed a high level of expression (Fig. 5A7). BRCA2 expression in oocytes was markedly increased in 1 μM bpv(HOpic) in primary follicles (36%) compared to control (20%, $P = 0.010$) (Fig. 5B6). There was no significant difference in expression within granulosa cells among all the groups in primary and secondary follicles (Fig. 5B7).

In contrast, Rad51 expression in oocytes was significantly reduced in both bpv(HOpic) groups in primary follicles (control versus 1 and 10 μM bpv[HOpic]: 48 versus 34 versus 24%) ($P < 0.05$), without significant changes in secondary follicles (Fig. 5C6). Rad51 expression was observed infrequently (<10%) in granulosa cells, mainly in secondary follicles with no significant changes observed among the groups ($P > 0.05$) (Fig. 5C7).

Discussion

Consistent with our previous finding using human tissue (McLaughlin *et al.*, 2014), bovine ovarian tissue fragments exposed to 1 and 10 μM bpv(HOpic) for 24 h showed increased primordial follicle activation. The culture system used in this study supports significant primordial follicle activation in the control group: recent studies indicate that this is as a result of disrupting the Hippo signaling pathway during the preparation of the tissue (Kawamura *et al.*, 2013; Hsueh *et al.*, 2015). Hippo disruption increases expression of downstream growth factors but manipulation of the PI3K pathway results in further activation (Kawamura *et al.*, 2013; McLaughlin *et al.*, 2014; Hsueh *et al.*, 2015; Grosbois and Demeestere, 2018). PI3K pathway activation resulting from PTEN inhibition was confirmed by increased phosphorylated Akt expression and nuclear exclusion of FOXO3. However, a deleterious

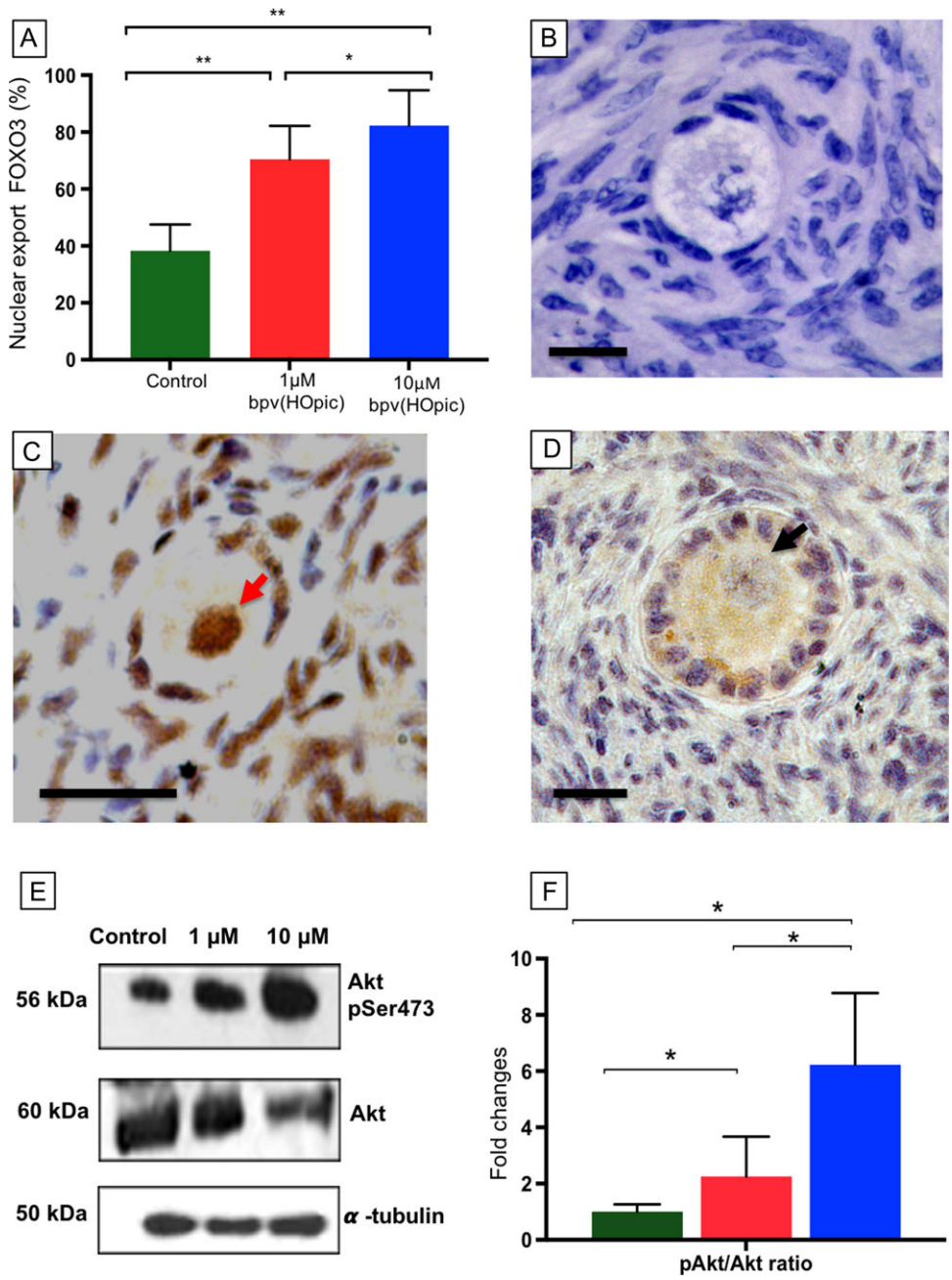

Figure 2 Expression of nuclear export of FOXO3 and ratio of phosphorylated Akt and Akt in control and bpv(HOpic) treated tissue. (**A**) Comparison of oocyte nuclear export of FOXO3 in control and bpv(HOpic) groups. Histogram shows mean percentage ± SEM (from three cultures per treatment with a minimum of 100 follicles analysed per group) of oocytes showing non-nuclear detection of FOXO3. **B**-**D**: Photomicrographs showing localisation of FOXO3 in bovine follicles. Negative control (B). Non-growing follicles with brown staining in the nucleus indicating inactivated FOXO3 (red arrow, C), nuclear export of FOXO3 from the nucleus of the activated primary follicles in bpv(HOpic) group indicated by brown staining in the ooplasm and negative staining in the nucleus (black arrow, D). Scale bar = 20 μm. (**E**) Western blot showing Akt and phosphorylated Akt (pAkt) expression in all groups. (**F**) pAkt/Akt ratio following 24 h exposure cultured control (green), 1 μM bpv(HOpic) (red), 10 μM bpv(HOpic) (blue). Lines represent significant differences between groups with a *P* value of ≤0.05 *.

effect on follicle morphological health was observed with the higher dose bpv(HOpic), in agreement with data from human ovary (Lerer-Serfaty *et al.*, 2013; McLaughlin *et al.*, 2014). The present data extend this by demonstrating that increased activation is associated with increased DNA damage and reduced DNA repair in ovarian follicles and, particularly, in oocytes.

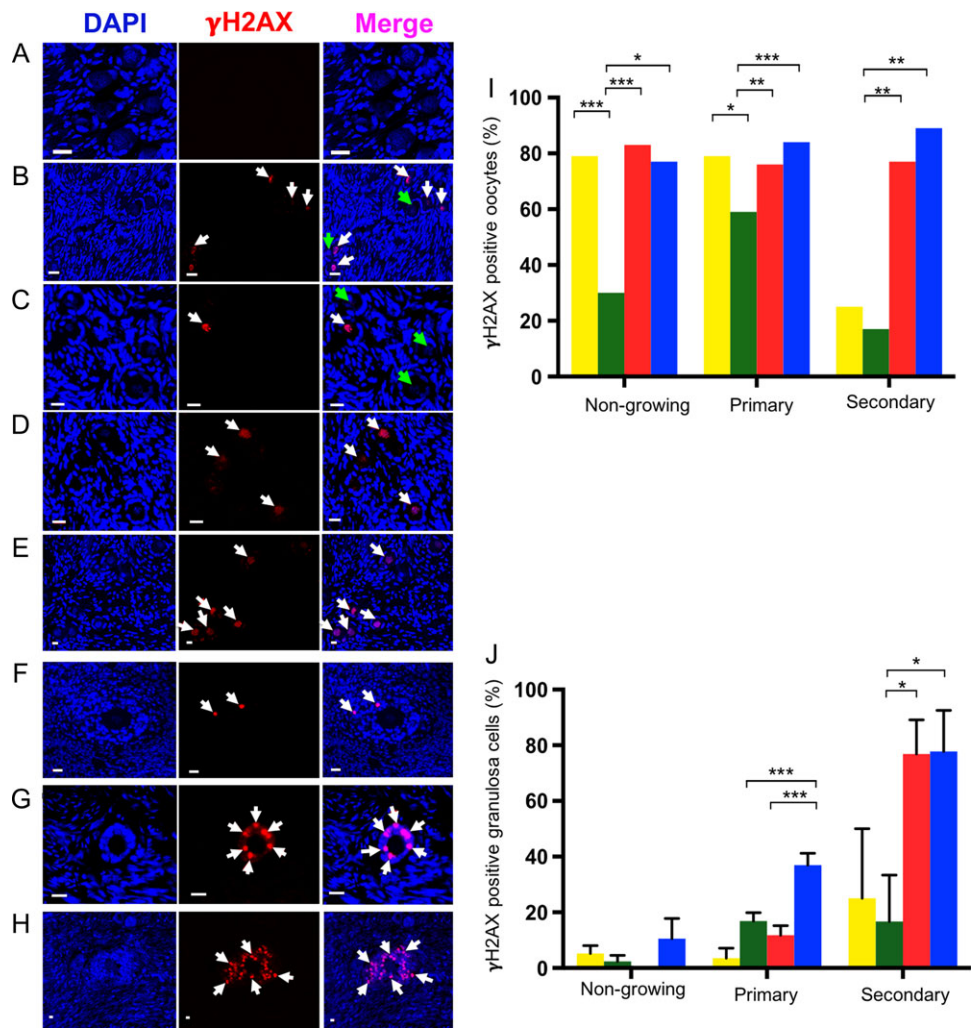

Figure 3 Representative images showing localisation by immunofluorescence of γH2AX bovine ovarian tissue in each treatment group. γH2AX (red) and DAPI (blue) staining in oocyte and granulosa cells (**A**–**H**). γH2AX staining appeared as bright points (foci) within nuclei (white arrows) in oocytes (A-E). The green arrows indicate areas where there is no γH2AX expression (B,C). Negative control (A), γH2AX positive and negative in the oocytes of day zero (D0) (B) positive and negative staining in cultured control (C); positive staining in 1 μM bpv(HOpic) (D) and 10 μM bpv(HOpic) (E). Localisation of γH2AX expression (white arrows) in granulosa cells (F–H) in control (F), 1 μM (G) and 10 μM bpv(HOpic) (H). Scale bar = 20 μm. Comparison of proportion of follicles showing γH2AX positive staining in the oocytes (**I**) and granulosa cells (**J**) of all groups. Analysis of 567 follicles from three independent experiments (I and J). The proportion of γH2AX positive oocytes per total number of follicles in each stage of follicle development (I); expression of γH2AX in granulosa cells (J), mean ± SEM. ***$P \leq 0.001$, **$P \leq 0.01$ and *$P \leq 0.05$. Yellow, D0; green, cultured control; red,1 μM bpv(HOpic) and blue, 10 μM bpv(HOpic).

The findings in this study support the view that the PTEN/Akt/PI3K pathway involves other intracellular pathways (Blanco-Aparicio *et al.*, 2007) that may have negative impacts on follicle growth. PTEN/PI3K/Akt activity impacts on DNA damage and repair (Hunt *et al.*, 2012; Ming and He, 2012) and has a central role in coordinating the apoptosis cascade activity (Weng *et al.*, 2001; Lu *et al.*, 2016). As DNA damage precedes the apoptotic process and can be present without any significant morphological changes, we investigated the effect of PTEN inhibition on DNA damage and DNA repair capacity of oocytes and granulosa cells. The bpv(HOpic) concentrations used in this study were low with a short-term incubation compared to other studies in human (Novella-Maestre *et al.*, 2015). However, these low concentrations clearly increased DNA damage and compromised DNA repair capacity of the follicles.

The DNA damage repair pathway involves γH2AX, and this binds specifically to the location of damage and controls recruitment of DNA repair proteins. Phosphorylation of γH2AX initiates the downstream pathway that leads to DNA repair or cell cycle arrest (Oktay *et al.*, 2015). We found that γH2AX expression was significantly higher in uncultured D0 tissue compared to control. However, the high γH2AX expression level in the D0 group was associated with increased expression of the DNA DSBs repair proteins MRE11, ATM

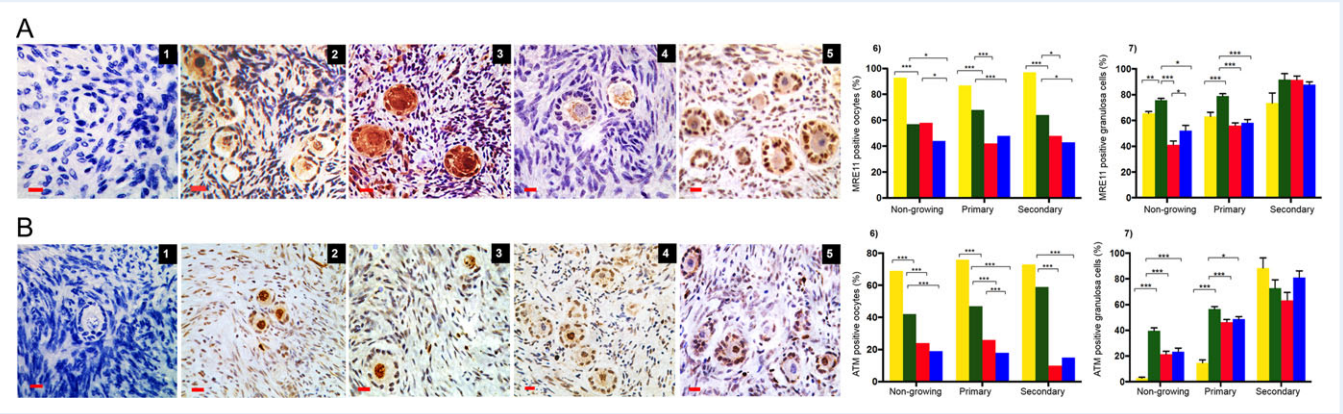

Figure 4 Immunohistochemical detection of MRE11 and ATM in oocytes and granulosa cells of follicles in all groups. Photomicrographs of MRE11 localisation (**A**1–5) and ATM (**B**1–5) expression in oocytes and granulosa cells. Negative control (1); positive staining (brown) in the oocytes and granulosa cells of day zero (D0; 2), control (3); 1 μM (4) and 10 μM bpv(HOpic) (5). Scale bar = 20 μm. The proportion of MRE11 and ATM in oocytes (A6, B6) and granulosa cells (A7, B7) shown as mean percentage ± SEM. Yellow bars, D0; green bars, cultured control; red bars, bpv(HOpic) 1 μM and blue bars, bpv(HOpic) 10 μM. Total number of follicles analysed: 4659 (MRE) and 5309 (ATM). ***≤0.001, **≤0.01, *≤0.05. *P* value was assigned at ≤0.05.

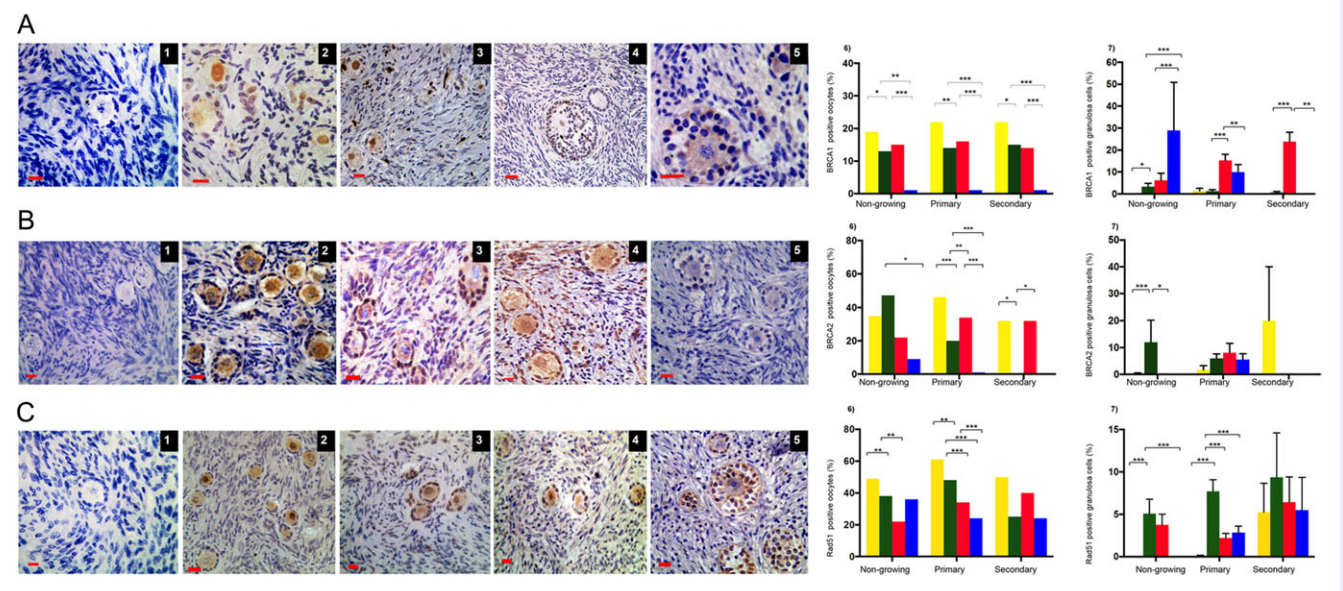

Figure 5 Immunohistochemical detection of BRCA1, BRCA2 and Rad51. Photomicrographs of BRCA1 (**A**1–5), BRCA2 (**B**1–5) and Rad51 (**C**1–5) expression in oocytes and granulosa cells. Negative control (A1, B1 and C1); positive staining (brown) in the oocytes and granulosa cells of day zero (D0; A2,B2,C2), control cultures (A3, B3 and C3); 1 μM (A4, B4 and C4) and 10 μM bpv(HOpic) (A5, B and B6). Scale bar = 20 μm. The proportion of oocytes (A6, B6 and C6) and granulosa cells (A7, B7 and C7) expressing BRCA1, BRCA2 and Rad51 in each treatment group (yellow bars, D0; green bars, cultured control; red bars, bpv(HOpic) 1 μM and blue bars, bpv(HOpic) 10 μM). Analysis of 1315 (BRCA1), 1134 (BRCA2) and 4148 (Rad51) follicles. ***≤0.001, **≤0.01, *≤0.05. *P* value was assigned at ≤0.05.

and Rad51 at all stages of follicle development. These breaks could reflect latent damage due to mild injury during tissue preparation and transport that appear to be rapidly resolved and may not cause serious consequences. This type of damage can be repaired directly without cell cycle arrest (Menezo *et al.*, 2010), as was indicated by the reduction in γH2AX expression following tissue culture and there being fewer morphologically unhealthy follicles in the cultured control tissue. All types of follicles in control cultures generated adequate DNA repair

capacity compared to treatment groups, which may reflect a culture medium with a nutrient-rich environment that is beneficial to cell metabolism (Paynter *et al.*, 1999).

DNA damage persisted or increased in the oocytes of both bpv (HOpic) treatment groups and was not associated with increasing DNA repair protein expression. In the DNA damage repair pathway, BRCA2 is indispensable in regulating the activity of Rad51. Increased BRCA2 expression in oocytes was consistent with the expression of Rad51 except in the higher dose of bpv(HOpic) of non-growing follicles wherein low level of BRCA2 did not affect Rad51 expression. In contrast, BRCA2 expression was high in 1 μM bpv(HOpic) exposed primary follicles but was not associated with increased Rad51 expression. This may indicate compromised homologous recombination. This finding may describe the association between Akt activation by bpv(HOpic) and defects in DNA damage repair protein interactions. Deficiencies in these interactions have previously been reported in human and mouse ovarian studies and associated with ageing (Titus *et al.*, 2013). DNA DSB repair capacity as reflected in BRCA1, BRCA2 and Rad51 was markedly reduced in oocytes exposed to the higher dose of bpv(HOpic). Activation of Akt has been shown to abolish the G2 cell cycle checkpoint by delaying nuclear translocation of BRCA1 during DNA DSB repair in a breast cancer cell line. This leads to deactivation of Chk1 following DNA damage process (Tonic *et al.*, 2010; Wu *et al.*, 2010). Although we did not quantitatively measure the intensity of DNA damage indicated by γH2AX expression in this study, our findings suggest that the DNA damage in the presence of bpV(HOpic) might be severe with limited repair, which may result in permanent cell cycle arrest.

Increased expression of γH2AX was observed in granulosa cells of growing follicles in the bpv(HOpic) treated groups. DNA DSB repair capacity of secondary follicles was not compromised in all groups, except BRCA1, which was apparently decreased with higher dose bpv (HOpic). Interestingly, the lower dose bpv(HOpic) did not affect expression of BRCA1 in all follicle types. Most of the follicles in higher dose bpv(HOpic) showed apoptosis after 6 days of culture. One possible explanation of these findings is that as actively dividing cells, such as granulosa cells, demonstrate a high metabolic activity and proliferation rate that will increase with the activation of Akt. In this context, granulosa cells of secondary follicles are more vulnerable to DNA induced damage. It seems likely that a decline in the capacity of DNA repair in granulosa cells happens more slowly than DNA damage, similar to the process that occurs with ageing (Zhang *et al.*, 2015). The proportion of morphologically normal follicles did not vary between 1 μM bpv(HOpic) and control group regardless of the presence of DNA damage and lack of DNA repair capacity. This may reflect a better response to DNA damage in low-dose compared to high-dose group but a study on human tissue has shown that the growth of apparently healthy preantral follicles isolated after treatment with 1 μM bpv(HOpic) was compromised after a further six days of culture (McLaughlin *et al.*, 2014). It has been reported that different factors affect the time period between the occurrence of DNA damage and apoptotic events (Xiao *et al.*, 2017). This study indicates that the dose of bpv(HOpic) could also affect this time frame.

It is worth considering the broader significance of these findings since PTEN inhibition has been used to activate primordial follicles in POI patients by activating follicles in tissue that is subsequently grafted back to patients (Suzuki *et al.*, 2015). The present data suggest that this strategy may be associated with increased DNA breaks and reduced DNA repair capacity. The impact of DNA damage on oocytes may range from meiotic dysfunction to cell death (Oktay *et al.*, 2015), possibly leading to reduced fertility (Kirk and Lyon, 1982; Meirow *et al.*, 2001; Menezo *et al.*, 2007; Adriaens *et al.*, 2009). More than 50% of oocytes with severe DNA DSBs can escape apoptosis and eventually achieve resumption of meiosis to the germinal vesicle breakdown stage in mice, but none of these oocytes develop to metaphase II (Lin *et al.*, 2014). This indicates that intact DNA DSB repair capacity in oocytes is pivotal to achieving mature and competent oocytes capable of fertilisation. This study is limited to primordial follicle activation and implications for later stages of follicle development have not been assessed. Impairment of human preantral follicle growth has been demonstrated after bpv(HOpic) treatment *in vitro* (McLaughlin *et al.*, 2014), but the implications for mature oocyte development are unexplored. We have recently demonstrated that a human *in vitro* growth (IVG) system (whose first stage is as used here) can support complete follicle development resulting in metaphase II oocytes (McLaughlin *et al.*, 2018). This methodology may be useful to provide additional insights into DNA damage and DNA repair of oocytes and granulosa cells, which may subsequently lead to improved IVG systems.

In summary, this study demonstrates that increasing activity of the PI3AKT pathway by a short exposure of bovine ovarian tissue fragments to bpV(HOpic) results in increased primordial follicle activation. However, this was accompanied by increased DNA damage and compromised DNA DSB repair capacity, in both oocytes and granulosa cells. These findings highlight the complexities and interactions between the regulation of initiation of follicle growth and the maintenance of follicle health and indicate the need for caution in developing pharmacological approaches to manipulation of this pathway for clinical use.

Acknowledgements

The authors thank John Binnie for collecting the bovine ovaries and Anisha Kubasik-Thayil of the IMPACT imaging facility (Centre for Discovery Brain Sciences, The University of Edinburgh) for assistance with image acquisition and analysis.

Authors' roles

M.M. contributed to the conception and design of study, experimental work and data acquisition, analysis and interpretation, and manuscript preparation. YLC contributed to the experimental work and data acquisition, analysis and interpretation, and final approval of manuscript. MMcL contributed to the conception and design of study, experimental work and data acquisition, analysis and interpretation, and final approval of manuscript. RAA contributed to the conception and design of study, data analysis and editing and final approval of manuscript. EET contributed to the conception and design of study, data analysis and editing and final approval of manuscript.

Funding

Funded by LPDP (Indonesia Endowment Fund for Education) as a scholarship to MM.

Conflict of interest

None relevant to this work.

References

Adriaens I, Smitz J, Jacquet P. The current knowledge on radiosensitivity of ovarian follicle development stages. *Hum Reprod Update* 2009;**15**: 359–377.

Altiok S, Batt D, Altiok N, Papautsky A, Downward J, Roberts TM, Avraham H. Heregulin induces phosphorylation of BRCA1 through phosphatidylinositol 3-Kinase/AKT in breast cancer cells. *J Biol Chem* 1999;**274**:32274–32278.

Blanco-Aparicio C, Renner O, Leal JF, Carnero A. PTEN, more than the AKT pathway. *Carcinogenesis* 2007;**28**:1379–1386.

Brunet A, Bonni A, Zigmond MJ, Lin MZ, Juo P, Hu LS, Anderson MJ, Arden KC, Blenis J, Greenberg ME. Akt promotes cell survival by phosphorylating and inhibiting a Forkhead transcription factor. *Cell* 1999;**96**: 857–868.

Bzymek M, Thayer NH, Oh SD, Kleckner N, Hunter N. Double Holliday junctions are intermediates of DNA break repair. *Nature* 2010;**464**: 937–941.

Carroll J, Marangos P. The DNA damage response in mammalian oocytes. *Front Genet* 2013;**4**:117.

Clarkson YL, McLaughlin M, Waterfall M, Dunlop CE, Skehel PA, Anderson RA, Telfer EE. Initial characterisation of adult human ovarian cell populations isolated by DDX4 expression and aldehyde dehydrogenase activity. *Sci Rep* 2018;**8**:6953.

Dupont J, Scaramuzzi RJ. Insulin signalling and glucose transport in the ovary and ovarian function during the ovarian cycle. *Biochem J* 2016;**473**: 1483–1501.

Fraser M, Zhao H, Luoto KR, Lundin C, Coackley C, Chan N, Joshua AM, Bismar TA, Evans A, Helleday T *et al*. PTEN deletion in prostate cancer cells does not associate with loss of RAD51 function: implications for radiotherapy and chemotherapy. *Clin Cancer Res* 2012;**18**:1015–1027.

Golding SE, Morgan RN, Adams BR, Hawkins AJ, Povirk LF, Valerie K. Pro-survival AKT and ERK signaling from EGFR and mutant EGFRvIII enhances DNA double-strand break repair in human glioma cells. *Cancer Biol Ther* 2009;**8**:730–738.

Grosbois J, Demeestere I. Dynamics of PI3K and Hippo signaling pathways during in vitro human follicle activation. *Hum Reprod* 2018;**33**: 1705–1714.

Hsueh AJ, Kawamura K, Cheng Y, Fauser BC. Intraovarian control of early folliculogenesis. *Endocr Rev* 2015;**36**:1–24.

Hunt CR, Gupta A, Horikoshi N, Pandita TK. Does PTEN loss impair DNA double-strand break repair by homologous recombination? *Clin Cancer Res* 2012;**18**:920–922.

Jackson SP, Bartek J. The DNA-damage response in human biology and disease. *Nature* 2009;**461**:1071–1078.

Jagarlamudi K, Liu L, Adhikari D, Reddy P, Idahl A, Ottander U, Lundin E, Liu K. Oocyte-specific deletion of Pten in mice reveals a stage-specific function of PTEN/PI3K signaling in oocytes in controlling follicular activation. *PLoS One* 2009;**4**:e6186.

Jia Y, Song W, Zhang F, Yan J, Yang Q. Akt1 inhibits homologous recombination in Brca1-deficient cells by blocking the Chk1-Rad51 pathway. *Oncogene* 2013;**32**:1943–1949.

Kao GD, Jiang Z, Fernandes AM, Gupta AK, Maity A. Inhibition of phosphatidylinositol-3-OH kinase/Akt signaling impairs DNA repair in glioblastoma cells following ionizing radiation. *J Biol Chem* 2007;**282**: 21206–21212.

Kawamura K, Cheng Y, Suzuki N, Deguchi M, Sato Y, Takae S, Ho CH, Kawamura N, Tamura M, Hashimoto S *et al*. Hippo signaling disruption and Akt stimulation of ovarian follicles for infertility treatment. *Proc Natl Acad Sci U S A* 2013;**110**:17474–17479.

Khanna KK, Jackson SP. DNA double-strand breaks: signaling, repair and the cancer connection. *Nat Genet* 2001;**27**:247–254.

Kirk M, Lyon MF. Induction of congenital anomalies in offspring of female mice exposed to varying doses of X-rays. *Mutat Res* 1982;**106**:73–83.

Lerer-Serfaty G, Samara N, Fisch B, Shachar M, Kossover O, Seliktar D, Ben-Haroush A, Abir R. Attempted application of bioengineered/biosynthetic supporting matrices with phosphatidylinositol-trisphosphate-enhancing substances to organ culture of human primordial follicles. *J Assist Reprod Genet* 2013;**30**:1279–1288.

Lin F, Ma XS, Wang ZB, Wang ZW, Luo YB, Huang L, Jiang ZZ, Hu MW, Schatten H, Sun QY. Different fates of oocytes with DNA double-strand breaks in vitro and in vivo. *Cell Cycle* 2014;**13**:2674–2680.

Liu K, Rajareddy S, Liu L, Jagarlamudi K, Boman K, Selstam G, Reddy P. Control of mammalian oocyte growth and early follicular development by the oocyte PI3 kinase pathway: new roles for an old timer. *Dev Biol* 2006;**299**:1–11.

Lu XX, Cao LY, Chen X, Xiao J, Zou Y, Chen Q. PTEN inhibits cell proliferation, promotes cell apoptosis, and induces cell cycle arrest via down-regulating the PI3K/AKT/hTERT pathway in lung adenocarcinoma A549 cells. *Biomed Res Int* 2016;**2016**:2476842.

McLaughlin M, Albertini DF, Wallace WHB, Anderson RA, Telfer EE. Metaphase II oocytes from human unilaminar follicles grown in a multi-step culture system. *Mol Hum Reprod* 2018;**24**:135–142.

McLaughlin M, Kinnell HL, Anderson RA, Telfer EE. Inhibition of phosphatase and tensin homologue (PTEN) in human ovary in vitro results in increased activation of primordial follicles but compromises development of growing follicles. *Mol Hum Reprod* 2014;**20**:736–744.

McLaughlin M, Telfer EE. Oocyte development in bovine primordial follicles is promoted by activin and FSH within a two-step serum-free culture system. *Reproduction* 2010;**139**:971–978.

Meirow D, Epstein M, Lewis H, Nugent D, Gosden RG. Administration of cyclophosphamide at different stages of follicular maturation in mice: effects on reproductive performance and fetal malformations. *Hum Reprod* 2001;**16**:632–637.

Menezo Y, Dale B, Cohen M. DNA damage and repair in human oocytes and embryos: a review. *Zygote* 2010;**18**:357–365.

Menezo Y Jr., Russo G, Tosti E, El Mouatassim S, Benkhalifa M. Expression profile of genes coding for DNA repair in human oocytes using pangenomic microarrays, with a special focus on ROS linked decays. *J Assist Reprod Genet* 2007;**24**:513–520.

Ming M, He YY. PTEN in DNA damage repair. *Cancer Lett* 2012;**319**: 125–129.

Novella-Maestre E, Herraiz S, Rodriguez-Iglesias B, Diaz-Garcia C, Pellicer A. Short-term PTEN inhibition improves in vitro activation of primordial follicles, preserves follicular viability, and restores amh levels in cryopreserved ovarian tissue from cancer patients. *PLoS One* 2015;**10**: e0127786.

Oktay K, Turan V, Titus S, Stobezki R, Liu L. BRCA mutations, DNA repair deficiency, and ovarian aging. *Biol Reprod* 2015;**93**:67.

Paynter SJ, Cooper A, Fuller BJ, Shaw RW. Cryopreservation of bovine ovarian tissue: structural normality of follicles after thawing and culture in vitro. *Cryobiology* 1999;**38**:301–309.

Pedersen T, Peters H. Proposal for a classification of oocytes and follicles in the mouse ovary. *J Reprod Fertil* 1968;**17**:555–557.

Plo I, Laulier C, Gauthier L, Lebrun F, Calvo F, Lopez BS. AKT1 inhibits homologous recombination by inducing cytoplasmic retention of BRCA1 and RAD51. *Cancer Res* 2008;**68**:9404–9412.

Puc J, Parsons R. PTEN loss inhibits CHK1 to cause double stranded-DNA breaks in cells. *Cell Cycle* 2005;**4**:927–929.

Reddy P, Liu L, Adhikari D, Jagarlamudi K, Rajareddy S, Shen Y, Du C, Tang W, Hamalainen T, Peng SL *et al*. Oocyte-specific deletion of Pten causes premature activation of the primordial follicle pool. *Science* 2008; **319**:611–613.

Shen WH, Balajee AS, Wang J, Wu H, Eng C, Pandolfi PP, Yin Y. Essential role for nuclear PTEN in maintaining chromosomal integrity. *Cell* 2007; **128**:157–170.

Sobinoff AP, Nixon B, Roman SD, McLaughlin EA. Staying alive: PI3K pathway promotes primordial follicle activation and survival in response to 3MC-induced ovotoxicity. *Toxicol Sci* 2012;**128**:258–271.

Suzuki N, Yoshioka N, Takae S, Sugishita Y, Tamura M, Hashimoto S, Morimoto Y, Kawamura K. Successful fertility preservation following ovarian tissue vitrification in patients with primary ovarian insufficiency. *Hum Reprod* 2015;**30**:608–615.

Telfer EE, McLaughlin M, Ding C, Thong KJ. A two-step serum-free culture system supports development of human oocytes from primordial follicles in the presence of activin. *Hum Reprod* 2008;**23**:1151–1158.

Thacker J. The RAD51 gene family, genetic instability and cancer. *Cancer Lett* 2005;**219**:125–135.

Titus S, Li F, Stobezki R, Akula K, Unsal E, Jeong K, Dickler M, Robson M, Moy F, Goswami S *et al*. Impairment of BRCA1-related DNA double-strand break repair leads to ovarian aging in mice and humans. *Sci Transl Med* 2013;**5**:172ra121.

Tonic I, Yu WN, Park Y, Chen CC, Hay N. Akt activation emulates Chk1 inhibition and Bcl2 overexpression and abrogates G2 cell cycle checkpoint by inhibiting BRCA1 foci. *J Biol Chem* 2010;**285**:23790–23798.

Torgovnick A, Schumacher B. DNA repair mechanisms in cancer development and therapy. *Front Genet* 2015;**6**:157.

van Wezel IL, Rodgers RJ. Morphological characterization of bovine primordial follicles and their environment in vivo. *Biol Reprod* 1996;**55**: 1003–1011.

Weng L, Brown J, Eng C. PTEN induces apoptosis and cell cycle arrest through phosphoinositol-3-kinase/Akt-dependent and -independent pathways. *Hum Mol Genet* 2001;**10**:237–242.

Winship AL, Stringer JM, Liew SH, Hutt KJ. The importance of DNA repair for maintaining oocyte quality in response to anti-cancer treatments, environmental toxins and maternal ageing. *Hum Reprod Update* 2018;**24**:119–134.

Wu J, Lu LY, Yu X. The role of BRCA1 in DNA damage response. *Protein Cell* 2010;**1**:117–123.

Xiao S, Zhang J, Liu M, Iwahata H, Rogers HB, Woodruff TK. Doxorubicin has dose-dependent toxicity on mouse ovarian follicle development, hormone secretion, and oocyte maturation. *Toxicol Sci* 2017;**157**: 320–329.

Xu N, Hegarat N, Black EJ, Scott MT, Hochegger H, Gillespie DA. Akt/PKB suppresses DNA damage processing and checkpoint activation in late G2. *J Cell Biol* 2010;**190**:297–305.

Zhang D, Zhang X, Zeng M, Yuan J, Liu M, Yin Y, Wu X, Keefe DL, Liu L. Increased DNA damage and repair deficiency in granulosa cells are associated with ovarian aging in rhesus monkey. *J Assist Reprod Genet* 2015; **32**:1069–1078.

Zhou L, Xie Y, Li S, Liang Y, Qiu Q, Lin H, Zhang Q. Rapamycin prevents cyclophosphamide-induced over-activation of primordial follicle pool through PI3K/Akt/mTOR signaling pathway in vivo. *J Ovarian Res* 2017; **10**:56.

cells

MDPI

Review

Crosstalk between PTEN/PI3K/Akt Signalling and DNA Damage in the Oocyte: Implications for Primordial Follicle Activation, Oocyte Quality and Ageing

Mila Maidarti [1,2,3], Richard A. Anderson [1] and Evelyn E. Telfer [2,*]

1 MRC Centre for Reproductive Health, Queens Medical Research Institute, University of Edinburgh, Edinburgh EH16 4TJ, UK; mila.maidarti@ed.ac.uk (M.M.); richard.anderson@ed.ac.uk (R.A.A.)
2 Institute of Cell Biology, University of Edinburgh, Edinburgh EH9 3FF, UK
3 Obstetrics and Gynaecology Department, Faculty of Medicine, Universitas Indonesia, Jakarta 10430, Indonesia
* Correspondence: evelyn.telfer@ed.ac.uk; Tel.: +44-(0)131-650-5393

Received: 31 October 2019; Accepted: 13 January 2020; Published: 14 January 2020

Abstract: The preservation of genome integrity in the mammalian female germline from primordial follicle arrest to activation of growth to oocyte maturation is fundamental to ensure reproductive success. As oocytes are formed before birth and may remain dormant for many years, it is essential that defence mechanisms are monitored and well maintained. The phosphatase and tensin homolog of chromosome 10 (PTEN)/phosphatidylinositol 3-kinase (PI3K)/protein kinase B (PKB, Akt) is a major signalling pathway governing primordial follicle recruitment and growth. This pathway also contributes to cell growth, survival and metabolism, and to the maintenance of genomic integrity. Accelerated primordial follicle activation through this pathway may result in a compromised DNA damage response (DDR). Additionally, the distinct DDR mechanisms in oocytes may become less efficient with ageing. This review considers DNA damage surveillance mechanisms and their links to the PTEN/PI3K/Akt signalling pathway, impacting on the DDR during growth activation of primordial follicles, and in ovarian ageing. Targeting DDR mechanisms within oocytes may be of value in developing techniques to protect ovaries against chemotherapy and in advancing clinical approaches to regulate primordial follicle activation.

Keywords: PTEN/PI3K/Akt; follicle activation; DNA damage response (DDR); ageing

1. Introduction

In mammalian females, oocytes are formed before birth and are surrounded by somatic cells (granulosa cells) to form structures known as follicles. Oocytes have entered meiosis and are arrested at the dictyate stage of prophase I with the most immature stage (primordial follicles) forming the store of female germ cells that will be utilised throughout reproductive life (reviewed in [1]). The pool of primordial follicles is progressively reduced with age leading to reproductive senescence [2–4]. Follicles are gradually lost from the pool either through death or by activation of the growth pathway. Therefore the rates of activation and degeneration determine the size of the pool and the time to onset of menopause [5]. Once follicles are recruited into the growing pool, pre-granulosa cells differentiate to form a single layer of cuboidal cells surrounding the oocyte. In parallel, the oocyte increases in size and undergoes further growth and maturation whilst still being maintained in meiotic arrest. These processes are referred to as primordial follicle activation [6]. Primordial follicles may be quiescent for many years and in humans for several decades, highlighting the importance of potential DNA

damage accumulation [7] that may threaten genomic integrity. In this context, a robust surveillance mechanism is essential to ensure that oocytes with DNA damage have it repaired or are eliminated with prevention of further growth and development [8,9], thus maintaining the quality of oocyte and any resulting embryo throughout the reproductive lifespan [10].

The phosphatase and tensin homolog of chromosome 10 (PTEN)/phosphatidylinositol 3-kinase (PI3K)/protein kinase B (PKB, Akt) pathway is one of the major non-gonadotropic insulin signalling pathways that coordinates the activation, growth and differentiation of follicles [6,11]. The pathway functions to control a myriad of cellular functions involving cell metabolism, proliferation and survival [12,13]. There is evidence to support the existence of crosstalk between the PI3K/Akt signalling pathway and the DNA damage response (DDR) in cells [14–16], indicating the importance of the consequences of interference with one of these pathways on the other. High PI3K/Akt activity is linked to a decline in the number of primordial follicles and ovarian ageing [17,18]. Ovarian ageing is associated with impaired DDR within oocytes [19–22] and this can also be induced following exposure to DNA damaging agents [23–28]. Nevertheless, taking advantage of PI3K/Akt signalling pathway effects on follicular recruitment, PTEN inhibition, as a central negative regulator of the pathway, has been widely used to activate primordial follicles in a range of species [18,29–33]. Most importantly, pregnancies have been achieved in women following transplantation of small fragments of ovarian cortex after exposure to pharmacological inhibitors of PTEN [34]. Recent studies suggest that activation of follicles by these methods may be damaging to subsequent growth and survival of follicles [35–37], indicating that further investigation is required to fully understand the impact and implications of follicle activation using pharmacological manipulation of this pathway.

A great deal of evidence, discussed below, suggests that the PI3K/PTEN/Akt pathway is essential in regulating cell-cycle checkpoint initiation and DNA repair and that the lack of PTEN in cells may cause genomic instability [38,39]. The ability to respond to such damage is crucial to ensure primordial follicle survival and to support the production of mature oocytes with a minimised risk of meiotic abnormalities against the adverse effects of age (reviewed in [40]) and ultimately to maintain reproductive lifespan. Surveillance mechanisms within oocytes to ameliorate DNA damage are essential as, during reproductive life, oocytes (and granulosa cells) can be subjected to DNA damage: this mainly occurs in the long-lived primordial follicles as a consequence of external and internal insults [21]. DNA double strand-breaks (DSBs) do not occur as frequently as other lesions, but persistent unrepaired DNA DSBs are the most severe type of damage and may lead to genomic instability [21,41–43].

In this review, we will limit the discussion to the DNA damage/DSBs repair pathway, and primarily focus on the mechanisms used by oocytes within primordial follicles to protect themselves against DNA damage throughout their lifespan. The DDR mechanism in granulosa cells will be discussed where relevant. Crosstalk between the PI3K/PTEN/Akt pathway and DDR has been linked to increased DNA damage and impaired DNA repair protein interactions in ovarian follicles activated in vitro [29]. Such findings will be important in elucidating the impact of pharmacological activation of primordial follicles by manipulation of the PI3K/PTEN/Akt pathway and its impact on DDR.

2. Methods

Published articles including original research, peer-reviewed and reviews were searched systematically in PubMed (Medline) database using specific terms such as ‘DNA damage’, ‘oocytes’, ‘primordial follicle activation’, ‘PI3K/Akt’, ‘ovarian ageing’ and ‘chemotherapy’. Abstracts and conferences proceeding were not included. The search yielded 757 relevant references of English language literature. Article selection was conducted using Preferred Reporting Items for Systematic Reviews and Meta-Analyses (PRISMA) guidelines [44]. The references in these articles were searched manually to retrieve additional articles, and an additional 19 articles were included. These were then screened for duplication, to ensure only articles related to DNA damage repair mechanism in primordial follicles were included. Only original research articles meeting the following eligibility criteria were included in the final search results: original research articles published from 1990 to 2019,

full articles available, articles in English and not symposia proceeding. Manuscripts were selected concerning primordial follicle activation in association with PI3K signalling pathway, ovarian ageing and DDR in oocytes of immature follicles. A total of 52 published full-text articles were included after cross-referencing, and 40 articles were analysed qualitatively (Figure 1).

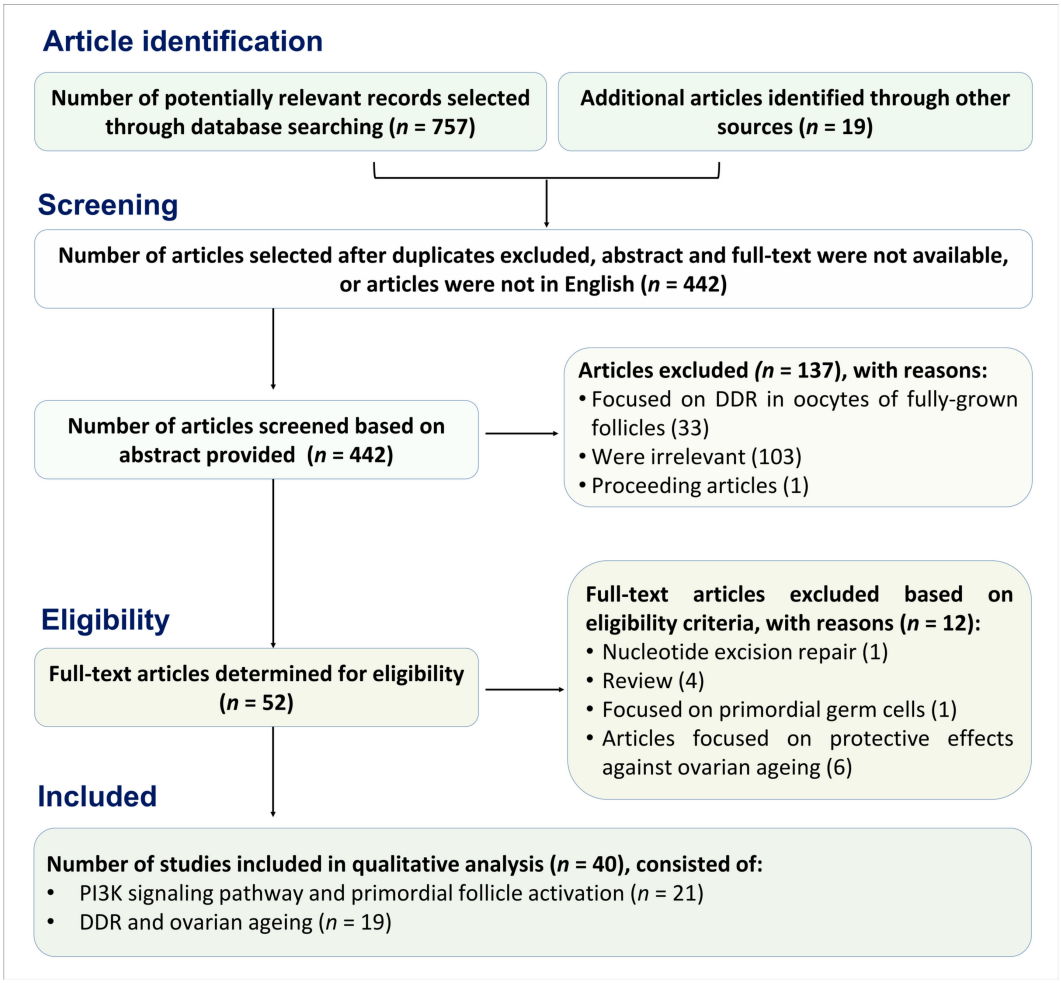

Figure 1. Flow chart following Preferred Reporting Items for Systematic Reviews and Meta-Analyses (PRISMA) guidelines to determine the study included into qualitative analysis.

3. DNA Damage Repair Pathway within Primordial Follicles

The DNA of a cell is continuously threatened by various types of damage that may cause a reduction in cellular function, cell cycle progression and DNA repair [45]. Exogenous sources of DNA damage include environmental agents such as ultraviolet, radiation and chemotherapeutic drugs [24]. Reactive oxygen species (ROS) are also an endogenous source of damage within somatic cells [46] and oocytes [20,47]. DNA damage constitutes a significant issue in non-dividing or slowly dividing cells as a large amount of DNA damage may accumulate over time. Any damage that does not cause cell cycle arrest will tend to induce replication errors leading to mutations [20]. However, all cells are endowed with the capacity to ameliorate the threats to DNA, which occurs mainly at the G1/S and G2/M-phase transition. Cells with DNA damage respond in various ways to activate an appropriate DDR pathway. A mild injury may not result in serious consequences as it can be repaired directly without cell cycle arrest. While severe DNA damage may result in cell cycle arrest, allowing sufficient time to repair DNA damage. During this time, a sequence of DDR proteins is activated and the cell's fate depends on its capacity to repair the damage [48].

DNA DSBs can be repaired by two main mechanisms: non-homologous end-joining (NHEJ) [49], and homologous recombination (HR) [20,50]. NHEJ is error-prone since it mediates the direct re-ligation of the two ends of broken DNA and is not based on a complementary DNA template. Given its error-prone nature, NHEJ is commonly accompanied by deletion or insertion of base pairs [51,52]. NHEJ primarily occurs at the G0/G1 phase [53] and can be independent of the cell cycle [54]. NHEJ is the most common type of DNA damage repair in mitotic cells. In contrast, HR is largely error-free and is functionally dominant at S and G2/M phases of the cell cycle when sister chromatids are available as a template for accurate DNA repair [55]. In this context, HR is the primary mode of DNA DSBs repair in meiotic cells. Both pathways are evident and can be functionally active in mammalian oocytes [56,57], although HR predominates in oocytes at all stages of development [10,48,58–62]. Given that primordial follicles are arrested at G2/M and accurate repair is a prerequisite to conserve genetic information [63], HR appears to be the pathway of choice for oocytes within primordial (immature) follicles [10,48,58,59]. While NHEJ can occur in the late stage of oocyte development [49,60,64].

HR requires the recognition of the DNA DSBs by the meiotic recombination 11 (MRE11)-Rad50-nijmegen breakage syndrome 1 (NBS1) (MRN) complex. The binding of MRN complex to DSB free ends allows the NBS1 protein to interact with ataxia telangiectasia mutated (ATM) dimers leading to autophosphorylation of ATM at a serine residue (367, 1893 and 1981) [65]. Detection of DNA damage attracts ATM kinase to the DNA DSB sites, through direct interaction between ATM and the C-terminal region of NBS1 [66]. It has been reported that ovaries from MRE11 mutant mice showed a marked increase in unrepaired DSBs, with primordial follicle loss and infertility although the number of mature follicles did not differ between wild type and mutant mice [67]. However, meiotic progression in mutant mice was delayed with only 5% of oocytes being able to complete synapsis [67], suggesting a key role of MRE11 in oocyte DDR.

ATM in turn phosphorylates a specific histone protein, H2AX, at the C-terminal serine 139 to generate γH2AX, which binds specifically to the DNA damage sites and controls the recruitment of DNA repair proteins. The critical role of ATM in DDR is demonstrated by a study using mouse ovaries in culture exposed to phosphoramide mustard (PM), a metabolite of cyclophosphamide (CP). Increased γH2AX in oocytes occurred 24 h after exposure and consequently induced substantial follicle loss. Interestingly, the administration of the ATM inhibitor KU55933, reduced the adverse impact of PM on follicle depletion, emphasising the importance of ATM in the DDR [68]. Phosphorylation of γH2AX initiates a downstream pathway resulting in DNA repair or cell cycle arrest (reviewed in [20]). γH2AX is extensively phosphorylated from minutes to hours following the detection of DNA breaks, quantitatively reflecting the severity of the damage [69–71]. Mediator DNA damage checkpoint protein (MDC1) is then activated and bound to γH2AX, mediated by breast cancer susceptibility gene 1 (*BRCA1*; Figure 2A). MDC1 forms foci that co-localise with γH2AX within minutes after the damage occurs and provides positive feedback, recruiting additional MRN complexes and thus leading to propagation of γH2AX at sites of DNA breaks [72].

Phosphorylation of ATM is the first step in the initiation of G2 checkpoint activation in the DNA damage repair pathway [73]. Activation of ATM upregulates downstream pathways leading to effective DNA repair through HR/NHEJ (HR in oocytes of primordial follicle, Figure 2A), initiation of checkpoint kinase 2 (Chk2, Figure 2A) or apoptosis (through activation of TAp63α, Figure 2B,C, and discussed in detail below) [20,74]. Activation of HR generates single-strand DNA (ssDNA) at multiple steps and requires a specific factor, replication protein A (RPA). In oocytes, the ssDNA binding protein complex RPA is replaced by Rad51 and meiotic cDNA1 (Dmc1). BRCA2 mediates the interaction between Rad51, Dmc1 and ssDNA to form the meiotic presynaptic nucleofilament, resulting in the initiation of HR (Figure 2A). Dmc1 deficiency in mouse oocytes leads to synapsis failure, which is HR-dependent and ultimately reduces follicle survival [75].

The role of Rad51 is of paramount importance in the final step of HR and in preventing oocyte death, as is evident from studies in mouse and bovine [48,62,76]. Inhibition of Rad51 prior to irradiation

exposure increases damage to DNA, whereas enhancing Rad51 expression by injecting recombinant Rad51 is sufficient to prevent DNA damage [48,76].

In the presence of DSBs, Chk2 activation delays the cell cycle transiently to provide sufficient time for DNA repair [77]. DNA damage checkpoints are primarily expressed when oocytes are in meiotic arrest. Their expression persists at this stage leading to increased sensitivity of oocytes in primordial follicles to DNA damage-inducing agents [75]. Activation of Chk2 simultaneously inhibits cell division cycle (Cdc) phosphatases including Cdc25a, Cdc25b and Cdc25c. This in turn activates cyclin-dependent kinase (Cdk) and consequently blocks the cell cycle progressing from G1 to S and G2/M phase (reviewed in [50]). The activation of p53 family members is another downstream target of ATM and functions to maintain checkpoint activation at G1/S of the cell cycle [53,78]. Inhibition of ATM in mouse oocytes exposed to irradiation results in a failure to activate p63, which then blocks the apoptosis pathway and prevents oocyte death [79].

4. A Unique p63 Pathway Links DNA Damage and Apoptosis in Oocytes within Primordial Follicles

In conditions resulting in severe DNA damage or with ineffective DNA repair, DNA DSBs accumulation is more likely to initiate the activity of p53 family members. This process is critical to abolish oocytes with unrepaired DNA damage and safeguard against germline mutations. The apoptosis process of oocytes within primordial follicles is mediated by a distinct cell surveillance mechanism involving N-terminal transactivation domain p63 (TAp63α) [24,80–82], a p53 family member [83]. TAp63α functions to respond to DNA damage primarily after prophase 1 of meiosis and is constitutively active only in female germ cells once DNA breaks occur [81]. The essential role of TAp63α in the apoptosis process makes it an essential regulator in follicle loss during chemotherapy, which may result in a reduced primordial follicular pool. Oocytes in the quiescent state demonstrate a high TAp63α expression. Wild-type mice exposed to radiation show primordial follicle loss (without loss of growing preantral follicles), whilst TAp63-deficient mice are insensitive to irradiation-induced apoptosis, confirming the indispensable role of TAp63α in the DDR of the oocyte within primordial follicles [80].

The *p63* gene encodes two major isoforms of TAp63, one with the transactivation (TA) domain and the other, ΔN-p63 (N-terminal truncated), lacking the TA domain [84]. TAp63α is the main p63 isoform expressed in the nuclei of oocytes within primordial follicles [80,81,83]. TAp63α is maintained in inactive dimeric form by the transcriptional inhibitory domain (TID) and further stabilised by the interaction of N-terminal transactivation (TAD) with TID and the oligomerization domain. In the dimeric state, the transactivation of TAp63α is suppressed by decreasing its DNA binding affinity and repressing the activity of the domain responsible for the transcriptional process [85]. Exposure to genotoxic agents such as radiation trigger a conformation change in TAp63α to its active tetrameric state, which in turn increases its DNA binding affinity and may ultimately cause apoptosis [85–87] and elimination of damaged oocytes (Figure 2C). The presence of TAp63α in oocytes of immature follicles highlights the need for adequate surveillance mechanism to ensure only oocytes with complete DNA damage repair are recruited to ovulation [80,81,84].

Mouse oocytes within primordial follicles also express all necessary kinases required to trigger p63 activation. Once DNA damage ensues, it may activate p63 directly, resulting in enhanced oocyte sensitivity to DNA damage compared to granulosa cells [88]. This vulnerability of oocytes to DNA damage is confirmed by a study using a low dose irradiation treatment in mice that is sufficient to induce oocyte death while the surrounding cells of the ovaries are not affected [79]. TAp63α is also expressed in oocytes within primary and preantral follicles, but expression is downregulated with oocyte growth [80,81], resulting in growing oocytes being less sensitive to DNA damage. The sensitivity to DNA damage diminishes once follicles reach the antral stage owing to complete loss of TAp63α expression at this stage [88].

TAp63 activation in oocytes within primordial follicles requires consecutive phosphorylation by Chk2 at serine 582 [89]. TAp63α is not phosphorylated in Chk2 deficient mice following exposure to irradiation [75] with ineffective oocyte elimination, whereas the entire primordial follicle pool

in wild type mouse ovary is eradicated [75]. Transcriptional activation of BH3-only pro-apoptotic BCL-2 family members PUMA (p53 upregulated modulator of apoptosis) and NOXA [24] are critical downstream targets of oocytes apoptosis mediated by TAp63 [82]. PUMA and NOXA trigger apoptosis by binding and suppressing the pro-survival B-cell lymphoma 2 (Bcl2) activity, an anti-apoptotic protein implicated in repairing mitochondrial permeability. PUMA and NOXA binding to Bcl-2 unleashes the pro-apoptotic protein B-cell lymphoma (Bcl)-associated X (BAX), precipitating an imbalance between BAX and Bcl2, which then activates apoptosis [90] (Figure 2B). It has been reported that oocytes of PUMA and NOXA deficient mice are not affected by γ-irradiation and are capable of producing healthy offspring [24]. Primordial follicle loss is also much reduced in PUMA knockout mice treated with CP and cisplatin [26]. Alternatively, upregulation of p53 elicits p21 transcription that directly prevents Cdk2 and Cdk4 transcription and eventually induces cycle arrest (reviewed in [50,91]), thus allowing DNA repair [90].

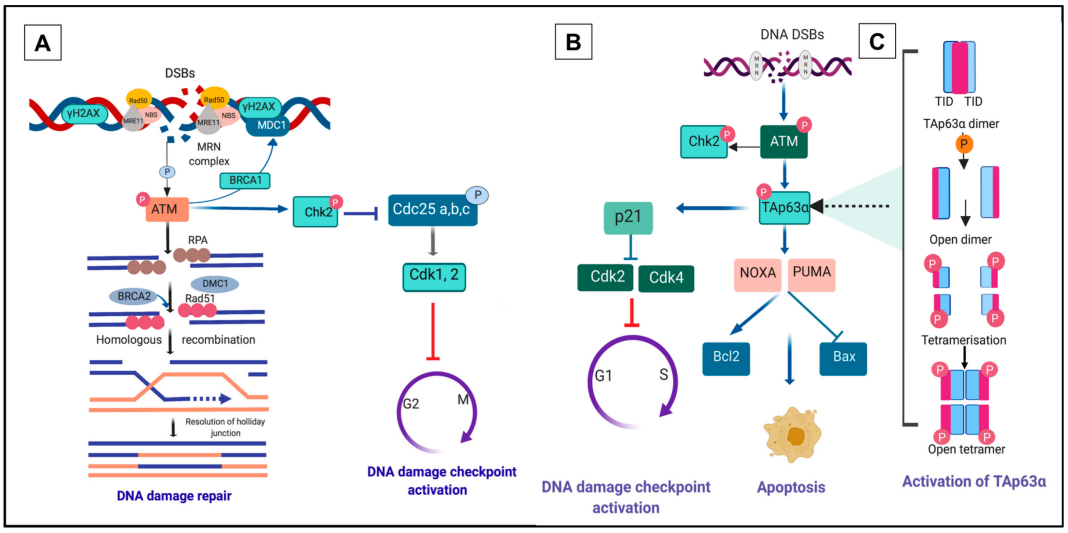

Figure 2. DNA double-strand breaks (DSBs) response pathway. (**A**) Homologous recombination (HR) repair pathway to combat DNA DSBs. Detection and recognition of DNA DSBs by the meiotic recombination 11-Rad50-nijmegen breakage syndrome 1 (MRN) complex (MRE11-RAD50-NBS1) triggers phosphorylation of ataxia telangiectasia mutated (ATM). Activation of ATM results in the phosphorylation of several DNA damage response (DDR) kinases such as histone protein, H2A variant, H2AX, at Serine 139 to generate γH2AX, checkpoint kinase 2 (Chk2) and p53 (TAp63α in primordial oocytes), mediating the effects of ATM on DNA damage repair, cell-cycle arrest and apoptosis. p63 induces cell-cycle arrest by activating the transcription of p21, which may hinder cell cycle progression through inhibition of cyclin-dependent kinase 2 (Cdk2) and Cdk 4 activity. Mediator DNA damage checkpoint protein 1 (MDC1) binds to γH2AX via breast cancer susceptibility gene 1 (*BRCA1*) and forms foci that co-localise with γH2AX. In oocytes, the DNA strand resection is activated and leads to homologous recombination (HR). Activation of HR generates single-strand DNA (ssDNA) at multiple steps and requires a specific factor, replication protein A (RPA). The ssDNA binding protein complex RPA in oocytes is replaced by Rad51 and meiotic cDNA1 (Dmc1). (**B**) Activated Chk2 promotes degradation of cell division cycle (Cdc25) and ultimately provokes cell cycle arrest through phosphorylation of Cdk2 and 4. Alternatively, in response to excessive or irreparable DNA damage, p63 may induce a cascade of apoptotic signalling pathway that requires transcriptional induction of p53 upregulated modulator of apoptosis (PUMA) and NOXA [24,92]. Apoptosis is controlled by the balance between pro-apoptosis B-cell lymphoma 2 (Bcl2) and anti-apoptosis B-cell lymphoma (Bcl)-associated X (BAX) activity. (**C**) An interplay of dimeric to the tetrameric formation of TAp63α. Phosphorylation of TAp63α ultimately transforms the inactive dimeric form of TAp63α to the active tetrameric form (figure adapted from [84,85,87]).

5. The PI3K/Akt Pathway Links Primordial Follicle Growth and the DDR

The regulation of recruitment of primordial follicles to grow is strictly controlled by a delicate balance between inhibitory and stimulatory factors to preserve the primordial follicle pool from premature exhaustion. Evidence from genetically modified mice supports the central role of the PTEN/PI3K/Akt signalling pathway in controlling the initiation of primordial follicle growth [93]. Thus, the size of the primordial follicle pool is determined by the dynamic activity of this pathway [17,18]. Accordingly, many studies involving pharmacological and non-pharmacological manipulation of this pathway have been conducted to investigate the activation of primordial follicles in vitro and in vivo [18,31,33,36,94–99].

Upregulation of the PI3K/Akt signalling pathway within the oocyte triggers a cascade of reactions that ultimately initiates activation of primordial follicles [6]. PI3K is comprised of a heterodimer of the p85 regulatory subunit and p110 catalytic subunit. In response to growth factors, all regulatory subunits of PI3K interact with the insulin receptor substrate, and thereby activate the catalytic subunit. The interaction induces the phosphorylation of membrane phospholipid phosphatidylinositol 4,5-biphosphonate (PIP2). PIP2 is converted to phosphatidylinositol 3,4,5-trisphosphate (PIP3), which then serves as a second messenger to enable phosphoinositide-dependent kinase 1 (PDK1) activation. PTEN, expressed by the oocyte, reverses this process by converting PIP3 to PIP2. PIP3 binds to Pleckstrin homology (PH) domain of PDK1 and Akt and recruits these two kinases to the subcortical area. This in turn activates PDK1 and subsequent Akt phosphorylation at threonine 308. Akt is further phosphorylated by mammalian target of rapamycin complex 2 (mTORC2) at serine 473 for its full activation, which then regulates a number of downstream targets [6].

PDK1 is indispensable in maintaining primordial follicle survival and preserving reproductive lifespan. It seems likely that both PTEN and PDK1 loss leads to premature ovarian failure (POF) but through different mechanisms. PTEN loss is associated with excessive primordial follicle activation and subsequent follicular atresia, whereas PDK1 deficiency instigates accelerated clearance of primordial follicles straight from their quiescent state [17]. Both types of primordial follicle loss are suggested to underlie ovarian ageing [17]. However, PTEN deletion in oocytes of primary and late stages of growing follicles does not reveal any significant effects on follicular growth [18].

mTORC1 is a further downstream substrate of Akt. mTORC1 is upregulated by the destabilisation of the heterodimeric complex of tuberous sclerosis complex 1 (TSC1) and 2 (TSC2). mTORC1 phosphorylates S6 protein kinase (S6K1), which promotes cell growth and proliferation and activates ribosomal protein S6 (rpS6), which increases protein translation [6] (Figure 3). The lack of TSC1 and TSC2 in mouse oocytes instigates massive primordial follicle activation, leading to POF [100]. Forkhead transcription factor FOXO3 (forkhead box O3) is a key target of the PTEN/PI3K/Akt pathway. Once activated, FOXO3 is shuttled from the nucleus to the cytoplasm, which then suppresses its transcriptional function leading to primordial follicle activation [93,101]. The FOXO3 deleted mouse model displays global primordial follicle activation at the neonatal stage leading to primordial follicle loss and POF [102,103]. Conversely, overexpression of constitutively active FOXO3 in the nucleus of mouse oocytes preserves them in a dormant state [104]. FOXO3 can thus be considered as a guardian of the primordial follicle pool, enhancing the ovarian reserve and maintaining reproductive capacity [102–104].

PI3K-related protein kinases (PIKKs) are considered to be the main regulators of DNA damage repair capacity of cells. Akt activation implicates the cell cycle checkpoint kinase 1 (Chk1), which has an important role in the DNA damage repair mechanism as it delays the cell cycle progression in S and G2 phase to correct an error of DNA damage before cell division [105]. *PTEN* is a tumour suppressor gene and is an essential factor in promoting normal cell proliferation and coordinating oocyte growth alongside granulosa cell proliferation [18,30]. Oocyte-specific PTEN deletion increases primordial follicle activation and prevents follicles from undergoing apoptosis but may be associated with accelerated clearance of follicles leading to primordial follicle pool exhaustion and POF [17,18].

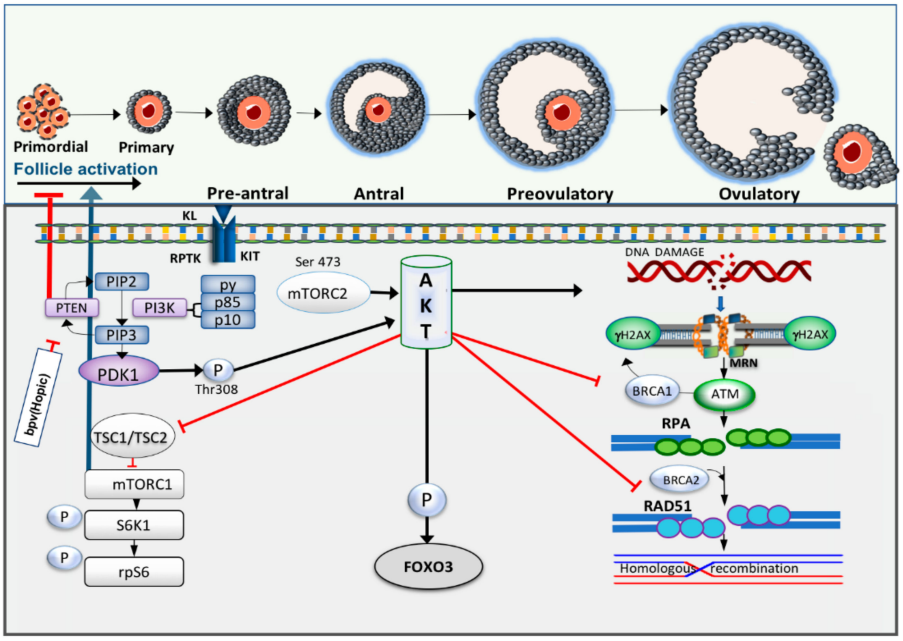

Figure 3. Crosstalk between primordial follicle activation and DDR pathway. Receptor protein tyrosine kinase (RPTK) Kit and its ligand activate phosphoinositide 3-kinase (PI3K) and as a response to this activation, the catalytic subunits of PI3K, p85 and p110, will be activated. In turn, it converts phosphatidylinositol-4,5-bisphosphate (PIP2) to phosphatidylinositol-3,4,5-bisphosphate (PIP3), which then serves as the second messenger to enable phosphoinositide-dependent kinase-1 (PDK1) activation. Phosphatase and tensin homolog deleted on chromosome 10 (PTEN) reverses this process and increases PIP2 expression. PDK1 and Akt are recruited through binding of their pleckstrin homology (PH) domains to PIP3, leading to phosphorylation of protein kinase B (Akt) by PDK1. Akt activation consequently triggers phosphorylation of forkhead box O3 (FOXO3) resulting in cytoplasmic localisation of this transcription factor. Increased in Akt activity also induces phosphorylation of mammalian target of rapamycin complex I (mTORC1) through inactivation of tuberous sclerosis complex 1 and 2 (TSC 1, 2). S6 protein kinase (S6K) activity is then upregulated and simultaneously triggers phosphorylation of ribosomal protein S6 (rpS6). Meanwhile, high intracellular levels of Akt have been reported to increase DNA damage, repress nuclear translocation of breast cancer susceptibility gene 1 (*BRCA1*) and compromise homologous recombination (HR) in breast cancer cells.

Hyperactivation of Akt due to PTEN inhibition may impair HR activity leading to genomic instability. Notably, a high endogenous level of Akt may be of significant importance in the pathology of cancer as Akt inhibits apoptosis and increases cell proliferation [15]. In cancer cells, excessive Akt activation has also been linked to suppressed NHEJ and DNA DSB repair [106]. PI3K/Akt signalling compromises DNA DSB repair by inactivating the G2 checkpoint [107], with increased Chk1 phosphorylation [108] or cytoplasmic sequestration of BRCA1 [15]. In addition, lack of PTEN in the cell leads to deficient DNA DSBs repair capacity and high incidence of spontaneous DNA breaks [16]. A study using a mouse model has shown that the expression of γH2AX was upregulated by seven-fold in PTEN-null mouse embryonic fibroblasts [109]. Furthermore, PTEN deletion is sufficient to markedly reduce the level of Rad51 that in turn leads to chromosomal instability [110,111]. In normal cells, increased Akt and DNA damage accumulation due to inefficient DNA repair are associated with Ras-induced senescence [112]. Crosstalk between PTEN/PI3K/Akt signalling pathway and DNA damage repair interactions is summarised in Figure 3.

Despite the role of PI3K/Akt in the pathology of cancer, the modulation of this pathway has been adopted as a potential approach for women with premature ovarian insufficiency (POI) and pregnancies have been achieved [34,113]. However, it has become increasingly evident that this pharmacological approach may be detrimental to oocyte/follicle development [29,35–37]. We have demonstrated that

dipotassium bisperoxo (5-hydroxypyridine-2-carboxyl) oxovanadate (bpv(HOpic)), a potent PTEN inhibitor, compromises the growth of apparently healthy human preantral follicles [36]. Likewise, the use of alginate scaffold and polyethylene glycol (PEG)-fibrinogen to culture human ovarian cortical strips in the presence of 100 µM bpv(HOpic) did not support follicular development [35]. Furthermore, constitutive PI3K activation in the perinatal period in transgenic mouse oocytes leads to lack of co-ordination between oocyte and granulosa cell growth, leading to enlarged oocytes surrounded by immature pre-granulosa cells. These mice are anovulatory, but follicles develop, and oocytes are meiotically competent. The inability to ovulate is likely the result of endocrine factors due to unregulated follicle growth [114]. PI3K over-activation in mouse oocytes has also been associated with granulosa cell tumour (GCT), characterised by excessive granulosa cell proliferation [115].

A recent finding from our lab utilising bovine ovarian cortical fragments exposed to the PTEN inhibitor bpv(HOpic) for 24 h showed increased primordial follicle activation after six days of culture. However, γH2AX expression in oocytes was upregulated and not associated with increased expression of the DNA repair enzymes ATM and Rad51. A low dose of bpv(HOpic) did not affect BRCA1 and 2 expression and more follicles in this group survived after six days of culture compared to high doses of bpv(HOpic). Nevertheless, a marked decrease in BRCA1 and 2 expression was observed after exposure to high doses suggesting a compromised DDR. Interestingly, despite high γH2AX expression being observed in granulosa cells of secondary stage follicles, DNA repair capacity of these cells was not significantly affected, as indicated by increased MRE11, ATM and Rad51 expression and a non-significant decline of BRCA1 and 2 [29] (Figure 4). Although the mechanism by which PI3K/Akt upregulation induces DNA damage in oocytes has not been elucidated, accelerated primordial follicle growth has been linked to decreased estradiol production indicating impaired granulosa cell function, whilst lowering the activation rate results in normal estradiol production [37]. This suggests that the rapid growth may be associated with a disordered intrafollicular oocyte and somatic cell relationship [116]. This condition may lead to uncoordinated oocyte and granulosa cell growth, as reported in mice [114].

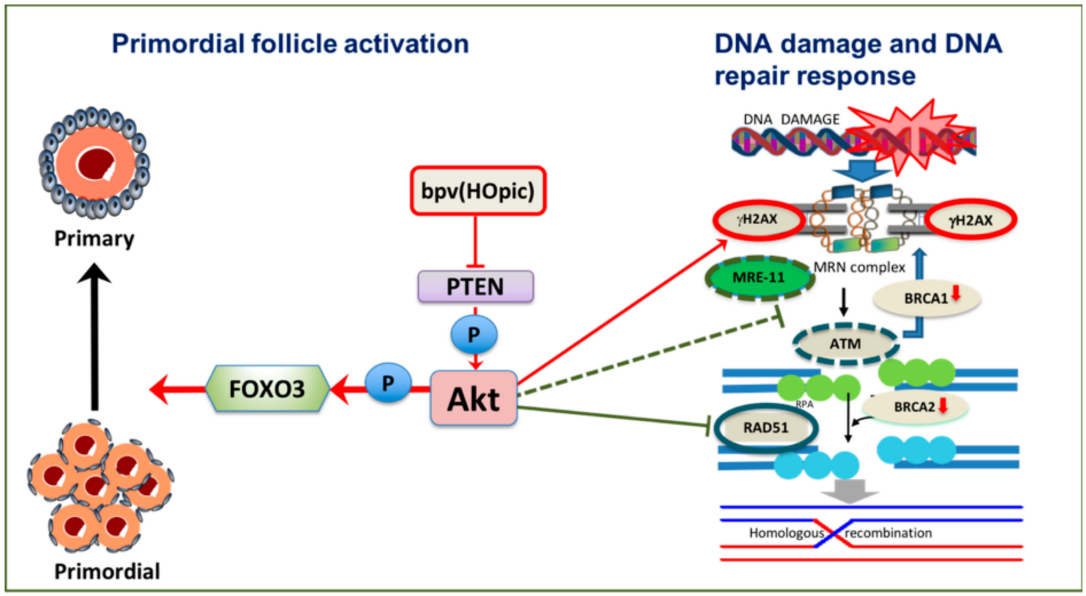

Figure 4. Potential effects of phosphoinositide 3-kinase /protein kinase B (PI3K/Akt) activation on DNA damage and DNA repair response of oocytes in vitro. Inhibition of PTEN by low dose Dipotassium bisperoxo(5-hydroxypyridine-2-carboxyl) oxovanadate (V) (bpv(HOpic)) is sufficient to induce primordial follicle activation. However, gamma H2AX (γH2AX) increases and DNA repair proteins meiotic recombination 11 (MRE11), ataxia telangiectasia mutated (ATM) and Rad51 are downregulated, as are breast cancer susceptibility gene 1 (*BRCA1*) and breast cancer susceptibility gene 2 (*BRCA2*).

Several publications utilising mouse models have provided evidence that oocytes within resting follicles may be directly targeted by chemotherapy treatments, including CP, cisplatin and doxorubicin [24,26,117,118]. It has also been proposed that primordial follicle depletion following chemotherapy may be induced by the loss of growing follicles with an increase in primordial follicle activation [119,120]. A study investigating the mechanism by which cisplatin induced ovarian failure showed that cisplatin reduced PTEN expression in oocytes leading to primordial follicle activation. Once follicles were activated to grow, they became more vulnerable to apoptosis with a loss of luteinising hormone (LH) receptor expression resulting in decreased oocyte meiotic competence and ovulation failure [23]. These direct and indirect effects of chemotherapy treatments on primordial follicles can form the basis to develop potential methods to protect ovaries against the adverse impacts of chemotherapy [121].

In addition to chemotherapy, another clinical problem that is linked to DNA damage, PI3K/Akt signalling pathway and ovarian ageing is endometriosis. Increased PI3K/Akt activity has been suggested in endometriosis [122–127], with loss of nuclear PTEN [128]. Primordial follicle loss in endometriosis has been associated with PI3K/Akt upregulation in mice and human [125] and is suggested to be responsible for ovarian ageing [129]. A diminished ovarian reserve in endometriosis occurs concomitantly with increased DNA damage and compromised DSB repair mechanism, indicated by low Rad51 and BRCA1 expression [130]. Experimental studies in rats indicate that an mTOR inhibitor is effective to suppress the growth of endometriotic implants, supporting the engagement of this pathway [131].

The effects of PI3K/Akt/mTOR on primordial follicle activation following chemotherapy treatment have led to research utilising this mechanism to reduce the adverse impact of chemotherapy on the ovary. In human, as mTOR hyperactivation is a common feature of cancers, mTOR inhibitors are becoming a therapeutic target in certain type of cancers. In a study utilising mouse embryonic fibroblast cell lines, constitutive mTOR activation enhanced apoptosis triggered by chemotherapy through persistent DNA damage as was shown by the upregulation of γH2AX. In parallel, the absence of both PTEN and TSC2 upregulates γH2AX expression. Intriguingly, mTOR inhibition prior to treatment is able to protect cells from etoposide-induced apoptotic cell death [132]. Substrates that inhibit mTOR have been shown to reduce excessive primordial activation and maintain the primordial follicle pool [133–135]. This positive effect is due to mTOR downregulation during chemotherapy and subsequently reduced Akt and S6K phosphorylation resulting in decreased primordial follicle loss and maintenance of the ovarian reserve and fertility [136]. Studies investigating the PI3K/Akt pathway are detailed in Table 1.

Table 1. Recent studies investigating the impact of phosphatase and tensin homolog deleted on chromosome 10/phosphoinositide 3-kinase/protein kinase B/mammalian target of rapamycin complex (PTEN/PI3K/Akt/mTORC) pathway either as a part of genetic modification/pharmacological activation, chemotherapy treatment or ovotoxicity exposure on primordial follicle activation, follicular growth and survival.

Agents Used/Compounds/Concentration	Mechanism of Action	Species/Methods	Effects on Follicular Growth/Survival	Specific Effects on Granulosa Cells/Oocyte	Study
1 and 10 μM Dipotassium bisperoxo (5-hydroxypyridine-2-carboxyl) oxovanadate (V) (bpv(HOpic)) for 24 h/ PTEN inhibitors.	Increase PI3K/Akt	Bovine/ovarian cortical fragments cultured.	Decreases in higher dose.	Compromises DNA damage response (DDR).	[29]
20, 40, 60, 80, 120 and 140 μM diazinon (DZN)	Inhibit PI3K/Akt	Porcine isolated granulosa cells.	Granulosa cells death	Increase DNA damage, mRNA level of Ataxia telangiectasia mutated (ATM), Rad51 and breast cancer susceptibility gene1 (*BRCA1*) increase p53 leading to granulosa cell death.	[137]
30 μM bpv (HOpic) + 150 μg/mL 740Y-P for 24 and 48 h or 100 nM everolimus.	Increase PI3K/Akt and inhibit mTOR activation respectively	Cryopreserved human ovarian cortical fragments cultured	Lowering the rate of activation improves follicular growth.	PTEN inhibition compromises granulosa cell estradiol production.	[37]
Cyclophosphamide (CP) 75 mg, 100 mg, 150 mg per kg body weight and 5 mg/kg body weight per day 1 week before and after CP administration.	PI3K/Akt activation	Mice, in vivo	CP induces non-growing and growing follicle loss. Rapamycin prevents CP induced primordial follicle activation.	Anti-mullerian hormone (AMH) expression decreases after CP exposure.	[133]
Transgenic mouse model	Increase PI3K activation in transgenic mice, Cre+	Transgenic mice, Cre+ and Cre−	Normal secondary follicles, granulosa cell tumour (GCT) in primordial and primary follicles.	Bilateral GCT due to increased activin A.	[115]
440 μM bisphenol A(BPA).	Increases PI3K/Akt activation	Rat ovarian fragment culture exposed to BPA.	BPA induces DNA damage both in oocytes and granulosa cells. PI3K signalling pathway involved in BPA-induced DNA damage.	Primordial follicle is activated to replace the larger follicle depletion.	[138]
Transgenic mouse model	Increase PI3K activation in transgenic mice, Cre+	Transgenic mice, Cre+ and Cre−	Increases follicles survival	Asynchronous oocytes and granulosa cells growth.	[114]
100 μM bpv(HOpic) for 25 h	Increase PI3K/Akt activation	Human ovarian cortical fragments cultured.	No damage to the follicular growth.	Enhance estradiol production without any damage to follicles compared to control group.	[33]
200 μM phosphatidic acid (PA) and 50 μM propranolol (PRO) for 24 h in mice; bpv(HOpic)(100 μM) /740Y-P (250 μM /mL) for 24 h, 740Y-P (250 μM /mL) only for another 24 h; PA (100 mM)/740Y-P (200 μM)/PRO (50 μM) for 24 h in human.	Increase PI3K/Akt /mTOR activation.	Mice and human ovaries transiently incubated in mTOR activators followed by grafting into female mice.	No damage to the follicular growth.	NA	[139]
30 μM of bpv(HOpic), and 150 μM /mL of 740YP for 24 h followed by incubation with 740YP alone for another 24 h	Increase PI3K/Akt activation.	Human ovarian cortical fragments transplantation following in vitro activation (IVA).	Autografting of ovarian fragments following in vitro activation (IVA) procedure to infertility related primary ovarian insufficiency (POI) patients.	NA	[34]

Table 1. *Cont.*

Agents Used/Compounds/Concentration	Mechanism of Action	Species/Methods	Effects on Follicular Growth/Survival	Specific Effects on Granulosa Cells/Oocyte	Study
1 μM bpv(HOpic) and 10 and 100 μM bpv(HOpic) (unpublished)	Increase PI3K/Akt activation	Human ovarian cortical fragments and isolated preantral follicle culture.	Higher dose compromises follicular growth. The lower dose is associated with deleterious effects on subsequent growth of preantral follicles.	NA	[36]
Cisplatin, once daily at doses of 0.5, 1.0, 1.5 and 2.0 mg/ kg for 5 to 14 days	Activation of PI3K/Akt	Intraperitoneal injection of cisplatin in mice	Increases the proportion of growing follicles.	Induces ovarian failure.	[23]
100 μM bpv(HOpic) and 500 μM /mL 740Y-P for 24 and 48 h	Increase PI3K/Akt activation.	Human ovarian cortical fragments cultured in polyethylene glycol (PEG)-fibrinogen hydrogels.	Compromises follicle survival.	NA	[35]
30 μM bpv(HOpic) and 150 μg/mL 740YP for 24 h	Increase PI3K/Akt activation.	Mice ovarian transplantation and human ovarian fragments transplantation following IVA.	Promotes primordial follicle activation both in mice and human.	NA	[113]
Female mice deficient in PTEN	Increase PI3K/Akt activation	PTEN knockout mice	Rapamycin reduces the primordial follicles activation in PTEN knockout mice.	Rapamycin prevents global primordial follicles activation induced by the absence of PTEN.	[134]
1 μM bpv(HOpic) for 24 h	Increase PI3K/Akt activity.	Mice cortical fragments IVA followed by transplantation and bpv(HOpic) directly injected to female mice.	Does not compromise follicular health.	More mature and fertilised oocytes in PTEN inhibition group.	[32]
100 μM bpv(HOpic) and/or 500 μg/mL 740Y-P for 48 h or bpv(HOpic) plus 740Y-P together with the Akt inhibitor SH-550 μM or the PI3K inhibitor Wortmannin 25 μM.	Increase PI3K/Akt, Akt inhibitor decreases the activation.	Mice and human cortical fragments incubated in Akt activators followed by xenografting.	Increases in the number of secondary and antral stage follicles following xenografting and does not affect follicular health.	No malignancy observed after long term ovarian transplantation.	[140]
Mice lacking Tuberous sclerosis complex 1 (TSC1), PTEN; TSC1 and PTEN; Phosphatidylinositol-dependent kinase 1 (PDK1) and PDK1 and TSC1 in oocytes.	Enhances mTOR activation.	Mutant female mice	Degenerated activated primordial follicles (short term), diminished follicular health (long term).	Rapamycin prevents global primordial follicle activation. Activation does not cause tumour development.	[100]
Homozygous mutant female mice deficient Tuberous sclerosis complex 2 (TSC2) in oocytes.	Enhances mTOR activation.	Mutant female mice.	Massive primordial follicle activation.	Depletion of follicle reserve.	[93]
Female mice lacking PTEN, PDK1 and r ibosomal protein S6 kinase (rpS6)	Increases PI3K/Akt	Mutant female mice.	Follicles with degenerating oocytes in PDK1 deletion and enlarged oocytes in PTEN deletion.	The absence of PTEN causes Primary Ovarian Insufficiency (POI) that can be reversed by PDK1 deletion.	[17]
PTEN deletion in mice.	Increases PI3K/Akt	PTEN mutant mice	Tends to be normal follicle morphology but with enlarged oocytes and flattened granulosa cells.	PTEN deletion leads to excessive primordial follicle activation.	[18]

NA: Not available.

6. DNA Damage Associated with Ovarian Ageing, a Crosstalk between PI3K/Akt/PTEN Signalling, Ageing and DNA Damage Response

Ovarian ageing as a physiological process varies substantially among women depending on the number of primordial follicles and the rate of follicle loss [141,142]. It is also very closely associated with reduced oocyte quality [143]. A link between these is suggested by the increasing rate of primordial follicle activation with age [144] with PI3K/Akt signalling pathway being a key regulator of this growth activation [17,18]. Compromised DNA repair protein interactions as a consequence of ovarian ageing has been connected to increase PI3K/Akt activity [19–22].

There is increasing evidence of an association between DNA damage and repair capacity of oocytes and maternal age, with DNA repair becoming less efficient with ageing [19–21,58]. A study in non-human primates confirmed a lack of DNA repair efficiency with advancing age, with cytoplasmic sequestration of BRCA1 in oocytes [22]. Although DNA damage and repair mechanisms in granulosa cells are not the main focus of this review, it is worth mentioning that γH2AX expression in granulosa cells of growing follicles was not different between old and young mice [22]. This finding may suggest less effective DNA repair in oocytes within primordial follicles compared to surrounding somatic cells. Accordingly, mouse oocytes of all follicle types exhibit high expression of γH2AX with increasing age. At the same time, the oocyte appears to have an ineffective DNA repair mechanism as was shown by a profound drop in BRCA1, MRE11 and ATM but not BRCA2. Mutations in *BRCA1* but not *BRCA2* perturb ovarian stimulation leading to smaller litter size. Interestingly, DNA damage was not evident in pre-granulosa cells within primordial follicles [21]. In line with these findings, the mRNA level of *BRCA1*, *Rad51* and *H2AX* were reduced in aged female rat and buffalo oocytes within primordial follicles [19,58].

Women with *BRCA2* mutations do not show a reduced response to ovarian stimulation [145]. However, BRCA2 deficient mice are able to produce competent and fertilised oocytes but more abnormal embryos are observed [146], indicating an important role of BRCA2 in the oocyte. In women, complete loss of BRCA2 function leads to ovarian dysgenesis resulting in primary amenorrhea, with reduced Rad51 function in HR indicated by low Rad51 expression at the site of DNA damage [147]. A genome-wide association study (GWAS) analysis also shows association between DNA damage repair and age at menopause [148], particularly highlighting links with BRCA1. Likewise, a diminished ovarian reserve mirrored by low AMH levels in women with *BRCA1* but not *BRCA2* mutations [149] supports findings from a transgenic mouse model [21]. In addition, primordial follicles with *BRCA1* mutations are more susceptible to DNA damage accumulation, as shown by high γH2AX expression in primordial follicles [25].

As ageing is thus associated with a reduction in DNA repair capacity, oocytes from older women may be more susceptible to genotoxic insults with increased primordial follicle loss due to apoptosis [10]. It is evident that the degree of doxorubicin induced DNA damage is independent of age, but apoptotic events are more apparent in oocytes of old mice. This may be related to the finding that oocytes from young mice have a greater DNA repair capacity [48]. Qualitative analysis of recent findings of studies in DNA damage and ovarian ageing are summarised in Table 2.

ROS accumulation in mitochondria can be an underlying factor in ageing, by increasing oxidative damage leading to a gradual decrease in follicle quality [150]. Increased ROS activity due to senescence parallels diminished activity of the oxidative defence system and may lead to increased lipid peroxidation, oxidative stress and damage to macromolecules including DNA with either single-strand breaks (SSBs) or DSBs [151]. High ROS expression in follicular fluid of patients undergoing in vitro fertilisation (IVF) has been linked to reduced oocyte fertilisation and poor embryo quality [152]. Mitochondria have been hypothesised to be the first organelle affected by ROS since they are the source of oxygen radical production; ageing is also associated with increased mitochondrial DNA (mtDNA) deletions [153,154]. PTEN upregulation, through modulation of the PI3K/Akt pathway, decreases ROS production in cells (reviewed in [155,156]). Increased ROS concentration in mitochondria due to ageing may inhibit PTEN leading to accumulation of PIP3, which then increases Akt activation and further

increases ROS production. This pathway suggests a positive feedback loop between PTEN, PIP3 and ROS [157]. The impact of ageing on the PI3k/Akt signalling pathway, DDR and resting pool depletion is summarised in Figure 5.

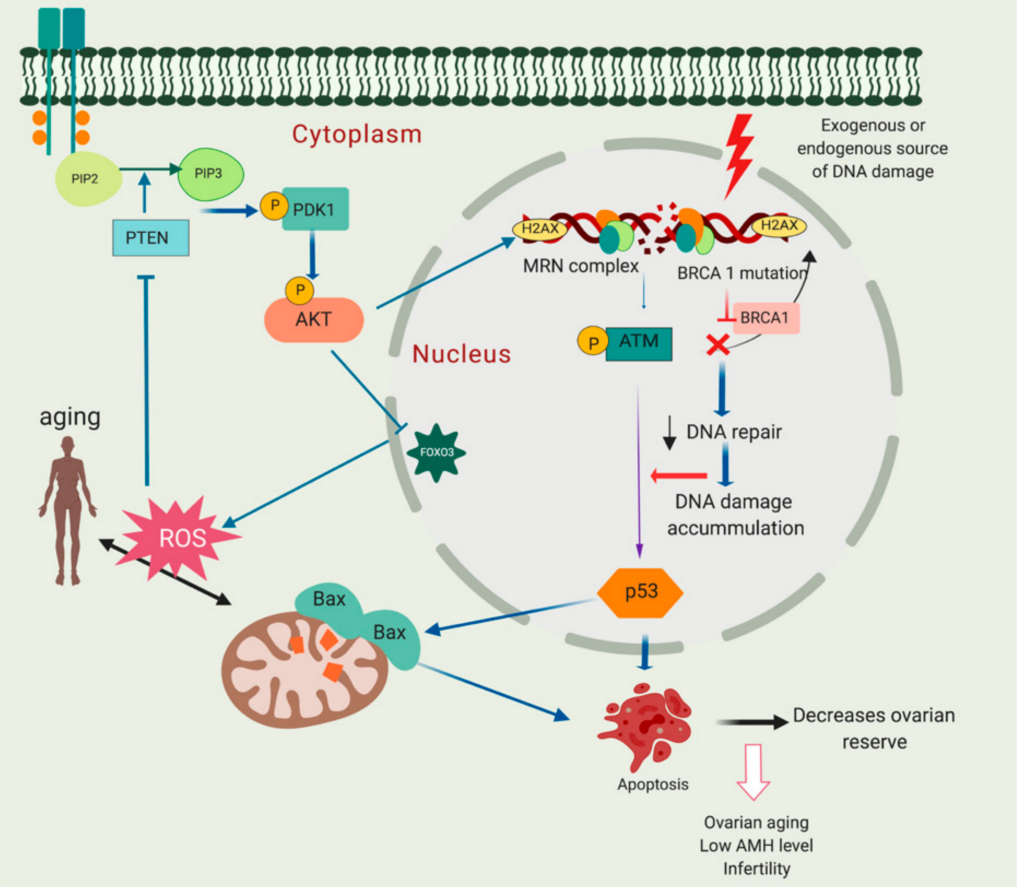

Figure 5. Molecular relationship between phosphoinositide 3-kinase/protein kinase (PTEN/Akt) activation, DNA damage and decreased ovarian reserve. Breast cancer susceptibility gene 1 (*BRCA1*) mutation may lead to compromised DNA repair pathway and eventually primordial follicle apoptosis leading to follicle loss and decreased ovarian reserve. In addition, mitochondria can be one of the major sources of DNA damage. Excessive reactive oxygen species (ROS) production may harm macromolecules in the cells including DNA leading to single-stand breaks (SSBs) or double-strand breaks (DSBs). High ROS expression in mitochondria may lead to PTEN inhibition and increase Akt activation. This may eventually further increase ROS production due to inactivation of forkhead box O3 (FOXO3).

Table 2. Summary of recent clinical and experimental studies providing evidence linking DNA damage response (DDR), ovarian ageing and ovarian reserve.

Study Focus	Study Type	DDR Pathway Affected	Main Outcomes	References
Oocyte maturation rate of breast cancer patient with breast cancer susceptibility gene 1 (*BRCA1*) and Breast cancer 2 (*BRCA2*) mutation.	Retrospective cohort study.	BRCA1 and BRCA2	The number of mature oocytes resulted from in vitro maturation (IVM) procedure is not different between women with *BRCA1* and without *BRCA* mutation.	[158]
Ovarian reserve of patients with *BRCA* mutation carriers and non-carriers with or without malignancy.	Retrospective cohort study.	BRCA1 and BRCA2	Patients with *BRCA* mutation carriers and noncarriers show comparable ovarian reserve and number of oocytes yield following ovarian stimulation.	[159]
The role of BRCA2 in ovarian development and puberty onset.	A case control study in human.	BRCA2 and Rad51	Lack of BRCA2 reduces Rad51 recruitment during homologous recombination.	[147]
Ovarian reserve in patients with *BRCA1* mutation.	Case-control study.	γH2AX, BRCA1 and BRCA2	DNA double-strand breaks (DSBs) increase in *BRCA1* mutation group but not *BRCA2*. DNA damage increases with age in *BRCA1/2* mutation.	[25]
Oocyte yield following ovarian stimulation in patients with *BRCA1/2* mutation.	Retrospective cohort study.	BRCA1 and BRCA2	The number of oocytes produced by women with *BRCA* mutation is lower than without BRCA1 mutation.	[160]
DNA damage and repair capacity of aged and young buffalo ovaries.	Experimental study in buffalo ovaries.	BRCA1, γH2AX, MRE11, Rad51 and ATM	mRNA expression of BRCA1, meiotic recombination 11 (MRE11), Rad51 and ataxia telangiectasia mutated (ATM) decline significantly in aged buffalo ovaries.	[58]
The effects of *BRCA* mutation on anti-Mullerian hormone (AMH) serum level.	Prospective cohort study	BRCA1 and BRCA2	Patients with *BRCA2* mutations exhibit a lower AMH level compare to low-risk control patients.	[161]
Anti-mullerian hormone (AMH) serum level in patients with *BRCA1/2* mutation.	Cross-sectional study	BRCA1 and BRCA2	AMH serum level of patients with *BRCA1/2* mutation carriers does not significantly different from non-carriers.	[162]
AMH serum level in women with *BRCA1* and *BRCA2* mutation.	Cross-sectional study	BRCA1 and BRCA2	*BRCA1* but not in *BRCA2* mutation carriers have a lower AMH level.	[149]
Ovarian ageing effects on DNA damage repair response in rat ovaries.	Experimental	γH2AX, BRCA1, MRE11, Rad51, ATM, BRCA1 and BRCA2	DNA repair proteins BRCA1, Rad51, ATM and γH2AX in aged rat primordial follicles declined compared to immature rats.	[19]
Comparison of proteins profile of primordial follicles isolated from immature rat and aged rat.	Experimental	Heat shock cognate 71kDa (Hsp71C), calreticulin, Bcl-2-related ovarian killer protein (BOK)	Protein expression for DSBs response decreases significantly in aged rats.	[59]
The association between DNA DSBs in granulosa cells and ageing.	Experimental	γH2AX, BRCA1, Telomeric repeat binding factor (TRF2)	Increased γH2AX and decreased BRCA1 expression in all follicle types with age.	[22]
The association between AMH serum level and *BRCA* mutation.	Cross-sectional study	BRCA1 and BRCA2	AMH serum level of patients with a *BRCA1* mutation is lower than without *BRCA1* mutation.	[163]
The effect of ovarian ageing on DNA DSBs of oocytes and granulosa cells.	Experimental	γH2AX, BRCA1, MRE11, Rad51, ATM, BRCA1 and BRCA2	Increased DNA damage and decreased DDR capacity with advancing age.	[21]
Time to menopause in *BRCA1* and 2 mutations carriers.	Case control study.	BRCA1 and BRCA2	Both *BRCA1* and *2* mutation patients experience menopause earlier than control.	[164]
Doxorubicin effects on ovarian ageing.	Experimental	γH2AX, ATM and activated caspase 3	γH2AX expression is higher in ovarian tissue exposed to doxorubicin in vitro.	[118]
Transactivation p73 (TAp73) expression in young and aged female oocytes.	Experimental	TAp73	TAp73 is downregulated in older women's oocytes.	[165]
The effects of age on the occurrence of aneuploidy in mouse oocytes.	Experimental	BRCA1	*BRCA1* expression is decreased in oocytes of aged mice. Aneuploidy increases in aged oocytes.	[166]
The role of BRCA2 in male and female gametogenesis.	Experimental	BRCA2	BRCA2 deficiency in mice leads to infertility.	[146]

7. Conclusions and Future Directions

It is clear that mammalian oocytes have distinct DNA damage surveillance mechanisms. There is evidence linking the regulation of primordial follicle growth activation through the PI3K pathway with increased DNA damage/reduced repair, and this provides a model for the development of new approaches to the investigation and potentially therapeutic intervention in both these key aspects of oocyte biology. Evidence from both genetic mouse models and the culture of mammalian ovarian cortical fragments supports the contention that imbalance in signalling events between oocytes and granulosa cells may contribute to impaired follicle function after aberrant primordial follicle growth activation.

Data reviewed here explore the links between the regulation of primordial follicle growth activation and DNA damage repair pathways. The primordial follicle and particularly the oocyte within it has unique physiological challenges, being required to maintain genomic integrity and quality from birth over several decades without cell growth or replication. Thus, the opportunity for repeated DNA surveillance during cell division is absent, and oocyte-specific pathways from DNA damage to apoptosis exist. There is increasing research activity linking follicle growth regulation with oocyte DNA damage and repair capacity in the context of potential prevention of ovarian damage against chemotherapy, radiation or environmental toxicants. The elucidation of the possibility to confer resistance against chemotherapy through identification of key factors in the oocyte apoptotic pathway may lead to clinical trials building on the differences in these pathways between the oocyte and somatic cells.

Rad51, a critical protein involved in oocyte resilience to apoptosis, is a feasible candidate to promote DNA repair capacity in oocytes and ultimately conserve fertility in women undergoing cancer treatment. Administration of recombinant Rad51 into mouse oocytes has been demonstrated to increase DDR, prevent apoptosis, improve the defective DNA repair capacity in oocyte and restore embryo development [48,76]. Future investigation into the safety and efficacy of modulating Rad51 as a clinical application to preserve functional germ cells may be beneficial to improve oocyte and embryo development following chemotherapy exposure and in ageing.

Targeting the PI3K/PTEN/Akt/mTOR pathway, mTOR inhibition with rapamycin [133] and everolimus [136] have also been investigated as a means to protect ovaries during exposure to chemotherapy in mice. Melatonin and ghrelin have also been proposed to protect the ovaries against cisplatin and may also affect this pathway, though perhaps indirectly. Both ghrelin and melatonin suppress cisplatin-mediated PI3K/Akt pathway upregulation and inhibit FOXO3 nuclear shuttling, thus preserving the primordial follicle pool [167]. This is a promising avenue, though it will be essential to ensure that the effects of chemotherapy on cancer cells are not compromised [10].

It has been shown that either complete loss of PUMA or partial loss of TAp63 in mice oocytes could retain the primordial follicle pool following CP and cisplatin exposure. This is a promising approach to reduce the negative effects of chemotherapy on the ovaries [26,117] as the salvage process exclusively occurs within the oocyte without interfering with the cancer treatments [10].

An intriguing novel approach to the protection of ovaries against chemotherapy has been suggested by a recent study introducing microRNAs (miRNAs) [168]. It is reported that miRNAs are differentially expressed in mouse postnatal ovaries exposed to 4-hydroperoxy-cyclophosphamide (4-HC), some of which have been implicated in DDR and apoptosis and affect cellular susceptibility to DNA damaging agents [169]. MiRNAs can be effective techniques as their expression can be adjusted with their microenvironment during chemotherapy treatment, thus minimising off-target toxicity. Lethal 7 (let-7a) mimic is an example of a new miRNA based therapeutic to minimise follicle injury following chemotherapy treatment [170]. However, this work is at an early stage, with challenges including how to deliver miRNAs to a specific target organ with minimum side effects.

In vitro activation (IVA) methods have generated controversy regarding efficacy and safety with in vitro studies indicating that manipulating activation by pharmacological methods has an impact on subsequent quality of oocytes [35–37]. Pharmacological primordial activation utilising a PTEN inhibitor

has been associated with increased DNA damage and impaired DNA repair capacity particularly in oocytes [29]. While an IVA protocol utilising both PI3K/Akt and Hippo signalling pathways prior to ovarian tissue transplantation may have major negative consequences on follicle health [119,171,172], the PI3K/Akt signalling pathway may also be a potential target to prevent follicle activation and loss following ovarian tissue transplantation, maximising the longevity of the transplanted tissue. A recent study showed that short exposure to a specific inhibitor of mTORC1 partially hindered follicular activation while improving follicle survival and steroidogenesis [37]. Since precocious follicular growth in vitro has been a major constraint in developing in vitro follicle growth systems, lowering the activation rate by using an mTORC inhibitor may have additional value as a promising strategy for the derivation of mature oocytes in vitro. Finally as the canonical PI3K/Akt signalling pathway is interconnected with many feedback loops that are essential for optimal cell function during ageing [157], future research investigating the potential of manipulation of PTEN and PI3K to reduce ROS accumulation and thus damage in ageing oocytes will be essential.

Funding: The work was supported by LPDP (Indonesia Endowment Fund for Education) as a part of Ph.D. scholarship to MM. Work conducted in this area in EET and RAA's laboratories has been funded by MRC grants G0901839 and G1100357.

Acknowledgments: Figures 2 and 5 were created by Biorender web-based illustration.

Conflicts of Interest: None to declare.

References

1. Telfer, E.E.; Zelinski, M.B. Ovarian follicle culture: Advances and challenges for human and nonhuman primates. *Fertil. Steril.* **2013**, *99*, 1523–1533. [CrossRef] [PubMed]
2. Faddy, M.J.; Gosden, R.G. A mathematical model of follicle dynamics in the human ovary. *Hum. Reprod.* **1995**, *10*, 770–775. [CrossRef] [PubMed]
3. Hansen, K.R.; Knowlton, N.S.; Thyer, A.C.; Charleston, J.S.; Soules, M.R.; Klein, N.A. A new model of reproductive aging: The decline in ovarian non-growing follicle number from birth to menopause. *Hum. Reprod.* **2008**, *23*, 699–708. [CrossRef] [PubMed]
4. Broekmans, F.J.; Knauff, E.A.; te Velde, E.R.; Macklon, N.S.; Fauser, B.C. Female reproductive ageing: Current knowledge and future trends. *Trends Endocrinol. Metab.* **2007**, *18*, 58–65. [CrossRef]
5. McGee, E.A.; Hsueh, A.J. Initial and cyclic recruitment of ovarian follicles. *Endocr. Rev.* **2000**, *21*, 200–214. [CrossRef]
6. Adhikari, D.; Liu, K. Molecular mechanisms underlying the activation of mammalian primordial follicles. *Endocr. Rev.* **2009**, *30*, 438–464. [CrossRef]
7. Wang, Q.; Sun, Q.Y. Evaluation of oocyte quality: Morphological, cellular and molecular predictors. *Reprod. Fertil. Dev.* **2007**, *19*, 1–12. [CrossRef]
8. Ashwood-Smith, M.J.; Edwards, R.G. DNA repair by oocytes. *Mol. Hum. Reprod.* **1996**, *2*, 46–51. [CrossRef]
9. Tilly, J.L. Commuting the death sentence: How oocytes strive to survive. *Nat. Rev. Mol. Cell Biol.* **2001**, *2*, 838–848. [CrossRef]
10. Winship, A.L.; Stringer, J.M.; Liew, S.H.; Hutt, K.J. The importance of DNA repair for maintaining oocyte quality in response to anti-cancer treatments, environmental toxins and maternal ageing. *Hum. Reprod. Update* **2018**, *24*, 119–134. [CrossRef]
11. Dupont, J.; Scaramuzzi, R.J. Insulin signalling and glucose transport in the ovary and ovarian function during the ovarian cycle. *Biochem. J.* **2016**, *473*, 1483–1501. [CrossRef]
12. Stokoe, D. The phosphoinositide 3-kinase pathway and cancer. *Expert. Rev. Mol. Med.* **2005**, *7*, 1–22. [CrossRef]
13. Engelman, J.A.; Luo, J.; Cantley, L.C. The evolution of phosphatidylinositol 3-kinases as regulators of growth and metabolism. *Nat. Rev. Genet.* **2006**, *7*, 606–619. [CrossRef]
14. Karimian, A.; Mir, S.M.; Parsian, H.; Refieyan, S.; Mirza-Aghazadeh-Attari, M.; Yousefi, B.; Majidinia, M. Crosstalk between phosphoinositide 3-kinase/akt signaling pathway with DNA damage response and oxidative stress in cancer. *J. Cell. Biochem.* **2019**, *120*, 10248–10272. [CrossRef]
15. Plo, I.; Laulier, C.; Gauthier, L.; Lebrun, F.; Calvo, F.; Lopez, B.S. Akt1 inhibits homologous recombination by inducing cytoplasmic retention of brca1 and rad51. *Cancer Res.* **2008**, *68*, 9404–9412. [CrossRef]

16. Puc, J.; Keniry, M.; Li, H.S.; Pandita, T.K.; Choudhury, A.D.; Memeo, L.; Mansukhani, M.; Murty, V.V.; Gaciong, Z.; Meek, S.E.; et al. Lack of pten sequesters chk1 and initiates genetic instability. *Cancer Cell.* **2005**, *7*, 193–204. [CrossRef]
17. Reddy, P.; Adhikari, D.; Zheng, W.; Liang, S.; Hamalainen, T.; Tohonen, V.; Ogawa, W.; Noda, T.; Volarevic, S.; Huhtaniemi, I.; et al. Pdk1 signaling in oocytes controls reproductive aging and lifespan by manipulating the survival of primordial follicles. *Hum. Mol. Genet.* **2009**, *18*, 2813–2824. [CrossRef]
18. Reddy, P.; Liu, L.; Adhikari, D.; Jagarlamudi, K.; Rajareddy, S.; Shen, Y.; Du, C.; Tang, W.; Hamalainen, T.; Peng, S.L.; et al. Oocyte-specific deletion of pten causes premature activation of the primordial follicle pool. *Science* **2008**, *319*, 611–613. [CrossRef]
19. Govindaraj, V.; Keralapura Basavaraju, R.; Rao, A.J. Changes in the expression of DNA double strand break repair genes in primordial follicles from immature and aged rats. *Reprod. Biomed. Online* **2015**, *30*, 303–310. [CrossRef]
20. Oktay, K.; Turan, V.; Titus, S.; Stobezki, R.; Liu, L. Brca mutations, DNA repair deficiency, and ovarian aging. *Biol. Reprod.* **2015**, *93*, 67. [CrossRef]
21. Titus, S.; Li, F.; Stobezki, R.; Akula, K.; Unsal, E.; Jeong, K.; Dickler, M.; Robson, M.; Moy, F.; Goswami, S.; et al. Impairment of brca1-related DNA double-strand break repair leads to ovarian aging in mice and humans. *Sci. Transl. Med.* **2013**, *5*, 172ra21. [CrossRef]
22. Zhang, D.; Zhang, X.; Zeng, M.; Yuan, J.; Liu, M.; Yin, Y.; Wu, X.; Keefe, D.L.; Liu, L. Increased DNA damage and repair deficiency in granulosa cells are associated with ovarian aging in rhesus monkey. *J. Assist. Reprod. Genet.* **2015**, *32*, 1069–1078. [CrossRef]
23. Chang, E.M.; Lim, E.; Yoon, S.; Jeong, K.; Bae, S.; Lee, D.R.; Yoon, T.K.; Choi, Y.; Lee, W.S. Cisplatin induces overactivation of the dormant primordial follicle through pten/akt/foxo3a pathway which leads to loss of ovarian reserve in mice. *PLoS ONE* **2015**, *10*, e0144245. [CrossRef]
24. Kerr, J.B.; Hutt, K.J.; Michalak, E.M.; Cook, M.; Vandenberg, C.J.; Liew, S.H.; Bouillet, P.; Mills, A.; Scott, C.L.; Findlay, J.K.; et al. DNA damage-induced primordial follicle oocyte apoptosis and loss of fertility require tap63-mediated induction of puma and noxa. *Mol. Cell.* **2012**, *48*, 343–352. [CrossRef]
25. Lin, W.; Titus, S.; Moy, F.; Ginsburg, E.S.; Oktay, K. Ovarian aging in women with brca germline mutations. *J. Clin. Endocrinol. Metab.* **2017**, *102*, 3839–3847. [CrossRef]
26. Nguyen, Q.N.; Zerafa, N.; Liew, S.H.; Morgan, F.H.; Strasser, A.; Scott, C.L.; Findlay, J.K.; Hickey, M.; Hutt, K.J. Loss of puma protects the ovarian reserve during DNA-damaging chemotherapy and preserves fertility. *Cell Death Dis.* **2018**, *9*, 618. [CrossRef]
27. Rinaldi, V.D.; Hsieh, K.; Munroe, R.; Bolcun-Filas, E.; Schimenti, J.C. Pharmacological inhibition of the DNA damage checkpoint prevents radiation-induced oocyte death. *Genetics* **2017**, *206*, 1823–1828. [CrossRef]
28. Wang, Y.; Liu, M.; Johnson, S.B.; Yuan, G.; Arriba, A.K.; Zubizarreta, M.E.; Chatterjee, S.; Nagarkatti, M.; Nagarkatti, P.; Xiao, S. Doxorubicin obliterates mouse ovarian reserve through both primordial follicle atresia and overactivation. *Toxicol. Appl. Pharmacol.* **2019**, *381*, 114714. [CrossRef]
29. Maidarti, M.; Clarkson, Y.L.; McLaughlin, M.; Anderson, R.A.; Telfer, E.E. Inhibition of pten activates bovine non-growing follicles in vitro but increases DNA damage and reduces DNA repair response. *Hum. Reprod.* **2019**, *34*, 297–307. [CrossRef]
30. Jagarlamudi, K.; Liu, L.; Adhikari, D.; Reddy, P.; Idahl, A.; Ottander, U.; Lundin, E.; Liu, K. Oocyte-specific deletion of pten in mice reveals a stage-specific function of pten/pi3k signaling in oocytes in controlling follicular activation. *PLoS ONE* **2009**, *4*, e6186. [CrossRef]
31. Jagarlamudi, K.; Reddy, P.; Adhikari, D.; Liu, K. Genetically modified mouse models for premature ovarian failure (pof). *Mol. Cell. Endocrinol.* **2010**, *315*, 1–10. [CrossRef]
32. Adhikari, D.; Gorre, N.; Risal, S.; Zhao, Z.; Zhang, H.; Shen, Y.; Liu, K. The safe use of a pten inhibitor for the activation of dormant mouse primordial follicles and generation of fertilizable eggs. *PLoS ONE* **2012**, *7*, e39034. [CrossRef]
33. Novella-Maestre, E.; Herraiz, S.; Rodriguez-Iglesias, B.; Diaz-Garcia, C.; Pellicer, A. Short-term pten inhibition improves in vitro activation of primordial follicles, preserves follicular viability, and restores amh levels in cryopreserved ovarian tissue from cancer patients. *PLoS ONE* **2015**, *10*, e0127786. [CrossRef]
34. Suzuki, N.; Yoshioka, N.; Takae, S.; Sugishita, Y.; Tamura, M.; Hashimoto, S.; Morimoto, Y.; Kawamura, K. Successful fertility preservation following ovarian tissue vitrification in patients with primary ovarian insufficiency. *Hum. Reprod.* **2015**, *30*, 608–615. [CrossRef]

35. Lerer-Serfaty, G.; Samara, N.; Fisch, B.; Shachar, M.; Kossover, O.; Seliktar, D.; Ben-Haroush, A.; Abir, R. Attempted application of bioengineered/biosynthetic supporting matrices with phosphatidylinositol-trisphosphate-enhancing substances to organ culture of human primordial follicles. *J. Assist. Reprod. Genet.* **2013**, *30*, 1279–1288. [CrossRef]
36. McLaughlin, M.; Kinnell, H.L.; Anderson, R.A.; Telfer, E.E. Inhibition of phosphatase and tensin homologue (pten) in human ovary in vitro results in increased activation of primordial follicles but compromises development of growing follicles. *Mol. Hum. Reprod.* **2014**, *20*, 736–744. [CrossRef]
37. Grosbois, J.; Demeestere, I. Dynamics of pi3k and hippo signaling pathways during in vitro human follicle activation. *Hum. Reprod.* **2018**, *33*, 1705–1714. [CrossRef]
38. Brandmaier, A.; Hou, S.Q.; Shen, W.H. Cell cycle control by pten. *J. Mol. Biol.* **2017**, *429*, 2265–2277. [CrossRef]
39. Yin, Y.; Shen, W.H. Pten: A new guardian of the genome. *Oncogene* **2008**, *27*, 5443–5453. [CrossRef]
40. Adriaens, I.; Smitz, J.; Jacquet, P. The current knowledge on radiosensitivity of ovarian follicle development stages. *Hum. Reprod. Update* **2009**, *15*, 359–377. [CrossRef]
41. Jackson, S.P.; Bartek, J. The DNA-damage response in human biology and disease. *Nature* **2009**, *461*, 1071–1078. [CrossRef]
42. Khanna, K.K.; Jackson, S.P. DNA double-strand breaks: Signaling, repair and the cancer connection. *Nat. Genet.* **2001**, *27*, 247–254. [CrossRef]
43. Menezo, Y.; Dale, B.; Cohen, M. DNA damage and repair in human oocytes and embryos: A review. *Zygote* **2010**, *18*, 357–365. [CrossRef]
44. Moher, D.; Shamseer, L.; Clarke, M.; Ghersi, D.; Liberati, A.; Petticrew, M.; Shekelle, P.; Stewart, L.A.; Group, P.-P. Preferred reporting items for systematic review and meta-analysis protocols (prisma-p) 2015 statement. *Syst. Rev.* **2015**, *4*, 1. [CrossRef]
45. Branzei, D.; Foiani, M. Regulation of DNA repair throughout the cell cycle. *Nat. Rev. Mol. Cell. Biol.* **2008**, *9*, 297–308. [CrossRef]
46. Lindahl, T.; Barnes, D.E. Repair of endogenous DNA damage. *Cold Spring Harb. Symp. Quant. Biol.* **2000**, *65*, 127–133. [CrossRef]
47. Oktay, K.; Moy, F.; Titus, S.; Stobezki, R.; Turan, V.; Dickler, M.; Goswami, S. Age-related decline in DNA repair function explains diminished ovarian reserve, earlier menopause, and possible oocyte vulnerability to chemotherapy in women with brca mutations. *J. Clin. Oncol.* **2014**, *32*, 1093–1094. [CrossRef]
48. Kujjo, L.L.; Laine, T.; Pereira, R.J.; Kagawa, W.; Kurumizaka, H.; Yokoyama, S.; Perez, G.I. Enhancing survival of mouse oocytes following chemotherapy or aging by targeting bax and rad51. *PLoS ONE* **2010**, *5*, e9204. [CrossRef]
49. Martin, J.H.; Bromfield, E.G.; Aitken, R.J.; Lord, T.; Nixon, B. Double strand break DNA repair occurs via non-homologous end-joining in mouse mii oocytes. *Sci. Rep.* **2018**, *8*, 9685. [CrossRef]
50. Collins, J.K.; Jones, K.T. DNA damage responses in mammalian oocytes. *Reproduction* **2016**, *152*, R15–R22. [CrossRef]
51. Lieber, M.R. The mechanism of double-strand DNA break repair by the nonhomologous DNA end joining pathway. *Annu. Rev. Biochem.* **2010**, *79*, 181–211. [CrossRef]
52. Rodgers, K.; McVey, M. Error-prone repair of DNA double-strand breaks. *J. Cell. Physiol.* **2016**, *231*, 15–24. [CrossRef]
53. Heijink, A.M.; Krajewska, M.; van Vugt, M.A. The DNA damage response during mitosis. *Mutat. Res.* **2013**, *750*, 45–55. [CrossRef]
54. Bekker-Jensen, S.; Mailand, N. Assembly and function of DNA double-strand break repair foci in mammalian cells. *DNA Repair* **2010**, *9*, 1219–1228. [CrossRef]
55. Stringer, J.M.; Winship, A.; Liew, S.H.; Hutt, K. The capacity of oocytes for DNA repair. *Cell. Mol. Life Sci.* **2018**, *75*, 2777–2792. [CrossRef]
56. Menezo, Y., Jr.; Russo, G.; Tosti, E.; El Mouatassim, S.; Benkhalifa, M. Expression profile of genes coding for DNA repair in human oocytes using pangenomic microarrays, with a special focus on ros linked decays. *J. Assist. Reprod. Genet.* **2007**, *24*, 513–520. [CrossRef]
57. Jaroudi, S.; Kakourou, G.; Cawood, S.; Doshi, A.; Ranieri, D.M.; Serhal, P.; Harper, J.C.; SenGupta, S.B. Expression profiling of DNA repair genes in human oocytes and blastocysts using microarrays. *Hum. Reprod.* **2009**, *24*, 2649–2655. [CrossRef]

58. Govindaraj, V.; Krishnagiri, H.; Chauhan, M.S.; Rao, A.J. Brca-1 gene expression and comparative proteomic profile of primordial follicles from young and adult buffalo (bubalus bubalis) ovaries. *Anim. Biotechnol.* **2017**, *28*, 94–103. [CrossRef]
59. Govindaraj, V.; Rao, A.J. Comparative proteomic analysis of primordial follicles from ovaries of immature and aged rats. *Syst. Biol. Reprod. Med.* **2015**, *61*, 367–375. [CrossRef]
60. Fiorenza, M.T.; Bevilacqua, A.; Bevilacqua, S.; Mangia, F. Growing dictyate oocytes, but not early preimplantation embryos, of the mouse display high levels of DNA homologous recombination by single-strand annealing and lack DNA nonhomologous end joining. *Dev. Biol.* **2001**, *233*, 214–224. [CrossRef]
61. Rimon-Dahari, N.; Yerushalmi-Heinemann, L.; Alyagor, L.; Dekel, N. Ovarian folliculogenesis. *Results Probl. Cell. Differ.* **2016**, *58*, 167–190.
62. Perez, G.I.; Acton, B.M.; Jurisicova, A.; Perkins, G.A.; White, A.; Brown, J.; Trbovich, A.M.; Kim, M.R.; Fissore, R.; Xu, J.; et al. Genetic variance modifies apoptosis susceptibility in mature oocytes via alterations in DNA repair capacity and mitochondrial ultrastructure. *Cell. Death Differ.* **2007**, *14*, 524–533. [CrossRef]
63. Turan, V.; Oktay, K. Brca-related atm-mediated DNA double-strand break repair and ovarian aging. *Hum. Reprod. Update* **2019**, *26*, 43–57. [CrossRef]
64. Goedecke, W.; Vielmetter, W.; Pfeiffer, P. Activation of a system for the joining of nonhomologous DNA ends during xenopus egg maturation. *Mol. Cell. Biol.* **1992**, *12*, 811–816. [CrossRef]
65. So, S.; Davis, A.J.; Chen, D.J. Autophosphorylation at serine 1981 stabilizes atm at DNA damage sites. *J. Cell Biol.* **2009**, *187*, 977–990. [CrossRef]
66. You, Z.; Chahwan, C.; Bailis, J.; Hunter, T.; Russell, P. Atm activation and its recruitment to damaged DNA require binding to the c terminus of nbs1. *Mol. Cell Biol.* **2005**, *25*, 5363–5379. [CrossRef]
67. Inagaki, A.; Roset, R.; Petrini, J.H. Functions of the mre11 complex in the development and maintenance of oocytes. *Chromosoma* **2016**, *125*, 151–162. [CrossRef]
68. Ganesan, S.; Keating, A.F. The ovarian DNA damage repair response is induced prior to phosphoramide mustard-induced follicle depletion, and ataxia telangiectasia mutated inhibition prevents pm-induced follicle depletion. *Toxicol. Appl. Pharmacol.* **2016**, *292*, 65–74. [CrossRef]
69. Rogakou, E.P.; Pilch, D.R.; Orr, A.H.; Ivanova, V.S.; Bonner, W.M. DNA double-stranded breaks induce histone h2ax phosphorylation on serine 139. *J. Biol. Chem.* **1998**, *273*, 5858–5868. [CrossRef]
70. Tomilin, N.V.; Solovjeva, L.V.; Svetlova, M.P.; Pleskach, N.M.; Zalenskaya, I.A.; Yau, P.M.; Bradbury, E.M. Visualization of focal nuclear sites of DNA repair synthesis induced by bleomycin in human cells. *Radiat. Res.* **2001**, *156*, 347–354. [CrossRef]
71. Nazarov, I.B.; Smirnova, A.N.; Krutilina, R.I.; Svetlova, M.P.; Solovjeva, L.V.; Nikiforov, A.A.; Oei, S.L.; Zalenskaya, I.A.; Yau, P.M.; Bradbury, E.M.; et al. Dephosphorylation of histone gamma-h2ax during repair of DNA double-strand breaks in mammalian cells and its inhibition by calyculin a. *Radiat. Res.* **2003**, *160*, 309–317. [CrossRef]
72. Jungmichel, S.; Stucki, M. Mdc1: The art of keeping things in focus. *Chromosoma* **2010**, *119*, 337–349. [CrossRef]
73. Marangos, P.; Carroll, J. Oocytes progress beyond prophase in the presence of DNA damage. *Curr. Biol.* **2012**, *22*, 989–994. [CrossRef]
74. Jazayeri, A.; Falck, J.; Lukas, C.; Bartek, J.; Smith, G.C.; Lukas, J.; Jackson, S.P. Atm- and cell cycle-dependent regulation of atr in response to DNA double-strand breaks. *Nat. Cell Biol.* **2006**, *8*, 37–45. [CrossRef]
75. Bolcun-Filas, E.; Rinaldi, V.D.; White, M.E.; Schimenti, J.C. Reversal of female infertility by chk2 ablation reveals the oocyte DNA damage checkpoint pathway. *Science* **2014**, *343*, 533–536. [CrossRef]
76. Kujjo, L.L.; Ronningen, R.; Ross, P.; Pereira, R.J.; Rodriguez, R.; Beyhan, Z.; Goissis, M.D.; Baumann, T.; Kagawa, W.; Camsari, C.; et al. Rad51 plays a crucial role in halting cell death program induced by ionizing radiation in bovine oocytes. *Biol. Reprod.* **2012**, *86*, 76. [CrossRef]
77. Zannini, L.; Delia, D.; Buscemi, G. Chk2 kinase in the DNA damage response and beyond. *J. Mol. Cell Biol.* **2014**, *6*, 442–457. [CrossRef]
78. Basu, A.; Haldar, S. The relationship between bci2, bax and p53: Consequences for cell cycle progression and cell death. *Mol. Hum. Reprod.* **1998**, *4*, 1099–1109. [CrossRef]
79. Kim, D.A.; Suh, E.K. Defying DNA double-strand break-induced death during prophase i meiosis by temporal tap63alpha phosphorylation regulation in developing mouse oocytes. *Mol. Cell. Biol.* **2014**, *34*, 1460–1473. [CrossRef]

80. Suh, E.K.; Yang, A.; Kettenbach, A.; Bamberger, C.; Michaelis, A.H.; Zhu, Z.; Elvin, J.A.; Bronson, R.T.; Crum, C.P.; McKeon, F. P63 protects the female germ line during meiotic arrest. *Nature* **2006**, *444*, 624–628. [CrossRef]
81. Livera, G.; Petre-Lazar, B.; Guerquin, M.J.; Trautmann, E.; Coffigny, H.; Habert, R. P63 null mutation protects mouse oocytes from radio-induced apoptosis. *Reproduction* **2008**, *135*, 3–12. [CrossRef]
82. Amelio, I.; Grespi, F.; Annicchiarico-Petruzzelli, M.; Melino, G. P63 the guardian of human reproduction. *Cell Cycle* **2012**, *11*, 4545–4551. [CrossRef]
83. Levine, A.J.; Tomasini, R.; McKeon, F.D.; Mak, T.W.; Melino, G. The p53 family: Guardians of maternal reproduction. *Nat. Rev. Mol. Cell Biol.* **2011**, *12*, 259–265. [CrossRef]
84. Gebel, J.; Tuppi, M.; Krauskopf, K.; Coutandin, D.; Pitzius, S.; Kehrloesser, S.; Osterburg, C.; Dotsch, V. Control mechanisms in germ cells mediated by p53 family proteins. *J. Cell Sci.* 2017. [CrossRef]
85. Deutsch, G.B.; Zielonka, E.M.; Coutandin, D.; Dotsch, V. Quality control in oocytes: Domain-domain interactions regulate the activity of p63. *Cell Cycle* **2011**, *10*, 1884–1885. [CrossRef]
86. Straub, W.E.; Weber, T.A.; Schafer, B.; Candi, E.; Durst, F.; Ou, H.D.; Rajalingam, K.; Melino, G.; Dotsch, V. The c-terminus of p63 contains multiple regulatory elements with different functions. *Cell Death Dis.* **2010**, *1*, e5. [CrossRef]
87. Deutsch, G.B.; Zielonka, E.M.; Coutandin, D.; Weber, T.A.; Schafer, B.; Hannewald, J.; Luh, L.M.; Durst, F.G.; Ibrahim, M.; Hoffmann, J.; et al. DNA damage in oocytes induces a switch of the quality control factor tap63alpha from dimer to tetramer. *Cell* **2011**, *144*, 566–576. [CrossRef]
88. Coutandin, D.; Osterburg, C.; Srivastav, R.K.; Sumyk, M.; Kehrloesser, S.; Gebel, J.; Tuppi, M.; Hannewald, J.; Schafer, B.; Salah, E.; et al. Quality control in oocytes by p63 is based on a spring-loaded activation mechanism on the molecular and cellular level. *Elife* **2016**, *5*, e13909. [CrossRef]
89. Tuppi, M.; Kehrloesser, S.; Coutandin, D.W.; Rossi, V.; Luh, L.M.; Strubel, A.; Hotte, K.; Hoffmeister, M.; Schafer, B.; De Oliveira, T.; et al. Oocyte DNA damage quality control requires consecutive interplay of chk2 and ck1 to activate p63. *Nat. Struct. Mol. Biol.* **2018**, *25*, 261–269. [CrossRef]
90. Nowsheen, S.; Yang, E. The intersection between DNA damage response and cell death pathways. *Exp. Oncol.* **2012**, *34*, 243–254.
91. Guo, X.; Keyes, W.M.; Papazoglu, C.; Zuber, J.; Li, W.; Lowe, S.W.; Vogel, H.; Mills, A.A. Tap63 induces senescence and suppresses tumorigenesis in vivo. *Nat. Cell Biol.* **2009**, *11*, 1451–1457. [CrossRef] [PubMed]
92. Tavana, O.; Benjamin, C.L.; Puebla-Osorio, N.; Sang, M.; Ullrich, S.E.; Ananthaswamy, H.N.; Zhu, C. Absence of p53-dependent apoptosis leads to uv radiation hypersensitivity, enhanced immunosuppression and cellular senescence. *Cell Cycle* **2010**, *9*, 3328–3336. [CrossRef] [PubMed]
93. Adhikari, D.; Flohr, G.; Gorre, N.; Shen, Y.; Yang, H.; Lundin, E.; Lan, Z.; Gambello, M.J.; Liu, K. Disruption of tsc2 in oocytes leads to overactivation of the entire pool of primordial follicles. *Mol. Hum. Reprod.* **2009**, *15*, 765–770. [CrossRef]
94. Dole, G.; Nilsson, E.E.; Skinner, M.K. Glial-derived neurotrophic factor promotes ovarian primordial follicle development and cell-cell interactions during folliculogenesis. *Reproduction* **2008**, *135*, 671–682. [CrossRef]
95. Nilsson, E.; Parrott, J.A.; Skinner, M.K. Basic fibroblast growth factor induces primordial follicle development and initiates folliculogenesis. *Mol. Cell. Endocrinol.* **2001**, *175*, 123–130. [CrossRef]
96. Ojeda, S.R.; Romero, C.; Tapia, V.; Dissen, G.A. Neurotrophic and cell-cell dependent control of early follicular development. *Mol. Cell. Endocrinol.* **2000**, *163*, 67–71. [CrossRef]
97. Nilsson, E.E.; Skinner, M.K. Kit ligand and basic fibroblast growth factor interactions in the induction of ovarian primordial to primary follicle transition. *Mol. Cell. Endocrinol.* **2004**, *214*, 19–25. [CrossRef]
98. Nilsson, E.E.; Kezele, P.; Skinner, M.K. Leukemia inhibitory factor (lif) promotes the primordial to primary follicle transition in rat ovaries. *Mol. Cell. Endocrinol.* **2002**, *188*, 65–73. [CrossRef]
99. McLaughlin, E.A.; McIver, S.C. Awakening the oocyte: Controlling primordial follicle development. *Reproduction* **2009**, *137*, 1–11. [CrossRef]
100. Adhikari, D.; Zheng, W.; Shen, Y.; Gorre, N.; Hamalainen, T.; Cooney, A.J.; Huhtaniemi, I.; Lan, Z.J.; Liu, K. Tsc/mtorc1 signaling in oocytes governs the quiescence and activation of primordial follicles. *Hum. Mol. Genet.* **2010**, *19*, 397–410. [CrossRef]
101. Adhikari, D.; Liu, K. Mtor signaling in the control of activation of primordial follicles. *Cell Cycle* **2010**, *9*, 1673–1674. [CrossRef]

102. Castrillon, D.H.; Miao, L.; Kollipara, R.; Horner, J.W.; DePinho, R.A. Suppression of ovarian follicle activation in mice by the transcription factor foxo3a. *Science* **2003**, *301*, 215–218. [CrossRef]
103. John, G.B.; Shirley, L.J.; Gallardo, T.D.; Castrillon, D.H. Specificity of the requirement for foxo3 in primordial follicle activation. *Reproduction* **2007**, *133*, 855–863. [CrossRef]
104. Pelosi, E.; Omari, S.; Michel, M.; Ding, J.; Amano, T.; Forabosco, A.; Schlessinger, D.; Ottolenghi, C. Constitutively active foxo3 in oocytes preserves ovarian reserve in mice. *Nat. Commun.* **2013**, *4*, 1843. [CrossRef]
105. Hunt, C.R.; Gupta, A.; Horikoshi, N.; Pandita, T.K. Does pten loss impair DNA double-strand break repair by homologous recombination? *Clin. Cancer Res.* **2012**, *18*, 920–922. [CrossRef]
106. Liu, P.; Gan, W.; Guo, C.; Xie, A.; Gao, D.; Guo, J.; Zhang, J.; Willis, N.; Su, A.; Asara, J.M.; et al. Akt-mediated phosphorylation of xlf impairs non-homologous end-joining DNA repair. *Mol. Cell.* **2015**, *57*, 648–661. [CrossRef]
107. Xu, N.; Hegarat, N.; Black, E.J.; Scott, M.T.; Hochegger, H.; Gillespie, D.A. Akt/pkb suppresses DNA damage processing and checkpoint activation in late g2. *J. Cell Biol.* **2010**, *190*, 297–305. [CrossRef]
108. Pedram, A.; Razandi, M.; Evinger, A.J.; Lee, E.; Levin, E.R. Estrogen inhibits atr signaling to cell cycle checkpoints and DNA repair. *Mol. Biol. Cell* **2009**, *20*, 3374–3389. [CrossRef]
109. Shen, W.H.; Balajee, A.S.; Wang, J.; Wu, H.; Eng, C.; Pandolfi, P.P.; Yin, Y. Essential role for nuclear pten in maintaining chromosomal integrity. *Cell* **2007**, *128*, 157–170. [CrossRef]
110. Thacker, J. The rad51 gene family, genetic instability and cancer. *Cancer Lett.* **2005**, *219*, 125–135. [CrossRef]
111. Brunet, A.; Bonni, A.; Zigmond, M.J.; Lin, M.Z.; Juo, P.; Hu, L.S.; Anderson, M.J.; Arden, K.C.; Blenis, J.; Greenberg, M.E. Akt promotes cell survival by phosphorylating and inhibiting a forkhead transcription factor. *Cell* **1999**, *96*, 857–868. [CrossRef]
112. Astle, M.V.; Hannan, K.M.; Ng, P.Y.; Lee, R.S.; George, A.J.; Hsu, A.K.; Haupt, Y.; Hannan, R.D.; Pearson, R.B. Akt induces senescence in human cells via mtorc1 and p53 in the absence of DNA damage: Implications for targeting mtor during malignancy. *Oncogene* **2012**, *31*, 1949–1962. [CrossRef]
113. Kawamura, K.; Cheng, Y.; Suzuki, N.; Deguchi, M.; Sato, Y.; Takae, S.; Ho, C.H.; Kawamura, N.; Tamura, M.; Hashimoto, S.; et al. Hippo signaling disruption and akt stimulation of ovarian follicles for infertility treatment. *Proc. Natl. Acad. Sci. USA* **2013**, *110*, 17474–17479. [CrossRef]
114. Kim, S.Y.; Ebbert, K.; Cordeiro, M.H.; Romero, M.; Zhu, J.; Serna, V.A.; Whelan, K.A.; Woodruff, T.K.; Kurita, T. Cell autonomous phosphoinositide 3-kinase activation in oocytes disrupts normal ovarian function through promoting survival and overgrowth of ovarian follicles. *Endocrinology* **2015**, *156*, 1464–1476. [CrossRef]
115. Kim, S.Y.; Ebbert, K.; Cordeiro, M.H.; Romero, M.M.; Whelan, K.A.; Suarez, A.A.; Woodruff, T.K.; Kurita, T. Constitutive activation of pi3k in oocyte induces ovarian granulosa cell tumors. *Cancer Res.* **2016**, *76*, 3851–3861. [CrossRef]
116. Smitz, J.E.; Cortvrindt, R.G. The earliest stages of folliculogenesis in vitro. *Reproduction* **2002**, *123*, 185–202. [CrossRef]
117. Nguyen, Q.N.; Zerafa, N.; Liew, S.H.; Findlay, J.K.; Hickey, M.; Hutt, K.J.; Bezerra, M.E.S.; Gouveia, B.B.; Barberino, R.S.; Menezes, V.G.; et al. Cisplatin- and cyclophosphamide-induced primordial follicle depletion is caused by direct damage to oocytes resveratrol promotes in vitro activation of ovine primordial follicles by reducing DNA damage and enhancing granulosa cell proliferation via phosphatidylinositol 3-kinase pathway. *Mol. Hum. Reprod.* **2019**, *53*, 1298–1305.
118. Soleimani, R.; Heytens, E.; Darzynkiewicz, Z.; Oktay, K. Mechanisms of chemotherapy-induced human ovarian aging: Double strand DNA breaks and microvascular compromise. *Aging* **2011**, *3*, 782–793. [CrossRef]
119. Roness, H.; Gavish, Z.; Cohen, Y.; Meirow, D. Ovarian follicle burnout: A universal phenomenon? *Cell Cycle* **2013**, *12*, 3245–3246. [CrossRef]
120. Kalich-Philosoph, L.; Roness, H.; Carmely, A.; Fishel-Bartal, M.; Ligumsky, H.; Paglin, S.; Wolf, I.; Kanety, H.; Sredni, B.; Meirow, D. Cyclophosphamide triggers follicle activation and "burnout"; as101 prevents follicle loss and preserves fertility. *Sci. Transl. Med.* **2013**, *5*, 185ra62. [CrossRef]
121. Spears, N.; Lopes, F.; Stefansdottir, A.; Rossi, V.; De Felici, M.; Anderson, R.A.; Klinger, F.G. Ovarian damage from chemotherapy and current approaches to its protection. *Hum. Reprod. Update* **2019**, *25*, 673–693. [CrossRef]
122. Govatati, S.; Kodati, V.L.; Deenadayal, M.; Chakravarty, B.; Shivaji, S.; Bhanoori, M.; Yin, X.; Pavone, M.E.; Lu, Z.; Wei, J.; et al. Mutations in the pten tumor gene and risk of endometriosis: A case-control study increased activation of the pi3k/akt pathway compromises decidualization of stromal cells from endometriosis. *Hum. Reprod.* **2014**, *29*, 324–336. [CrossRef]

123. Madanes, D.; Bilotas, M.A.; Baston, J.I.; Singla, J.J.; Meresman, G.F.; Baranao, R.I.; Ricci, A.G.; Takeuchi, A.; Koga, K.; Satake, E.; et al. Pi3k/akt pathway is altered in the endometriosis patient's endometrium and presents differences according to severity stage endometriosis triggers excessive activation of primordial follicles via pi3k-pten-akt-foxo3 pathway inhibition of pi3k/akt/mtor pathway for the treatment of endometriosis. *Gynecol. Endocrinol.* **2019**, *104*, 1–5.
124. Makker, A.; Goel, M.M.; Das, V.; Agarwal, A. Pi3k-akt-mtor and mapk signaling pathways in polycystic ovarian syndrome, uterine leiomyomas and endometriosis: An update. *Gynecol. Endocrinol.* **2012**, *28*, 175–181. [CrossRef]
125. Takeuchi, A.; Koga, K.; Satake, E.; Makabe, T.; Taguchi, A.; Miyashita, M.; Takamura, M.; Harada, M.; Hirata, T.; Hirota, Y.; et al. Endometriosis triggers excessive activation of primordial follicles via pi3k-pten-akt-foxo3 pathway inhibition of pi3k/akt/mtor pathway for the treatment of endometriosis. *J. Clin. Endocrinol. Metab.* **2019**, *104*, 5547–5554. [CrossRef]
126. Yin, X.; Pavone, M.E.; Lu, Z.; Wei, J.; Kim, J.J. Increased activation of the pi3k/akt pathway compromises decidualization of stromal cells from endometriosis. *J. Clin. Endocrinol. Metab.* **2012**, *97*, E35–E43. [CrossRef]
127. Barra, F.; Ferro Desideri, L.; Ferrero, S. Inhibition of pi3k/akt/mtor pathway for the treatment of endometriosis. *Br. J. Pharmacol.* **2018**, *175*, 3626–3627. [CrossRef]
128. Zhang, H.; Zhao, X.; Liu, S.; Li, J.; Wen, Z.; Li, M. 17betae2 promotes cell proliferation in endometriosis by decreasing pten via nfkappab-dependent pathway. *Mol. Cell. Endocrinol.* **2010**, *317*, 31–43. [CrossRef]
129. Kitajima, M.; Dolmans, M.M.; Donnez, O.; Masuzaki, H.; Soares, M.; Donnez, J. Enhanced follicular recruitment and atresia in cortex derived from ovaries with endometriomas. *Fertil. Steril.* **2014**, *101*, 1031–1037. [CrossRef]
130. Choi, Y.S.; Park, J.H.; Lee, J.H.; Yoon, J.K.; Yun, B.H.; Park, J.H.; Seo, S.K.; Sung, H.J.; Kim, H.S.; Cho, S.; et al. Association between impairment of DNA double strand break repair and decreased ovarian reserve in patients with endometriosis. *Front Endocrinol.* **2018**, *9*, 772. [CrossRef]
131. Kacan, T.; Yildiz, C.; Baloglu Kacan, S.; Seker, M.; Ozer, H.; Cetin, A. Everolimus as an mtor inhibitor suppresses endometriotic implants: An experimental rat study. *Geburtshilfe Frauenheilkd.* **2017**, *77*, 66–72. [CrossRef]
132. Wang, Y.; Hu, Z.; Liu, Z.; Chen, R.; Peng, H.; Guo, J.; Chen, X.; Zhang, H. Mtor inhibition attenuates DNA damage and apoptosis through autophagy-mediated suppression of creb1. *Autophagy* **2013**, *9*, 2069–2086. [CrossRef]
133. Zhou, L.; Xie, Y.; Li, S.; Liang, Y.; Qiu, Q.; Lin, H.; Zhang, Q. Rapamycin prevents cyclophosphamide-induced over-activation of primordial follicle pool through pi3k/akt/mtor signaling pathway in vivo. *J. Ovarian. Res.* **2017**, *10*, 56. [CrossRef]
134. Adhikari, D.; Risal, S.; Liu, K.; Shen, Y. Pharmacological inhibition of mtorc1 prevents over-activation of the primordial follicle pool in response to elevated pi3k signaling. *PLoS ONE* **2013**, *8*, e53810. [CrossRef]
135. Zhang, X.M.; Li, L.; Xu, J.J.; Wang, N.; Liu, W.J.; Lin, X.H.; Fu, Y.C.; Luo, L.L. Rapamycin preserves the follicle pool reserve and prolongs the ovarian lifespan of female rats via modulating mtor activation and sirtuin expression. *Gene* **2013**, *523*, 82–87. [CrossRef]
136. Goldman, K.N.; Chenette, D.; Arju, R.; Duncan, F.E.; Keefe, D.L.; Grifo, J.A.; Schneider, R.J. Mtorc1/2 inhibition preserves ovarian function and fertility during genotoxic chemotherapy. *Proc. Natl. Acad. Sci. USA* **2017**, *114*, 3186–3191. [CrossRef]
137. Wang, W.; Luo, S.M.; Ma, J.Y.; Shen, W.; Yin, S. Cytotoxicity and DNA damage caused from diazinon exposure by inhibiting the pi3k-akt pathway in porcine ovarian granulosa cells. *J. Agric. Food Chem.* **2019**, *67*, 19–31. [CrossRef]
138. Ganesan, S.; Keating, A.F. Bisphenol a-induced ovotoxicity involves DNA damage induction to which the ovary mounts a protective response indicated by increased expression of proteins involved in DNA repair and xenobiotic biotransformation. *Toxicol. Sci.* **2016**, *152*, 169–180. [CrossRef]
139. Sun, X.; Su, Y.; He, Y.; Zhang, J.; Liu, W.; Zhang, H.; Hou, Z.; Liu, J.; Li, J. New strategy for in vitro activation of primordial follicles with mtor and pi3k stimulators. *Cell Cycle* **2015**, *14*, 721–731. [CrossRef]
140. Li, J.; Kawamura, K.; Cheng, Y.; Liu, S.; Klein, C.; Liu, S.; Duan, E.K.; Hsueh, A.J. Activation of dormant ovarian follicles to generate mature eggs. *Proc. Natl. Acad. Sci. USA* **2010**, *107*, 10280–10284. [CrossRef]
141. Faddy, M.J.; Gosden, R.G.; Gougeon, A.; Richardson, S.J.; Nelson, J.F. Accelerated disappearance of ovarian follicles in mid-life: Implications for forecasting menopause. *Hum. Reprod.* **1992**, *7*, 1342–1346. [CrossRef]

142. De Bruin, J.P.; Dorland, M.; Spek, E.R.; Posthuma, G.; van Haaften, M.; Looman, C.W.; te Velde, E.R. Age-related changes in the ultrastructure of the resting follicle pool in human ovaries. *Biol. Reprod.* **2004**, *70*, 419–424. [CrossRef]
143. Li, Q.; Geng, X.; Zheng, W.; Tang, J.; Xu, B.; Shi, Q. Current understanding of ovarian aging. *Sci. China Life Sci.* **2012**, *55*, 659–669. [CrossRef]
144. Gougeon, A. Dynamics of follicular growth in the human: A model from preliminary results. *Hum. Reprod.* **1986**, *1*, 81–87. [CrossRef]
145. Oktay, K.; Kim, J.Y.; Barad, D.; Babayev, S.N. Association of brca1 mutations with occult primary ovarian insufficiency: A possible explanation for the link between infertility and breast/ovarian cancer risks. *J. Clin. Oncol.* **2010**, *28*, 240–244. [CrossRef]
146. Sharan, S.K.; Pyle, A.; Coppola, V.; Babus, J.; Swaminathan, S.; Benedict, J.; Swing, D.; Martin, B.K.; Tessarollo, L.; Evans, J.P.; et al. Brca2 deficiency in mice leads to meiotic impairment and infertility. *Development* **2004**, *131*, 131–142. [CrossRef]
147. Weinberg-Shukron, A.; Rachmiel, M.; Renbaum, P.; Gulsuner, S.; Walsh, T.; Lobel, O.; Dreifuss, A.; Ben-Moshe, A.; Zeligson, S.; Segel, R.; et al. Essential role of brca2 in ovarian development and function. *N. Engl. J. Med.* **2018**, *379*, 1042–1049. [CrossRef]
148. Day, F.R.; Ruth, K.S.; Thompson, D.J.; Lunetta, K.L.; Pervjakova, N.; Chasman, D.I.; Stolk, L.; Finucane, H.K.; Sulem, P.; Bulik-Sullivan, B.; et al. Large-scale genomic analyses link reproductive aging to hypothalamic signaling, breast cancer susceptibility and brca1-mediated DNA repair. *Nat. Genet.* **2015**, *47*, 1294–1303. [CrossRef]
149. Phillips, K.A.; Collins, I.M.; Milne, R.L.; McLachlan, S.A.; Friedlander, M.; Hickey, M.; Stern, C.; Hopper, J.L.; Fisher, R.; Kannemeyer, G.; et al. Anti-mullerian hormone serum concentrations of women with germline brca1 or brca2 mutations. *Hum. Reprod.* **2016**, *31*, 1126–1132. [CrossRef]
150. Shi, L.; Zhang, J.; Lai, Z.; Tian, Y.; Fang, L.; Wu, M.; Xiong, J.; Qin, X.; Luo, A.; Wang, S. Long-term moderate oxidative stress decreased ovarian reproductive function by reducing follicle quality and progesterone production. *PLoS ONE* **2016**, *11*, e0162194. [CrossRef]
151. Yang, B.; Oo, T.N.; Rizzo, V. Lipid rafts mediate h2o2 prosurvival effects in cultured endothelial cells. *FASEB J.* **2006**, *20*, 1501–1503. [CrossRef]
152. Das, S.; Chattopadhyay, R.; Ghosh, S.; Ghosh, S.; Goswami, S.K.; Chakravarty, B.N.; Chaudhury, K. Reactive oxygen species level in follicular fluid–embryo quality marker in ivf? *Hum. Reprod.* **2006**, *21*, 2403–2407. [CrossRef]
153. Kitagawa, T.; Suganuma, N.; Nawa, A.; Kikkawa, F.; Tanaka, M.; Ozawa, T.; Tomoda, Y. Rapid accumulation of deleted mitochondrial deoxyribonucleic acid in postmenopausal ovaries. *Biol. Reprod.* **1993**, *49*, 730–736. [CrossRef]
154. Keefe, D.L.; Niven-Fairchild, T.; Powell, S.; Buradagunta, S. Mitochondrial deoxyribonucleic acid deletions in oocytes and reproductive aging in women. *Fertil. Steril.* **1995**, *64*, 577–583. [CrossRef]
155. Nogueira, V.; Hay, N. Molecular pathways: Reactive oxygen species homeostasis in cancer cells and implications for cancer therapy. *Clin. Cancer Res.* **2013**, *19*, 4309–4314. [CrossRef]
156. Kitagishi, Y.; Matsuda, S. Redox regulation of tumor suppressor pten in cancer and aging (review). *Int. J. Mol. Med.* **2013**, *31*, 511–515. [CrossRef]
157. Tait, I.S.; Li, Y.; Lu, J. Pten, longevity and age-related diseases. *Biomedicines* **2013**, *1*, 17–48. [CrossRef]
158. Grynberg, M.; Dagher Hayeck, B.; Papanikolaou, E.G.; Sifer, C.; Sermondade, N.; Sonigo, C. Brca1/2 gene mutations do not affect the capacity of oocytes from breast cancer candidates for fertility preservation to mature in vitro. *Hum. Reprod.* **2019**, *34*, 374–379. [CrossRef]
159. Gunnala, V.; Fields, J.; Irani, M.; D'Angelo, D.; Xu, K.; Schattman, G.; Rosenwaks, Z. Brca carriers have similar reproductive potential at baseline to noncarriers: Comparisons in cancer and cancer-free cohorts undergoing fertility preservation. *Fertil. Steril.* **2019**, *111*, 363–371. [CrossRef]
160. Derks-Smeets, I.A.P.; van Tilborg, T.C.; van Montfoort, A.; Smits, L.; Torrance, H.L.; Meijer-Hoogeveen, M.; Broekmans, F.; Dreesen, J.; Paulussen, A.D.C.; Tjan-Heijnen, V.C.G.; et al. Brca1 mutation carriers have a lower number of mature oocytes after ovarian stimulation for ivf/pgd. *J. Assist. Reprod. Genet.* **2017**, *34*, 1475–1482. [CrossRef]
161. Johnson, L.; Sammel, M.D.; Domchek, S.; Schanne, A.; Prewitt, M.; Gracia, C. Antimullerian hormone levels are lower in brca2 mutation carriers. *Fertil. Steril.* **2017**, *107*, 1256–1265. [CrossRef]

162. Van Tilborg, T.C.; Derks-Smeets, I.A.; Bos, A.M.; Oosterwijk, J.C.; van Golde, R.J.; de Die-Smulders, C.E.; van der Kolk, L.E.; van Zelst-Stams, W.A.; Velthuizen, M.E.; Hoek, A.; et al. Serum amh levels in healthy women from brca1/2 mutated families: Are they reduced? *Hum. Reprod.* **2016**, *31*, 2651–2659. [CrossRef]
163. Wang, E.T.; Pisarska, M.D.; Bresee, C.; Chen, Y.D.; Lester, J.; Afshar, Y.; Alexander, C.; Karlan, B.Y. Brca1 germline mutations may be associated with reduced ovarian reserve. *Fertil. Steril.* **2014**, *102*, 1723–1728. [CrossRef]
164. Finch, A.; Valentini, A.; Greenblatt, E.; Lynch, H.T.; Ghadirian, P.; Armel, S.; Neuhausen, S.L.; Kim-Sing, C.; Tung, N.; Karlan, B.; et al. Frequency of premature menopause in women who carry a brca1 or brca2 mutation. *Fertil. Steril.* **2013**, *99*, 1724–1728. [CrossRef]
165. Guglielmino, M.R.; Santonocito, M.; Vento, M.; Ragusa, M.; Barbagallo, D.; Borzi, P.; Casciano, I.; Banelli, B.; Barbieri, O.; Astigiano, S.; et al. Tap73 is downregulated in oocytes from women of advanced reproductive age. *Cell Cycle* **2011**, *10*, 3253–3256. [CrossRef]
166. Pan, H.; Ma, P.; Zhu, W.; Schultz, R.M. Age-associated increase in aneuploidy and changes in gene expression in mouse eggs. *Dev. Biol.* **2008**, *316*, 397–407. [CrossRef]
167. Jang, H.; Na, Y.; Hong, K.; Lee, S.; Moon, S.; Cho, M.; Park, M.; Lee, O.H.; Chang, E.M.; Lee, D.R.; et al. Synergistic effect of melatonin and ghrelin in preventing cisplatin-induced ovarian damage via regulation of foxo3a phosphorylation and binding to the p27(kip1) promoter in primordial follicles. *J. Pineal Res.* **2017**, 63. [CrossRef]
168. Alexandri, C.; Stratopoulou, C.A.; Demeestere, I. Answer to controversy: Mir-10a replacement approaches do not offer protection against chemotherapy-induced gonadotoxicity in mouse model. *Int. J. Mol. Sci.* **2019**, *20*, 4958. [CrossRef]
169. Wang, Y.; Taniguchi, T. Micrornas and DNA damage response: Implications for cancer therapy. *Cell Cycle* **2013**, *12*, 32–42. [CrossRef]
170. Alexandri, C.; Stamatopoulos, B.; Rothe, F.; Bareche, Y.; Devos, M.; Demeestere, I. Microrna profiling and identification of let-7a as a target to prevent chemotherapy-induced primordial follicles apoptosis in mouse ovaries. *Sci. Rep.* **2019**, *9*, 9636. [CrossRef]
171. Dolmans, M.M.; Martinez-Madrid, B.; Gadisseux, E.; Guiot, Y.; Yuan, W.Y.; Torre, A.; Camboni, A.; Van Langendonckt, A.; Donnez, J. Short-term transplantation of isolated human ovarian follicles and cortical tissue into nude mice. *Reproduction* **2007**, *134*, 253–262. [CrossRef] [PubMed]
172. Gavish, Z.; Spector, I.; Peer, G.; Schlatt, S.; Wistuba, J.; Roness, H.; Meirow, D. Follicle activation is a significant and immediate cause of follicle loss after ovarian tissue transplantation. *J. Assist. Reprod. Genet.* **2018**, *35*, 61–69. [CrossRef] [PubMed]